University of Alberta

ASSESSMENT AND REHABILITATION OF FC GIRDER BRIDGES

by

Nadeem Ahmad Khattak ©

A thesis submitted to the Faculty of Graduate Studies and Research in partial fulfillment of the requirements for the degree of Doctor of Philosophy

in

Structural Engineering

Department of Civil and Environmental Engineering

Edmonton, Alberta

Spring 2003

Canada

Library Release Form

Name of Author: Nadeem Ahmad Khattak

Title of Thesis: Assessment and Rehabilitation of FG Girder Bridges

Degree: Doctor of Philosophy

Year this Degree granted: 2003

Permission is hereby granted to the University of Alberta Library to reproduce single copies of this thesis and to lend or sell such copies for private, scholarly or scientific research purposes only.

The author reserves all other publication and other rights in association with the copyright in the thesis, and except as herein provided, neither the thesis or any substantial portion thereof may be printed or otherwise reproduced in any form whatever without the author's prior written permission.
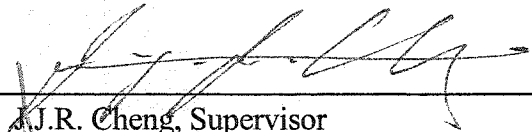
Nadeem Ahmad Khattak
45/D-1, Phase – I
HayatAbad, Peshawar
Pakistan

April 3, 2003

University of Alberta
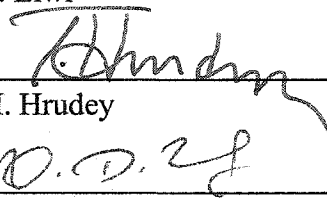
Faculty of Graduate Studies and Research

The u ndersigned c ertify t hat t hey have read, and recommend to the Faculty of Graduate Studies and Research for acceptance, a thesis entitled Assessment and Rehabilitation of FC Girder Bridges submitted by Nadeem Ahmad Khattak in partial fulfillment of the requirements for the degree of Doctor of Philosophy in Structural Engineering.

_____
J.R. Cheng, Supervisor

_____
A.E. Elwi

_____
T.M. Hrudey

_____
X. Wang

_____
T.G. Brown (External Examiner)

APRIL 2, 2003

DEDICATION

I would like to dedicate this thesis to my family, wife Noor-e-Irum, sons Muhammad Azam and Hashim Ahmad and parents Dr. Ghaus Muhammad Khattak and Farhat Jehan for inspiring me to get into this wonderful world of research.

ABSTRACT

Almost two hundred precast prestressed FC girder bridges were built in the province of Alberta over a twenty year period from 1960 to 1980. Many of these bridges have required rehabilitation due to the deterioration and failure of the field grouted longitudinal shear keys between the girders. Many rehabilitat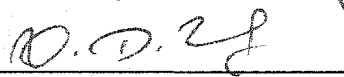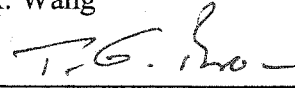ion schemes have been tried by Alberta Transportation in the past, but none have successfully rectified the problem. No thorough study has been carried out on monitoring the field performance of these structures and most bridge reviews are based on visual inspections that focus on the appearance of alarming signs.

This research program was designed to investigate and better understand the behaviour of FC girder bridges by conducting a three fold research program. The first part consisted of an extensive field survey meant to review the current condition of these bridges, visually assess severity of the field problem and verify shear key cracking concerns. While the second part constituted field testing and assessment of FC girder bridges to observe load sharing concerns as well as the response of the bridge to service loads. Load and vibration testing was conducted to measure deflections, strains and natural frequencies and mode shapes of the bridges. All the test measurements complemented each other and indicated partial load sharing between the girders as a result of shear key cracking.

The third and final phase of this research consisted of the development of a finite element model based on results from the field tests. A comparative study of the performance of the different rehabilitation schemes, in the finite element model, indicated that all

rehabilitation strategies improved load sharing among the girders. However, a combination of transverse prestressing and transverse steel underslung diaphragms was the best rehabilitation technique to avoid future shear key cracking. Differential movement at shear key joints in the form of deflections and rotations generally accelerate shear key cracking and must be arrested by increasing the stiffness of the transverse span. The success of the proposed scheme lies in its ability to transform the transverse cross section into a stiff plate hence eliminating all differential movement at the shear key lines.

ACKNOWLEDGEMENTS

This research was conducted under the supervision of Dr. J.J. Roger Cheng. His able guidance and unlimited patience are greatly appreciated.

I would also like to express my appreciation of the staff of the I.F. Morrison Structural Laboratory, Larry Burden and Richard Helfrich for their technical assistance and cooperation during the experimental part of this study.

The field testing on FC girder bridges was made possible by the logistic support provided by Alberta Transportation and the City of Fort Saskatchewan. I would like to sincerely thank Mr. Raymond Yu of the Alberta Transportation and Mr. John Alexander of Stantec Consulting for invaluable advice and providing access to bridge records. I would also like to acknowledge the help of Dr. Shahab Afhami of UMA Engineering in planning the testing phase of this program and providing useful tips from time to time.

The wealth of information obtained as a result of discussions with fellow graduate students was always useful in the research and the assistance of fellow students Adnan Shakir, Munnawar Hussain, Mohammad Behbahanifard, Sreekanta Das and Salman Mobeen is highly appreciated.

Last but certainly not the least I would like to thank my family, wife Irum, sons Azam and Hashim and parents Ghaus and Farhat for their untiring support and patience which was the biggest source of inspiration in completing this research.

Finally, I would like to thank the Almighty Allah on giving me the endurance and courage to accomplish this work.

TABLE OF CONTENTS

LIST OF TABLES

LIST OF FIGURES

LIST OF ABBREVIATIONS AND SYMBOLS

Abbreviations

AADT	Annual Average Daily Traffic
AASHTO	American Association of State Highway and Transportation Officials
ACI	American Concrete Institute
AE	Acoustic Emission
AT	Alberta Transportation
BIM	Bridge Inspection and Management Report
CA	Cawley & Adams Method
CHBDC	Canadian Highway Bridge Design Code
CM	Condition Monitoring
CMP	Correlated Mode Pairs
CSA	Canadian Standards Association
DAQ	Data Acquisition
DC	Direct Current
DI	Damage Identification
DLA	Dynamic Load Allowance
ft	foot
GPa	GigaPascal
Hz	Hertz
ISIS	Intelligent Sensing for Innovative Structures
kg	kilogram
kHz	kilohertz
kN	kiloNewton
LLDF	Lateral Live Load Distribution factor
LS	Lateral Stressing
LSt	Lateral Stiffening
LVDT	Linear Variable Differential Transducer
lbs	Pounds

MAC	Modal Assurance Criterion
mm	millimetre
MHz	Megahertz
MPa	MegaPascal
MTO	Ministry of Transportation of Ontario
NDE	Non-destructive Evaluation
NDT	Non-destructive Testing
ODS	Operating Deflected Shapes
ODOT	Ohio Department of Transportation
OHBDC	Ontario Highway Bridge Design Code
OC	On Centres
PCI	Prestressed Concrete Institute
PS	Prestressing
Psi	Pounds per square inch
SHM	Structural Health Monitoring
TRRL	Transport and Road Research Laboratory
USD	Underslung diaphragm
VBI	Vibration Based Inspection

Symbols

A	Gross Area
A_k	Axial stiffness
A_i	Area of part "i"
A_s	Area of steel
b	Width
C	Channel
C_s	Coefficient for curing
@	At
d	Distance between the centroids of the part and the gross
E	Modulus of elasticity
E_c	Modulus of elasticity of concrete

E	Error matrix
F	Force
F_{MxNE}	M x NE Damage sensitivity matrix
f	Frequency
f_r	Modulus of rupture of concrete
f_c'	Compressive strength of concrete
G	Shear Modulus of elasticity
G	Strain Gauges
h	Height or depth
I	Gross moment of inertia
I_i	Moment of inertia of part "i"
$I_{strong\ axis}$	Moment of inertia about the strong axis
$I_{weak\ axis}$	Moment of inertia about the weak axis
J	Torsion Constant
K^d	Stiffness matrix of the damaged structure
K^u	Stiffness matrix of the undamaged structure
$K_{shell\ element}$	Axial stiffness of the shell element
k	Axial stiffness
L	Length
L	Cable Transducers
M	Number of eigenvalues
M_A	Moment at end A
M_B	Moment at end B
N	Number of nodes
n	Number of readings
n	Modular ratio
NE	Number of members (or member groups)
P_c	Factor for cement content
P_f	Factor for ratio of fine to total aggregate
P_h	Factor for relative humidity
P_r	Factor for volume surface ratio

P_s	Factor for slump of concrete
P_v	Factor for percentage of air
P_{sh}	Correction factor for conditions other than standard conditions
R	Reaction
RD_i	Relative change or damage in the ith mode shape
T	Tons
t	thickness
t	Time in days
W	Wide flange
w	Width
Z	M x 1 matrix containing fractional changes in Eigen values
α	NE x 1 matrix containing changes in stiffness between model & structure
ψ_x	Experimentally measured mode shape vector
ψ_A	Theoretically predicted mode shape vector
θ_d	Angle of rotation of the bridge deck
θ_s	Angle of rotation of the shear key
Δ	Deflection
Δ_i	Deflection of ith girder
Δ_{Total}	Total deflection measured by all the girders
$^\circ C$	Degree centigrade
γ	Density of material
λ	Modification factor for concrete density
$\mu\varepsilon$	microstrain
Ω	Ohms
$\varnothing^u_i$	ith mode shape function in the undamaged state
$\varnothing^d_i$	ith mode shape function in the damaged state
$\sum$	Summation of
ε_{sh}	Shrinkage strain
ε_{shu}	Ultimate shrinkage strain

1.0   INTRODUCTION

1.1 History and Evolution

The FC girder is an inverted U shaped precast prestressed concrete girder (Figure1.1). The first series of FC girder bridges were built in Alberta in the early and mid 1960's, by erecting the FC girders adjacent to each other and joining longitudinally, with the help of field grouted shear keys and erection bolts. A layer of asphalt is normally laid directly on top of the girders to provide the wearing surface. Hence the top flanges of these girders provide the bridge deck for the traffic. Figure 1.2 shows a cross section of a FC girder bridge.

The elimination of the field cast deck, because of the side-by-side precast girder bridge construction, brought several advantages. Both cost and time were reduced by eliminating the form-work for the bridge deck, the pace of work could accelerate with no time wasted in curing of wet concrete and work quality could be assured by factory produced girders. The procedure was also useful for remote areas with no access to ready-mix concrete plants.

The name initials FC are derived from the fact that the first FC girders were originally developed by Fenrich Concrete in Alberta, which then became Supercrete and eventually turned into Lafarge. The FC girders directly evolved from the family of the earlier reinforced concrete girders, extensively used in bridge structures in Alberta, like the type E and G girders, which were mainly used for shorter spans and first presented the idea of providing a road surface for direct traffic without the need of laying a separate deck. These simple reinforced concrete girders were succeeded by a family of prestressed precast concrete girders (FC, MC, etc.) when longer spans had to be constructed. The FC girders have also been called FM (Metric) and LF (with lightweight concrete) girders. These girders have been generally designed for HS20 loading whereas the ones designed for HS25 loading have been labelled as type VF girders.

1

The first FC Girder Bridge was built in Alberta in 1961 at Cardston, over St. Mary River. This was a three span bridge with span lengths of 30 metres each. Between 1960 and 1995, 178 bridges were built in the province of Alberta alone. The provinces of Saskatchewan and British Columbia have also used FC girders for medium and short span bridges.

Figure 1.3 shows the number of FC girder bridges built in Alberta plotted against a ten-year window. The plot demonstrates an increased interest in the construction of these bridges in the 1970s, after ten years of successful service of the bridges constructed in the 1960s. However, numerous field problems started appearing in the 1980s and the construction frequency of these bridges dropped significantly in the 1980s and 1990s.

1.2 The Field Problem

After providing ten to twenty years of service, some of these bridges started to form longitudinal cracks in the deck directly over the shear key locations. Once a crack was formed in the shear key, salt and water would penetrate the wearing surface and weaken the shear key grout. As the grout would weaken, the cracks would widen leading to an eventual failure of the shear keys and a loss of load sharing and composite action. Moreover, the absorption of de-icing salts through the concrete caused corrosion of the prestressing tendons and spalling of concrete. Alberta Transportation (AT) regular bridge inspections identified advanced deterioration in the shear keys in many bridges and significant gaps between adjacent girders were observed in some bridges. Figure 1.4 illustrates one such shear key crack.

Typically, individual girders are designed for a fraction of the actual concentrated live wheel load according to the lateral load distribution factors given by the Bridge Codes like AASHTO or OHBDC. However the lateral load distribution can be impaired by the failure of the shear keys with a result that the girders are subjected to higher live loads than what they were designed for. Even though leakage may be the major problem with these bridges, in extreme cases the keys may crack severely enough that the shear key

2

cannot distribute load to adjacent girders, causing an overstress condition in the loaded girder.

Initially it was thought that shear key cracking was isolated to very long span bridges but later it became apparent that the problem was generally present in bridges of all spans and sizes. There has been some discussion on the causes of shear key cracking in FC girder bridges, though no experimental investigation has taken place so far. Some researchers have indicated that thermal effects are really what crack the shear key grout. Once the crack has formed, it grows progressively with loading and fatigue. Figure 1.5 shows an exaggerated view of the bridge transverse bending. It can be easily seen that such a situation can occur with bridge vibrations under moving traffic, thus producing distress in the grouted shear keys. Even though the objective of this research was not to study the causes of shear key failure, it is never the less useful to have some insight on it.

Shear key based bridge systems have been used extensively for short and medium span bridges in the United States, Canada, Japan and many other countries all around the world. These bridges have been built in a variety of different shapes, ranging from the channel sections, to the box sections and the single and double tee sections (Figure 1.6). The concrete box girder shape basically evolved from the channel section where a bottom flange was added to impart torsional rigidity to the channel section. However, all the shear key based systems have reported problems with shear key cracking and deterioration. Compared with other types of bridge systems, these bridges have showed highest deficiency percentages. According to the Alberta Transportation bridge maintenance records, the rehabilitation of FC girder bridges consumes a large share of their annual maintenance budgets.

1.3 Rehabilitation Techniques Used

Most of the remedial measures initially applied by the "Alberta Transportation and Utilities" (AT&U), now called the Alberta Transportation, were based on visual site inspections and previous experiences. The initial repair schemes mainly focussed on the malfunctioning of connector bolts. A thorough inspection routine on the existing bridges

3

showed that the bolts were often improperly grouted, loose or even sometimes missing. Variations of improving the grouted connection were attempted but after receiving only partial success from these improvements the main focus shifted towards lateral stressing and transverse stiffening of the system.

In 1980, a six span FC girder bridge at Whitecourt over Athabasca River was rehabilitated by lateral post tensioning, using 25.4 mm diameter Dywidag bars on each side of each diaphragm in combination with a high density concrete overlay placed over the girders. This system was not suitable for skewed bridges and involved some degree of difficulty in drilling through the girder webs to place the Dywidag bars. Some bridges were rehabilitated, in the following years, by improving the connections between the girders. The conventional bolts were replaced by high tension Super bolts and lightweight Foam Crete was filled in the space between the girders. All these efforts were made to strengthen the connections and generate adequate shear transfer between the girders.

Most of the rehabilitation schemes that followed were some variation or combination of lateral stressing of the system and shear transfer between the girders. Lateral strengthening of FC girder bridges was first accomplished by super bolts, then by short and staggered Dywidag bars and finally by using prestressing strands. Later it was felt that a transverse diaphragm was needed in addition to the lateral stressing system to increase the torsional rigidity of the bridge transverse cross section and to better distribute the load among the girders. In some bridges, a concrete deck was also added on top of the girders to further facilitate load sharing among all the components of the bridge.

1.4 Need for research

The response to any single rehabilitation scheme has not been very encouraging. Most of the rehabilitation techniques have been somewhat successful in improving the load sharing between the girders but the reappearance of longitudinal cracks in the bridge deck, after some years, indicates persistent movement at shear key locations. Deck

4

cracking may be a serviceability concern, but may turn into a strength concern with age if it results in corroding tendons and steel.

Different rehabilitation schemes, their variations and combinations have been used from around 1979 to date, but a thorough comparative analysis of the performance of optimum arrangements of these rehabilitation schemes, has not been conducted. Improvements and modifications were refined over the years, based on response to previous schemes. However, consistent success has not been achieved for any one scheme because of the lack of a broad available knowledge base on the analysis of these rehabilitation schemes and their influence on the performance of the bridges. The role of many factors in affecting the behaviour of these bridges as in any real life structure; make it a complex problem to handle.

The behaviour resulting from a combination of rehabilitation schemes is even harder to assess and analyze, based on visual inspections of results, because it may be complicated to isolate the effect coming from each of the components of the rehabilitation scheme, separately. Besides, the assumptions going into such a break down of the analysis may sometimes be wrong because the behaviour of the real structure is at times heavily governed by factors not considered in our analysis. An extensive study to understand the behaviour of the FC girder bridges is yet to be done and hence this significant portion of the Alberta infrastructure stands at risk, in the years to come.

1.5 Objectives and Scope

The primary objective of this research was to extensively study the behaviour of the FC girder bridges and suggest an effective and generic rehabilitation scheme for its field problem. The main objective can be split into three sub objectives:

- Understanding the behaviour of FC Girder Bridges under vehicular loads;
- Assessing the performance of the existing rehabilitation schemes;
- Recommending the best possible rehabilitation schemes for existing FC girder bridges.

5

To address some of the concerns mentioned earlier, real life bridges were monitored for strains, deflections and vibration characteristics. Based on the field data from these bridges, a finite element model was prepared and validated with the help of the field measurements. The validated model was then used for parametric studies for the assessment of the existing rehabilitation schemes, their variations and combinations.

A physical inspection survey was also conducted on 38 FC girder bridges in Alberta, which constitutes 21% of the total number of FC girder bridges in Alberta, and the current response of the bridges to various rehabilitation schemes was noted to assess the performance of the different schemes.

The thesis, in the end, proposes a rehabilitation scheme, which is best suited to be applied on FC Girder Bridges of all spans and widths and provides Alberta Transportation the required knowledge base to use the rehabilitation scheme on these bridges with full confidence.

1.6 Lay out of Thesis

The thesis has been laid out in paper format, in accordance with the "Faculty of Graduate Studies and Research (FGSR) Manual of Regulations and Guidelines for Thesis Preparation". Each chapter has its own introduction and bibliography. However, the first "Introduction" chapter and the last "Conclusion" chapter are relevant to the whole thesis. Figures for each chapter have been grouped together at the end of each chapter; however the tables are arranged within the text and are placed close to their reference. References have been shown as superscript numerals wherever they need to be quoted. Portions of this work, which have been published or are intended to be published, have been marked with an asterisk with a footnote giving the reference on that page. The following list illustrates an overview of the thesis and the arrangement of the different chapters.

6

Chapter 1: Introduction to the Thesis

Chapter 2: Provides a summary of the current state of knowledge in this area and discusses similar concerns with other shear key based bridge systems.

Chapter 3: Describes the current state of FC girder bridges in the province of Alberta by compiling a physical and statistical database survey of all FC girder bridges and studying the impact of certain parameters on the performance of these bridges.

Chapter 4: Provides a methodology review by scanning the available published literature on load and vibration testing of highway bridges.

Chapter 5: Includes a comprehensive case study on the field-testing and instrumentation of the FC Girder Bridge rehabilitation in Fort Saskatchewan, Alberta.

Chapter 6: Shows the formation of a three-dimensional finite element model, which is able to predict the behaviour of the FC Girder Bridge, in Fort Saskatchewan, Alberta, when subjected to field testing, and comments on the performance of the rehabilitation schemes used on that bridge.

Chapter 7: Shows results from the Ambient Vibration Test conducted on a number of FC girder bridges and the comparison with their respective finite element model results.

Chapter 8: Constitutes a performance comparison study of the different rehabilitation schemes used on the finite element model.

Chapter 9: Provides the Summary and Conclusions.

7

A typical FC girder
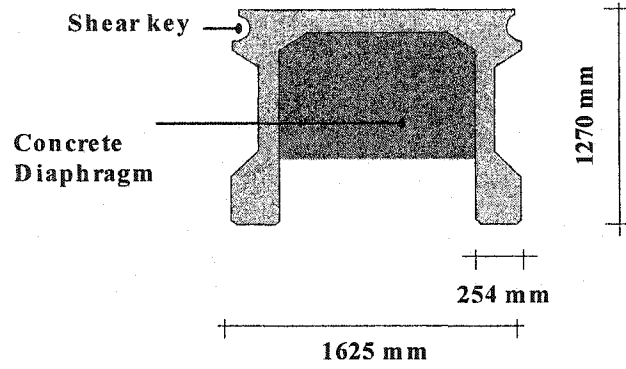
Fig. 1.1: Cross section of a FC Girder
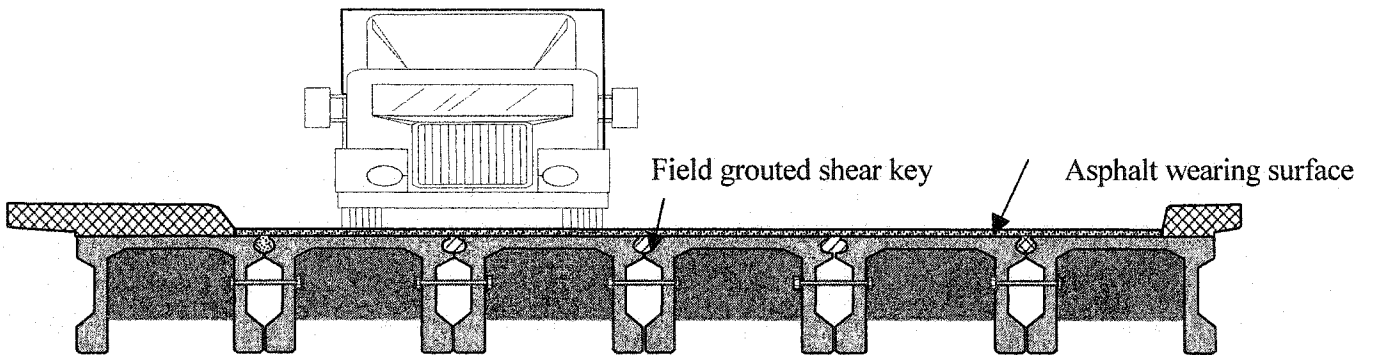
Fig 1.2: Cross Section of a FC girder bridge

8

Total Number of existing FC Girder Bridges = 180
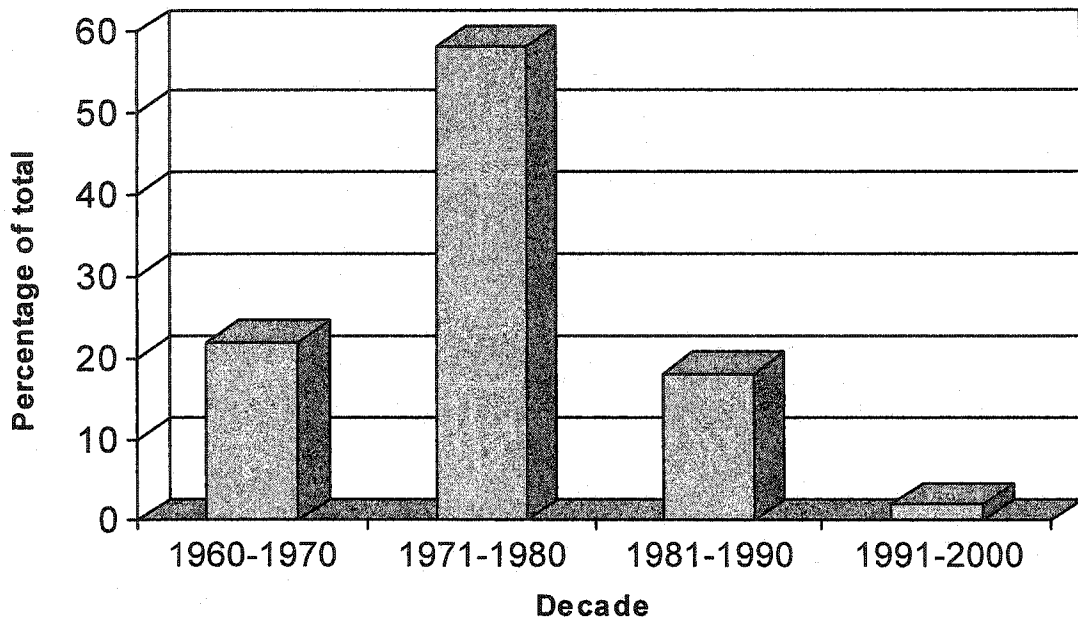
Fig. 1.3: A break up of FC girder bridges constructed in different years
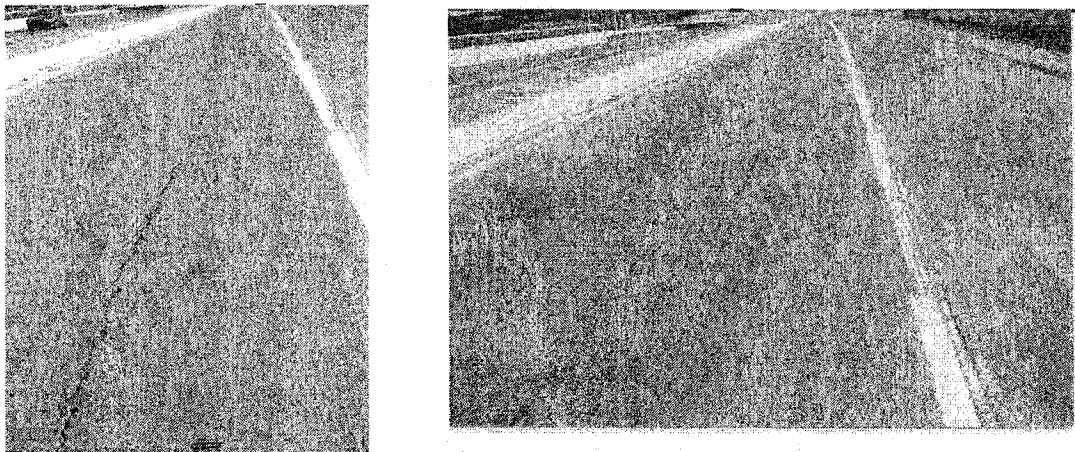
Fig. 1.4: Significant cracking over shear keys

9
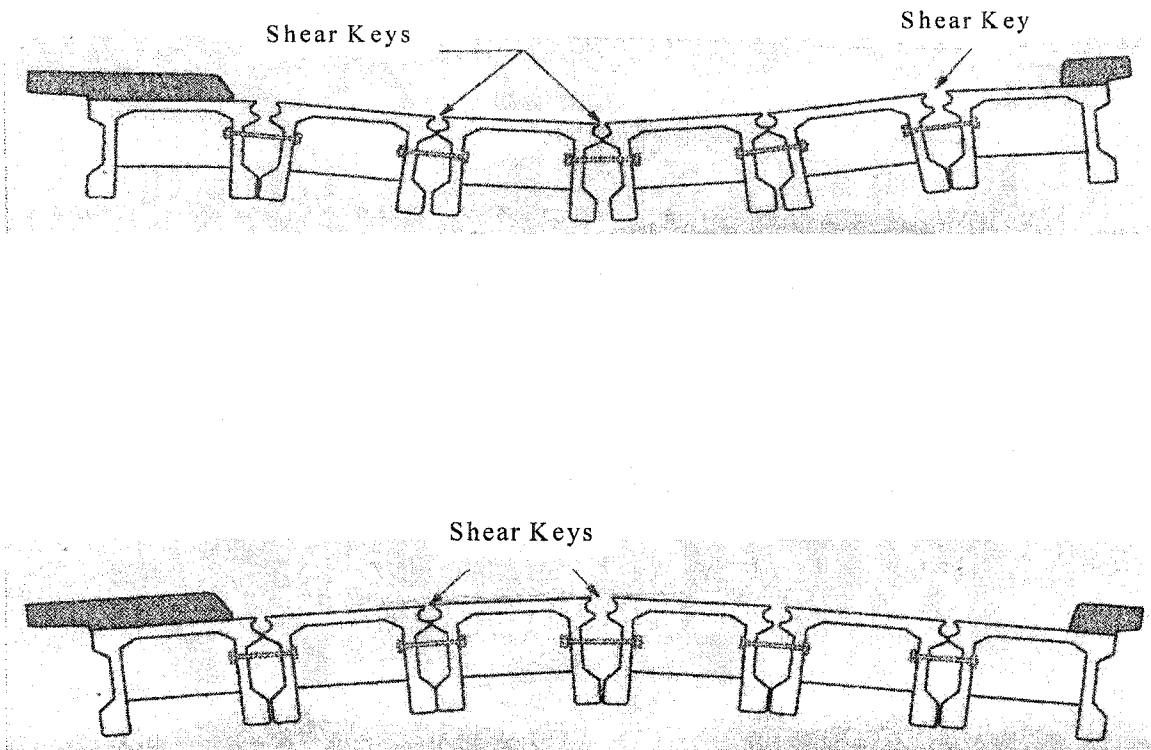
Fig. 1.5: Transverse deflected shape of the bridge under vibration

Precast concrete channel sections
joined by field grouted shear keys
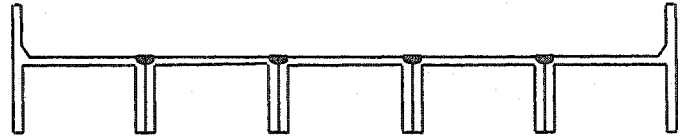
Channel shaped girders with field
cast shear keys and concrete deck
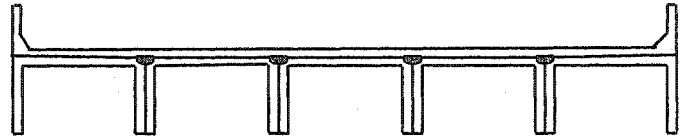
Precast concrete box girders with
field grouted shear keys
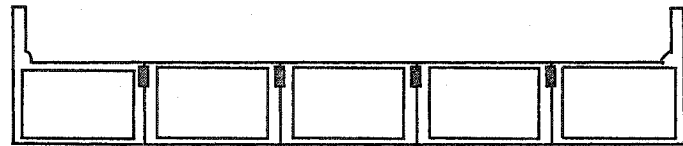
Precast concrete box girders with
field cast shear keys and concrete
deck
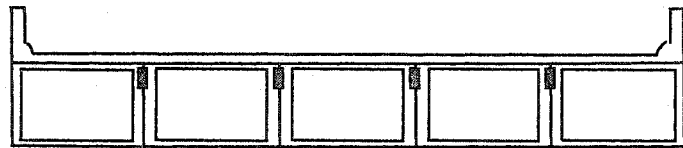
Precast concrete Tee sections
with shear keys
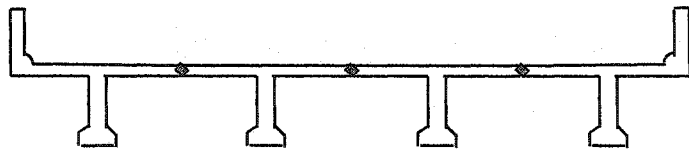
Precast concrete double tee
sections with shear keys
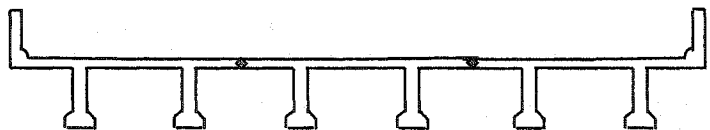
Fig. 1.6: Cross sections of various types of shear key based bridge systems

11

2.0 PERFORMANCE OF SHEAR KEY BRIDGE SYSTEMS: A LITERATURE REVIEW

2.1 Introduction

Shear key based bridge systems have been used all around the world in different forms and shapes. Major advantages gained due to convenience and portability made these systems very popular for medium and short span bridges. However, rehabilitation needs plagued these bridges after some years of service. The quality assurance of plant produced girders was offset by deterioration of the field grouted shear keys.

Frequent problems with shear keys led researchers to investigate the causes and suggest remedies. It was observed that shear keys deteriorated regardless of the shape and size of the girder cross section. For example, even though the behaviour of a box girder bridge may be different from a channel-shaped girder bridge, damage always occurred in the form of longitudinal cracking at shear key locations.

In some cases, prototype models were prepared and tested in the laboratory whereas in other cases, conclusions were drawn from field inspection and monitoring of these bridges. While laboratory testing has its own merits, generally it is also important to investigate the bridge in its real working condition under real time traffic. This is made possible and easy now with the help of fast computers, reasonably accurate instruments and portable data acquisition systems, which can be easily carried to site.

Based on geometrical information of the bridge, a finite element model of the structure can be prepared and calibrated with field results. This refined model, which can now predict the true behaviour of the bridge, may be used for investigating the performance of various rehabilitation schemes, which can be applied to the bridge. Presently the bridge codes do not give specific guidelines for selecting deficient bridges for rehabilitation. Most departments of transportation prepare their own criteria for each particular case, which are usually heavily dependent on visual site inspections. The Alberta Transportation (AT) observes the benefit cost ratio of using a particular rehabilitation scheme, which is dictated by the life cycle cost analysis of the bridge.

12

2.2 Concrete Multi-girder Bridges

Bakht, et al.[1] have shown that the field grouted shear keys provide some transverse flexural rigidity but the load transfer from one beam to another takes place mainly by transverse shear. The common tools of analysis and design like the AASHTO[2] Bridge Code and the Ontario Bridge Code (OHBDC)[3] do not provide information on this structural response and hence shear keys are generally designed by previously established empirical methods. This approach does not allow the designer to assess the margin of safety in the design. The authors have presented a simplified method, for evaluating the transverse shear intensity in the shear keys, by calculating a dimensionless characterizing parameter from the bridge properties, and reading governing intensities of transverse shear from the provided charts.

2.2.1 Grouting issues with shear keys

Gulyas, et al.[4] have reported that strict quality control goes into the production of the precast girders as well as the prestressing strands, but unfortunately a second class treatment is often given to the shear key grouts, which are intended to provide effective long term vertical shear transfer between adjacent members. Therefore the grout frequently becomes the weak link in the system. Generally, the keyways are filled with different types of non-shrink grouts, which do not have prescribed requirements for maximum shrinkage limits or minimum bond strength. Both properties are critical for effective load transfer. A laboratory study was undertaken to compare component material tests and composite grouted keyway specimens using two different grouting materials: non-shrink grouts and magnesium ammonium phosphate mortars. Comparative composite specimens were tested in vertical shear, longitudinal shear and direct tension. Results indicate significant differences in performance between the materials. Composite testing of grouted keyway assemblies, rather than component materials testing was shown to be a more accurate way to evaluate the performance of the grouting material. Based on the findings in this paper resulting from field, laboratory and other investigative sources, magnesium ammonium phosphate ($Mg-NH_4-PO_4$) mortars show good properties, have lower drying shrinkage rates, significantly lower chloride absorption and can be successfully used in field applications for keyway grouting.

Nottingham[5] has attributed grouted joint problems to three key issues. Weak grout, poor joint details and inconsistent grouting procedures. Grout specifications in the earlier Alaskan designs for bridges and dock decks were not thorough enough and left much to the expertise of the construction contractor. A sample specification according to Nottingham might read, "When the plans provide for keyways between adjacent concrete members to be filled with grout, the grout shall consist by volume of one part Portland cement, three parts clean concrete sand, and minimum water necessary for placement. The grout shall be thoroughly mixed, before placement, until a uniform consistency is obtained." The very nature of Portland cement grouts, virtually assure some shrinkage cracks in grout joints, regardless of quality control. Some high quality Portland cement concrete was tried as joint grout with better success, but shrinkage cracks, although moderate, were still common. Often overlooked, precast element tolerance can lead to improper joint fit and incomplete grouting hence sometimes joints may not reach full strength and can be much weaker than envisioned by the designer. Nottingham indicated that a high quality, low shrinkage, impermeable, high bond, high early strength grout with low temperature curing ability was needed and to date, the closest material to meeting these requirements has been prepackaged magnesium ammonium phosphate based grout often extended with pea gravel.

2.2.2 Effects of size, shape and position of the shear keys

Issa et al.[6] conducted an extensive survey to study the field performance of full depth precast concrete panels in bridge decks and have commented that the size and shape of the shear keys have an obvious impact on their long term performance. They also concluded that post tensioning across the grouted joints was necessary to secure the tightness of the joints, guard against leakage and to keep the joints in compression.

Huckelbridge et al.[7] did a series of field tests to study the performance of the grouted shear keys in prestressed concrete multi-girder bridges. Response in the form of relative inter-girder displacements and flexural strains in the girders was recorded during passages of the test vehicle. All of the tests (even the post repair structure) exhibited relative displacements across some joints that would be indicative of fractured shear

14

keys. In the test program, relative displacements between 0.08 and 0.5 mm were observed at joints that must be presumed to have at least partially fractured shear keys. However, the largest observed live load strain for a test vehicle weighing approximately 214 kN was less than 30 µε, indicating substantial reserve capacity in the bridge despite the damaged joints.

In the tested structures, these fractured keys were generally limited to those joints in closest proximity to the normal wheel positions, in the driving lane most often used by heavy truck traffic. The joints that exhibit the largest relative deflections are also adjacent to the normal wheel positions and hence are subjected to more intense shear transfer requirements. Joints that exhibited obvious outward signs of distress (leakage of water, or reflective cracking in the deck above the joint) always indicated relatively large intergirder deflections. The actual length of the fracture, stiffness of the girders, and magnitude and proximity of the wheel load to the fractured joint were the parameters that affected the magnitude of relative displacement.

Esnawi[8] conducted an extensive study to evaluate the problem of shear key failure in prestressed concrete box girder bridges and to propose a new shear key design. Using a finite element analysis, he suggested that shear key failure probably occurs due to tensile stresses, from negative transverse moment in the top flange of the bridge. These stresses arise due to continuity provided by the shear key in its current top location. Esnawi looked at various remedial solutions including the transverse post tensioning of the system. It was observed that for the transverse post-tensioning to be fully effective, the scheme had to be applied at such close intervals that most of the economic attractiveness of this design would be sacrificed. Esnawi proposed the shear key to be placed at a new location i.e. at the neutral axis. This hypothesis was put to test in the laboratory and succeeded in both static and fatigue tests. Static load capacity increased three times while the fatigue life of the new shear key design was extended to over 8,000,000 cycles. All modifications were done keeping the same non-shrink grout material for the shear keys, as used previously in the current designs. The vertical passage above the shear key was

filled with foam filler and the top sealed with a joint sealant. This girder assembly would now be ready to take a wearing course of bituminous material.

In reviewing the practices in other countries, it was found that cases of longitudinal cracking are seldom reported in Japanese adjacent prestressed concrete girder bridges. Yamane et al.[9] has shown that cross sectional shapes and design criteria for prestressed girders in Japan are similar to those in the United States, except for size and shape of the longitudinal joint between the girders and the amount of transverse post-tensioning. I.E. the shear keys are placed in relatively wide and deep joints between the girders and higher levels of post-tensioning are used. Moreover, most bridges in Japan do not use cast in place structural slabs in composite action with the girders, though a wearing surface is required on all bridge decks. Figures 2.1 to 2.3 illustrate the cross sectional shapes commonly used in Japan whereas Figures 2.4 and 2.5 shows a comparison of the American and Japanese cross sectional box girder bridge shapes.

El-Remaily, et al.[10] have reported that precast multi-girder bridges in the United States, as compared with other types of prestressed concrete highway bridges, have the highest deficiency percentages. The problem of reflective cracking is due to insufficient consideration of the structural behaviour of a bridge. Both shear and bending must be transferred at the transverse joint between girders in order to control both translational and rotational deformations. Some states use a combination of heavy structurally composite topping and a large amount of transverse post tensioning. Composite topping is not a structurally efficient solution because it does not control differential rotation of the box, nor is it an economical solution. While comparing American and Japanese design and construction practices El- Remaily et al. attribute shear key problems to insufficient connection between the girders which give rise to transverse moments inducing tensile stresses and longitudinal hinging along the shear keys. Transverse restraint at the top and bottom can eliminate the longitudinal hinging, hence distributing the load across the entire cross section and giving rise to a stiffer system in the transverse direction. El-Remaily has proposed a design methodology that combines the performance requirements for a Japanese bridge with the simplicity of American construction

16

practices. The proposed design involves provision of post-tensioned transverse diaphragms at quarter points of the bridge span. The diaphragms would be made continuous in the space between the boxes through deep blockouts filled with grout. Post tensioning is provided, based on bridge width and loading, assuming the bridge consists of an assembly of rigidly connected stringers and diaphragms.

Martin and Osborn[11] have also indicated that shear and bending must both be transferred at the joints of adjacent girders to limit translational as well as rotational deformations. Often girder joints cannot transmit transverse moments and hence act like hinges, only transferring vertical loads across the joints by shear.

In the state of New York, 219 adjacent precast concrete box beam bridges were built during 1985 to 1990[12]. An adjacent girder precast box beam bridge in the state of New York is composed of precast beams connected by 12 in. deep grouted keyways to transfer shear forces along the structure. After the grout hardens, the beams are transversely post tensioned and a composite, cast in place deck is poured over them with stirrups projecting from the beams into the deck overlay. Lall et al.[12] undertook a study in 1990 to investigate causes of longitudinal shear key cracking and suggest remedies. The 1990 study showed that 54 percent of these bridges had developed longitudinal cracks over the shear keys. Based on a survey of construction practices in other states two of the suggested changes were adopted in the New York's design standards in 1992. These consisted of increasing the depth of the shear keys to almost the full depth of the box beams and increasing the number of transverse tendons to three for span lengths less than 50 ft. and to five for longer spans. 91 bridges were built between 1993 to 1995 in the short to medium span range and a follow up study was organized in 1996 to determine the effectiveness of the new full depth shear key/ transverse tendon system. Survey responses were analyzed and the results showed that shear key related longitudinal cracking was found on 21 bridges (out of 91) or 23 percent of the sample. This shows that the shear key cracking had been reduced significantly.

17

Lall et al. reported that the frequency of shear key cracking appeared unrelated to maximum span length or total bridge length. Bridges with higher annual average daily traffic (AADT) appeared to be more susceptible to shear key related cracking. Those with AADTs of 5000 or more exhibited more cracking than those with AADT values less than 5000. Based on literature search, site visits and consultation with bridge designers Lall et al. proposed changes to the shear key shape and size, increased reinforcement in concrete overlays and a greater post tensioning force in the transverse post tensioning system.

Badie et al.[13] have described the longitudinal cracking of the shear keys as a result of the large torsional stiffness of the box shape girders and the lack of adequate transverse connection to transfer forces between the boxes. Commenting on the solution of a transverse diaphragm and post tensioning system by El-Remaily, Badie et al. have raised the question of a doubtful cost benefit ratio. To cut down on cost and to reduce the number of pieces required for shipping and handling and erecting the multi-beam bridge, Badie et al. have proposed a trapezoidal box section of such girders. By making comparisons with the existing shapes, the authors claim that the new cross section is structurally more efficient, cost effective, aesthetically pleasing and less prone to maintenance problems.

A recent survey by the PCI Bridge Committee[14] showed that adjacent precast, prestressed box girder bridges are used in at least 30 states throughout the United States. The open channel design with shear keys in the top flange, used to transfer the load between the adjacent girders, gave rise to the closed box girder design. As the vertical load gets transferred by shear at the joints, it has to be carried across the member to the next joint by torsion. Since open sections are flexible in torsion, a bottom flange is added to the open channel to create a box girder with a higher torsional rigidity.

2.2.3 Influence of temperature on shear key cracking

Miller et al.[14] conducted full scale testing of the shear keys at the University of Cincinnati. Three tests were carried out. The first test used the standard non-shrink grout and the top shear key (i.e. 150 mm from the top), the second test used the mid depth shear

key (i.e. 300 mm from the top) with the standard non-shrink grout and the third test used the top shear key with the epoxy grout. Diaphragms and transverse tie rods were provided as required by Ohio DOT specifications. No appreciable transverse post tensioning was provided and four hydraulic actuators (each applying 44.5 KN) were used to load the bridge, in pairs of two, at the midspan of each of the interior beams.

Miller et al. observed that the first cracking in the shear keys, even before the application of any load, was caused by temperature stresses. Cracks in the keyways were detected using ultrasonic pulse velocity method. It was seen that temperature effects caused thermal strains and deflections, which were large enough to crack the shear keys. Transverse omega clip gauges placed across the joints showed maximum transverse tensile strains of more than 300 $\mu\varepsilon$ at top of the shear key, due to thermal stresses. This is enough to crack the shear keys. Thus it appears that the shear keys crack almost immediately due to temperature effects. After the girders were loaded, it was observed that initial cracks caused by temperature propagated during loading and that loading did not cause new cracks.

On a second trial it was seen that the shear keys also cracked due to the temperature gradient about the ambient temperature in a normal day. During daytime, heat from the sun causes the upper part of the girders and deck to deflect up whereas night time brings cooling to the same, hence causing a downward deflection. These temperature-induced movements cause the girders to rotate about their axes, opening and closing the shear key joints. Figure 2.6 shows the movement of the girders due to temperature changes. The authors describe the shear keys to be acting like hinges, about which the beams rotate with each temperature cycle. Since the area above the key is grouted and hence restrained against movements, it accumulates stresses, which eventually crack the grout.

With the epoxy shear key tests, no cracking was found. Thus, epoxy shear keys had superior performance against cracking. However the authors warn against potential problems with using epoxy shear keys. Firstly, epoxy has a coefficient of thermal expansion, which is three times that of concrete. This may cause temperature induced

19

cracking if there were a wide variation in ambient temperatures. Secondly, it was observed that it was very difficult to fail the epoxy shear keys, but when they did fail, the failure occurred through the concrete, which could be an undesirable failure mode.

2.3 Concrete Channel Shaped Girder Bridges (FC Girder Bridges)

There are close to 200 FC girder bridges in the province of Alberta alone. The provinces of Saskatchewan and British Columbia have also used FC girder bridges and other shear key based bridge systems. Rehabilitation needs of many of these bridges due to shear key cracking led the Alberta Transportation in 1995, to initiate finite element studies, aimed at a better understanding of the cracking problem.

Serink and Hrudey[15] have given an account of the damage and deterioration in FC girder bridges in the province of Alberta, due to shear key cracking, and a historical review of the different rehabilitation schemes tried to date. The authors carried out a finite element study of FC girder bridges to simulate the crack causing mechanism and evaluate the performance of various rehabilitation schemes as well as experiment with new remedial measures. The parameter chosen to assess the relative performance of each rehabilitation scheme was the relative rotation about a longitudinal axis, between the top corners of adjacent girders. This parameter was very sensitive to many of the variables tested and directly related to the shear key curvature. Relative rotations of the model were plotted against the longitudinal distance of the bridge and it was noticed that peak values of relative rotation occurred at diaphragm locations. The differential rotations in the shear keys on both the straight and skewed bridges at diaphragm locations were three to five times as high as they were midway between the diaphragms. This phenomena was explained as follows:

"At regions away from the diaphragms, the girder legs were observed to open outward as a result of curvature in the top flange. However, at the diaphragms the girder legs and the top flange are constrained and the positive curvature due to dishing is concentrated at the shear keys." This effect is illustrated in Figure 2.7. Based on this observation, it was suggested that cracking of the shear keys initiated at diaphragm locations.

20

The authors suggested that there were three options available for preventing the shear keys from cracking: increase the capacity of the shear keys to absorb the rotations through prestressing or more flexible materials, reduce the global deformations by increasing the transverse rigidity, or force more of the global dishing into the deck by increasing the relative stiffness of the shear keys and removing the diaphragms. The following synthesis was reached after exploring four rehabilitation alternatives:

- Lateral post-tensioning is most effective when placed in individual strands at deck level;
- Lateral post-tensioning also increases the capacity of the shear keys;
- The retrofit stirrups and underslung diaphragms are effective in reducing differential rotations. They are not, however as effective as the single strand prestressing and do not contribute to the strength of the shear keys;
- Skewed bridges require sufficient lateral post-tensioning in the end zones to compensate for the tension stresses which cannot be significantly reduced or eliminated.

Serink and Hrudey concluded that the optimum solution to rehabilitate these bridges was through a system consisting of closely spaced strands at deck level and continuous transverse underslung channel diaphragms at the concrete diaphragm locations. The effectiveness of this scheme in arresting the problem of shear key cracking was based on how well it reduced the relative rotations between the girders. However it was noticed that all rehabilitation methods tried were less effective on skewed bridges than on straight bridges. This may be because differential rotations in the shear keys on skewed bridges are heavily influenced by the twisting caused by the skewed support.

Reid Crowther & Partners Ltd.[16] prepared a finite element analysis report for the design of rehabilitation for five bridges. Four primary categories of deformational and stress analysis results were assembled and evaluated during the finite element study.

21

The main objective of this study was to accurately assess the rotational response of the girder connection (shear keys) zones to vehicular loading effects. Relative rotation of adjacent units was taken as the governing criteria in selecting rehabilitation schemes. The best retrofit type for these bridges was expected to reduce the tendency of adjacent girders to rotate relative to each other. It was also mentioned that the relative rotation of the adjacent girders contributed to longitudinal cracking of the wearing course, which led to the deterioration of the bridge deck and girder elements because of water and chloride absorption through these cracks. It was felt that shear transfer between the adjacent girders was adequate and no retrofit to improve the load sharing was generally required.

Based on their finite element study, Reid Crowther & Partners Ltd. suggested a rehabilitation scheme consisting of a combination of the underslung diaphragms and a bonded composite concrete overlay. It was stated that a reduction of 50% in bridge flexibility was predicted by the provision of the underslung diaphragms whereas a reduction of 30% was made possible by the use of concrete overlay. The percentages showing reduction in bridge flexibility were calculated from the measured magnitudes of the shear key rotations. However, the authors indicate that this decrease in flexibility is only possible if the flexural stiffness of the shear key zones is the same as that of the uncracked composite overlay deck system. To ensure this behaviour, lateral precompression of the deck is recommended by providing prestressing at the deck level.

Azarnejad et al.[17] from CH2M Gore & Storrie Ltd. conducted a finite element analysis for the rehabilitation of Lawrence River Bridge. Constructed in 1974, this bridge had three spans and consisted of six adjacent FC type girders. A stress analysis was performed on a three dimensional finite element model using the solid element as the main building block and it was shown that high tensile stresses existed at shear key locations, for the case of bridge loading by a truck on one side. This would happen as a result of negative transverse bending in the other lane. It was thought that these tensile stresses could easily crack the shear keys. In a report[18] for the Alberta Transportation, CH2M Gore & Storrie Limited indicated that the normal transverse tensile stresses produced in the shear keys as a result of truck loading were in the range of 3.5 MPa

which was about the same as the tensile strength of concrete. Hence, stresses occurring from heavy vehicular traffic were sufficient to crack the shear key grout. In positive bending, the transverse tensile stresses occurred at the bottom of the shear keys whereas in negative bending they occurred at the top of the shear keys. The high tensile stresses occurring at the bottom of the shear key under positive transverse deck bending could produce vertical cracks, which will close after the load passes. However, repeated loading or the effects of loading on other parts of the bridge could cause permanent cracking through the shear keys.

As noticed in earlier studies, these stresses had sharp peaks at the diaphragm locations. The explanation given for this effect was that the diaphragms imparted a higher transverse rigidity to the girder and hence tensile stresses will get concentrated at the shear key locations.

Based on the results of their finite element analysis, the authors recommended that the addition of a concrete overlay slab provided the greatest strengthening effect for FC girder bridges. When a 100 mm overlay slab was added, the extent and level of tensile stress concentrations were reduced considerably. Tension stresses of around 1.5 MPa were observed after the concrete deck was placed and this stress level was comfortably within the tensile strength of a silica fume fibre reinforced concrete deck of 5 MPa. Some joint reinforcement to minimize or arrest cracks along joint lines was also advised. From variations in the model, it was shown that the addition of a 100 mm concrete overlay slab reduced the tensile stresses by almost 70%, whereas the provision of steel boots, to connect the adjacent girder legs at diaphragm locations provided a further strengthening effect of 10 to 15%. Deck post tensioning was thought to be contributing 15 to 30% to the overall strengthening. However it was mentioned that post tensioning might cause tensile stresses at the joint, if the shear keys were deteriorated.

23

2.4 Conclusions

An apparent deficiency with most of the finite element studies mentioned above is that they do not have any test data to validate their numerical models. For example the overall stiffness of the concrete overlay has field limitations because of shrinkage and temperature effects. Composite topping is not a structurally efficient solution because it does not control differential rotation of the girders, nor is it an economical solution. In the case of a non-composite topping, as is used in most FC Girder Bridges, the slab girder bond can be highly variable which casts a shadow of doubt on the overall stiffness of the system. Prestressing losses with time are obviously the worst enemy of any prestressing system, which again raise questions of the long-term reliability of any rehabilitation system. And finally the behaviour simulation through simplified models can be misleading, unless those simple models have been calibrated and validated with test data. Such concerns point towards the necessity of a periodic or continuous monitoring system which will collect periodic or continuous data and provide the opportunity to collect a time history for observing changes in behavioural characteristics of the bridges.

24

Figures
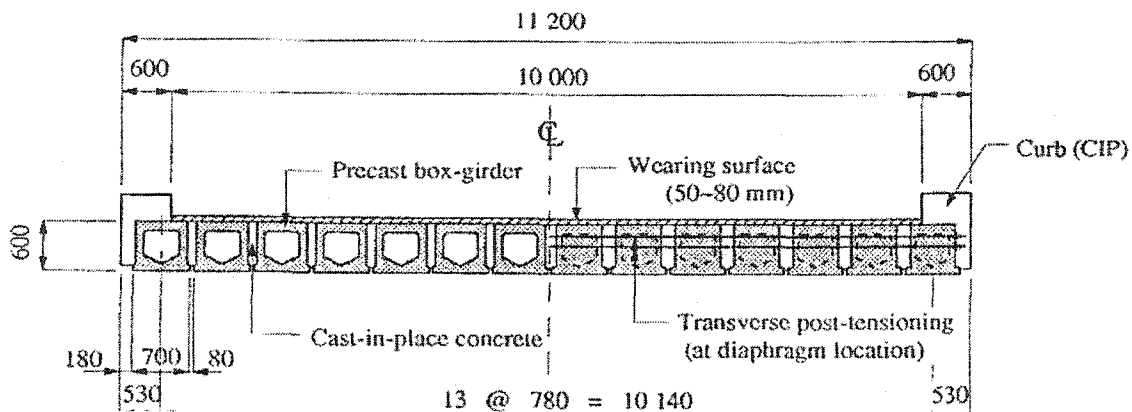
Fig. 2.1[7]: Cross Section of Box Girder Bridges used for short spans in Japan
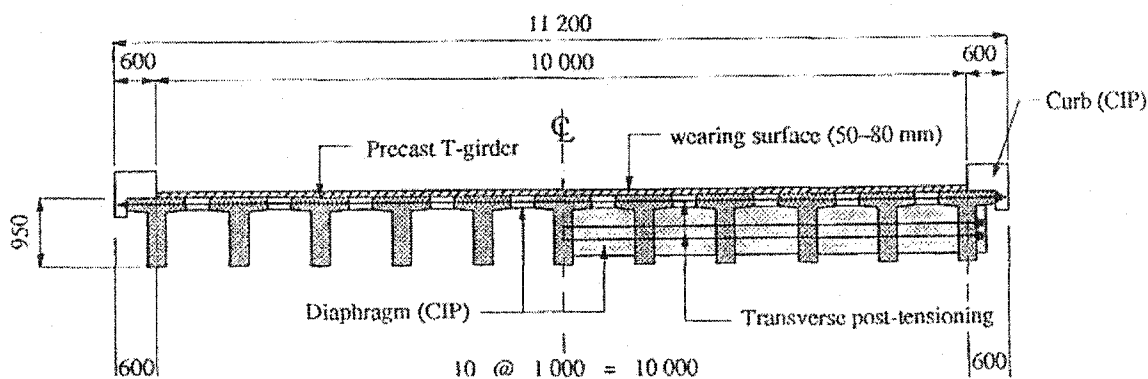
Fig. 2.2[7]: Cross Section of T Girder Bridges used for short spans in Japan
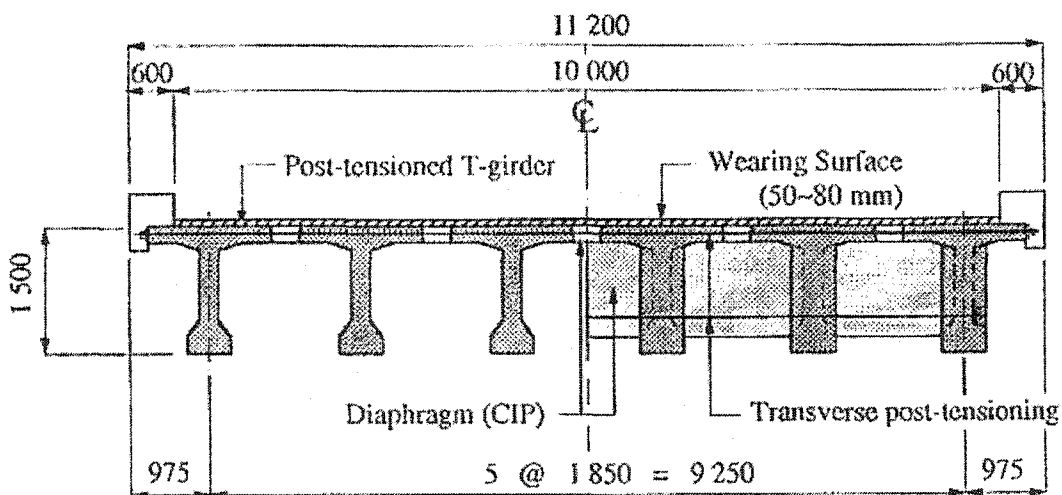
Fig. 2.3[7]: Cross Section of T Girder Bridges used for medium spans in Japan

25
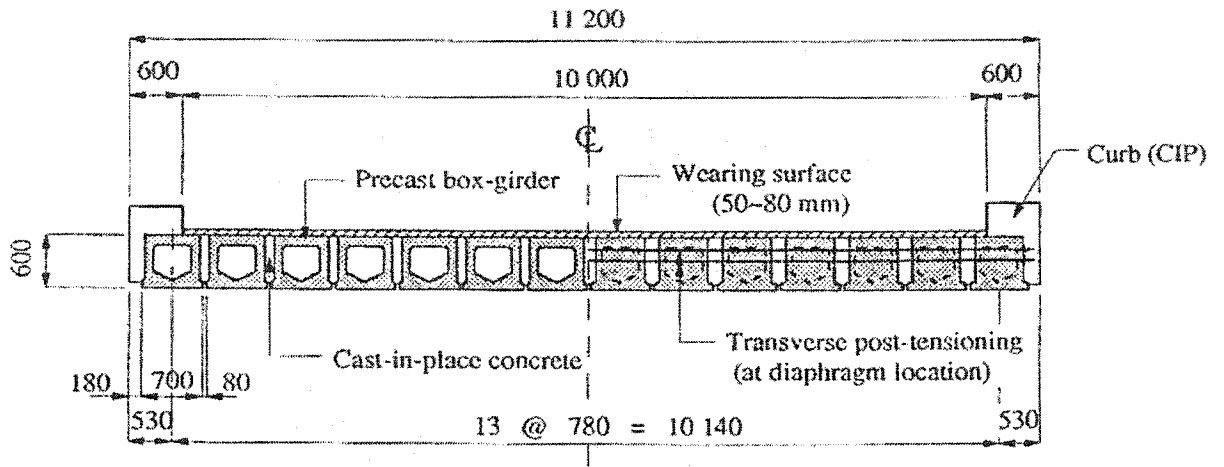
Fig. 2.4[8]: Box girder bridge in Japan
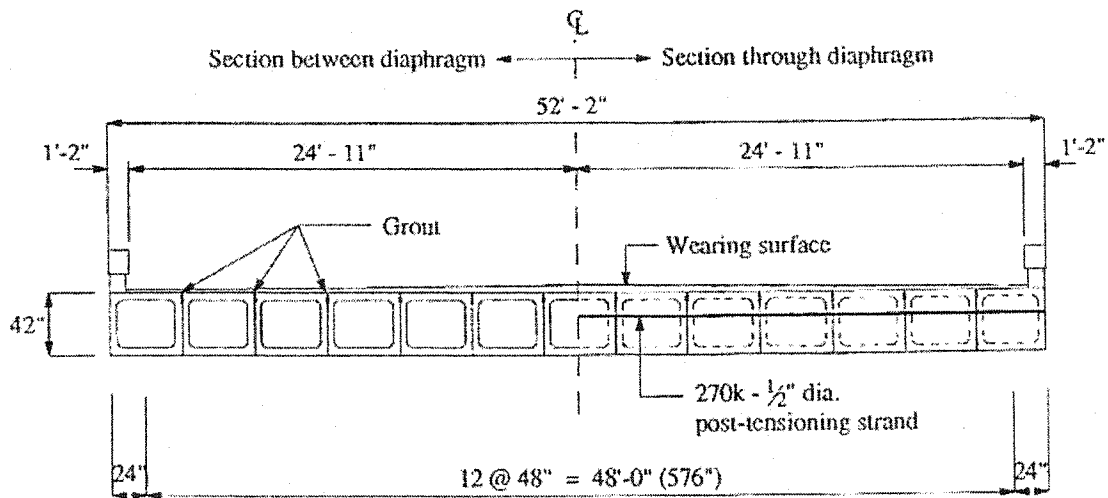
Fig. 2.5[8]: Box girder bridge in the United States

26
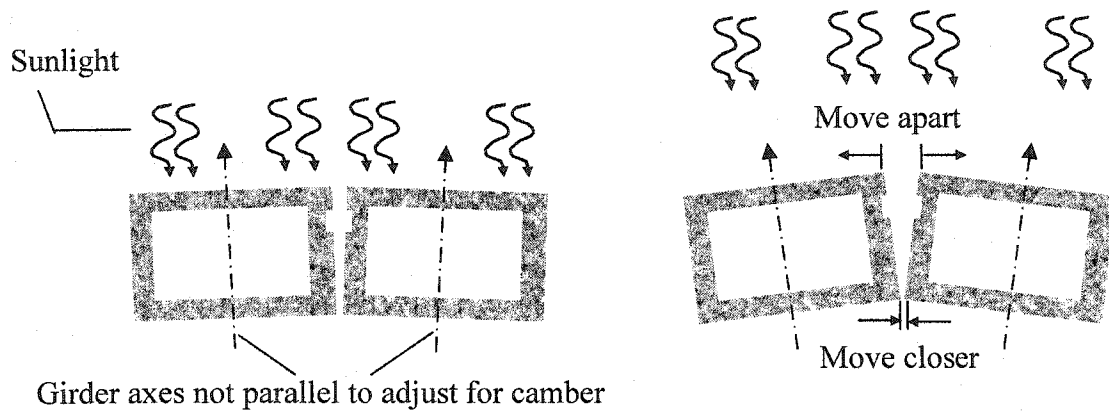
Fig. 2.6[12]: Rotation of girders due to heat from the sun – exaggerated view
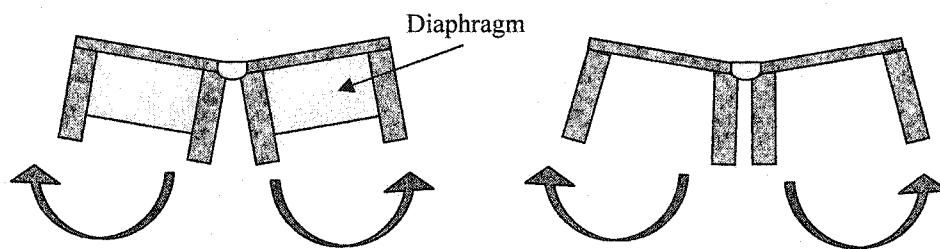
Fig. 2.7: Transverse girder rotation with and without diaphragms – exaggerated view

27

2.4 References

1. Bakht B., Jaeger L. G. and Cheung M. S. (1983). "Transverse Shear in Multibeam Bridges", Journal of Structural Engineering, ASCE, Vol. 109, No. 4, April, pp. 936 – 949.

2. AASHTO (American Association of the State Highway and Transportation Officials) Bridge Design Code.

3. OHBDC – Ontario Highway Bridge Design Code.

4. Gulyas R. J., Wirthlin G. J., and Champa J. T. (1995). "Evaluation of Keyway Grout Test Methods for Precast Concrete Bridges", PCI Journal, Vol.40, No. 1, January-February, pp. 44 – 57.

5. Nottingham D. (1996). "Joint Grouting in Alaskan Bridges and Dock Decks", Concrete International, Vol. 18, No. 2, February, pp. 45 – 48

6. Issa M. A., Issa M. A., Khayyat S. Y., Yousif A. A. and Kaspar I. I. (1995). "Field Performance of Full Depth Precast Concrete Panels in Bridge Deck Reconstruction", PCI Journal, Vol. , No. , May-June, pp. 82 – 108

7. Huckelbridge A. A., Esnawi H. E. and Moses F. (1995). "Shear Key Performance in Multibeam Box Girder Bridges", Journal of Performance of Constructed Facilities, Vol. 9, No. 4, November, pp. 271 – 285

8. EL-Esnawi H. H., (1996) May. "Evaluation of Improved Shear Key Design for Multi-Beam Prestressed Concrete Box Girder Bridges." Ph.D. Thesis, Department of Civil Engineering, Case-Western Reserve University, Cleveland, OH,

9. Yamane T., Tadros M. K., and Arumugasaamy P. (1994). "Short to Medium Span Precast Prestressed Concrete Bridges in Japan," PCI Journal, Vol. 39, No. 2, March-April, pp. 74 – 100

10. EL-Remaily A., Tadros M. K., Yamane T. and Krause G. (1996). "Transverse Design of Adjacent Precast Prestressed Concrete Box Girder Bridges", PCI Journal, Vol. 41, No. 4, July-August, pp. 96 – 113

11. Martin L.D. and Osborn A. E. N. (1983). "Connections for Modular Concrete Bridge Decks", FHWA-82/106, NTIS Document PB84-118058, Consulting Engineers Group Inc., Glenview, IL, August.

12. Lall J., Alampalli S. and Dicocco E. F. (1998). "Performance of Full-Depth Shear Keys in Adjacent Prestressed Box Beam Bridges", PCI Journal, Vol.43, No. 2, March-April, pp.72 – 79

13. Badie S. S., Kamel M. R. and Tadros M. K. (1999). "Precast Pretensioned Trapezoidal Box Beam for Short Span Bridges", PCI Journal, January-February, pp. 48 – 59

14. Miller R. A., Hlavacs G. M., Long T. and Greuel A. (1999). "Full-Scale Testing of Shear Keys for Adjacent Box Girder Bridges", PCI Journal, November-December, pp. 80 – 90

15. Serink D. and Hrudey T. M. (1996). "Finite Element Analysis of Shear Key Behaviour in FC Girder Bridges", 1st Structural Specialty Conference, Canadian Society for Civil Engineering, Edmonton, Alberta.

16. Reid Crowther & Partners LTD (1996). Report prepared for Alberta Transportation on finite element analysis of five FC girder bridges, leading to the selection of appropriate rehabilitation scheme

17. Azarnejad A., Tadros G. and Mcwhinnie K. (1999) "Rehabilitation of FC Girder Bridges: Analysis and Construction", Annual Conference of the Canadian Society for Civil Engineering, Regina, Saskatchewan, June 2-5, pp. 165-174

18. CH2M Gore & Storrie Limited, "Lawrence River Bridge Strengthening Analysis", Report No. BF 75694, prepared for the Alberta Transportation, December 1998

3.0   CURRENT ASSESSMENT AND REHABILITATION OF FC GIRDER BRIDGES[*]

3.1 Introduction

To assess the severity of the field problem as well as to select bridges for field testing, an extensive survey was undertaken to observe the longitudinal cracking on these bridge decks. The objectives of the field survey were to look for possible trends or relationships between various influencing parameters and the performance of these bridges as well as to assess the success or failure of various rehabilitation schemes used on these bridges in the past.

38 bridges, which constitute 21% of the total, were visited in Alberta to conduct a sample survey consisting of visual inspections and looking for longitudinal cracking. Additional information on various parameters was obtained from the Alberta Transportation FC girder bridge databases and individual bridge inspection and management reports (BIM). The parameters investigated to have an influence over bridge performance were span length, span width, bridge skew, service age, and traffic volume.

Almost all of the FC girder bridges are simple span bridges and only a few have been constructed as continuous structures. From most of the visual as well as record inspections, it appears that the volume of traffic has the biggest share in the long-term deterioration of these bridges.

Most of the rehabilitation schemes used on the FC girder bridges so far constitute some form of lateral stressing of the system. However, longitudinal cracks have reappeared on many of the rehabilitated bridges. There is no particular favourite to date, which can be referred to as the successful strategy. The apparent failure of the rehabilitation schemes to arrest the shear key cracking problem brings up two questions. The first question is whether lateral strengthening is the correct mode of rehabilitation to be used on these bridges and the second obvious query is whether the lateral strengthening techniques are

---

[*] Essentials of this chapter appear as a paper in the proceedings of the sixth international conference on short and medium span bridges held in Vancouver BC, 2002

30

using the optimum combination of their participating parameters (like spacing, sectional properties etc).

It is quite possible that the optimum combination of these participating parameters, which would solve the shear key cracking problem, could turn into an uneconomical combination that would largely offset the economic advantages gained out of constructing this type of bridges. However, even the most conservative combination of these conventional rehabilitation schemes would still cost only a small fraction of the expenditure required to replace these bridges with new structures. This is the obvious incentive for Alberta Transportation to resort to rehabilitation of old bridges instead of replacing them with new bridges. This chapter will summarize and tabulate the results of the FC girder bridge survey, undertaken in the summer of 2000.

3.2 Past Performance

180 FC girder bridges in the province of Alberta have been assessed for performance based on certain performance indicators. A randomly selected sample of 38 bridges out of the total number of 180 was personally visited for visual inspections. Information about the whole FC Girder Bridge population in the province of Alberta was obtained from Alberta Transportation files. A bridge generally exhibited an uncracked deck and no longitudinal shear key cracking on the bridge deck surface if it was still in its original form and had not been rehabilitated. This was verified by the observations from the visual inspections sample survey. According to the results of that survey, none of the 14 non-rehabilitated bridges surveyed, showed any signs of shear key cracking.

Hence, the rehabilitation factor was then a good indicator for assessing the influence of certain parameters on the performance of these bridges, and has been used in all the following tables calculating the rate of deterioration affected by different parameters. Since the scope of interest of this research was load sharing concerns due to shear key cracking and deterioration therefore bridge information from Alberta Transportation bridge records was only reported in the following tables if the bridge had been rehabilitated for shear key cracking. All other rehabilitation needs on these bridges due to

deteriorated deck joints (at the junction of various spans in a bridge) or collision damages etc were not taken into account for this survey. Most of the tables to follow are based on the assessment of the total number of bridges in the province of Alberta or the whole FC Girder Bridge population. However, some tables are instituted on only the number of bridges visited, or the selected sample, to show or verify a particular argument and have been clearly labelled as bridges assessed on that basis. Table 3.1 shows the number and percentage of the total FC girder bridges that have undergone rehabilitation[1] in the province of Alberta.

Table 3.1: Original vs. rehabilitated – Considering all existing FC girder bridges

Total Number of FC girder bridges	Number of bridges rehabilitated	% Rehabilitated
180	76	42.2

3.2.1 Performance indicator results

The performance indicators that were used to evaluate the bridges were span length, span width, straight or skew, service age and traffic loads. This exercise was carried out to see if one of these indicators visibly affected the long-term performance of these bridges.

Table 3.2 shows the influence of span length upon deterioration in the bridge shear keys, which leads to its rehabilitation. Our survey showed that 27 percent of the bridges which were shorter than 20 metres had to be rehabilitated as compared to 42 percent of the bridges which were between 20 and 30 metres and 44 percent of the bridges which had span lengths greater than 30 metres. This seems to indicate that longer bridges were more susceptible to shear key deterioration than shorter bridges. However the same table also shows that most of the bridges which were rehabilitated were located on main highways and very few bridges located on local roads had to undergo rehabilitation. The span width of the bridge also shows some correlation with the conditions leading to rehabilitation. From Table 3.3 we see that 48 percent of the wider bridges had to be rehabilitated whereas 38 percent of the relatively narrower bridges were rehabilitated. This difference between 48 and 38 percent further goes up if we chose the cut-off width at 10.5 meters instead of 12 meters. Increased shear key deterioration with increasing width is an

32

outcome of more bending in the transverse span which puts extra demand on the shear keys.

Table 3.2: Performance indicators – Span length

	Less than 20 m.			20 to 30 m.			Greater than 30 m.		
	M	S	L	M	S	L	M	S	L
Existing	5	2	4	35	12	29	42	15	36
Rehabilitated	3	0	0	25	6	1	28	8	5
% Rehabilitated	27.27			42.10			44.08		

M = Main Highways,   S = Secondary Highways,   L = Local roads and urban streets

Table 3.3: Performance indicators – Span Width

	Over 12 meters (Wide bridges)	Under 12 meters (Narrow bridges)
Existing	75	105
Rehabilitated	36	40
% Rehabilitated	48	38

Table 3.4 shows that skewed bridges were more susceptible to shear key deterioration than straight bridges. This could be possible because of a relative twist in the bridge deck due to the skewed shape of the bridge. Tables 3.5 and 3.6 illustrate that shear key cracking seems to be a product of long term bridge usage and that most of the bridges have actually completed at least 20 years of active service before they had to require rehabilitation. Perhaps the best performance indicator is "Traffic Loads", as shown in Table 3.7. This table shows that the bridge deck deterioration is directly influenced by the extent and frequency of loading on the bridges.

Table 3.4: Performance indicators – Skew

	Skewed bridges	Straight bridges
Existing	68	112
Rehabilitated	36	40
% Rehabilitated	53	36

33

Table 3.5: Performance indicators – Service Age (constructed before and after 1980)

	Bridges in service since before 1980	Bridges in service since 1980
Existing	160	20
Rehabilitated	76	0
% Rehabilitated	47.5	0

Table 3.6: Performance indicators – Service Age (based on years of service)

Total Number of bridges rehabilitated = 76	Bridges with service age of 20 years or more	Bridges with service age of less than 20 years
	58	18
% of total rehabilitated	76	24

Table 3.7: Performance indicators – Traffic loads

	Bridges on main[a] highways	Bridges on local[b] roads
Existing	77	36
Rehabilitated	58	4
% Rehabilitated	75	11

Main[a] Highways: Inter-provincial primary highways (for example highways 1, 2, 16 et.)
Local[b] Roads: City or town streets

Bridges located on main highways obviously have a higher Annual Average Daily Traffic (AADT) value than the bridges, which are located on local roads and dirt tracks. This seems to explain why only 11 percent of the bridges on local roads were rehabilitated, whereas as much as 75 percent of the bridges on main highways had to be rehabilitated for shear key related deck cracking concerns.

The three indicators (i.e. skew, width and traffic loads) showing a positive correlation with bridge deterioration were then further investigated for isolating the effect of one from the other. For example the question would arise that if skewed bridges are more

34

susceptible to cracking how do we know if all skewed bridges are not under heavy and frequent loading cycles. To answer this question, we refer to Tables 3.8 and 3.9 below.

Table 3.8: Skew vs. traffic loads effects on FC Girder Bridges

	Skewed bridges on main highways	Skewed bridges on local roads
Existing	34	14
Rehabilitated	26	4
% Rehabilitated	76	28

Table 3.9: Straight spans vs. traffic loads effects on FC Girder Bridges

	Straight bridges on main highways	Straight bridges on local roads
Existing	43	22
Rehabilitated	32	0
% Rehabilitated	74	0

It is clearly visible from the above table that most of the skewed bridges that were located on main highways had undergone rehabilitation. However a comparison of Tables 3.8 and 3.9 also illustrate that the skewness of the bridge does have some detrimental effects. As 76 percent of the skewed bridges on main highways developed shear key problems and had to be rehabilitated, this deterioration remained the same in the case of straight bridges on main highways, which shows that traffic volume and intensity had an obvious dominant influence. However, in case of lightly used local roads, 28 percent of the skewed bridges were rehabilitated whereas no straight bridges had been rehabilitated, which points towards the fact that skewed bridges are more prone to shear key cracking.

A similar comparison is presented for the Span Width indicator in Tables 3.10 and 3.11 Again both these tables show that though traffic loads had a dominant influence in putting the shear keys into distress, the width of the span did still have some effect on shear key deterioration. Earlier in Table 3.5 we noticed that none of the 20 bridges which were constructed after 1980 had been rehabilitated. An explanation to this effect could be given by the bridge location distribution which can be seen in Table 3.12. This table

35

illustrates that most of the bridges constructed after 1980 are actually located on the lightly travelled local roads and only 3 of those bridges were placed on the main highways. Moreover there were some design improvements incorporated in the original design (like transverse prestressing etc) in some of the relatively newer bridges.

Table 3.10: Wide spans vs. traffic loads effects on FC Girder Bridges

	Wide bridges on main highways	Wide bridges on local roads
Existing	53	6
Rehabilitated	40	3
% Rehabilitated	75	50

Table 3.11: Narrow spans vs. traffic loads effects on FC Girder Bridges

	Narrow bridges on main highways	Narrow bridges on local roads
Existing	24	30
Rehabilitated	18	1
% Rehabilitated	75	3

Table 3.12: Location distribution of bridges constructed after 1980

Total Number of Bridges = 20	On Primary Highways	On Secondary Highways	On local roads and Urban Streets
Number of Bridges	3	3	14

Hence, traffic volume then seems to have the major effect on shear key deterioration of FC Girder Bridges. However, span length, span width and skewness of the bridge also have some minor influence on the deterioration process in FC Girder Bridges.

Supplementary information to the above survey is provided in the following tables. A full break up of the type of roadways supporting all the FC girder bridges is given in Table 3.13. This table shows that as the significance of the road type goes down, so does the percentage of rehabilitated bridges on that road type. Most of the multi span FC girder

bridges constructed in Alberta are simple span structures, though a few are continuous. The moment connection in these bridges is provided with the help of a field grouted connecting plate or rebar, between the precast girders. According to Alberta Transportation, the continuous bridges have performed better than the simple span bridges.

A break up of the bridges with different number of spans is provided in Table 3.14. This table shows that a greater number of bridges were rehabilitated which were spanning larger distances. For example, two to four span bridges had a larger percentage, which under went rehabilitation than single span bridges. Since these are simple span bridges therefore the length effect really comes down to the fact that again most of the multi span bridges are located on main or secondary highways. This may also be observed in Table 3.15.

Table 3.13: Road type vs. Percent rehabilitated

	Existing	Rehabilitated	% Rehabilitated
Bridges on Primary Highways	77	58	75
Bridges on Secondary Highways	30	13	43
Bridges on Local[a] Roads	36	6[b]	16
Bridges on Urban[c] Streets and Indian Reserve Roads	23	2	8
Bridges on Private Roads	6	0	0
Bridges on Forestry Trunk Roads	5	0	0

[a] Local roads are generally smaller roads within cities.
[b] Out of these six bridges, three are fairly wide Edmonton streets which see a lot of traffic.
[c] Urban streets include streets connecting portions of cities across highways

Table 3.14: Number of spans of Simple Span Bridges vs. Percent rehabilitated

	Total	Rehabilitated	% Rehabilitated
Single span bridges	40	10	25
Two span bridges	40	23	57
Three span bridges	52	21	40
Four span bridges	25	20	80
Five span bridges	11	6	54
Six span bridges	4	1	25
Seven span bridges	3	0	0
Eight span bridges	1	0	0

Table 3.15: Rehabilitated vs. non-rehabilitated for different span bridges

	Total	On highways	Number Rehabilitated	On light traffic roads	Number Rehabilitated
Single span bridges	40	19	9	21	1
Two span bridges	40	21	19	19	4
Three span bridges	52	32	20	20	1
Four span bridges	25	22	18	3	2
Five span bridges	11	9	6	2	0
Six span bridges	4	2	1	2	0
Seven span bridges	3	1	0	2	0
Eight span bridges	1	1	0	0	0

3.3 Rehabilitation

Over a twenty-year span, many different rehabilitation schemes were tested on the FC girder bridges in Alberta. The initial repair schemes mainly focused on the malfunctioning of erection bolts because many bridge inspection reports had suggested that bolts were often improperly grouted, loose or even sometimes missing. After receiving limited success from these improvements the rehabilitation focus shifted towards lateral stressing and transverse stiffening of the system.

38

Post-tensioned Dywidag bars were used to laterally stress the system on the earliest bridges. By lateral stressing, the idea was to impart compression to the shear keys. Two 25 mm Dywidag bars were usually provided, one on each side of the precast transverse girder diaphragm. Since this system could not be applied to skewed bridges, another form of this method was devised by using short and staggered Dywidag bars to laterally stress pairs of adjacent girders. After some years a new method was introduced which was applicable on both straight and skewed bridges. This time the lateral stressing was accomplished by 51-mm high strength rods post-tensioned by Super bolts. These bars would also connect pairs of adjacent girders and were staggered across the bridge, overlapping at the girder interfaces. Finally, lateral stressing was also achieved by using prestressing tendons. However, all those schemes involved some degree of difficulty in drilling through the girder webs to place the prestressing medium.

Later it was felt that a transverse diaphragm was needed in addition to the lateral stressing system to make the girders torsionally rigid and to better distribute the load among the girders. This was made possible with the help of a lateral steel under-slung diaphragm. Figure 3.1 shows a schematic of some of the rehabilitation schemes discussed above.

Most of the rehabilitation schemes that followed were some variation or combination of lateral stressing and lateral bracing of the system. Table 3.16 shows the number of bridges that were rehabilitated by using each of the rehabilitation schemes. Taking a closer look at the distribution among the schemes it can be easily observed that there was no particular favourite in the rehabilitation process of these bridges, though the largest number of bridges were rehabilitated by using post tensioned Dywidag bars. However, if we lump together the bridges that were rehabilitated by using strands and Dywidag bars in the same category of lateral stressing, it can be observed that 34 bridges were rehabilitated by lateral stressing only. Moreover, in most bridges a non-reinforced, non-composite, high-density concrete deck was added on top of the girders (as shown in Figure 3.1) to act as the wearing surface, no matter what the rehabilitation scheme was.

The rehabilitation schemes employing lateral stressing of the system tend to impart compression to the shear key area, through the prestressing force, and utilize additional load sharing capabilities obtained from grouting the hollow spaces between adjacent girder legs to improve load sharing between the girders. The addition of the concrete deck on top of the girders is meant to provide a rigid layer, which will improve both the load sharing and load distribution between the different girders, even though it does not improve the torsional rigidity of the girders. If the concrete overlay is a part of the structural rehabilitation, it is usually post tensioned in the transverse direction. In other cases, the concrete overlay may only be used as a wearing surface and not post tensioned. Figures 3.2 to 3.5 show pictures of some rehabilitation schemes used on FC Girder Bridges.

Table 3.16: Bridges rehabilitated with each scheme[2,3]

Straight Bridges							
Rehabilitation Scheme	LS[a] With DD[b]	LS[a] With Strands	LS[a] With Strands & USD[e]	LSt[d] With USD[e]	Transverse Prestressed Concrete Deck & USD[e]	LS[a] With DD[b] & USD[e]	LS[a] With SB[c]
Number of bridges	9	9	10	5	3	3	4

Rehabilitation Scheme	Skewed Bridges						
	LS[a] With DD[b]	LS[a] With Strands	LS[a] With Strands & USD[e]	LSt[d] With USD[e]	Transverse Prestressed Concrete Deck & USD[e]	LS[a] With DD[b] & USD[e]	LS[a] With SB[c]
Number of bridges	11	5	3	5	6	2	1

Total	20	14	13	10	9	5	5

LS[a] = Lateral stressing; DD[b] = Dywidag bars; SB[c] = Super bolts; LSt[d] = Lateral stiffening; USD[e] = Underslung diaphragms

Finally, the underslung diaphragm provides lateral bracing of the system, improves upon the torsional stiffness of the girders and clamps webs of adjacent girders in such a way so as to eliminate or greatly reduce inter-girder vertical differential deflections.

Table 3.17 illustrates the performance of the different rehabilitation categories, observed during the FC Girder Bridge sample field survey. For simplification, all lateral stressing techniques like stressing with strands or stressing with Dywidag bars have been combined together under, "Prestressing under girder flange". Similarly the strands and Dywidag combination with the underslung diaphragms when the lateral stressing is provided under the flange, is presented together as, "Prestressing under girder flange and steel underslung diaphragms".

From this table, we can observe that most of the bridges that were rehabilitated had shown signs of re-cracking on top of the newly laid concrete or asphalt, wearing surface. Though we can also see that the bridges rehabilitated with a combination of lateral prestressing and underslung diaphragms had a much better performance and most of those bridges remained uncracked.

41

Table 3.17: Bridges rehabilitated with each scheme, considering only the sample survey

	PS[a] Under Girder Flange	Transverse Prestressed Concrete Overlay & USD[b]	PS[a] Under Girder Flange & Steel USD[b]	US[b] Diaphragm only	Super Bolts
Surveyed	8	6	5	4	1
Re-cracked	7	1	1	4	0

PS[a] = Prestressing

USD[b] = Underslung diaphragms

3.4 Survey Errors

Even though care was taken to include only those bridges in this analysis that were rehabilitated for shear key deterioration concerns for consistency in the comparisons, errors in the conclusions based on the survey cannot be totally ruled out. Two types of errors can generally occur, when conducting a survey. These are known as sampling and non sampling errors. Sampling error is the error that occurs because not every element in a population is surveyed. Nonsampling error refers to all other types of errors that can occur when a survey is conducted, such as measurement errors, processing errors etc.

Sampling errors in the simple random sample of 38 bridges selected for this survey, were quite unavoidable to some extent because of proximity concerns. For better communication efficiency, only those bridges were selected in this survey which were located close to the city of Edmonton. Hence, to avoid confusion in the results because of sampling errors, most of the survey is based on the whole population, information for which was obtained from Alberta Transportation data bases and bridge files.

Non sampling errors in the population survey could come from inaccurate estimation of data from the available databases, the effect of borderline entries when limits were fixed on lengths, widths, skews etc. and the authenticity of information available in Alberta

Transportation bridge files and databases. The variation of other indicators while one was being considered would not change the results because this variation was quite evenly distributed across all sectors of the parameter being considered, hence cancelling out its effect.

For all practical purposes, the above mentioned errors were small and would not conclusively affect the results of this survey.

3.5 Conclusions

This study, based on the total population of 180 FC Girder Bridges, showed that most of the shear key deterioration and cracking is related to sustained use and ever increasing traffic loads. Span length, span width and skewness of the bridge also contribute minor damage to the shear key deterioration hence leading to bridge rehabilitation.

The sample survey of 38 bridges was quite useful in accomplishing a number of objectives. The first and the foremost being the verification of the presence of longitudinal cracking at shear key locations in many bridges. Observations on rehabilitated bridges that exhibited signs of re-cracking were useful in the performance evaluation of the rehabilitation schemes. It was observed from the sample survey that the FC Girder Bridges, which were rehabilitated by a combination of lateral prestressing and underslung diaphragms performed relatively better than other bridges which were rehabilitated by other schemes. And finally, the sample survey was used to confirm the trends established by the population survey.

Different rehabilitation schemes have been used on FC Girder Bridges; from around 1979 to date, and improvements and modifications have been refined over the years, based on response to previous schemes. Most of the remedial measures have been based on visual inspections and previous experiences as well as some finite element studies. The behaviour resulting from a combination of rehabilitation schemes is harder to assess and analyze, based on visual inspections of results because it may be complicated to isolate the effect coming from each of the components of the rehabilitation scheme, separately.

And the role of many factors in affecting the behaviour of these bridges, as in any real life structure, make it a complex problem to handle.

Hence it appears imperative in this case, to utilize field-monitoring techniques to assess the field-based performance of the bridges as well as calibrate the finite element models with field data.

3.6 Acknowledgements

44

Figures

Fiber Reinforced Silica Fume Concrete Deck

Post Tensioning Tendons

Side Curb

External Stirrups

Dywidag bars or tendons

Underslung Diaphragm Assembly

Grout
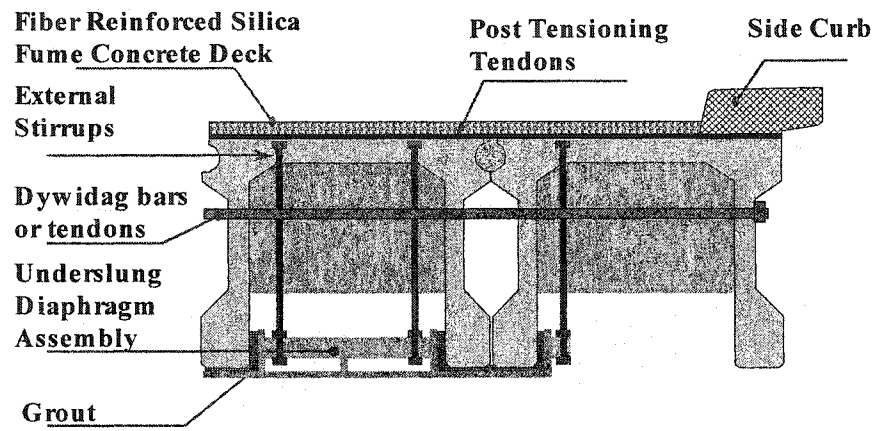
Figure 3.1: Schematic showing some rehabilitation schemes
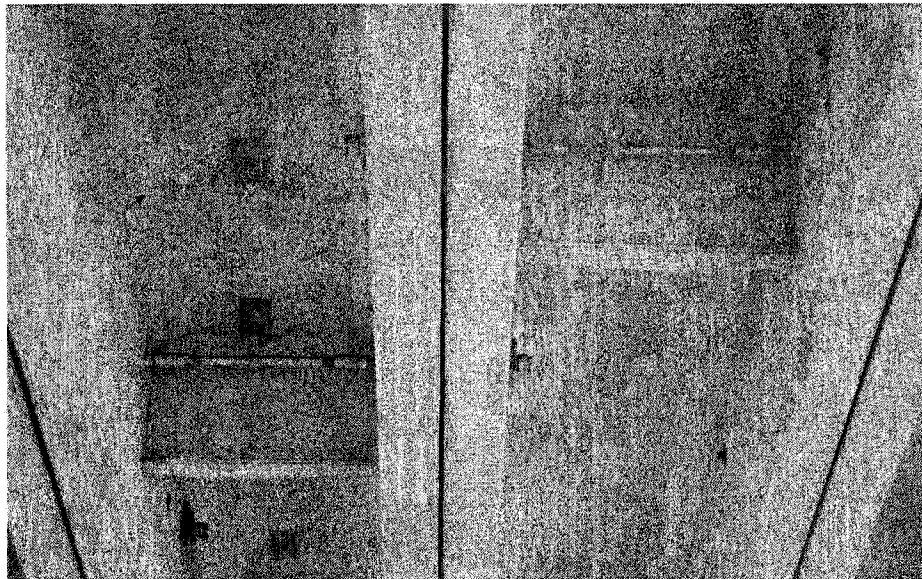
Figure 3.2: Lateral stressing with superbolts

45
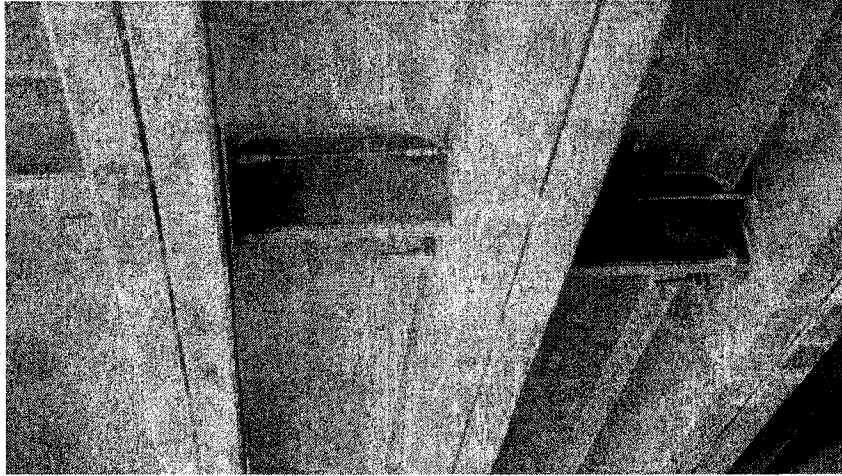
Figure 3.3: Lateral stressing with staggered dywidag bars
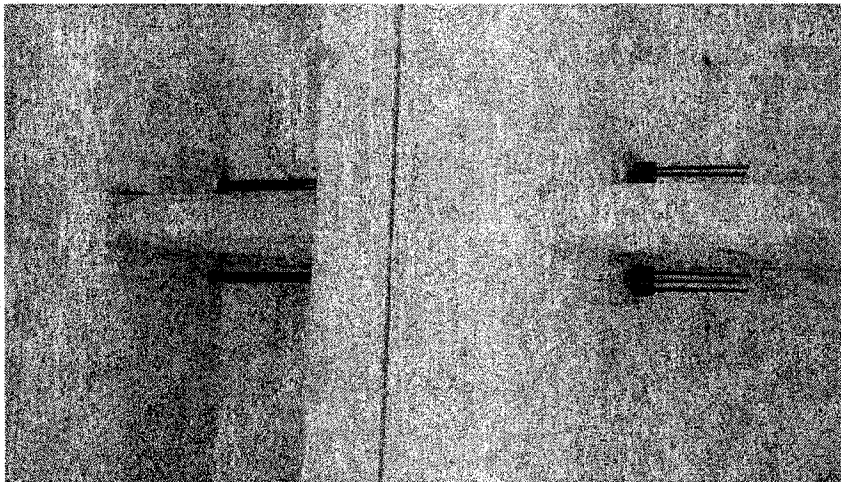
Figure 3.4: Lateral stressing with prestressing tendons
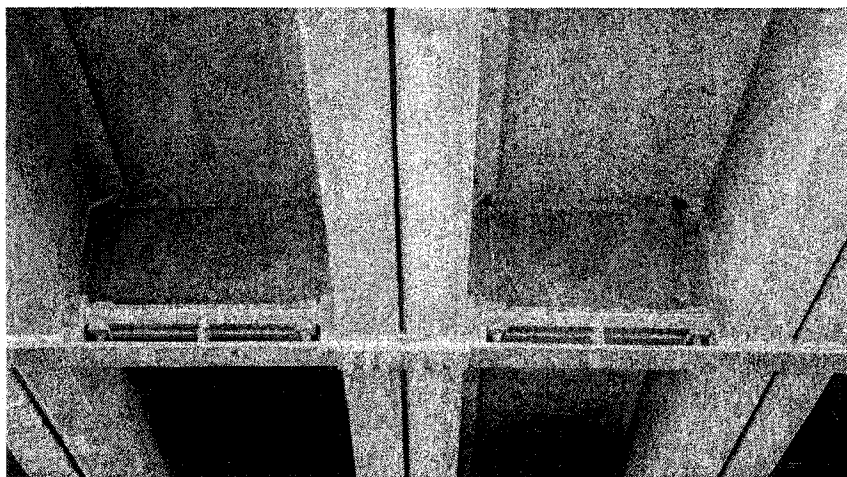
Figure 3.5: Lateral bracing with channel type underslung diaphragms

46

3.7 References

1. R. Yu, Type FC, FM, LF, VF Girder Report, Alberta Transportation Bridge Information System, January 20, 1998

2. Lateral Stressing and Shear Strengthening Projects on FC Girder Bridges, Alberta Transportation Bridge Records, September 11, 1995

3. FC Girder Rehabilitation Data (1995 to 1999), Alberta Transportation Bridge Records.

4.0 FIELD TESTING AND VIBRATION BASED DAMAGE ASSESSMENT A METHODOLOGY REVIEW

4.1 Introduction

Early detection of the damage in a structure can often imply increased reliability and safety and lower maintenance costs. Sometimes, structures need to be rehabilitated during their service life, however the timing and extent of the required rehabilitation are difficult to determine. The type of repair scheme and its ideal timing would be a direct function of the extent of damage but unfortunately this information is not always known and its effect on the global behaviour of the structure is difficult to judge.

Maintenance programs are generally designed, based on response to previous experiences. This approach may not always yield the best results and valuable time and finances can be spent on using a particular strategy and studying its response on a particular structure. Due to the complexity of a real life structure and its real operating conditions, numerical models may not always prove to be accurate. Hence the conventional means of rehabilitating essentially reduce to trial and error methods where rehabilitation design formulates on the degree of success achieved.

With the development of electronic data acquisition and storage systems it has become easier now to apply periodic or continuous monitoring to structures. The main idea is to replace visual, systematic inspections by health monitoring systems, which periodically or continuously acquire and analyze response data and indicate damage when it is not too late. The non-destructive nature of these techniques, which cause minimum service disruption are hence gaining immense popularity.

Several methods have been proposed and researched in the recent past, for indicating changes in the key characteristics of a structure. Most of these methods rely on the detection of frequency shifts, which lead to the investigation of modal data for damage detection, while other methods probe the Operating Deflected Shapes (ODS) or changes in strain measurements over time. Most methods make use of a model-based approach, using a finite element model refined with information from structural health monitoring.

48

Though most researchers agree on the Level 1 (i.e. damage results in frequency or strain shifts in a structure) accomplishment of these damage detection methods, considerable anomaly still exists over level 2, 3 and 4 of the same process where damage is quantified and located in a structure. Above all, the placement of intelligent instrumentation and the logical interpretation of scores of structural data into meaningful indicators require a long and strenuous effort in itself, to provide a stepwise result based strategy.

4.2 Non-Destructive Testing (NDT)

Non-destructive testing methods are those techniques that provide information on the health of a structure or its part without causing any alteration to the part itself. With growing concerns of environmental degradation and with ever improving technological procedures as a result of ongoing research, the field of non-destructive testing is more alive today than ever before. Its use with many technical disciplines involving corrosion monitoring, health physics, laser technology, process control, instrument development, medicine and nuclear power associate these NDT methods with a wide range of practical problems, from troubleshooting to the most sophisticated characterizations of materials and system behaviour. The detection of defects in solids is an essential part of quality control of engineering systems for their safe and successful use in practical situations.

The use of NDT methods for the assessment of Civil Engineering structures has also increased over the recent years. Most applications have been to the evaluation of damage and repair of bridge members or to identify internal cracks in concrete structures. ACI Committee 228, Non-destructive Testing of Concrete, was organized in 1982 to promote the use of non-destructive testing techniques for concrete construction and to disseminate up-to-date information on the application of these techniques[1]. In addition to the common NDT tools used in the past, aggressive research is presently undergoing in the fields of load and vibration testing of structures, which are still in service. This mode of NDT testing is now possible with the advent of powerful and portable computer systems and data acquisition systems.

4.2.1 Basic Review

Some of the NDT methods, which are in most common use, are:

- Radiography
- Magnetic particle testing
- Ultrasonic testing
- Liquid penetrant tests
- Electromagnetic testing methods
- Leak testing methods
- Acoustic Emissions
- Visual inspections

4.2.1.1 Radiography

Radiography is the technique of obtaining a shadow image of a solid using penetrating radiation such as x-rays or gamma rays. The x-ray source provides a diverging broad beam through the specimen onto a radiographic film or a fluorescent screen. The image obtained is in projection, with no details of depth within the solid. Images recorded on film are known as radiographs. The contrast in a radiograph is due to a different degree of absorption of x-rays in the specimen and depends on variations in specimen thickness, different chemical constituents, non-uniform densities, flaws, discontinuities or to the scattering processes within the specimen. The x-ray shadow image should be a faithful reflection of the inhomogeneities of the object[2]. It is necessary though to have access to opposite sides of the specimen.

4.2.1.2 Magnetic particle testing

This method makes use of the magnetic properties of ferro-magnetic materials to locate surface and subsurface discontinuities in manufactured materials and parts, by inducing magnetic fields into ferromagnetic parts. Surface and subsurface discontinuities such as cracks and seams cause a break in the magnetic uniformity and form a reliable visual indication of the discontinuity.

50

4.2.1.3 Ultrasonic testing

Ultrasonic testing is used widely by the industry for quality control and equipment integrity studies. Major uses include flaw detection and wall thickness measurements. It may be possible to detect flaws and determine their size, shape and location. Wall thickness measurements are specially important where corrosion can cause a uniform reduction in wall thickness over a period of time. Ultrasonic transducers are used for this purpose. These use a piezoelectric crystal, which is driven by high voltage electrical pulses. These voltage pulses make the crystal produce short bursts of high frequency vibrations. These sound waves generated by the ultrasonic transducer are transmitted into the material being tested. If flaws or discontinuities are present, an acoustic mismatch occurs and some or all of the ultrasonic energy is reflected back to the transducer[3]. The piezoelectric crystal in the transducer converts the reflected sound wave back into electrical pulses whose amplitude are related to flaw characteristics and whose time of travel through the material are proportional to the distance of the flaw from the entrant surface.

A number of sonic and ultrasonic non destructive testing and evaluation methods are available today to assess the condition of concrete structures, deep foundations, dams, pavements, tunnels etc. for safety and repair purposes[4]. Most of those methods are based on the measurement of stress wave propagation behaviour. The measurements provide data that are directly and indirectly related to physical conditions of the system under test. Ultrasonic stress waves are commonly used in "Pulse Echo" techniques to provide quality assurance of structural steel welds in construction. "Impact Echo" techniques are used to investigate honeycomb, crack evaluation and void conditions in structural concrete[5]. Ultrasonic Pulse Velocity testing is also sometimes conducted to define the severity of cracking damage in pre-cast bridge segments and for the quality assurance of epoxy injection repairs.

4.2.1.4 Liquid penetrant tests

The liquid penetrant testing is a simple method to apply. First, liquid penetrant containing a dye is applied to the surface of a part and allowed to stand for a period of time. During

51

this penetration or dwell time, the dye penetrant is absorbed into surface discontinuities by capillary action. After the predetermined dwell time has elapsed, excess penetrant is removed from the surface of the part. Finally, a light colored developer is applied to the surface that draws some of the dye penetrant out of the discontinuity. As the penetrant is absorbed by the developer, it spreads out creating indications that are considerably wider and more easily seen than the actual surface defects. Liquid penetrants are selected on the basis of their penetrating ability and dyes are selected for their brilliance. Today, the liquid penetrant testing is more reliable than the radiographic testing for locating minute surface discontinuities[3]. Since the dye penetrant is carried into surface defects by capillary action, it follows that the technique is limited to the detection of surface defects or subsurface defects with surface openings.

4.2.1.5 Electromagnetic Testing Methods – Eddy Current testing & Leakage flux inspection

Eddy current testing involves the use of alternating magnetic fields and can be applied to any conductor. The alternating magnetic field sets up circulating eddy currents in the test part. Any parameter that affects the electrical conductivity of the test area can be detected with eddy currents. Leakage flux testing involves the use of a permanent magnet or DC electromagnetic fields and can be applied only to ferromagnetic materials. With the flux leakage technique, any discontinuity that produces lines of leakage flux in the test area can be detected. These two techniques have been combined with other techniques such as ultrasonic testing and laser dimensional measuring to achieve specific results.

4.2.1.6 Leak Testing Methods

Leak tests are usually required to assure that airtight sealed electronic parts, valves, high pressure tubing and piping systems or welds do not leak. Leak tests may be Ultrasonic leak testing, Bubble leak testing, Dye penetrant leak testing and Pressure Change leak testing etc. Each method has its own standards to measure unacceptable leak.

52

4.2.1.7 Acoustic Emissions

An acoustic emission (AE) is a localized rapid release of strain energy in a stressed material. This energy release causes stress waves to propagate through the specimen. These acoustic emissions can be detected at the specimen surface and analyzed to deduce the nature of damage such as microcraking[6].

Acoustic emission is a NDT technique where the material being inspected generates signals that warn of impending failure. Acoustic emission testing is based on the fact that solid materials emit sound or acoustic emissions when they are mechanically or thermally stressed to the point where deformation or fracture occurs[3]. Acoustic emissions are generated by cracking in composite structures such as aircraft wings, pipes, circuit boards and industrial storage tanks. It is also generated by deformation and crack propagation in pipes, pressure vessels and weldments. Acoustic emission transducers are piezoelectric sensors operating at frequencies from 20 kHz to 1.5 MHz. Acoustic emission test equipment consists of transducers, preamplifiers, single channel signal processing instruments, multichannel signal processing systems, distributive and microprocessor-controlled systems, and AE weld, leak and bearing monitors.

4.2.1.8 Visual Inspections

Visual inspection, aided or unaided, direct or remote, is a valuable, if yet unrecognized non destructive evaluation tool. It is the oldest and the most commonly used inspection method in civil engineering and will probably never be abandoned. Visual inspection can be defined as an inspection procedure where the supervisor makes use of one or more of the human senses like the eye sight, hearing, taste to assess the condition of a structure or structural part.

The appearance and colour of a corroded area often provides valuable insights as to the cause and extent of corrosion. Similarly the pattern and location of cracking as well as shape deformation can sometimes provide useful information. Each NDT technique is unique with its own advantages and disadvantages, however nothing can be substituted for visual inspection, nor can visual inspection replace other established NDE techniques.

53

However, when direct visual inspections are difficult to make, these senses can be supplemented by some kind of auxiliary equipment like a hammer or magnifying glass. Sophisticated optical instruments can often be used to provide remote viewing of critical areas, for example small cracks in both steel and concrete structures.

However, the quality of a visual inspection is primarily dependent on the experience and imagination of the inspector, which may be supplemented by drawings and photographs and reports from previous inspections. This implies that the quality of the visual inspection report will heavily depend on the training of the inspector through past experience with similar inspections. Moreover, a visual inspection can only reveal defects at or close to the accessible surfaces. This means that the method cannot stand alone, but has to be supplemented with other inspection methods.

4.3 Load and vibration testing used as an NDT tool

All the experimental techniques mentioned above require that the vicinity of the damage be known prior to the test and that the portion of the structure being inspected be readily accessible. Under these limitations, the above methods can then detect damage on or near the surface of the structure. The need for additional global damage detection methods that can be applied to complex structures has led to the development of methods that examine changes in the vibration characteristics of the structure.

Field testing a structure under real working conditions and normal operating service loads is the preferred present way of condition assessment. Testing in its original operating environment enables the inspector to eliminate a number of assumptions that are usually made when designing the test set up for a laboratory specimen. For example, with a field tested structure there is no more a need of applying accurate boundary conditions and loading patterns, as in the case of a laboratory built and tested specimen. The non-destructive nature of most of these testing procedures makes them an effective addition to the previously mentioned NDT tools. However, field testing is mostly used to assess a structure under service loads and is seldom used to calculate ultimate capacities. Hence,

54

the magnitude of measurements is usually small which makes it a challenging task to track trend paths and draw meaningful conclusions.

Load and vibration testing in the field has been referred to by a number of different names by different researchers like, "VBI – Vibration based inspection[7] ", "CM – Condition Monitoring[8] " and "DI – Damage Identification[9]". However the most recent term that is being extensively used to encompass all field testing methods is that of, "SHM – Structural Health Monitoring[10] ", which derives its name from drawing analogies with the health monitoring of individuals by the medical doctor. Just as a trip to the doctor determines the cause of an ailment, field testing of structurally suspected bridges aims at evaluating the causes of suspicion in the bridges.

Though Structural Health Monitoring (SHM) may be a relatively new term in Civil Engineering, the use of instruments to assess the health and integrity of structures is very old. Field testing of bridges with the help of rudimentary measuring instruments has been carried out for a long time. Proof testing with the help of sandbags or other artificial loading procedures used to be carried out on earlier bridges in Europe before opening the bridge to normal traffic.

4.3.1 SHM – Structural Health Monitoring

The main objective of SHM is to accurately and efficiently monitor the in-situ behaviour of a structure to assess its performance under service loads, to detect damage or deterioration and to determine the current structural condition or in other words its health[10]. The Structural Health Monitoring system should be able to provide on demand reliable information pertaining to the safety and integrity of a structure. This information can then be incorporated into a bridge maintenance and management system and could result in the improvement of future design guidelines. Some of the obvious gains coming out of an effective structural monitoring system would be verification and reliability of innovative designs, early detection of problems, avoidance of catastrophic failures, effective allocation of resources and reduced service disruptions and maintenance costs.

55

Recent renewed interest in the area of condition assessment of structures can be attributed to three main developments, innovative materials and designs, aging structures and technological advances in test data acquisition, processing and storage.

The application of modern technology like high performance materials and refined analysis techniques has led to optimal design of new structures during the last couple of decades. However, these optimized structures can be vulnerable to failure and may sometimes contain very little redundancy in their support systems. Therefore, it is very important to detect damage like cracks, as early as possible. Furthermore, there is a large number of old structures, which have lived their design lives and are still in service. The amount of damage in these old bridges has increased due to age combined with an increase in traffic loads and intensity.

The risk of some sort of damage in most structures is very high and also very difficult to estimate. The Stochastic nature of environmental loads and service loads together with the uncertainties in the models for strength reduction due to aging, make it impossible to perform a reliable calculation of the state of damage at any time in the lifetime of the structure[7]. Hence, the use and reliability of inspection methods for damage detection have therefore become even more important in the safety evaluation of Civil Engineering structures. Besides, during the last two decades, it has become profitable to perform inspection and repair instead of demolition and replacement.

4.3.1.1 The System Composition

The complete structural health monitoring system should comprise of the following essential ingredients[10]:

i)   A sensor system

ii)   Data acquisition and communication

iii)   Data processing and storage

iv)   Diagnostics

v)   Data retrieval

i) A Sensor System

The first task in the preparation of a plan for the health monitoring of a structure is the installation layout of the various sensing devices, which can measure absolute values or changes in different parameters like load, strains, deformations, accelerations, temperature etc. The sensory system in a structure can be seen as the nervous system of the human body, which transmits sensory signals from the brain to the rest of the parts of the body. The effectiveness of the end results in a structural health monitoring project has a lot to do with the correct choice and placement of the instrumentation for that particular problem.

Most of the sensing devices are in direct physical contact with the structure and register the required data. Two common types of sensors are electronic and optical sensors. When subjected to a specific physical phenomenon, an electronic sensor reports the magnitude of the phenomenon by producing electrical signals in terms of electrical charge or a change in voltage. On the other hand, optical sensors report the magnitude of the physical change in forms of light signals. A large number of sensing devices are commercially available, for example electrical resistance strain gauges, vibrating wire strain gauges, deflection transducers, accelerometers, temperature probes and fibre optic gauges. In addition to the conventional sensors, which have been available commercially for a long time, there are many new sensor technologies, which are in different stages of development, including some advanced fibre optic sensors, di-electric measurement sensors and piezo-electric materials.

ii) Data Acquisition and Communication

Data acquisition consists of acquiring and collecting data from the sensors mounted on the structure, amplify, filter and condition the signal, provide bridge completion as well as excitation to the sensors and prepare the data signal for further analysis, whereas, data communication is the mode of data transfer from the sensors to the data acquisition system and from the data acquisition system to the processing and storing computer. Two common data acquisition systems are generally in use; the conventional and the computer based systems.

57

The conventional system employs simple read out units, which can be directly connected to the sensory system, and an operator visually reads the data from the read out units and manually records it. This is an economical and simple approach if a small number of sensors are to be read for a short period of time. However, for more general applications, dealing with large number of recording sensors, a computer based data acquisition system is better suited. This kind of system is usually equipped with a large number of recording channels, which enables the operator to read many sensors at the same time. The computer based data acquisition system is also equipped with a signal conditioner and a DAQ board, which converts the analog signals from the sensors into digital signals, which are then recognizable by a computer.

In its most basic form transmission of data is conducted by wires. The length and thickness of the wire can have an influence over the quality of the data and adjusting techniques like using a three-wire system are helpful in neutralizing the wire size effects. At the most sophisticated end of the communication continuum, the collected data is transmitted remotely, either through telephone lines or by other wireless modes. The selection of a suitable communication system is however an essential component of an effective structural monitoring system.

iii) Data Processing & Storage

The data acquired from the sensory system of a structure through a data acquisition system is finally routed to a computer for onward data processing and storage. A computer software handles the communication between the data acquisition system and the data processing and storing computer. The same software provides a trigger to read the sensors and supplies additional information like certain calibration factors or data sampling rates that may be required by the system to accurately interpret the data.

Sometimes the information collected from such a system may contain noise or extraneous data due to the presence of interfering devices in the vicinity of the test. Sensors that are not compensated for temperature are also prone to giving misleading results. Hence the data that comes directly from the structure has to be processed for all these effects.

58

Different filtration or processing techniques are used for this purpose to separate meaningful data from useless noise. Accurate processing of this data will obviously yield information that can be successfully used towards a realistic characterization of the structure's behaviour.

Raw data and processed data are two terms which are commonly used to distinguish the data collected directly from the structure from the information that has been labelled, plotted and corrected for external influences. Both the raw and processed data can be stored in a computer for future use.

iv) Diagnostics

One of the most important aspects of a structural health monitoring system is the interpretation or conversion of measured local parameters like deflections, strains and accelerations into global response functions like stiffness, stresses or frequencies of vibration. Currently no comprehensive techniques are available to facilitate this interpretation of data and the very small in service measurements of various parameters make it an extremely challenging task to draw meaningful conclusions. The use of a finite element model here comes in very handy. The model can be calibrated with results from field tests, and utilized for situations and scenarios, which are hard to simulate in an actual field test.

v) Data Retrieval

Finally, the test data recorded from a structural health monitoring system should be stored in such a way that it can be easily and efficiently retrievable. Since the interpretation value of this data is subjective to the individual performing the analysis therefore the ready availability of this information can enable a reanalysis of the problem or provide more researchers with opportunities of applying different techniques of analyzing the same data to compare with earlier results. Some data archival systems have been recently developed to store this data in such a way that it is safely stored and efficiently retrievable.

59

As mentioned in Article 4.3, we will break down field testing into:

- Load testing
- Vibration testing

While most load tests are conducted to measure deflections and strains in a structure, vibration tests are performed to measure vibration levels and modal parameters like natural frequencies and mode shapes of vibration and damping ratios of the different modal shapes.

4.3.2 Load Tests

Load testing of bridges can be conducted by subjecting the bridge structure to different kind of loading patterns that may simulate the live load vehicular traffic on the bridge. The objective is to assess the capacity of the bridge to sustain live loads. Load testing is not really a very new activity and has been in practice for centuries. However, with the involvement of modern technological procedures, it is probably convenient now to split load testing into:

A.) Static load testing

B.) Dynamic load testing

Static load testing utilizes static loads, which may be positioned on the bridge very slowly, so as to avoid any dynamic effects in the bridge. Dynamic load testing, on the other hand, uses dynamic or moving loads, which can excite the dynamic response of the bridge.

4.3.2.1 Static Load Testing

Static load testing employs ways and means to load the bridge with a static load. In some cases bridges were tested by applying a uniformly distributed load to simulate the traffic loading on the bridge, whereas in other instances a static load was placed on different positions on the bridge deck to evaluate the bridge response. In the early days, however, study of the bridge response was practically limited to observing deflections under the test loads and most of the times manual deflection meters were the only instruments used during this test. The bridge was considered to be safe if it did not exhibit excessive deflection under the load. Modern static load testing of the bridges in the field now uses

60

strain gauges in addition to various deflection meters like LVDTs (Linear variable differential transducer) and cable transducers to measure strains as well as deflections in the bridge deck. In the most common case, a gravel loaded dump truck or a multi axle truck trailer is parked on different marked points on the bridge deck and deflections and strains noted at points of interest. By plotting these measurements with the longitudinal location of the truck load, an influence line plot may be obtained for deflections or strains.

The response of the bridge to a static load test can be used to study a number of issues prevalent with bridges like load carrying capacity[10], load sharing between the girders[11], study of lateral load distribution factors[12], total deflection and the establishment of an alarm threshold for deflections[13] and the evaluation of in-situ strength and stiffness of structural elements to verify doubts over quality of construction[14]. This test has also been used to investigate the bridge response to new materials and new designs[15].

Types of Static Load Tests

Based on its purpose of use, the static load tests may be classified as Behaviour Tests, Diagnostic Tests and Proof Tests[12]. Behaviour tests may be carried out to study the behaviour of certain types of bridges, or to observe the load distribution characteristics of the bridge. Diagnostic tests, on the other hand may be conducted to diagnose a specific problem which may have become a recurring phenomena in many bridges and hence a serious cause of concern. And finally, the main purpose of conducting proof tests is to assess the safe load carrying capacity of the bridge. In a proof test, the bridge may be subjected to high static loads. However, to avoid the risk of damage, this static load is increased gradually but not allowed to increase beyond the linear elastic limit.

Static Test Loading

A good loading system for static load testing should have the following characteristics[16]:

i)   The load should be representative of the actual vehicular loads

ii)   The load should be adjustable, i.e. can be increased or decreased

iii)   The loading system should be easily manoeuvrable

iv)   The weight distribution and load location should be repeatable

Static loading in the past has been applied by either using concrete blocks, a truckload or hydraulic jacks[16]. Concrete blocks, of known weight, may represent uniformly distributed load on the bridge deck and are usually placed with the help of a crane. Lee et al.[17] used concrete blocks as test loads on the centre span of a three span concrete bridge, for conducting a static load test. The concrete blocks were meant to simulate a uniformly distributed load on the bridge and the maximum load that was applied was equivalent to a uniformly distributed load of about 20 kN/m^2, which was twice the design load.

An advantage with using concrete blocks or hydraulic jacks as the test load is the ability of the test set up to allow easy incrementing of the test load for measuring a load-deflection response. However, the biggest disadvantage with this type of loading is its lack of manoeuvrability, which doesn't allow testing with different load positions. A vehicle with pre weighed axles and measured axle spacings is the most efficient and easy way to statically load the bridges. This vehicle may be loaded with concrete blocks or gravel to simulate a heavy commercial vehicle on highways. The advantage in using this kind of a static load is its ease of placement in different positions and patterns to compare the load effects. The truckload is generally brought on to the bridge deck, very slowly, so as to act as a static load and to avoid any dynamic effects induced due to speed. Hydraulic jacks have also been used for applying loads through cables anchored in the ground, or weighted with heavy concrete mats.

Application of the Static Load Test

Numerous advantages of using field load testing to arrive at certain conclusions has led many departments of transportation all over the world to resort to field testing for this

62

purpose. Load testing of bridges to assess their load carrying capacity, was introduced in Ontario in the early 1970's by the Ministry of Transportation of Ontario (MTO)[12]. As a part of this program, more than 250 bridges were tested in Ontario. Similarly, many states in the United States are now developing extensive field testing programs for their highway infrastructure. For example, the Department of Transportation of Florida is one of the state departments which has established a comprehensive bridge-testing program. A computerized data base of over 200 load tests performed in Switzerland since 1973 has been established to study the behaviour of bridges subjected to a load test[13]. The Forsmo bridge in Norway was put to load testing shortly after its completion in September of 1995 to evaluate the response of the first aluminum road bridge in Norway[15].

Many bridges in Alberta have been recently put to load tests to observe different aspects of bridge behaviour. Load testing on Crowchild Trail Bridge in Calgary Alberta, was carried out to observe the response of the new steel free bridge deck[18]. Two trucks, each loaded to 80000 lbs were used to produce nine different load cases. In six of these load cases, the trucks were parked side by side at different positions along the bridge whereas the remaining three load cases involved a single truck. The tests conducted on the bridge on Highway 2, connecting to the city of Millet, were aimed at assessing the strength of the bridge girders which had been damaged as a result of broken prestressing tendons due to corrosion and high truck impacts[19]. Another objective of this test was to compare the performance of the conventional external post tensioning rehabilitation systems and FRP (fibre reinforced polymer) carbon strips and glass sheets.

A common concern with field-testing employing a mobile static load is the authenticity of the results, which may have been inflated or altered due to thermal effects. In a province like Alberta, where temperature changes of 20 degrees Celsius is a realistic possibility, a long test can possibly accumulate temperature related errors in the results. To avoid this problem, it is advisable to use temperature compensated Wheatstone bridge circuits and temperature compensated strain gauges for the material in use, i.e. steel or concrete. Taing et al.[23] took the truck load off the bridge after every five load point readings and measured a zero load reading. In most cases the difference was not

significant. Though Afhami et al.[18] noticed thermal effects in their measurements and a correction for the thermal output error was applied. Since their instrumentation layout also included six temperature probes, the change in the temperature of the active gauges was estimated, based on the readings of the six thermistors.

4.3.2.2 Dynamic Load Testing

Dynamic load testing is usually conducted on a bridge structure by running a loaded truck over the bridge at different speeds and various impact levels. This test is fairly similar to the static load test but draws its significance from the dynamic increment in the measurements due to the dynamic and vibratory effects of the interaction of the moving vehicle and the bridge. This dynamic increment is known as the DLA (Dynamic Load Allowance)[25], Dynamic Factor, Amplification Factor or Impact Factor[27] in the structural design and evaluation process.

Dynamic loads are usually applied to bridges by a combination of[25]:

a) Bumps in the riding surface or expansion joints, which result in direct impact to the bridge deck.

b) Dynamic variation in axle loads due to undulation and roughness in the riding surface

c) Dynamic response of the main longitudinal bridge components to the moving vehicle loads.

The current Canadian Bridge Design Code, S6-2000[25] presents the dynamic load allowance as an equivalent static load, expressed as a fraction of the design load and its value based on numerous dynamic load tests. Just like the static load test, the dynamic load test is also conducted to investigate issues related to the health of the bridge and consists of measuring deflections and strains as well as the natural frequencies and modes of vibration of the bridge.

Dynamic Test Loading

Loading for the Dynamic Load Test has been provided in the past in the following three modes[16]:

i) Normal traffic

ii) Test vehicle

iii) Vehicle Impact

The most realistic estimate of the bridge response to the dynamic effects of moving traffic can be obtained by subjecting the bridge to normal uncontrolled traffic and measuring its response for a reasonably long period of time. The results of this test can be used to obtain the dynamic characteristics of the bridge as well as realistic estimates of the stress ranges required for fatigue calculations[20]. However, the most common mode of dynamic loading during a dynamic load test has been the use of a test vehicle of known axle weights and spacings. This test vehicle is driven over the bridge at various speeds and the bridge response measured for each test run. The third type of dynamic loading, which has been referred to as Vehicle Impact, consists of either suddenly braking the speeding test vehicle on the bridge or driving the test vehicle on a bump or roughened surface on top of the bridge deck.

When a test vehicle is used for the dynamic load test, the test vehicle should have characteristics which can result in an upper bound value of the dynamic load allowance. The value of the dynamic load allowance obtained from an ordinary single vehicle load may hence be unconservative and can sometimes misleadingly result in values, which are not representative of the actual situation. Certain vehicle and bridge parameters that affect the value of the dynamic load allowance are[16]:

(a) Ratio of the natural frequencies of test vehicle and bridge: It has been shown by many researchers[24,25,26] in the past that the dynamic load allowance is a maximum if the first flexural frequencies of the test vehicle and the bridge are close to each other. Hence to obtain a large dynamic increment of the bridge response, if possible, the frequency of the vehicle should be brought close to that of the bridge.

65

(b) Ratio of the damping factors of the test vehicle and bridge: A small ratio of the two damping factors will result in a large value of the dynamic load allowance. This implies that the test vehicle should have low damping characteristics.

(c) Ratio of the test vehicle and bridge mass: A large value of this ratio will yield a large value of the dynamic load allowance implying that the test vehicle should be carrying a high load.

(d) Road roughness: The dynamic load allowance varies directly with the road roughness.

A dynamic load test can be measured with the help of strains, deflections or vibratory accelerations or natural frequencies. However, if dynamic testing is being conducted to evaluate the dynamic load allowance, it is preferable to monitor either strains or deflections because it is extremely difficult to obtain values of the dynamic factor from accelerometer output.

The ISIS "Guidelines for Structural Health Monitoring"[12] does not recommend carrying out a single dynamic load test to determine the dynamic load allowance for a given bridge owing to the presence of a fairly large scatter in the technical literature for the values of dynamic amplification factor. There is a very strong possibility that a single dynamic load test may yield a dynamic factor value, which is not representative of the worst possible case. The ISIS guidelines recommend using the CHBDC – 2000[25] values, which reflect the state of the art and are the product of a very large testing and statistical research exercise. Though, the guidelines still recommend the test as a useful research tool for improving specifications for the Dynamic Load Allowance for different types of bridges.

Dynamic Load Testing Procedure

Lee et al.[17] conducted a dynamic load test on an old concrete bridge to assess the bridge response and measure the natural frequencies and vibration characteristics. This bridge represented a large family of bridges that were built in Hong Kong immediately after the Second World War and for which no records exist regarding their design and construction. The dynamic load test was carried out by driving a truck weighing 2200 kg

at a varying speed. This truck was made to pass over a 60 mm high concrete bump, purposely constructed across the span to give vehicle impact to the bridge deck. The vehicle speed was measured by electrical contacts in steel strips, which get activated by the wheels of the vehicle and installed at the two ends of the span. Vibration of the bridge deck was measured by accelerometers and seismographs.

Rainer[21] and Pernica used passenger cars travelling at a speed of approximately 54 km/hr. and fully loaded tandem and single axle dump trucks running at approximately 32 km/hr. to test a three span prestressed concrete bridge to obtain its dynamic properties. Willmore Mark II seismometers were used to measure the vibrations of the bridge deck. The seismometer signals were recorded on a 7 channel FM tape recorder, displayed and refined on a 7 channel Honeywell visicorder and finally analyzed on a real-time Fourier spectrum analyzer to obtain the Fourier Amplitude Spectrum. The peaks in the plot exhibit the natural frequencies of vibration at various modes. The authors used the half-power bandwidth relation to determine the damping ratio for each natural mode.

Markey et al.[15] used the dynamic load test to determine the dynamic characteristics of the first Aluminum bridge built in Norway in September 1995. A twenty tonne lorry was used for this purpose. The truck was driven over the bridge at six different speeds between 5 km/hr. and 35 km/hr. and in four different test combinations, i.e. driving from east to west, west to east, driving over the undisturbed pavement and driving over the bridge with a neoprene plank placed across the deck to generate impact on the bridge deck. The measurements that were made during the test were those of acceleration, vertical deflection and strain.

The new steel free bridge deck of the Crowchild Trail Bridge in Calgary, Alberta was subjected to dynamic load testing first in 1997[22], before the new bridge deck was opened to traffic, and then in 1998[23], after the bridge had successfully completed one year of service. The static and dynamic load tests were carried out after one year of the bridge in service to observe any possible changes in the dynamic characteristics of the bridge. The major issues under observation during these tests were the strain distribution, deflection

67

profile, load sharing between the girders, dynamic behaviour of the new bridge deck and its dynamic and vibration characteristics. Afhami et al.[22] used the normal traffic on the bridge as the dynamic loading for the test. This consisted of a random mix of passenger cars and heavy and light trucks. Information such as the type of truck, number of axles and driving lanes was recorded on videotape. By combining the response data from instrumentation at two sections along the bridge, the time between the peak responses of the two gauges was measured and the speed of the vehicles was evaluated by using this time instant and the known distance between the two instrumented bridge sections. Taing et al.[23] used a three axle dump truck loaded to 40,220 kg. in all the tests. The front axle weighed 4290 kg and the second and third axles, which were tandem axles, weighed 15650 kg and 20280 kg respectively. Four truck speeds of 15, 30, 40 and 55 km/hr. were investigated during the test.

Billing et al.[24] carried out dynamic testing of 27 bridges of different materials (i.e. steel, concrete, timber) and various configurations in Ontario, to verify provisions of the dynamic load allowance and vibration included in the Ontario Highway Bridge Design Code (OHBDC). Four test vehicles which were representative of the heavy commercial trucks in Ontario were used. The first two were five axle tractor-trailers with gross weights of 391 and 414 kN. The third vehicle was an eight-axle combination with a gross weight of 580 kN and the fourth one was a three axle Inspector 50 service vehicle having a gross weight of 241 kN. Each test vehicle was driven over the bridge in each traffic lane at the maximum legal speed of 48 km/hr. In addition to the isolated truck test runs, scheduled runs were also made by the test vehicles closely following each other in the same lane or driving parallel in multi lanes where ever this was permitted as in the case of some one way bridges.

Data Acquisition for Dynamic Load Test

The data acquisition system, as described in article 4.3.1.1 of this chapter, can be used both for the static and dynamic load tests. However, the data acquisition system that is to be used in a dynamic load test must contain the continuous data scan feature, which is not a requirement in a static load test. This feature of the data acquisition board (DAQ) as

68

well as the data acquisition program instructs the computer on how often to scan the DAQ board. This setting is usually included in the DAQ program under the title of scan rate and measured in the units of Hz., which is basically the number of scans or samples that the program will record in a second. The continuous data scan feature in the data acquisition system provides the ability to record and produce a time series function of a measurement like strain or deflection.

Selecting a value of the scan rate mainly depends on the period of the monitoring program and the significance of the data size. Maintaining a fast scan rate for a long period of time will yield huge data files, which may not always be the feasible alternative. This is obviously due to the limitations in data storage space and efforts in strenuous data handling and processing. Many sophisticated programs may allow for scanning the DAQ board with a fast scan rate, screen for unwanted data and save only a small amount of data on the hard disk of the computer to efficiently use the storage space. In other cases, storage efficiency may be obtained by saving only the maximum, minimum and average values of each channel over a relatively long period of time. However, probably the simplest form of monitoring is to scan the DAQ board with a constant scan rate, for a relatively short period of time, and save all the data on the hard disk of the computer.

4.3.3 Vibration Tests

Highway bridges are usually susceptible to vibrations. Not only are most bridges sensitive to dynamic loads but they also have natural frequencies in the same range as those of heavy vehicles. The first resonant frequency of highway bridges is usually below 10 Hz. and often as low as 2 or 3 Hz. Because most heavy vehicles generate their dynamic wheel loads in the 1.5 to 4.5 Hz. frequency range therefore excitation of one system by the other can sometimes be significant[41]. Hence, knowledge of the modal parameters of a bridge can be useful and vibration testing has been successfully used for this purpose in the past.

Most of the early vibration testing on Civil Engineering structures consisted of safety inspection on railway bridges and involved monitoring vibration levels. In recent years it was realized that vibration testing could also be successfully used for estimating accumulated damage in a structure. The main objective of present day vibration testing is the estimation of the natural frequencies and associated mode shapes of vibration. These mode shapes of vibration for each natural frequency actually indicate the deflected shape, when the structure is vibrating at that frequency[28]. Since these modal parameters are functions of the physical properties of a structure like its stiffness, mass and damping, therefore a change in these physical properties should result in a change in the modal parameters of the structure. This relationship between the modal parameters and the physical properties of a structure can then be utilized to assess deterioration or damage in that structure from extended use, by monitoring the long-term dynamic response of the structure.

Vibration testing has been conducted on bridges in the field by the following two methods:

- Forced Vibration Testing
- Ambient Vibration Testing

4.3.3.1 Forced Vibration Testing

Forced vibration testing consists of inducing vibrations in the bridge with the help of an externally applied force of known magnitude and frequency. In most tests the input excitation is controlled as well as measured while in some tests the input may be controlled but not measured. The physical excitation devices used in a forced vibration test are generally known as vibrators, exciters or shakers. These excitation devices are usually designed to transmit a vibratory force into the structure. The structural response to forced vibration is measured with the help of accelerometers and converted to natural frequencies of vibration and their corresponding mode shapes.

70

Advantages and disadvantages of using the Forced Vibration Test

The main advantage of using this test is that the input excitation is in the control of the researcher who can alter the input loading to suit the test requirements. Besides, the forced vibration test is a better alternative for measuring higher modes and damping estimates because higher modes can only be excited to measurable levels by artificial excitation and damping estimates are known to be accurate under higher levels of excitation. However, there are several disadvantages associated with this test as well and the first and the foremost is the cost. Designing an adequate and safe artificial excitation system can be fairly costly and the bridge has to be taken out of service for conducting the test. Moreover, there is always some risk of causing damage in the bridge system as a result of the forced excitation.

Types of excitation systems

The external excitation systems are either of contacting or of non-contacting type. The contacting type systems are in contact with the structure during the whole test whereas the non-contact type systems do not have to be in contact with the structure throughout the test period. Different excitation systems used externally on bridges in the past can be described as:

i)   Contacting type

ii)   Impact type

iii)   Step relaxation or transient excitation

iv)   Other methods

i) Contacting type

The contacting type forced excitation systems remain in contact with the bridge throughout the test and are usually mounted on the bridge itself. The systems that have been used successfully in the past for this purpose are[29]:

•   Eccentric rotating mass vibrators

•   Electrohydraulic vibrators

The eccentric rotating mass vibrator uses a rotating shaft, with a mass, whose centre of mass is displaced from its centre of rotation. The vibratory motion of this exciter can be

71

either circular or rectilinear and the magnitude of the applied force as well as the operating frequency can be adjusted to suit the test requirements. This type of vibrator may have a single rotating mass or multiple rotating masses. The ones with multiple rotating masses are capable of generating forces in multiple directions[29]. However, the sinusoidal varying forces delivered by these exciters are proportional to the square of the rotational speed and reliable excitation is only achieved above 1 Hz[30]. Details on the design and construction of eccentric rotating mass exciters are given by Hudson[31] and Shepherd et al[32].

The electrohydraulic vibrators apply forces to the bridge deck, which are produced by the reciprocating motion of a mass that is driven by a hydraulic actuator. The weight of the mass can be adjusted to obtain different force magnitudes and the attainable stroke and frequency can be limited by the piston velocity and oil flow rate[33]. The Transport and Road Research Laboratory (TRRL) in England developed an electro-hydraulic pulse exciter that consists of four masses, each of which is driven by an electrohydraulic actuator[34]. The system is mounted on a mobile axle and hence capable of being moved on the bridge. The electrohydraulic vibrators generate forces of greater magnitude than the eccentric rotating mass vibrators but have not been used as much as the latter type, perhaps because of system cost and complications.

ii) Impact type

The impact type vibrators are generally not in contact with the structure continuously and only make contact when the impact is applied to the structure. These tests often use an instrumented hammer to provide the impact or a suspended mass to deliver blows to the structure[29]. The magnitude of the impulse can be varied by changing the mass of the hammer and the impact frequency range can be varied by changing the hammer head type. The impact type vibrators have been used by many researchers in the past[17,35] but they are not very suitable for use with large structures and there is always some risk of localized damage due to the application of high forces, at the point of contact.

72

iii) Step relaxation or transient excitation

The step relaxation or transient excitation methods usually consist of first deforming the structure to some predefined position and then releasing it to vibrate freely. These tests are sometimes also referred to as the "Pull Back Tests[12]". The initial deformation is provided by pulling the structure with cables or by loading it with hydraulic jacks[36,39,40]. The step relaxation methods are mechanically difficult to implement though these are known to be most effective for the determination of damping[12]. In most cases the input force is not measured and only the bridge response is observed.

iv) Other methods

A number of other methods which do not fall under the above mentioned categories or may be derivatives of these methods have also been used and published in the literature. Some of those methods consist of using a drop weight impact on a sand bed[37], a bolt gun[38], or vehicle impact[17].

4.3.3.2 Ambient Vibration Testing

The ambient vibration test, as the name suggests, is a test to record the ambient vibrations of a structure. This test determines the vibration characteristics of a structure that has been excited by wind, human activity or traffic. Unlike the forced vibration testing, input excitation is not under the control of the researcher and the structure is assumed to be excited by a relatively constant level of ambient sources of excitation like wind, waves, traffic or human activity. The response of the structure is measured by strategically placed accelerometers. An efficient placement of the instrumentation requires not only expertise in dynamic testing but also prior knowledge of the behaviour of the structure[39]. This may be accomplished by a detailed analysis of the structure, which is helpful in achieving the strategic placement of the accelerometers. The dynamic characteristics of a bridge experimentally obtained from an ambient vibration test can be used to refine the structure's numerical model.

Theory behind the test

The natural frequencies of a structure can be estimated using the Fourier transforms of the ambient vibration acceleration records[42,44]. The natural frequencies are determined from the peaks of the power spectral density of an ambient vibration acceleration record. The mode shapes can be determined experimentally using the ratios of the Fourier amplitudes at the natural frequencies. However these estimates are only possible if the natural frequencies are well separated and lightly damped, such that the response at a natural frequency is dominated by the corresponding mode shape.

Basic assumptions of the Ambient Vibration Test

The basic assumption of this method is that the excitation forces are a stationary random process with an acceptably flat frequency spectrum[29] and that only the response data of the structure can be used to evaluate the vibration parameters. Reliable estimates of modal frequencies and mode shapes can be obtained if the following conditions are met[42]:

i) Linearity

The structure behaves as a linear system. This means that a linear combination of individual force inputs will result in the same linear combination of the corresponding individual responses.

ii) Excitation

The structural modes of interest are significantly excited and the power spectrum of the excitation is continuous for the frequency range of interest.

iii) Modes well separated and lightly damped

The modes of interest are well separated and lightly damped. Thus the response at a natural frequency is characterized by the corresponding mode shape and the peaks in the power spectrum can be used to identify the natural frequencies.

74

Advantages of using the Ambient Vibration Test

Some advantages of using the ambient vibration test are as follows:

- The test is easy to conduct and involves the use of relatively simple instrumentation.

- The structure is still in service and hence there are no disruptions to traffic.

- There remains no need to assemble or erect special and expensive excitation devices.

- Since the test is conducted under service loading, therefore there is a possibility of correlating structural vibration response with the normal service loading.

- In long span bridges and other large structures, the ambient vibration test is the only practical method to apply because it will be very difficult to come up with a forced excitation device that is strong enough to shake a very large structure.

- By using this test, the cost of vibration measurement is reduced significantly.

Limitations of the Ambient Vibration Test

i) Low excitation levels

It is difficult to obtain good vibration records when the ambient excitation is very small or the structure is very stiff. In such cases it is important to use transducers that are very sensitive.

ii) Errors in damping measurement

Brownjohn (1988)[30] and Okauchi et al. (1992)[43] have shown that damping estimates from the same ambient vibration study can vary significantly, depending on the analysis technique used. Also it was observed that damping values depend on the amplitude of the excitation as well as the temperature of the structure. In some cases it was seen that the damping values would double for some of the modes when the excitation amplitude was doubled. At small amplitudes associated with ambient vibration, all of the damping estimates have shown to have significant amplitude dependence. This indicates that damping can not be reliably estimated using the ambient vibration techniques and the results from low level excitation may not be suitable to predict the structural response to high level excitation[45].

iii) Dominant excitation at specific frequencies

If rotating machinery is attached to the structure or is operated nearby at a particular frequency then the structure will respond at those frequencies. A similar dominant exciting force may also be provided by a heavy passing truck, if the test is being conducted under normal traffic[12]. This causes peaks in the power spectrum, which do not correspond to the natural frequencies of vibration of the structure and may be falsely identified as being the natural frequencies of the structure. Hence it is important to determine which dominant frequencies are caused by operating machinery or traffic. This can be done by comparing the identified frequencies with the analytically predicted frequencies to detect the extraneous frequencies.

iv) Added mass effects

When traffic is used to excite the bridges, the added mass of the vehicular traffic may make it difficult to identify the higher modes accurately, in an ambient vibration test. Ambient vibration measurements should be preferably taken when bridge traffic is light.

4.4 Vibration based damage assessment

Interest in the area of damage assessment based on field vibration measurements has increased significantly in the past two decades. This is mainly due to technological advancements, which have led to an improvement in vibration measurement techniques as well as field data acquisition and storage. As a consequence of the increased interest in research, many methods have been proposed by various researchers, dealing with vibration based damage assessment.

Rytter[7] has categorized these damage detection methods in four levels of interest:

- **Level 1** consists of the methods, which give an indication of the presence of damage in a structure.

- **Level 2** methods indicate damage in a structure as well as giving information about the possible location of that damage.

- **Level 3** methods estimate the magnitude of the damage in addition to detecting and localizing damage

- **Level 4** methods compile a complete picture and determine the safety levels of the structure, which may be subjected to some damage state.

While most methods are quite reliable within the level 1 scope of the problem, there is still considerable argument over the algorithms used by methods in levels 2 and 3. The structure is usually assumed to behave linearly both in the damaged and undamaged states and hence there is a need to incorporate non-linear models to improve the reliability of the results. Most methods require vibration signatures of the structure when it was newly built, for an accurate assessment, and these are rarely available. Moreover, many of these methods have been verified by simulation on simple structures and there has been too much emphasis on the analysis and determination of the behaviour of a structure with a known damage scenario instead of the detection of the damage scenario when the behaviour is known.

4.4.1 Damage Indicators

A damage indicator is a dynamic quantity that can be used to identify the existence of damage in a structure. Rytter[7] has given details of 16 conventional and non-conventional damage indicators that have been used in the past. However, only the damage indicators, which have been used more commonly, are outlined below:

- Natural Frequencies
- Mode Shapes
- Damping
- Transmissibility

4.4.1.1 Natural Frequencies

This is the most extensively used damage indicator available in the published literature. The observation that shifts in natural frequencies in a structure are caused by a change in the structural properties of a structure provides the basis of use for this indicator. The popularity of this indicator is due to the ease with which the natural frequencies of a structure can be determined with a high level of accuracy. Also, the natural frequencies

are sensitive to both local and global damage. Since most natural frequency formulations contain many geometric and material parameters like L, E, I etc. therefore a change in these parameters will be accompanied by a change in the natural frequency. Similarly localized damage can be detected by doing a comparative observation of the changes in the natural frequencies of various modes.

Natural frequencies depend on the square root of the stiffness change. Hence many researchers have observed that the natural frequency shifts, which are associated with structural changes or damage, are usually very small in magnitude. Either very precise measurements or extremely high levels of damage will produce appreciable shifts in the natural frequency damage indicator[9]. Farrar et al.[46] conducted testing on I-40 bridge and observed that no significant reduction in the modal frequencies were observed when the cross sectional stiffness at the centre of a main plate girder was reduced by 96 %. When damage is produced by cracking, the natural frequency indicator sometimes gives unreliable findings if crack closure occurs in a fatigue crack as opposed to an open crack[7]. Since most level 2 and 3 methods are based on linear elasticity, this effect often underestimates the cracking[47]. Fox[48] has concluded from his research that natural frequency is a reasonable damage indicator but does not yield sufficient information when used alone. In other words, the natural frequency indicator needs to be used in combination with other damage indicators to get conclusive meaningful information.

4.4.1.2 Mode Shapes

The change in the geometry of the mode shape of a structure is yet another parameter that has been extensively used in the past. Since damage will change the stiffness of certain localized areas, the mode shape of the damaged structure will differ from that of the undamaged structure in terms of deflection, rotation and curvature changes[7]. Hence a mode shape comparison of the damaged and undamaged states of the structure can provide useful information about the presence and location of damage. Some sort of a modal correlation technique is generally used for this purpose. Allemang[49], Kim[50] and Alampalli[51] have demonstrated the use of the Modal Assurance Criterion (MAC) technique for this purpose. However, accurate mode shape measurements are rather

difficult to make in the field and require a fairly extensive layout of the instruments, as compared to the natural frequency measurements. It has also been noticed that the efficiency of the mode shape as the damage indicator decreases as the extent of the damage increases[7]. This makes the use of the mode shape as an approximate indicator for locating damage. An alternative to the mode shapes, as shown by some researchers[52], is to use the mode shape derivatives like curvature.

4.4.1.3 Damping

The damping capacity of a structure often changes when damage occurs in a structure. This is evident from the fact that cracking would cause internal friction in the system which will change the damping as well as vibration characteristics of the structure.

Damping as been used as a potential damage indicator in some published work, but the sensitivity of this parameter to many external influences makes it an unreliable indicator if used alone. For example it was found that damping in a structure was highly sensitive to environmental conditions like temperature. Hence the use of damping as a damage indicator has been quite limited and restricted to use in conjunction with other damage parameters.

4.4.1.4 Transmissibility

The transmissibility ratio can be defined as the ratio of the amplitude of the response of a structure to the amplitude of the excitation, in steady-state forced vibration. The response of the structure can be measured in the form of displacement, velocity or acceleration. The introduction of damage in the structure, which will alter its stiffness, will also cause a change to this ratio. By reshaping the transmissibility ratio to some extent, this indicator has been utilized by some researchers towards verifying the presence of damage and locating it in the structure.

79

4.4.2 Methods for Damage Assessment

Several damage assessment methods have been proposed in the literature, which make use of various damage indicators and their combinations. Some of those methods also perform a sensitivity analysis to screen out the factors which may be affecting the changes in the damage indicators but do not constitute a structural stiffness change. A few of these methods are briefly described in this chapter.

4.4.2.1 Fox's Methods

Fox[48] proposed two relatively simple methods to detect and localize damage in a structure. The first method makes use of the changes in the natural frequencies and does a systematic comparison of the unaffected modal points to the affected modal points, to locate possible damage. The second method uses absolute and relative changes in the mode shapes of heavily affected modes. Fox evaluated the relative changes in the mode shapes by the following relationship:

$$RD_i = \frac{\phi_i^u - \phi_i^d}{\phi_i^u}$$

Where RD_i = Relative change in the ith mode shape

$\emptyset_i^u$ = ith mode shape function in the undamaged state

$\emptyset_i^d$ = ith mode shape function in the damaged state

The locations with significantly large values of the RD_i indicator on a RD_i vs. the modal span plot would point towards potential damaged areas. The method works well with simple structures but is difficult to apply to complex structures.

4.4.2.2 Dynamic Response Method

The Dynamic Response Method[7] records the dynamic response of the structure at predefined response stations, marked on the structure. This method makes use of the transmissibility ratio, which was described earlier in this chapter as a damage indicator. It was observed that the method would give better results if the excitation frequency was close to one of the natural frequencies and if the transmissibility ratio from more than one natural frequencies was used.

80

4.4.2.3 Stiffness Error Matrix Method

This method is based on the assumption that damage in a structure will cause changes to the stiffness matrix of the structural model. Hence, damage will be assessed by comparing the model stiffness matrices of the undamaged and damaged states of the structure. This is usually done by evaluating an error matrix E that gives the change between the two model matrices and is defined in its simplest form as:

$$E = K^d - K^u$$

Where,

K^d = Stiffness matrix of the damaged structure

K^u = Stiffness matrix of the undamaged structure

He et al.[53], Gysin[54] and Park et al.[55] have given different forms of the error matrix, which are advantageous to use and have wider application.

4.4.2.4 Stubbs and Osegueda method

Stubbs[56] and Osegueda[57] proposed a Level 2/3 method for damage identification, which uses a sensitivity relation to relate the changes in the natural frequencies of a structure to the changes in member stiffnesses due to damage. This sensitivity relation is formulated in the form of a damage sensitivity matrix. Hence, the fractional stiffness change of the members is obtained from the relation:

$$\alpha = F^{-1}Z$$

Where,

α = NE x 1 matrix containing fractional changes in the stiffnesses between the finite element model and the structure

Z = M x 1 matrix containing the fractional changes in eigen values

F = M x NE damage sensitivity matrix relating the fractional changes in stiffnesses to the fractional changes in eigen values.

This method uses a six step iterative algorithm to define a base line structure for comparisons with the damaged structure. The iterative sequence provides a modified

81

version of the initially assumed finite element model, which now has frequencies that are close (in the least square sense) to those of the existing damaged structure, even though none of the members of the baseline model are damaged. However the mode shapes of the base line model would be different from those of the damaged structure. Having identified the base line model, this method goes on to present the evaluation process for damage localization and severity estimation. The authors claim this method to be a level 3 method though it runs into difficulties when the number of modes is much fewer than the number of damage parameters.

4.4.2.5 Cawley and Adams method

Cawley and Adams[58] have presented a method to locate defects, which uses the measured changes in the natural frequencies of the structure. According to the CA method, the ratio of frequency changes in two modes is a function of the location of damage. A ratio between frequency shifts for modes i and j is worked out as $\delta\omega_i / \delta\omega_j$

A grid of possible damage points is considered and an error term is constructed that relates the measured frequency shifts to those predicted by a model based on a local stiffness reduction. A number of mode pairs are considered for each potential damage location and the pair giving the lowest error indicates the location of the damage. The formulation requires modal characteristics of the undamaged state of the structure and does not account for possible multiple damaged locations.

4.4.2.6 Flow chart of damage identification methods

Figure 4.1 provides a flow chart showing the family of existing damage identification methods, their damage detection parameters and a brief description of the principle of each of those methods. The flow chart is compiled in this form to provide a quick review of what presently exists in the literature regarding structural damage detection.

82

4.5 Conclusions

Field testing of structures has been successfully used in the past to evaluate useful information about the structural health. This chapter provides a complete picture of this process and summarizes the published literature, starting from field testing and data acquisition to the diagnosis of damage and defects in the structure. The field testing review in this chapter was used to constitute the test methodology of this thesis, while the damage detection theories provided the background for commenting on the shear key condition, based on the natural frequency and mode shape results. In general, most of the published literature requires the use of modal parameters from the structure, at the time of its construction, for effective comparison between the damaged and undamaged states of the structure. Unfortunately this information is not always available, which leaves the researcher to back track to the base line model (finite element model) with the help of information available from the damaged structure.

83

Based on observations that changes in structural properties cause changes in vibration frequencies. These methods relate damage detection to shifts in natural frequencies.

Based on the level of correlation between modes, from the test of undamaged structure and damaged structure, using some correlation technique like the MAC

An alternative to using mode shapes is using mode shape derivatives, such as curvature. It was shown by some researchers that absolute changes in mode shape curvature can be a good indicator of damage

Typically damage is detected by comparing the flexibility matrix synthesized using the modes of the damaged structure to the flexibility matrix synthesized using the modes of the undamaged structure or a FEM model

Using frequency changes

Using mode shape changes

Using mode shape curvature changes

Use direct comparison of the measured parameter matrices to estimate the location of damage

Based on dynamically measured flexibility matrix

Damage Identification Methods

Based on changes in measured stiffness matrix

Matrix Update Methods

Nonlinear Methods

Neural Network Based Methods

Other Methods

Based on modifying structural model matrices such as mass, stiffness and damping to reproduce as closely as possible the measured static or dynamic response from the data. Comparisons of the updated matrices to the original correlated matrices provide an indication of damage

Simulate non linear systems using linear techniques.

System of cascaded sigmoid functions where the outputs of one layer, multiplied by weights, summed, then shifted by a bias are used as the inputs to the next layer.

- Random decrement technique
- Changes in anti-resonances
- Non linear least squares meth.
- Contrast maximization meth.
- Modal energy transfer ratio
- Damage location vector
- Operating deflected shapes
- Use of Ritz and vectors

Figure 4.1: Flow Chart showing detail of damage detection methods

4.6 References

1.   Pessiki S., Olson L. (1997). "Innovations in non-destructive testing of concrete", ACI International SP-168.

2.   Cartz, Louis (1995). "Nondestructive Testing", The Materials Information Society ASM International, pp.15-23.

3.   Mix, Paul E. (1987). "Introduction to nondestructive testing – A training guide", John Wiley & Sons, Wiley – Interscience Publication, pp. 104-149.

4.   Olson, L.D., Wright, C.W.(1990). "Nondestructive Testing for Repair and Rehabilitation," American Concrete Institute, Concrete International, March, Vol. 12, No. 3, pp. 58-64.

5.   Olson, L.D. (1992) "Sonic NDE of Structural Concrete", Nondestructive Tesing of Concrete Elements and Structures, Proceedings of Sessions sponsored by the Engineering Mechanics Division of the American Society of Civil Engineers and the Structures Congress, San Antonio, Texas, April 13-15, pp. 70-81.

6.   Ouyang, C., Landis E., and Shah, S.P. (1992) "Damage Assessment in Concrete Using Acoustic Emission", Nondestructive Tesing of Concrete Elements and Structures, Proceedings of Sessions sponsored by the Engineering Mechanics Division of the American Society of Civil Engineers and the Structures Congress, San Antonio, Texas, April 13-15, pp. 13-24

7.   Rytter, Anders, (1993), "Vibration Based Inspection of Civil Engineering Structures" PhD Thesis, University of Aalborg,

8.   Ansari, Farhad, (2000), "Condition Monitoring of Materials and Structures", American Society of Civil Engineers (ASCE), Library of Congress Catalog Card no. 00-038086

9. Doebling, S.W., Farrar, C.R., Prime, M.B., & Shevitz, D.W. (1996), "Damage Identification and Health Monitoring of Structural and Mechanical Systems from Changes in Their Vibration Characteristics: A Literature Review", Los Alamos National Laboratory, New Mexico, Report No. LA-13070-MS, May 1996.

10. Bakht, B. (1981), "Testing of the Manitou Bridge to determine its load carrying capacity", Canadian Journal of Civil Engineering (Can. J.), 8(2), pp. 218-229.

11. Afhami, S., Khattak, N., Cheng, R. & Alexander, J. (2000), "Field Assessment of the Bridge Rehabilitation in Fort Saskatchewan, Alberta", Report Prepared for the City of Fort Saskatchewan by the Structures Group, University of Alberta.

12. ISIS (Intelligent Sensing for Innovative Structures) Canada, (2000), "Guidelines for Structural Health Monitoring", Design Manual of ISIS Canada, The Canadian Network of Centres of Excellence on Intelligent Sensing for Innovative Structures

13. Hassan, M., Burdet, O. & Favre, R., "Analysis and Evaluation of Bridge Behaviour Under Static Load Testing Leading to Better Design and Judgment Criteria", Proceedings of the Fourth International Bridge Engineering Conference, pp. 296-303.

14. Srinivasulu, P., et al., (1997), "Structural Assessment by in-situ Static and Dynamic Testing", Collection of papers published by E & FN Spon, 2-6 Boundary Row, London SE18HN and the book titled, "Structural Assessment – The role of large and full scale testing" edited by K.S. Virdi, pp. 355-362.

15. Markey, I., Ostlid, H. & Solaas, K. (1997) "Testing a New Aluminium Road Bridge", Collection of papers published by E & FN Spon, 2-6 Boundary Row, London SE18HN and the book titled, "Structural Assessment – The role of large and full scale testing" edited by K.S. Virdi, pp. 141-148.

16. Derucher, K.N., Moses, F. & Sweeney R.A.P. (1980), "A Guide for the Field Testing of Bridges" An ASCE publication prepared by the Working Committee on Safety of Bridges, pp. 38-42.

17. Lee, P.K.K., Ho, D., & Chung, H.W. (1987), "Static and Dynamic Tests of Concrete Bridge", ASCE Journal of Structural Engineering, January, 113(1), pp. 61-73.

18. Afhami, S. and Cheng J.J.R. (1999), "Field Instrumentation and Monitoring of Crowchild Trail Bridge in Calgary, Alberta", Report prepared for the City of Calgary by the Structures Research Group, University of Alberta.

19. Khattak, N., Afhami S., Cheng J.J.R., Alexander J., (1999), "Field Assessment of the Bridge Rehabilitation in Millet Alberta", Report prepared for Alberta Transportation, by the Structures Research Group, University of Alberta.

20. Cicci F. and Csagoly P. (1974), "Assessment of the Fatigue Life of a Steel Girder Bridge", Research Report 192, Ministry of Transportation and Communications of Ontario, Downsview. September.

21. Rainer, J.H. & Pernica G. (1979), "Dynamic testing of a modern concrete bridge", Canadian Journal of Civil Engineering (Can. J.), September, Vol.6, pp. 447-455.

22. Afhami S., Alexander S.D.B. & Cheng J.J.R., (1998), "Field Instrumentation and Monitoring of Crowchild Bridge in Calgary, Alberta", International Conference on Short & Medium Span Bridges (SMSB), Calgary, Alberta, July13-16.

23. Taing, K.K., Cheng J.J.R. & Afhami, S. (1999), "Field Assessment of Crowchild Bridge in Calgary, Alberta", CSCE Annual Conference.

24. Billing, J.R., (1984), "Dynamic Loading and Testing of Bridges in Ontario", Canadian Journal of Civil Engineering (Can.J.), December, Vol.11, pp. 833-843.

25. CAN/CSA-S6-2000, Canadian Highway Bridge Design Code & Commentary

26. Csagoly, P.F., Cambell, T.I. & Agarwal, A.C., (1972), "Bridge Vibration Study", Research Report 181, Ministry of Transportation and Communications of Ontario, Downsview, September.

27. AASHTO, American Highway Bridge Design Code.

28. Clough R. & Penzien J., (1993), "Dynamics of Structures" McGraw-Hill, New York,

29. Salawu O.S. & Williams C., (1995), "Review of full-scale dynamic testing of bridge structures", Engineering Structures, February, Volume 17, Number 2, pp.113-121.

30. Brownjohn, J.M.W., (1988), "Assessment of structural integrity by dynamic measurements", PhD Thesis, Department of Civil Engineering, University of Bristol, Bristol, UK.

31. Hudson, D.E., (1962), "Synchronized vibration generators for dynamic tests of full scale structures", Research Report, Earthquake Engineering Research Laboratory, California Institute of Technology, Pasadena, California, USA.

32. Shepherd, R.T. & Reay, A.M., (1967), "Some apparatus for small amplitude dynamic testing of multistorey buildings", Journal of the British Society for Strain Measurements, No. 4, pp. 16-21.

33. Salawu, O.S. & Williams C., (1994), "An Excitation System for Dynamic Testing of Large Structures", Journal of Testing and Evaluation, JTEVA, Vol.22, No.4, July, pp. 370-375.

34. Leonard, D.R., (1974), "Dynamic tests on highway bridges – Test procedures and equipment", TRRL Laboratory Report 654, Transport and Road Research Laboratory, Berkshire, UK.

35. Green, M.F. & Cebon, D., (1993), "Modal testing of two highway bridges", Proceedings of the 11th International Modal Analysis Conference (IMAC), Kissimme, FL, USA, Vol.2, pp. 838-844.

36. Douglas, B.M., Maragakis,E.A. and Nath, B., (1990) "Static deformations of bridges from quick release dynamic experiments", ASCE Journal of Structural Engineering, 116(8), pp. 2201-2213

37. Morgan, B.J. and Oesterle, R.G., (1985), "On-site modal analysis – a new powerful inspection technique", Proceedings of the 2nd International Bridge Conference, Pittsburg, PA, USA, pp. 108-114.

38. Wood, M.G., Friswell, M.I. and Penny, J.E.T., (1992), "Exciting large structures using a bolt gun", Proceedings of the 10th International Modal Analysis Conference (IMAC), San Diego, CA, USA, Vol 1, pp. 233-238.

39. Ventura, C.E., Felbar, A.J. and Stiemer, S.F., (1996), "Determination of the Dynamic Characteristics of the Colquitz River Bridge by Full-scale Testing", Canadian Journal of Civil Engineering, Vol. 23(2), pp. 536-548.

40. Dorton, R.A., Holowka M. and King, J.P.C., (1977), "The Conestogo River Bridge – Design and Testing", Canadian Journal of Civil Engineering, Vol. 4, No.1, March.

41. Green, M., (1990), "The dynamic response of short span highway bridges to heavy vehicle loads", Ph.D. Thesis, Department of Civil Engineering, Queens College, November.

42. Felber, A.J., (1995), "Development of the Hybrid Bridge Evaluation System", Ph.D. Thesis, Department of Civil Engineering, University of British Columbia.

43. Okauchi, L., Miyata, T., Tatsumi, M. & Kiyota, R. (1992), "Dynamic Field Tests and Studies on Vibration Characteristics of Long Span Suspension Bridges, JSCE Journal of Structural Engineering and Earthquake Engineering, Vol 9, pp.89-100

44. James,G.H., Carne,T.G., Lauffer, J.P. and Nord, A.R., (1992), " Modal testing using natural excitation", Proceedings of the 10th International Modal Analysis Conference (IMAC), San Diego, CA, USA, Vol. 2, pp. 1209-1216.

45. Abdel-Ghaffar, A.M. & Scanlan, R.H., (1985), " Ambient vibration studies of Golden Gate bridge", ASCE Journal of Engineering Mechanics, 111(4), pp. 463-482.

46. Farrar, C.R., Baker, W.E., Bell, T.M., Cone, K.M., Darling, T.W., Duffey T.A., Eklund A., and Migliori A. (1994), "Dynamic Characterization and Damage Detection in the I-40 Bridge Over the Rio Grande", Los Alamos National Laboratory Report LA-12767-MS.

47. Biswas, M., Pandey, A.K. & Samman, M.M., (1990), "Diagnostic experimental spectral modal analysis of a highway bridge", International Journal of Analytical and Experimental Modal Analysis, Vol.5, No.1, January.

48. Fox, C.H.J., (1992), "The Location of Defects in Structures: A Comparison of the Use of Natural Frequency and Mode Shape Data", Proceedings of the 10th

International Modal Analysis Conference (IMAC), San Diego, CA, USA, Vol. 1, pp. 522-528.

49.   Allemang, R.J. and Brown, D.L., (1982), "A Correlation Coefficient for Modal Vector Analysis", Proceedings of the 1st International Modal Analysis Conference, Orlando, Florida, USA, pp. 110-116.

50.   Kim, J.H., Jeon, H.S., and Lee, C.W., (1992), "Application of the Modal Assurance Criteria for Detecting and Locating Structural Faults", Proceedings of the 10th International Modal Analysis Conference (IMAC), San Diego, CA, USA, Vol. 1, pp. 536-540.

51.   Alampalli, S., Fu G., and Aziz, I.A., (1992), "Modal Analysis as a Bridge Inspection Tool", Proceedings of the 10th International Modal Analysis Conference (IMAC), San Diego, CA, USA, Vol. 2, pp. 1359-1366.

52.   Panday, A.K., Biswas, M. and Samman, M.M., (1991), " Damage Detection from Changes in Curvature Mode Shapes", Journal of Sound and Vibration, 145(2), pp.321-332.

53.   He, J. and Ewins, D.J., (1986), "Analytical Stiffness Matrix Correction Using Measured Vibration Modes", International Journal of Analytical and Experimental Modal Analysis, July, Vol.1, No.3, pp. 1-9.

54.   Gysin, H.P., (1986), "Critical Application of an Error Matrix Method for Location of Finite Element Modeling Inaccuracies", Proceedings of the 4th International Modal Analysis Conference (IMAC), pp. 1339-1351.

55.   Park, Y.S., Park, H.S., and Lee, S.S., (1988), "Weighted Error Matrix (WEM) Application to Detect Stiffness Damage by Dynamic Characteristic

Measurement", International Journal of Analytical and Experimental Modal Analysis, July, Vol.3, No.3, pp.101-107.

56. Stubbs N., Park S., Sikorsky C. and Choi S., (2000), " A global non-destructive damage assessment methodology for civil engineering structures", International Journal of Systems Science, Vol.31, No.11, pp. 1361-1373.

57. Stubbs, N., and Osegueda R., (1990), "Global Non-Destructive Damage Evaluation in Solids", The International Journal of Analytical and Experimental Modal Analysis, 5(2), pp. 67-79.

58. Cawley, P. and Adams R.D., (1979), "The Location of Defects in Structures from Measurements of Natural Frequencies", Journal of Strain Analysis, Vol.14, No.2, pp. 49-57.

5.0 FIELD ASSESSMENT OF THE BRIDGE REHABILITATION IN FORT SASKATCHEWAN, ALBERTA[*]

5.1 Introduction

The 99th Ave. Bridge in Fort Saskatchewan is a two-lane, single-span overpass. Its superstructure consists of six adjacent precast, prestressed channel shaped FC girders. The original bridge did not have a cast in place concrete deck. Due to extensive cracking of the asphalt in both transverse and longitudinal directions, the bridge asphalt pavement was replaced with a cast in place concrete deck in July of 1998. The new concrete deck has no longitudinal reinforcement, but was prestressed in the transverse direction. Underslung steel diaphragms were attached to the webs of the FC girders to improve the behaviour of the bridge.

To evaluate the effectiveness of the bridge rehabilitation and to better understand the behavior of the FC girder bridges, the bridge was instrumented with 28 strain gauges, 10 cable transducers, and 4 accelerometers. Of particular importance is the observation of longitudinal cracking at shear key locations and comparison of the behaviour of the bridge with and without a concrete deck. Hence, static and dynamic load tests, as well as ambient vibration tests, were conducted before and after the rehabilitation. Relevant information such as the influence line for deflection and strain, load sharing among the girders, dynamic factor, damping of the bridge, natural frequencies and their corresponding mode shapes was extracted from these tests.

Conclusions from three independent measurements, namely deflection, strain, and vibration were in excellent agreement and complemented each other. Relative vertical deflections of 1.5 to 2 mm between the adjacent legs of the girders, before rehabilitation,

---

[*] Essentials of this chapter include portions of the Structural Engineering Report prepared for the city of Fort Saskatchewan.

indicate some movement at the shear key lines. Transverse stressing of the deck and underslung diaphragms were effective in increasing the flexural stiffness of the bridge in the transverse direction, and hence, enhancing the load sharing among the girders.

5.2 The Fort Saskatchewan Bridge

The Fort Saskatchewan Bridge is located on the 99th Ave. in the city of Fort Saskatchewan and in the province of Alberta. It is a two-lane, single-span bridge built in 1975, to carry traffic over Highway 15. In 1998, to expand the 99th Avenue to four lanes, a second bridge was built parallel to but entirely separated from the original bridge. To strengthen the old bridge against shear key cracking and in order to match the structural capacities and certain aesthetic features of the two bridges, a rehabilitation program was carried out on the original bridge. During this rehabilitation, the traffic was diverted onto the new bridge.

Figure 5.1 shows the plan of the original 99th Ave. FC Girder Bridge in Fort Saskatchewan. Figures 5.2 and 5.70 show the elevation of the bridge. As illustrated in figures 5.3 and 5.71, the superstructure of the bridge consists of six precast prestressed channel-shaped FC girders. Before rehabilitation, the bridge had no cast in place concrete deck and its asphalt pavement was extensively cracked in both transverse and longitudinal directions. While cracks in asphalt, especially the transverse cracks, are usually related to material properties and temperature effects, initiation of the longitudinal cracks is a result of the relative movement of the adjacent girders. Figures 5.4 and 5.5 show the cracking of asphalt before rehabilitation.

The rehabilitation of the bridge consisted of replacing the asphalt with a fiber reinforced, silica fume, concrete overlay and installing steel underslung assemblies on the underside of the bridge. Figures 5.6 and 5.7 show that the 100mm concrete deck is prestressed in the transverse direction but has no longitudinal reinforcement. Details of the underslung diaphragms are illustrated in figures 5.8 and 5.9.

94

Underslung assemblies were designed to impart torsional stiffness to the transverse cross section, limit the vertical and lateral movement of adjacent girder legs, enhance the load sharing between the girders and increase the shear capacity of the bridge using external stirrups where needed. It was believed that this combination of the underslung assemblies and transverse post-tensioned deck would control any movement at shear key lines and prevent them from cracking in the future.

To evaluate the effectiveness of the bridge rehabilitation and to better understand the behaviour of the FC Girder Bridges, a field assessment program was developed at the University of Alberta in collaboration with ISIS Canada, City of Fort Saskatchewan, and Stantec Consulting Ltd. in Edmonton. Twenty-eight strain gages were installed on the FC girders, post tensioning tendons, and underslung diaphragms. Ten cable transducers and four accelerometers were used to measure deflections and vibrations, respectively. Static and dynamic load tests, as well as ambient vibration tests, were conducted both before and after the rehabilitation which made it possible to study the behaviour of the bridge with and without a concrete deck. In addition, strain in the underslung diaphragms, caused by deck stressing and passing vehicles was also measured. This chapter will describe the field instrumentation of the Fort Saskatchewan Bridge, the conducted tests, their results, and a discussion.

Information such as influence line for deflection and strain, load sharing among the girders, dynamic factor, and damping of the bridge was obtained from the load tests. Information such as natural frequencies of the bridge and their corresponding mode shapes was determined by the ambient vibration tests. All load tests were conducted once with a grader and once with a truck. To avoid repetition, only the results from load tests with the truck are presented.

95

5.3 Instrumentation and Conducted Tests

This section provides all relevant details on the field tests that were conducted on the Fort Saskatchewan Bridge and the accompanying instrumentation that was used for these tests.

5.3.1 Instrumentation

Twenty-eight strain gauges were installed on the FC Girders, post-tensioning tendons, and underslung diaphragms. During the load tests, ten cable transducers were attached to the girders to measure their deflections. Four accelerometers were used to perform the ambient vibration tests.

Figures 5.10 and 5.11 show the location of the twelve strain gauges installed on the FC girders. Strain gauges used were 120 Ω, 25mm foil gauges temperature compensated for concrete. Installation of these gauges involved traffic control on Highway 15 (beneath the bridge). To avoid closure of this highway, these strain gauges were located 4 meters off the mid-span of the bridge. This enabled the instrumentation team to install the gauges under the bridge, by closing only one lane and still allow room for traffic to drive on the Highway 15 underpass. Figures 5.72 and 5.73 show the installation of strain gauges on the girders in the field.

Two of the post-tensioning tendons, as shown in figure 5.6, were gauged with 120 Ω, 5mm gauges. To enhance strain measurements, four gauges were mounted on each tendon in a full-bridge configuration (figure 5.74). With such configuration, strain measurements become independent of the temperature change. Figures 5.12 and 5.74 show the location of the eight gauges mounted on the underslung diaphragms. These gauges were also 120 Ω, 5mm gauges compensated for steel. Half-bridge configuration was used to eliminate thermal errors and therefore, strains were measured at four locations. Location of the cable transducers is presented in figures 5.10 and 5.13. The cable transducers were mounted on the traffic rail in the middle of Highway 15 (figure

5.77), one meter off the mid-span of the bridge. Wires were stretched vertically from the cable transducers to the girders. The reliability of such deflection measurements was confirmed with a level survey in one of the load tests as seen in figure 5.75. To determine the natural frequencies, four accelerometers were attached to the top surface of the bridge using a double adhesive tape. The corresponding mode shapes were determined at the three sections shown in figure 5.14, by moving the accelerometers around. The circle mark in figure 5.14 indicates the positions of the accelerometers on the bridge deck plan. Figure 5.76 shows the accelerometers and signal conditioners on the bridge deck.

5.3.2 Conducted Tests

Load tests and ambient vibration tests were conducted before and after rehabilitation. In addition, strains in tendons and underslung diaphragms due to transverse deck stressing and passing trucks were measured. In the load tests, a 15.3 tonne grader and a 23 tonne truck were separately used (figures 5.78 and 5.79), however only the test results with the truck are described in this chapter. Table 5.1 provides a summary of the tests and measurements on the 99 Ave. Bridge.

Similar three axle trucks weighing 23 tonnes were used to perform the load tests before and after the rehabilitation of the bridge. Dimensions and load of axles of these trucks are presented in figures 5.15 and 5.16. Before rehabilitation, the truck was positioned on either right lane, centre mark, or left lane as illustrated in figures 5.17 through 5.19. After rehabilitation, however, as the bridge was open to traffic and it was not possible to close both lanes simultaneously, therefore tests with truck on centre mark were not performed.

Each static test was conducted in the shortest time possible so that temperature does not change during the test and hence its effects can be ignored. The second axle of the truck was positioned at four-meter intervals on the bridge deck. Other axles were positioned only at the supports ($x = 0$ and 32m) and at the strain gauge location ($x = 20$m). Dynamic tests were performed at varying truck speeds (intervals of about 15 km/hr). Actual speeds

of the truck have been verified by calculating directly from the collected strain and/or deflection data, and are presented in table 5.2. In some cases, the condition at the construction site was such that the driver could not speed up the truck to 45 km/hr or by doing so, could not bring it to stop safely. Table 5.2 also presents the scan rate and the total time of acquiring data. A digital low-pass filter of 19 Hz was used to eliminate electromagnetic noise.

Table 5.1 – Summary of the tests and measurements on the bridge

Date	Test	Measurements
May 21, 1998	Preliminary test – Passing trucks	Strain in girders
June 1, 1998	Static and dynamic load tests – Before rehabilitation Truck and Grader	Strain in girders Deflection by cable transducers
June 2, 1998	Static load tests – Truck	Deflection by level surveying
June 11, 1998	Ambient vibration test – Before rehabilitation	Accelerations Mode shapes
Aug. 19-23, 98	Evaluation of underslung assembly under deck stressing	Strain in tendons Strain in underslung diaphragms
Aug. 23, 1998	Ambient vibration test – After rehabilitation	Accelerations Mode shapes
Sept. 22, 1998	Evaluation of underslung assembly under passing trucks	Strain in tendons and girders Strain in underslung diaphragms
Oct. 6, 1998	Static and dynamic load tests – After rehabilitation Truck and Grader	Strain in girders Deflection by cable transducers

In the ambient vibration test, the bridge is randomly excited by low level forces such as wind and human activities; hence the measurements (accelerations) are taken for a long time. For each set of measurement 200 seconds of data was collected at the scan rate of

98

200 Hz, resulting in a resolution of 0.005 Hz for the frequencies. The first three mode shapes have been determined for the three axes shown in figure 5.14.

Table 5.2 – Dynamic load tests

Location of truck	Time Stamp	Speed	Scan Rate (Hz)	Total Time (Sec.)
Before rehabilitation – June 1, 1998				
Right Lane	P0521	18 km/hr	1000	20
	P0504	32 km/hr	1000	10
	P0507	33 km/hr	1000	10
Centre Mark	P0519	16 km/hr	1000	20
	P0509	34 km/hr	1000	10
	P0510	35 km/hr	1000	10
	P0527	60 km/hr	1000	10
Left Lane	P0522	18 km/hr	1000	20
	P0513	33 km/hr	1000	10
	P0515	34 km/hr	1000	10
After rehabilitation - Oct. 6, 1998				
Right Lane	P0128	16 km/hr	500	20
	P0131	29 km/hr	500	10
	P0136	51 km/hr	500	10
Left Lane	P0110	16 km/hr	500	20
	P0113	30 km/hr	500	10
	P0105	40 km/hr	500	10

In each axis, one accelerometer was kept as reference while others were moved around. The relative magnitude of the power spectrum between the reference sensor and all others are used to estimate the mode shapes at each natural frequency.

Tendons and underslung diaphragms have been studied in two load cases, 1) transverse stressing of the deck, and 2) live truck loadings. In the first load case, an initial set of

99

readings was taken on August 19, 1998 at air temperature of 22 °C. The final set of readings was done after stressing the deck on August 23, 1998 at air temperature of 26 °C. In the 2nd load case, strain caused by several passing trucks was measured for gauges on the tendons, gauges on the underslung diaphragms, and gauges G2, G4, G6, G8, G10, and G12 on the FC Girders.

5.4 Test Results

Results of the three field tests, i.e. the ambient vibration test, the static load test and the dynamic load test are presented in the following sections.

5.4.1 Ambient Vibration Test

The first three natural frequencies of the bridge before rehabilitation, have been identified as peaks in the power spectrum, as shown in figure 5.20, and were respectively 2.82, 3.25, and 5.43 Hz. Due to rehabilitation, as illustrated in figure 5.21, the first two natural frequencies changed to 2.77 and 3.38 Hz. An interesting finding is the lack of the previously third natural frequency. As illustrated in figures 5.22 and 5.23, in the longitudinal direction, all these frequencies associate with the first fundamental mode shape. However, as shown in figure 5.24, their corresponding mode shape in the transverse direction is totally different. In other words these three mode shapes may yield different deflected shapes of the whole bridge but all of them are really formed by the first fundamental mode shape of the individual girder and depend upon the timing of the movement of the girders with respect to each other.

At the frequency of 2.82 Hz, all the girders move up and down simultaneously with almost equal magnitude. This mode will be called the first vertical mode shape. At the frequency of 3.25 Hz, however, when the east edge girder moves down, the west edge girder moves up, and vice versa. The relative movement of the girders is almost linear. This mode will be referred to as the first torsional mode shape. Unlike the first two mode shapes, the frequency of 5.43 Hz is associated with the bending of the bridge in the

100

transverse direction; while the two edge girders move up on both the ends, the middle girders move down, and vice versa. This mode suggests that the bridge deck was not rigid before rehabilitation, and our inability to measure it after rehabilitation is evidence of a more rigid deck in the transverse direction, which is an obvious improvement.

5.4.2 Static Load Test

Deflections and strains were measured for three transverse position of a truckload before rehabilitation and two positions after the rehabilitation of the bridge. Note that the deflection measurements are at one meter off the mid-span of the bridge. For the truck specifications shown in figures 5.15 and 5.16, a simple analysis shows that the deflection at the mid-span should be only 0.5 percent larger than the deflections at one meter off the mid-span. Strain measurements, however, were at a section four meters off the mid-span. This would result in moments (and strains) that would be roughly 8.3% smaller than those expected at the mid-span.

5.4.2.1 Results of Deflection Measurements

Figure 5.25 summarizes the deflection results in one of the static tests, and is presented as an example. It can be seen that the maximum deflection is obtained when the second axle of the truck is located at the middle of the bridge (or the steering axle at $X = 16 + 4.54 = 20.54$ m). For the steering wheel at $X = 20.54$ m, load sharing among the girders based on the deflection measurements is presented in figures 5.27 through 5.29 for the cases of truck on the right lane, centre mark, and left lane, respectively. The behaviour of the bridge can be better visualized by superposing the two test results with the truck on the right and left lanes, as presented in figure 5.30. In this case, the four middle girders are directly loaded by two trucks, and the two edge girders share part of the load of the trucks. The largest measured deflection before rehabilitation was 12.8 mm. Due to rehabilitation, the largest deflection has reduced to 11.2 mm, which is an improvement in the load sharing of the edge girders.

101

To quantify load sharing, we will look at the lateral live load distribution factors, evaluated on the basis of measured deflections at each girder, during the load test. The lateral live load distribution factor (LLDF) was defined as the ratio of the deflection of a particular girder to the total deflection measured on all the girders.

$$LLDF = \frac{\Delta_i}{\Delta_{total}} \times 100 = \text{The percentage of the total load resisted by each girder}$$

Where $\Delta_{total} = \Delta_i + \Delta_j + \Delta_k$ .... , i.e. total deflection of all girders

Figure 5.80 shows an improvement in the load sharing after rehabilitation with respect to the LLDF before and after rehabilitation. When the truck was in the right lane, the LLDF for girder no.3 reduced from 24% to 18% after rehabilitation, whereas that for girder no. 6 increased to 8% from 3%. Similar effect was observed when the truck was placed in the left lane. This shows that load is now being shared away from the loaded girders and transferred on to the end giders, which are not directly under the load.

5.4.2.2 Results of Strain Measurements

Figure 5.26 shows that the maximum strain (measured at 4 m off mid-span) occurs when the second axle of the truck is at the gauge location (the steering axle at $X = 24.54$ m). The average strain at this section was about 50 $\mu\varepsilon$ for all the three transverse location of the truck. The plots showing load sharing among the girders, based on strain measurements with the steering axle of the truck at $X = 24.54$ m, are presented in figures 5.31 through 5.33. Superposition of the test results with the truck on right and left lanes is presented in figure 5.34. It can be seen that the edge girders are contributing more after the rehabilitation (closer to a uniform distribution of strains), and the maximum strain has decreased from 140 $\mu\varepsilon$ to 126 $\mu\varepsilon$.

5.4.3 Dynamic Load Test

Deflections and strains were measured in the dynamic load test, conducted by driving the 23 Tonne truck in different lanes over the bridge, at different speeds. Spray painted large

102

spots on the bridge deck as well as carefully placed and aligned rubber pylons guided the truck driver to drive straight on predetermined lines, on the bridge deck.

5.4.3.1 Results of Deflection Measurements

Figures 5.35 through 5.37 show the measured deflection in dynamic tests before rehabilitation. For the truck on the right lane and on the centre mark, the largest measured deflection was at the location of cable transducer L7 (Figures 5.35 and 5.36). For the truck on the left lane, the largest response was at the location of cable transducer L3 (Figure 5.37). Figures 5.38 and 5.39 show the deflection in dynamic tests after the rehabilitation. Cable transducers L9 and L1 show the largest response for the truck on the right and the left lanes, respectively.

Load sharing, based on the average of the deflections in the dynamic tests with different speed of the truck, is presented in figures 5.40 through 5.42. The load sharing information from the dynamic measurements is in excellent agreement with the information from the static test. It also confirms an improvement in the load sharing after rehabilitation, especially since a better contribution from the edge girders was achieved after rehabilitation.

Figures 5.43 through 5.47 are enlargements of figures 5.35 through 5.39 for the period of time that the truck was on the bridge. To allow for the comparison of the tests with different speed of the truck, the horizontal axis has been transformed from time to the location of the steering axle of the truck. Results of the static tests are added to these graphs for the ease of comparing static and dynamic test results. Vibration of the bridge was sometimes as large as ± 2 mm. Note that the level of vibration is much less when the truck is at speeds of about 30 km/hr compared to cases with speeds less than 20 km/hr or more than 40 km/hr.

103

5.4.3.2 Results of Strain Measurements

The influence line for strains, at the location of the strain gage with the largest response is plotted in figures 5.48 through 5.52. Load sharing based on strain measurements in dynamic tests is presented in figures 5.53 through 5.55, indicating an improvement due to rehabilitation. To allow for the comparison of the static test results and dynamic test results with varying speed of the truck, measured strains are plotted versus the location of the front axle in figures 5.56 through 5.60.

Digital filtration techniques were used to isolate any response within frequencies 2 and 4 Hz. Figures 5.61 and 5.62 show how a response can be broken into the vibratory and non-vibratory components. The non-vibratory component is referred to as the pseudo-static part, since it represents the response that remains after the vibrations have been filtered out and hence represents the static part. This exercise was conducted to compare the pseudo static portion of the dynamic load test with the results of the static load test. Before rehabilitation, the bridge vibrated at a frequency of 2.78 Hz in all tests. After rehabilitation, the frequency of vibration has reduced to 2.64 Hz. At these frequencies, as presented in figure 5.63, all girders move up and down simultaneously. Hence, these frequencies correspond to the first vertical mode. As shown in this figure, in some cycles G12 shows larger response than G1, while in other cycles G1 has the largest response. This indicates that the second mode (torsional mode) is combined with the main mode of vibration (vertical mode).

Damping of the bridge for its first vertical mode shape can be determined based on strain measurements. After the truck completely passes the bridge, the bridge vibrates freely at a combination of its natural frequencies. In measuring damping, it is ideal to isolate each natural frequency. However, for frequencies close to each other, there is always concern about filtering effects. A solution that avoids filtering problem and minimizes the effect of the torsional mode is to average the response of all the strain gages. Figures 5.65 and 5.66 respectively show the vibration of the bridge before and after the rehabilitation using this technique. Non-linear best fit analyses have been performed on the results of the tests

104

with large vibration. For each vibration, damping can be determined once based on the positive peak values and once based on the negative peak values. Table 5.3 provides a summary of the damping information. Before rehabilitation, for the natural frequency of 2.78 Hz, the damping ratio on average was determined to be 1.39%. After rehabilitation, for the natural frequency of 2.64 Hz, the damping ratio was determined to be 1.73%.

Table 5.3 – Summary of Damping Information

Truck Location	Speed (Km/hr)	Sign of The Peak	Frequency (Hz)	No. of Points	R^2	Damping Ratio (%)	Standard deviation
Before Rehabilitation of the Bridge							
Right	18	Positive	2.78	18	0.9902	1.51	0.04
Lane	18	Negative	2.78	19	0.9936	1.49	0.03
Center	16	Positive	2.78	18	0.9930	1.35	0.03
Mark	16	Negative	2.78	18	0.9866	1.20	0.04
Left	17	Positive	2.78	18	0.9970	1.42	0.02
Lane	17	Negative	2.78	19	0.9942	1.39	0.03
After Rehabilitation of the Bridge							
Right	16	Positive	2.64	17	0.9954	1.69	0.03
Lane	16	Negative	2.64	17	0.9977	1.70	0.02
Left	40	Positive	2.64	11	0.9935	1.75	0.05
Lane	40	Negative	2.64	12	0.9921	1.76	0.05

5.4.4 Tendons and Underslung Assemblies

Tendons and underslung diaphragms have been studied in two load cases, 1) transverse stressing of the deck, and 2) live truck loading. Due to post-tensioning, strain in tendons 1 and 2 increased 7216 and 7460 $\mu\varepsilon$, respectively. This corresponds approximately to a force of 140 kN per tendon and an average stress of 0.35 MPa in concrete. Strain change for underslung diaphragms at locations A through D were 6, 12, 0, and 7 $\mu\varepsilon$, respectively. These values are within the limits of the accuracy of the data acquisition and are essentially insignificant. Hence, the bottom of the adjacent webs remained stationary

105

relative to each other due to post-tensioning. The average strain of the girders for the heaviest passing truck was 31 $\mu\varepsilon$. Comparing this strain with the average strain of 50 $\mu\varepsilon$ in load tests with the 23-tonne truck, the weight of the passing truck is estimated to be

$31 / 50 \times 23 = 14.3$ tonnes. For this truck, maximum strains at locations A through D (see figure 5.12) were respectively 8, 13, 6, and 19 $\mu\varepsilon$. Figure 5.64 shows the response of gauge D on the underslung diaphragm and gauge G4 on the FC girder #2 to this truck.

5.5 Discussion

Three issues are being discussed in this chapter: longitudinal cracks in the asphalt pavement, rigidity of the bridge deck and change in various stiffnesses of the bridge.

5.5.1 Longitudinal cracks in asphalt before rehabilitation

The focus of discussion, in this section is the direct effect of the relative movement of the girders on the formation of longitudinal cracks in the pavement. Two possible scenarios would be discussed here which result in the formation and progression of longitudinal cracks in the bridge deck.

Figure 5.69 shows the transverse vibrating cycle of the bridge deck, on a highly exaggerated scale, under a vehicle driving over the bridge. When the transverse cross section bends as shown in figure 5.69 (b), asphalt is generally in compression, however when it bends as shown in figure 5.69 (c), the asphalt decking as well as the shear keys are in tension. These tensile stresses can crack the shear keys as well as the asphalt deck, directly over the shear keys. The third mode shape of 5.43 Hz. before rehabilitation, shown in figure 5.24 also confirms this scenario. The torsional stiffness of the edge girders is higher due to the concrete curb or the sidewalk, therefore, at the shear keys near the curbs, sometimes a reverse curvature might occur which will put the end shear keys in direct tension resulting in longitudinal cracks at those shear keys.

The second scenario, which confirms shear key cracking and is responsible for the progression of longitudinal cracks in the asphalt pavement, associates with shear slippage at the shear keys. Once the cracks have formed, inter-surface abrasion due to successive loading cycles will cause these cracks to grown in width. An indication of such slippage can be observed in figures 5.27 through 5.30 or figures 5.40 through 5.42. The difference between the vertical deflections of the bottom of adjacent girder legs was measured to be almost 2mm in some instances, which indicates some vertical movement at the shear keys, hence depleting the load sharing between the girders.

However figures 5.4 and 5.5 show that the cracks in the asphalt deck were a random mix of longitudinal and transverse cracks. Since shear key cracking should have produced only longitudinal cracks, it appears that other factors like temperature effects and the material properties of the asphalt batch were responsible for transverse asphalt cracking.

5.5.2 Rigidity of the bridge deck

Relative movement of the girders occur because of poor load sharing among the girders. The same relative movement results in the initiation of longitudinal cracks in the asphalt before rehabilitation. Deflection measurements in load tests are evidence of bending of the bridge in the transverse direction similar to what is shown exaggerated in figure 5.69(b). With this shape of transverse bending, assembly bolts are in tension, while concrete at the shear keys is in compression. Underslung diaphragms were designed to impart torsional rigidity to the bridge as well as increase its shear capacity. The middle diaphragm increases the flexural capacity of the bridge in the transverse direction, and hence improves the load sharing among the girders.

Before rehabilitation transverse shear had to be transferred between the adjacent girders through a small area at the shear key. Truckload tests before rehabilitation show inter girder relative deflections at shear key locations, which indicate some relative movement between the girders before rehabilitation. With the application of the rehabilitation

107

scheme of the new concrete deck and the underslung diaphragm assembly, it was thought that transverse shear transfer would not be a concern any more, especially after transverse stressing of the deck. Load tests after rehabilitation do indicate that inter girder relative deflections were greatly reduced.

Another shape of transverse bending before rehabilitation is presented in Figure 5.69. This mode was associated with the excitation of the bridge at the frequency of 5.4 Hz. and measured during the Ambient Vibrations Test. The new concrete deck, its transverse stressing, and the underslung assembly have practically eliminated such a mode shape, and hence the rehabilitation has been efficient in increasing load sharing among the girders.

5.5.3 Change in the stiffness of the bridge

The three modal frequencies, i.e. the vertical, torsional and transverse bending are taken as good indicators of the stiffness in each of these directions. At high levels of vibration, measured by strain gages, the natural frequency was observed to decrease from 2.78 Hz. before rehabilitation to 2.64 Hz after rehabilitation. This issue can be addressed by the fact that the natural frequency is related to the square root of the stiffness to mass ratio. Knowing that the mass of the bridge has increased approximately by about 7 percent due to the provision of the rehabilitation components, a change in the natural frequencies of the bridge will occur if a corresponding increase in the stiffness has not taken place. A drop in the natural frequency showed that the stiffness of the bridge in the longitudinal direction did not increase as a result of the rehabilitation process. At low level of vibration, measured by accelerometers, the frequency at the first vertical mode was observed to have decreased from 2.82 to 2.77. This difference in the modal frequencies between the two sets of dynamic testing data is in line with the available literature and is due to the presence of the vehicle mass on the bridge deck during the dynamic truckload test. However, for all practical purposes, all these changes are considered insignificant because the rehabilitation program was designed to boost the transverse stiffness of the bridge.

108

From the ambient vibration test results, the frequency of the first torsional mode has increased from 3.25 to 3.38 Hz due to rehabilitation. Considering the 7% increase in the mass of the bridge, it can very well be concluded that the torsional stiffness of the bridge has improved noticeably. Similarly, the disappearance of the third modal frequency representing the transverse bending mode shape is a very good indication of the fact that the transverse stiffness of the bridge improved significantly as a result of the rehabilitation process.

5.6 Major results and conclusions

1) Three independent measurements, namely strain, deflection, and vibration, prove that the load sharing among the girders has improved due to the rehabilitation of the bridge. Transverse stressing of the deck and underslung diaphragms were effective in improving load sharing by increasing the flexural stiffness of the bridge in the transverse direction. Disappearance of the third natural frequency (5.43 Hz) after rehabilitation is an important evidence of a more rigid deck in the transverse direction.

2) The changes in the vertical, torsional and transverse bending mode shapes were reasonable indication of the changes to the longitudinal, torsional and transverse bending stiffness of the bridge. An increase in the torsional and transverse bending modal frequencies verified the increase in the bridge stiffnesses in those directions however a drop in the vertical modal frequency showed that no stiffness increase occurred in the longitudinal direction of the bridge. Since the rehabilitation program was mainly meant to boost the transverse stiffness of the bridge and improve the load sharing between the girders, it can be concluded from the test results that the rehabilitation program was successful in achieving its main objective.

3) The differential settlements between the adjacent girder webs were measured to be around almost 2 mm before rehabilitation. This relative movement at the shear key lines

109

is a clear indication of deterioration and cracking inside the shear keys, which limits the load sharing between the girders and reduces the flexural stiffness of the cross section in the transverse direction of the bridge. The differential deflections at the adjacent girder webs went down to an average of 0.2 mm after the rehabilitation components were put in place. This indicates an obvious improvement due to rehabilitation of the bridge.

4) The first natural frequency at high levels of vibration (measured by strain gauges) was smaller than the measured frequency in the ambient vibration tests (measured by accelerometers). This difference has also been observed by other researchers and is due to the presence of the vehicle mass on the bridge in case of using the vehicle as the source of excitation. The difference was only 1.4% before rehabilitation and 4.9% after rehabilitation.

5.7 Acknowledgements
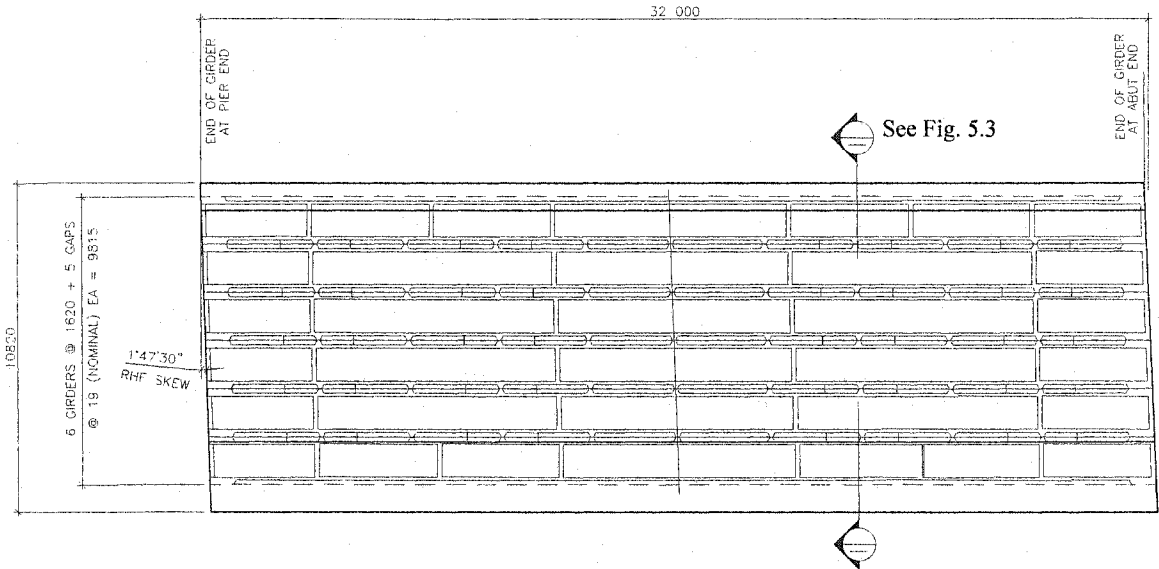
Figure 5.1: Plan of the 99th Ave. bridge in Fort Saskatchewan

Figure 5.2: Sectional Elevation (looking north)

111
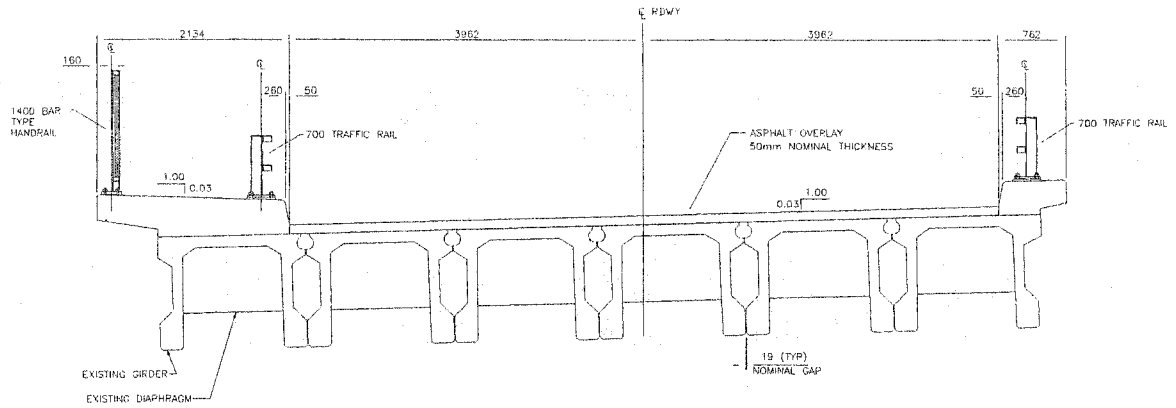
Figure 5.3: Section of the bridge, before rehabilitation
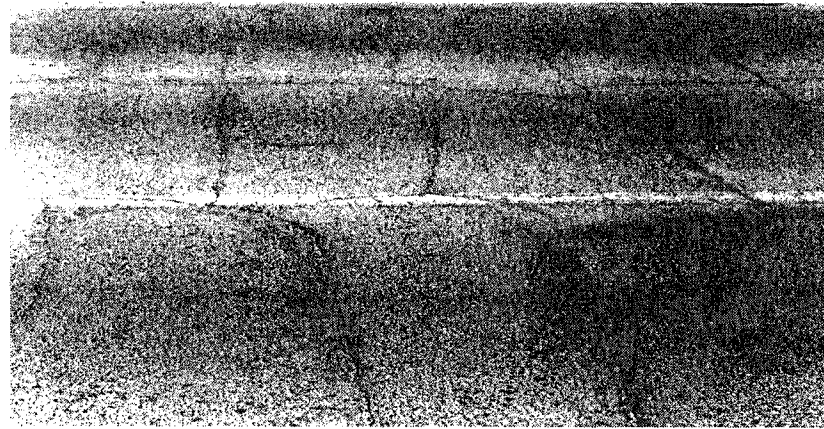
Figure 5.4: Longitudinal and transverse cracks in apshalt, before rehabilitation
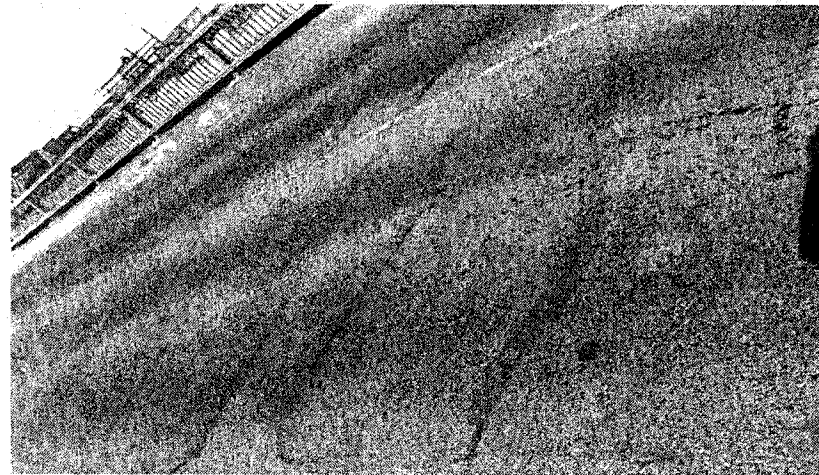
Figure 5.5: Cracks in the asphalt pavement, before rehabilitation

112
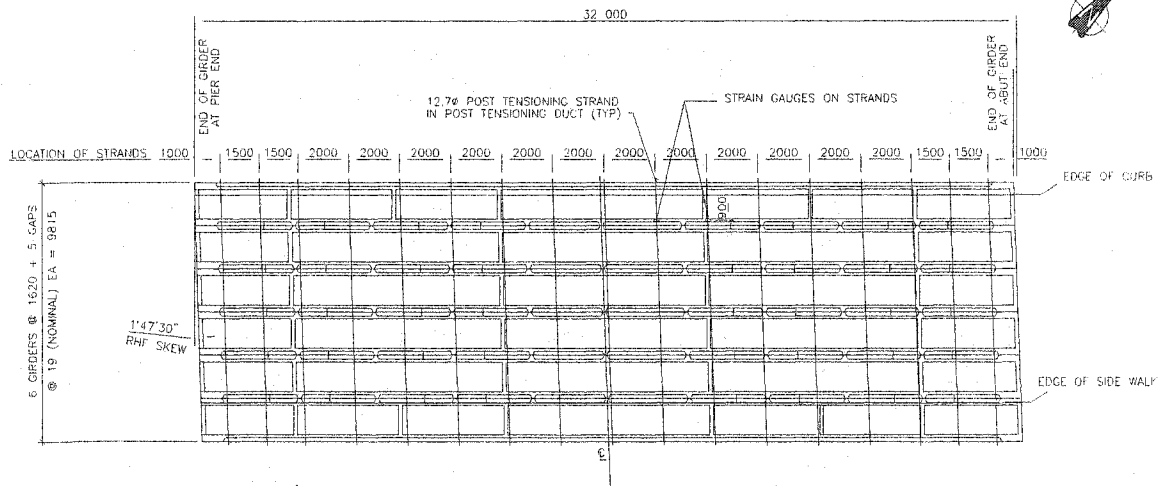
Figure 5.6: Deck Strand Layout and Strain Gauges on Tendons
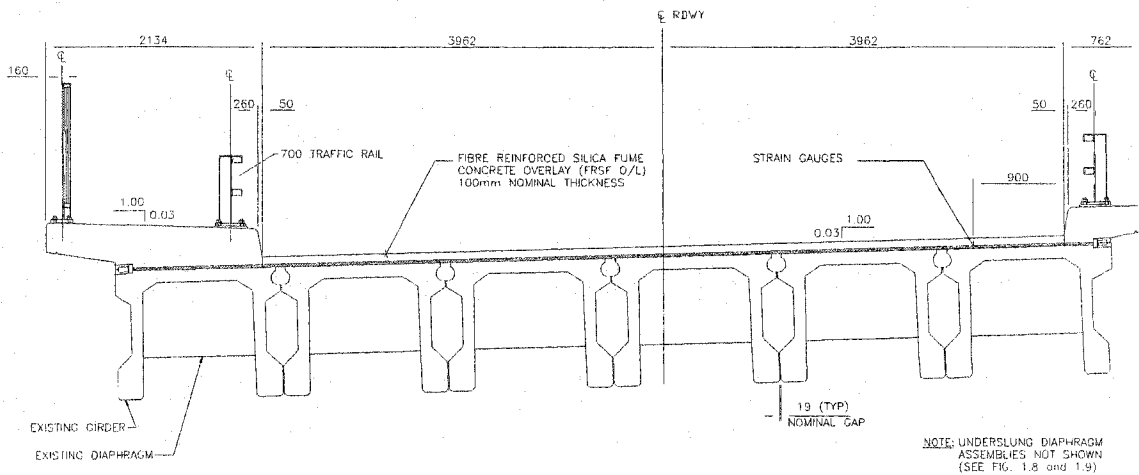
Figure 5.7: Section of the bridge, Deck Stressing

113
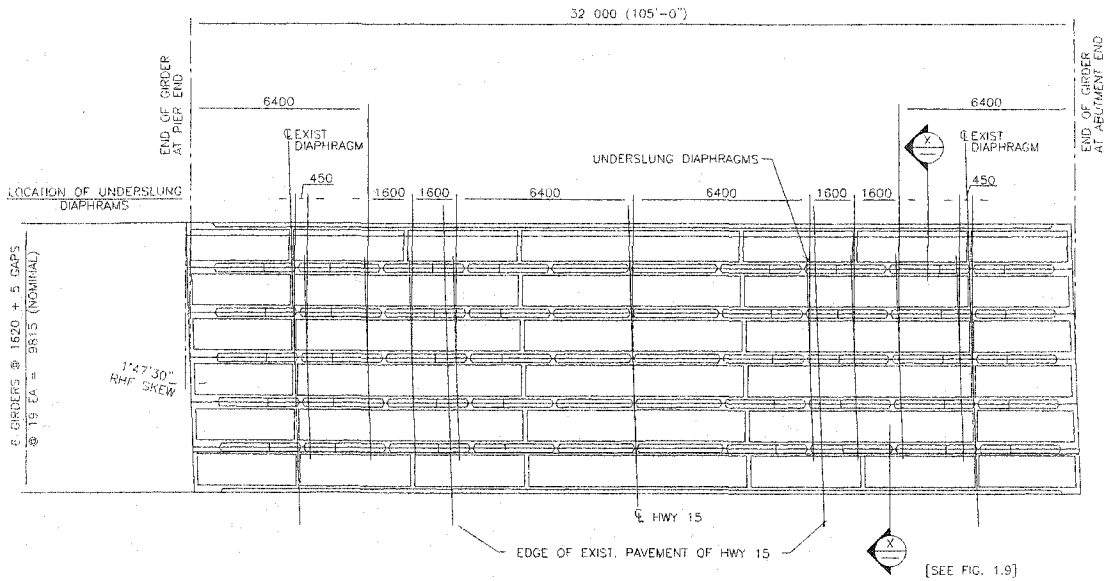
Figure 5.8: Layout of Underslung Diaphragms
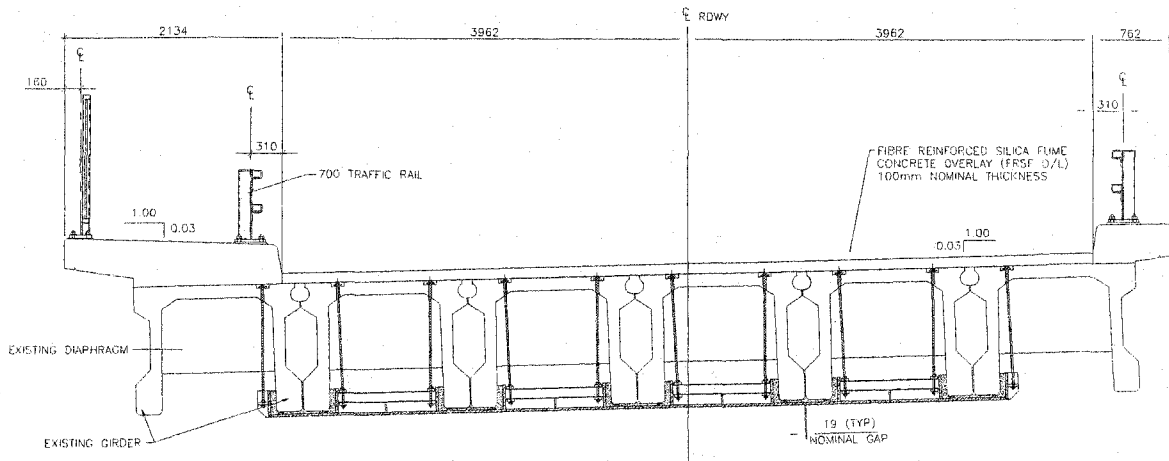
Figure 5.9: Section showing Underslung Diaphragms

114
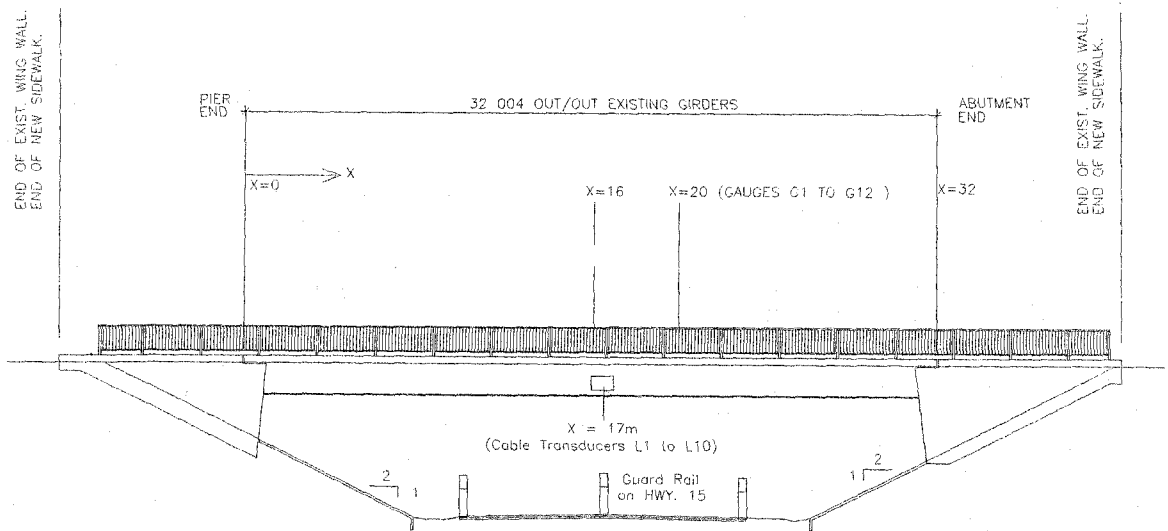
Figure 5.10: Elevation of the bridge showing location of sensors
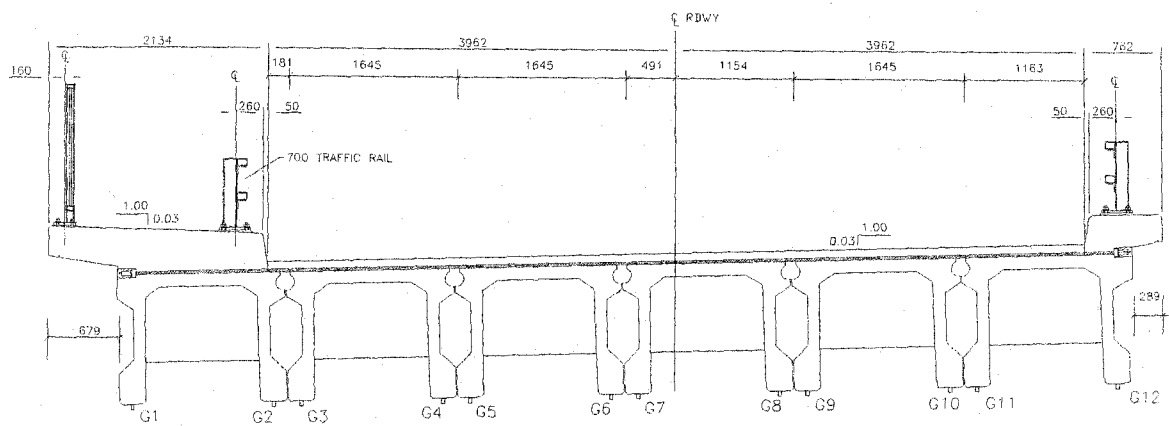
These Gauges are at X = 20m

Figure 5.11: Position of strain gauges on girders

115
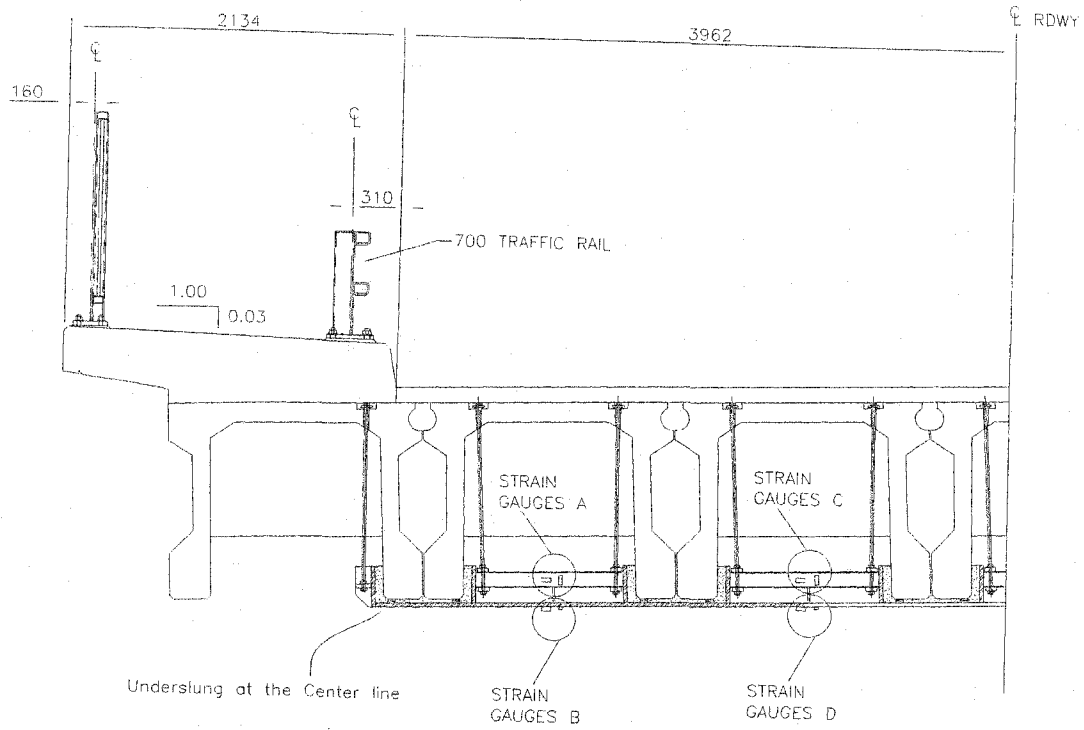
Figure 5.12: Strain gauges on underslung diaphragms
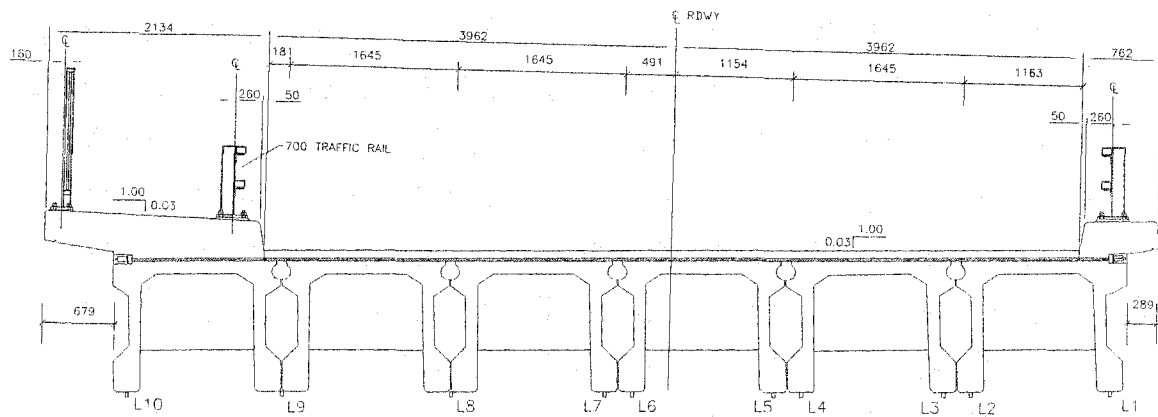
Figure 5.13: Cable transducer connections to girders

116
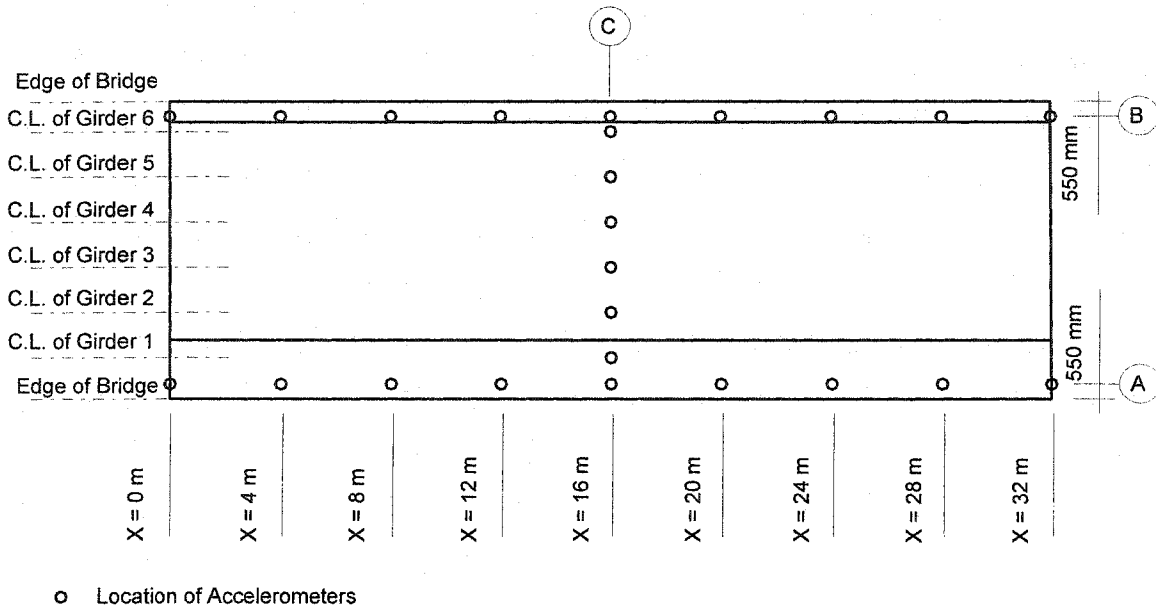
Figure 5.14: Accelerometer positions in Ambient Vibration Test
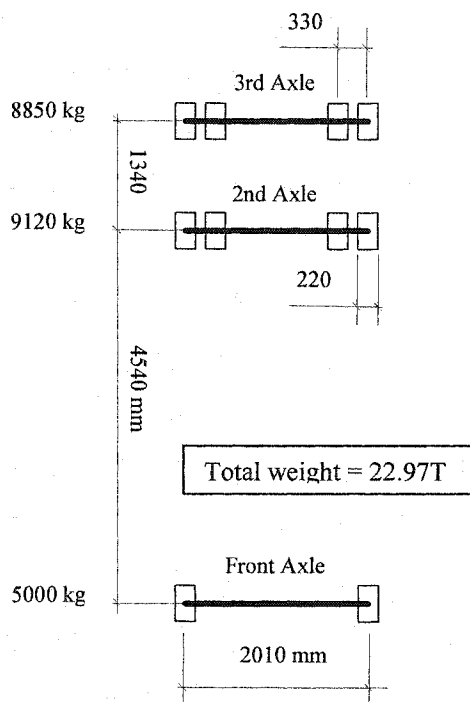
Figure 5.15: Truck information, before rehabilitation
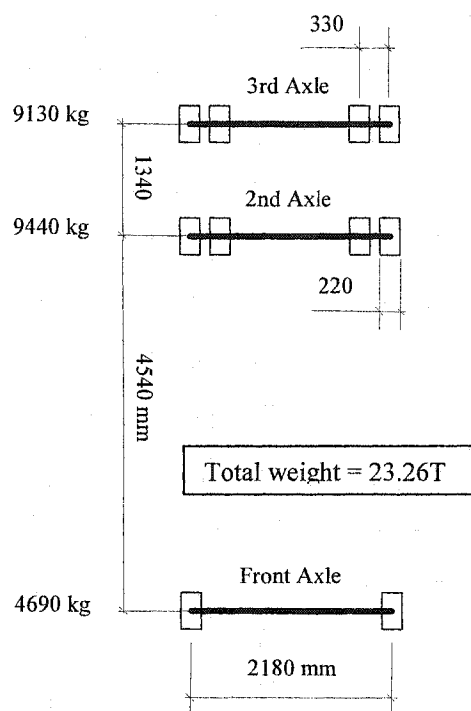
Figure 5.16: Truck information, after rehabilitation

117
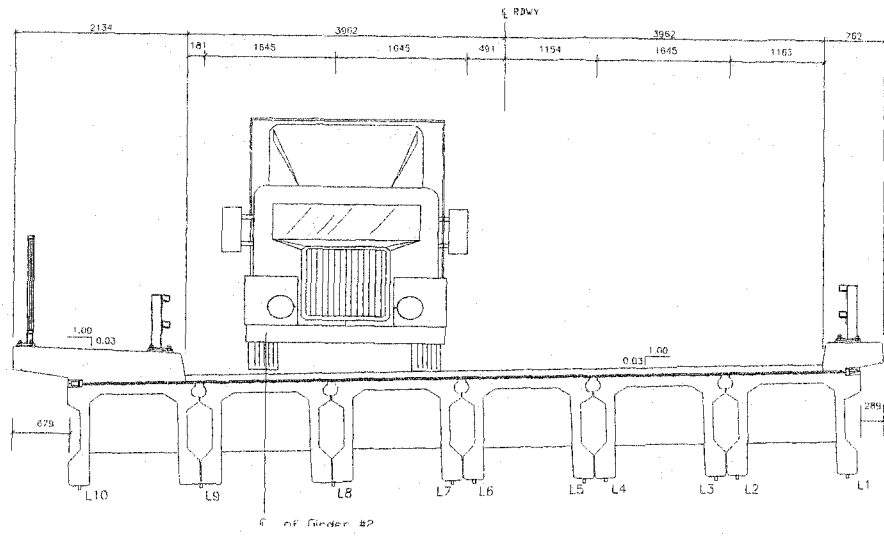
Figure 5.17: Truck on right lane
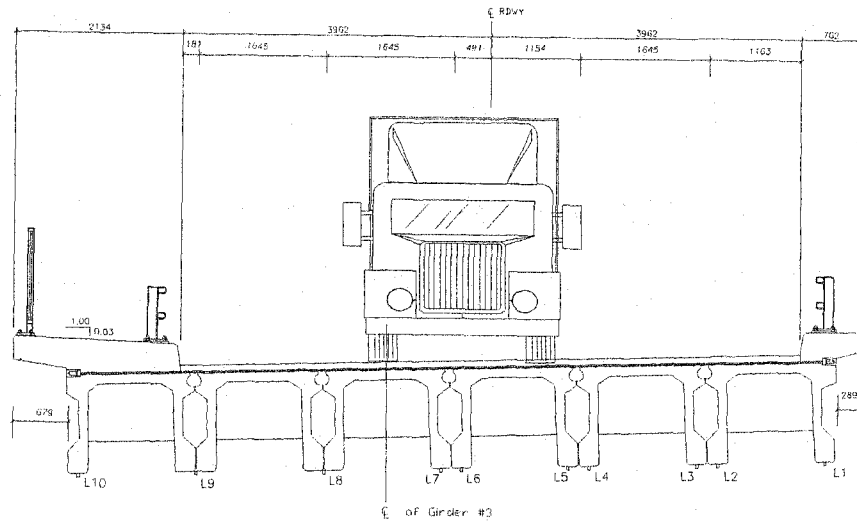
Figure 5.18: Truck on centre mark
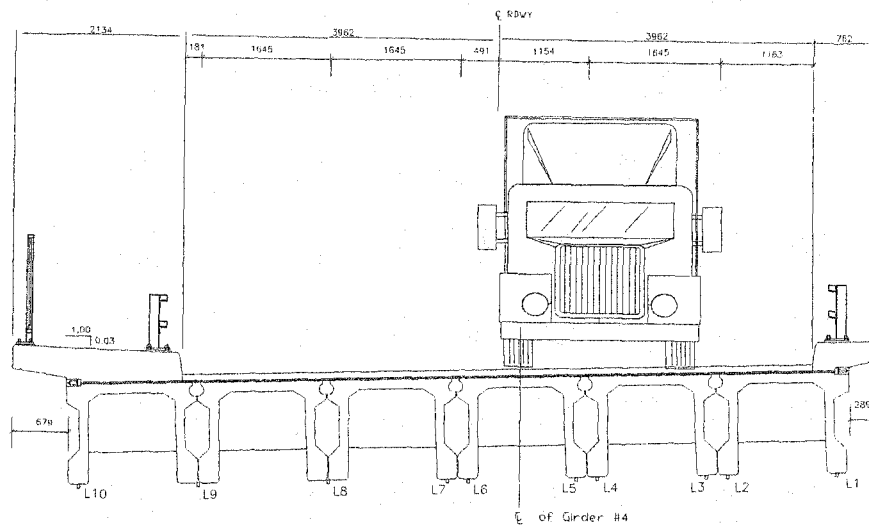
Figure 5.19: Truck on left lane

118
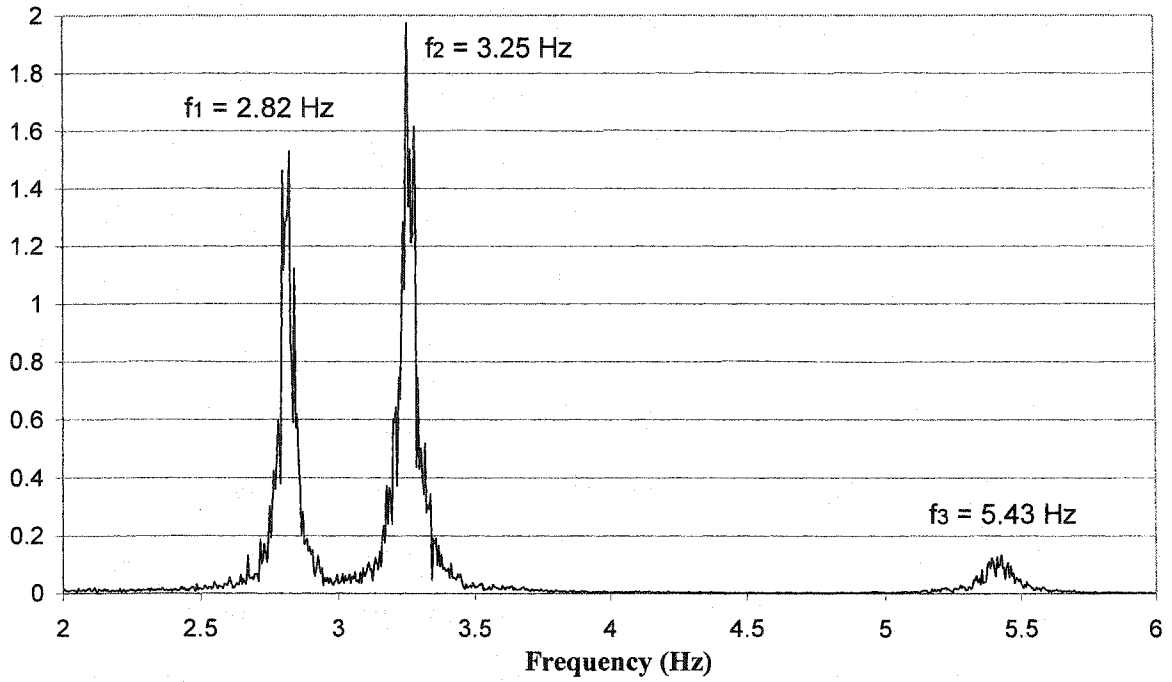
Figure 5.20: Power Spectrum of accelerometer 1, before rehabilitation
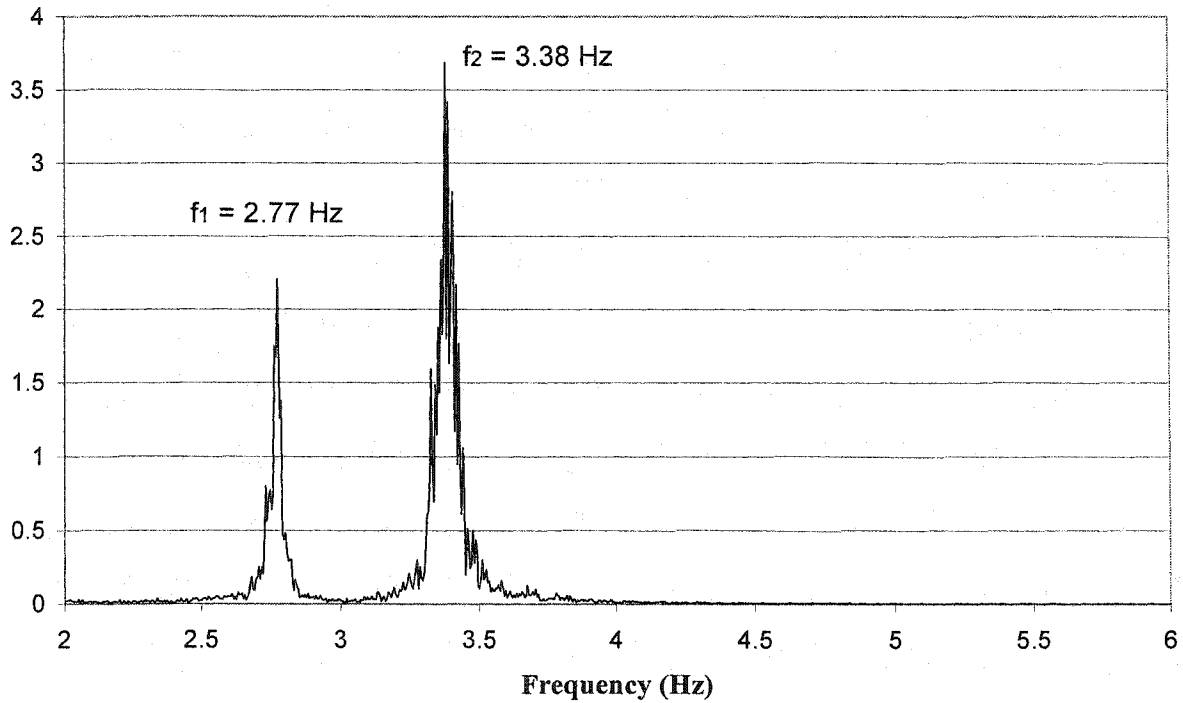
Figure 5.21: Power Spectrum of accelerometer 1, after rehabilitation

119
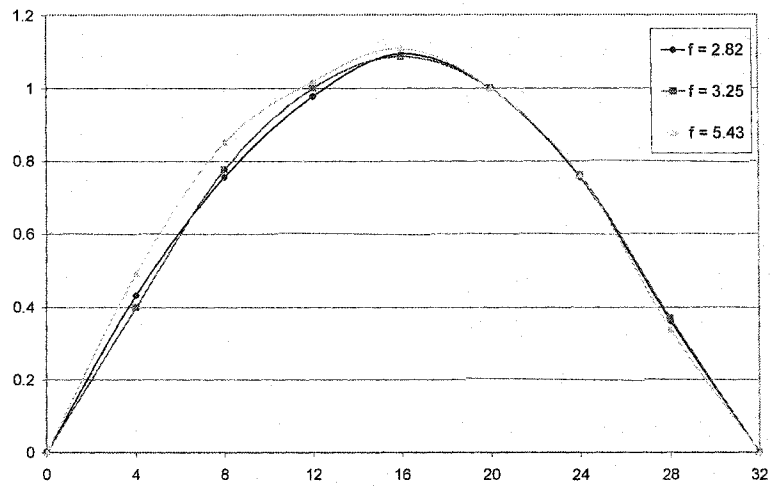
Figure 5.22: Mode shapes in longitudinal direction at axis A in Fig. 5.14, before rehabilitation
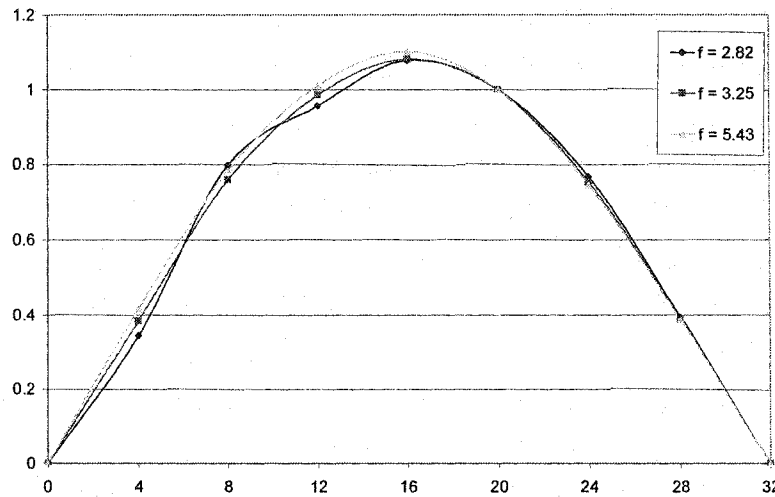
Figure 5.23: Mode shapes in longitudinal direction at axis B in Fig. 5.14, before rehabilitation
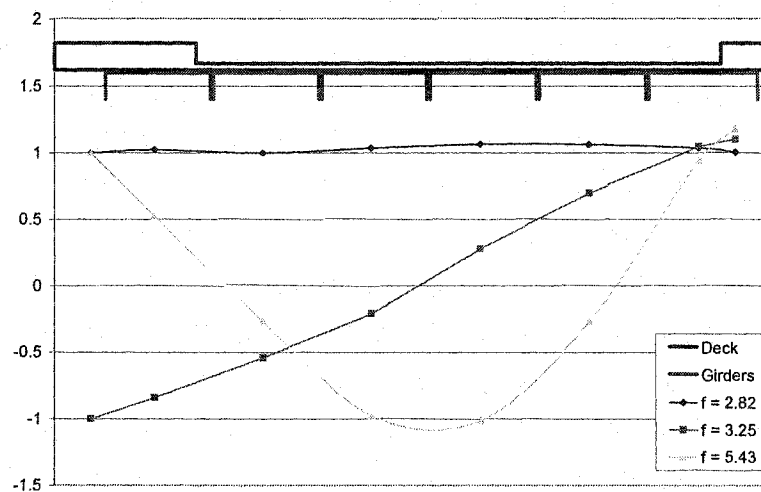
Figure 5.24: Mode shapes in transverse direction at axis C in Fig. 5.14, before rehabilitation

120

Truck on Right Lane - Before Rehabilitation
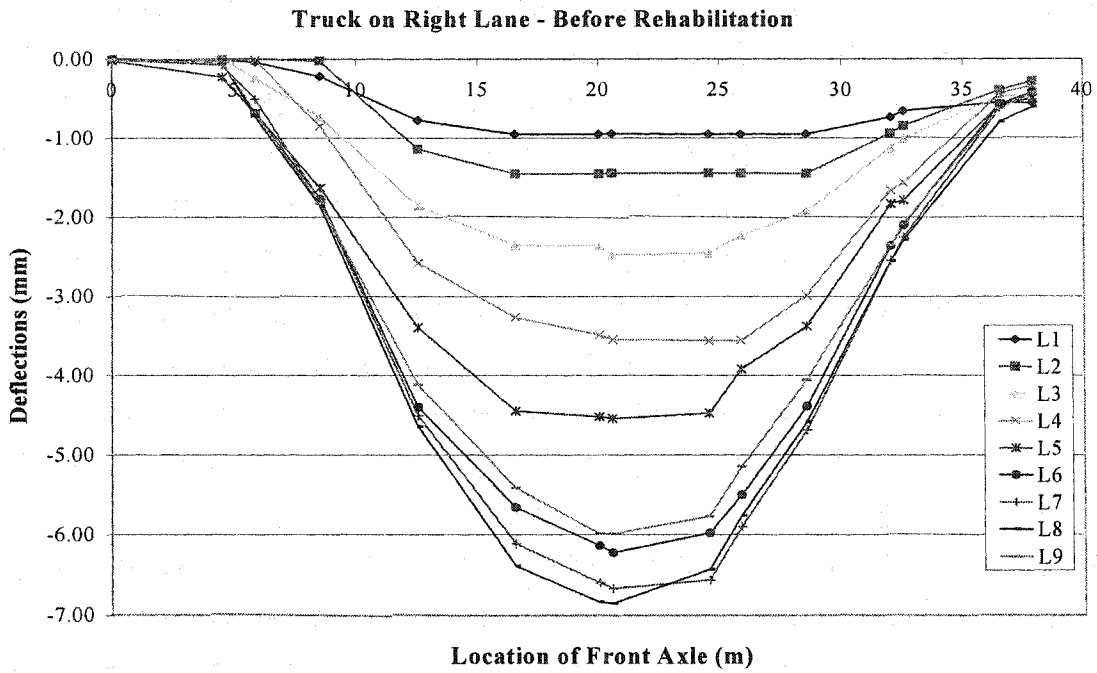
Figure 5.25: Deflections in static test, before rehabilitation, with truck on right lane

Truck on Right Lane - Before Rehabilitation
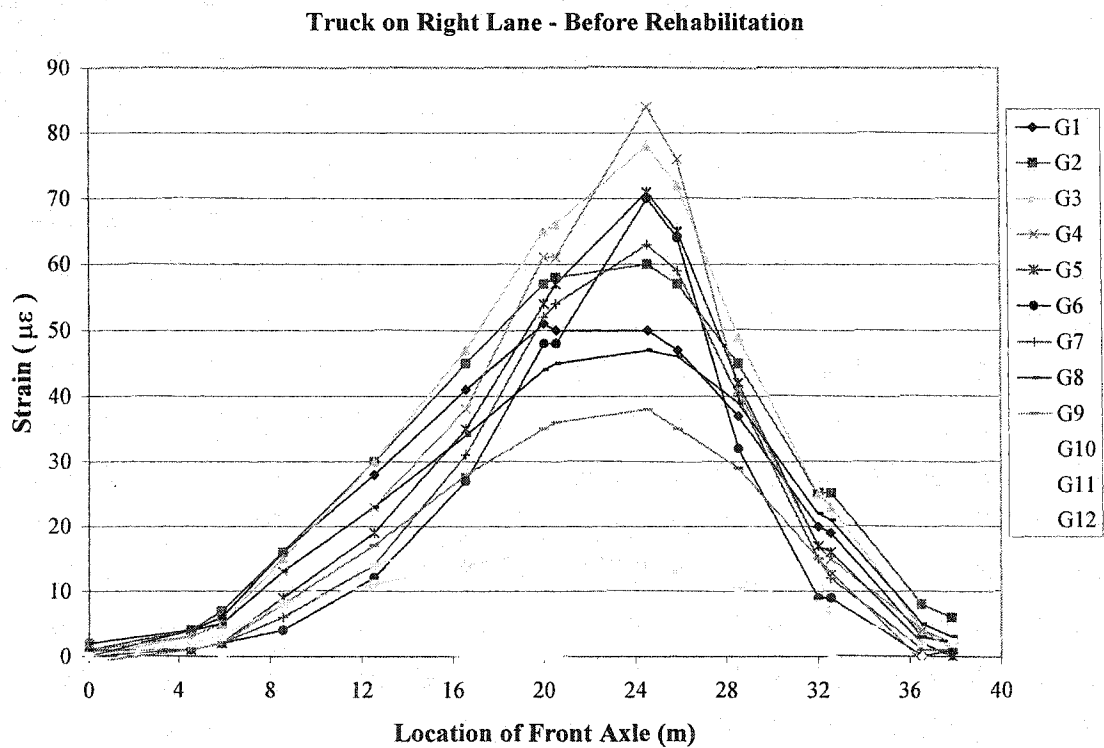
Figure 5.26: Strains in static test, before rehabilitation, with truck on right lane

121
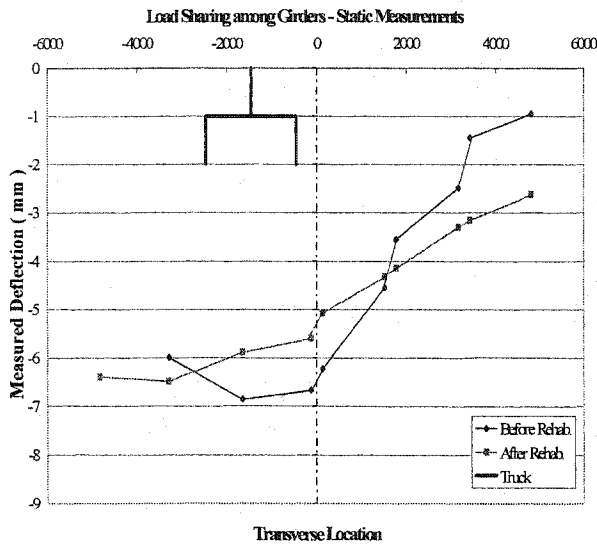
Figure 5.27: Load sharing based
on deflection, truck in right lane
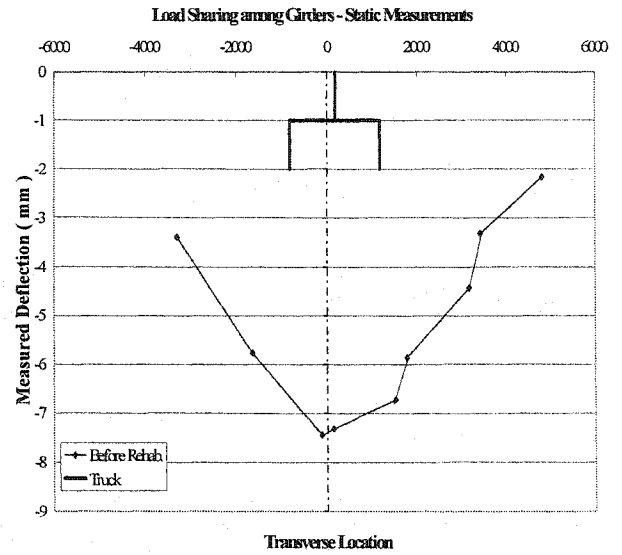
Figure 5.28: Load sharing based on
deflection, truck on centre mark
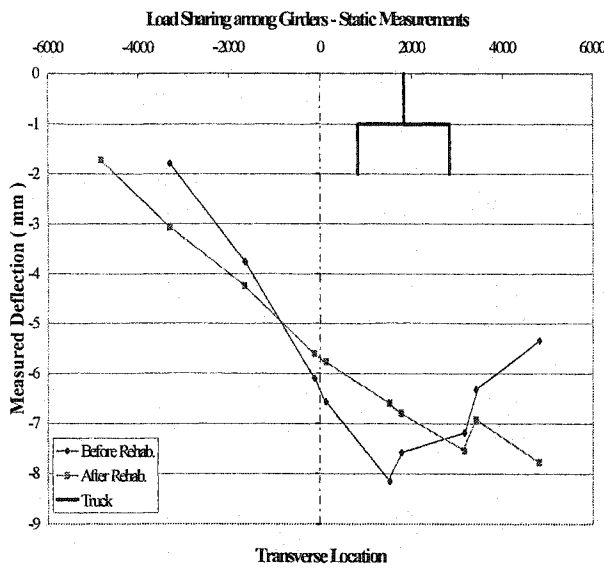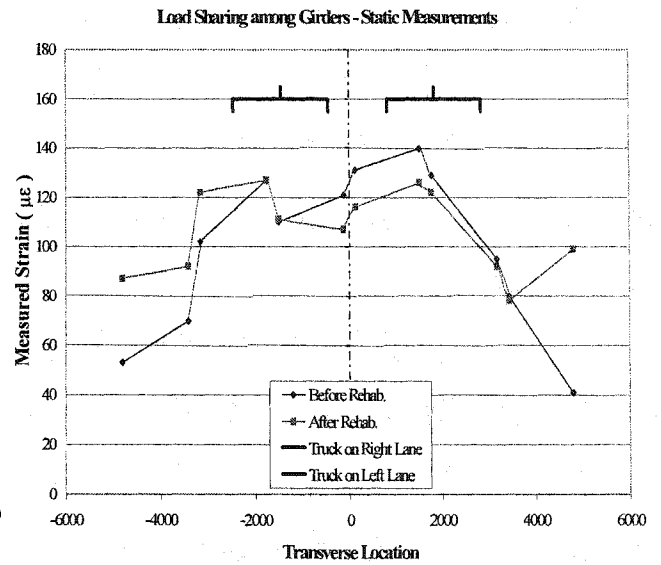

Figure 5.29: Load sharing based
on deflection, truck in left lane
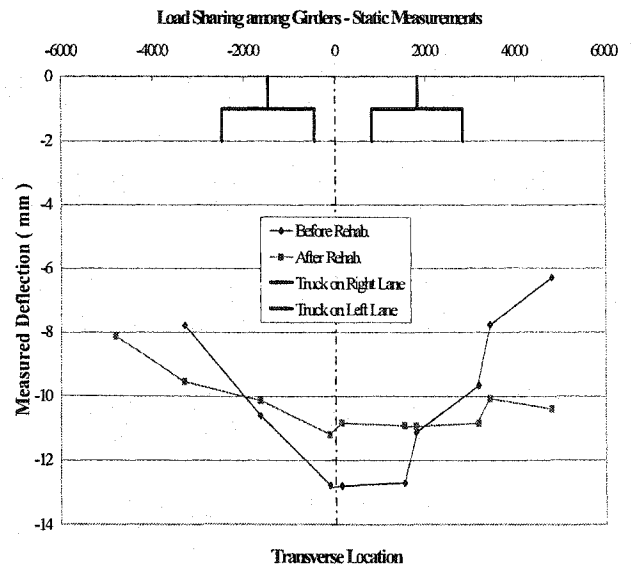
Figure 5.30: Load sharing based on
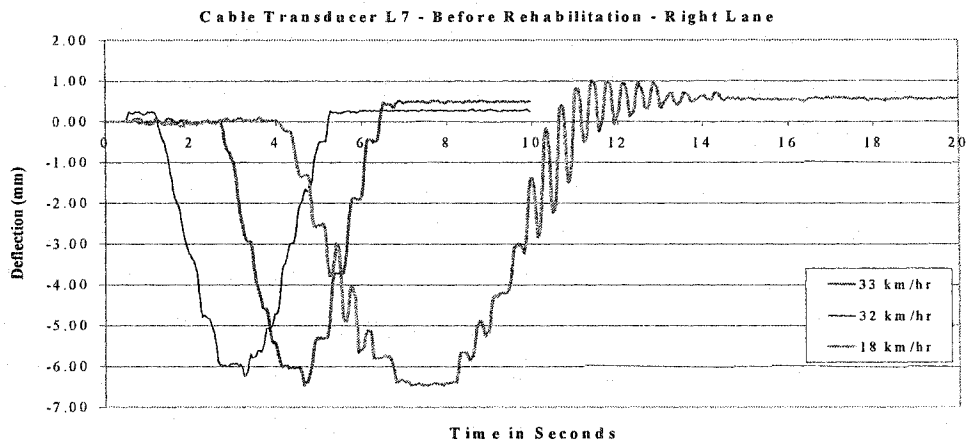deflection, superimposing figs. 5.27, 5.29

122
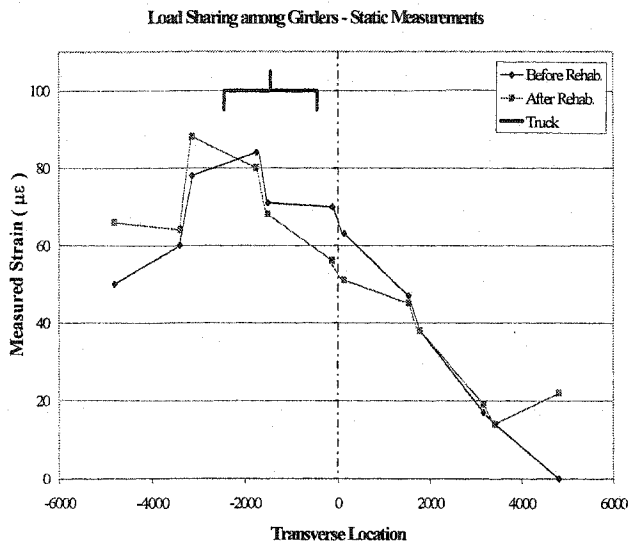
Figure 5.31: Load sharing based
on strain, truck in right lane
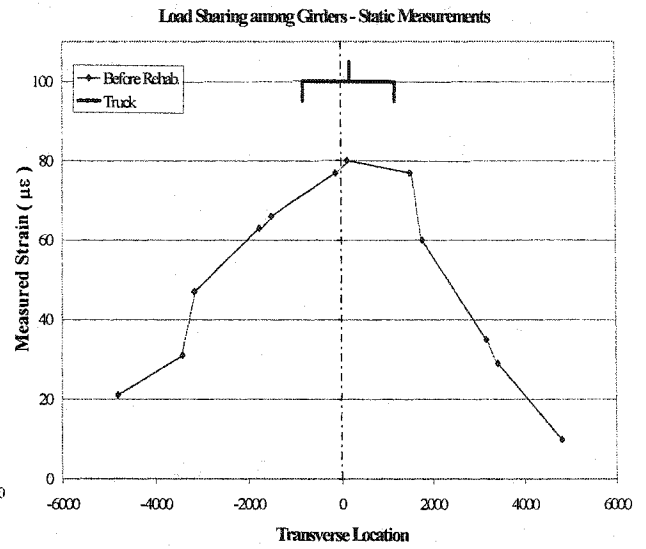
Figure 5.32: Load sharing based
on strain, truck on centre mark
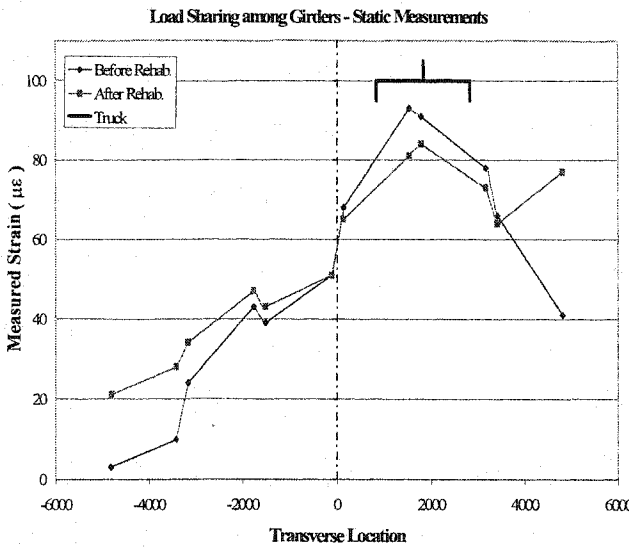
Figure 5.33: Load sharing based
on strain, truck in left lane

Figure 5.34: Load sharing based on
strain, superimposing figs. 5.31, 5.33

123

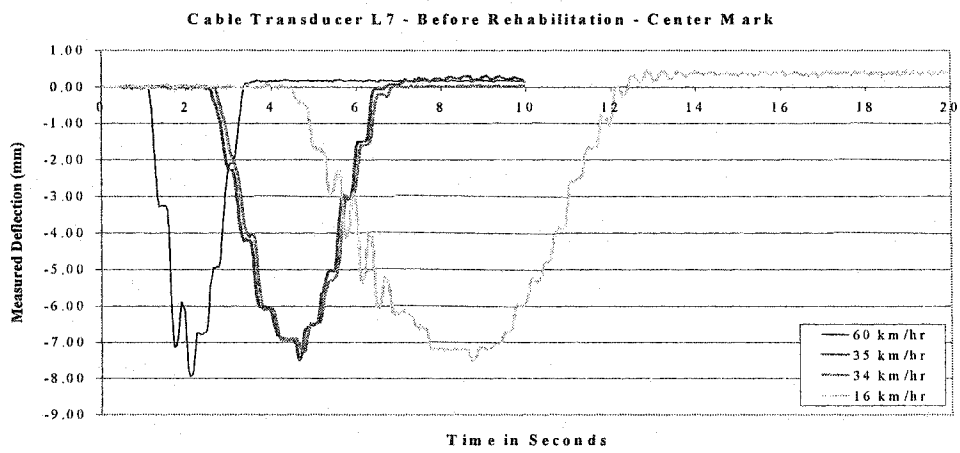Figure 5.35: Dynamic response of cable transducer L7, truck in right lane

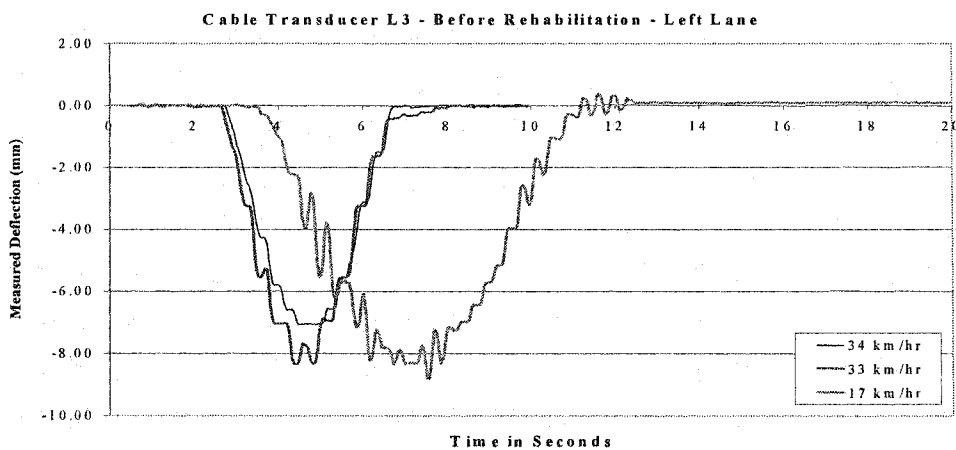Figure 5.36: Dynamic response of cable transducer L7, truck on centre mark

Figure 5.37: Dynamic response of cable transducer L3, truck in left lane
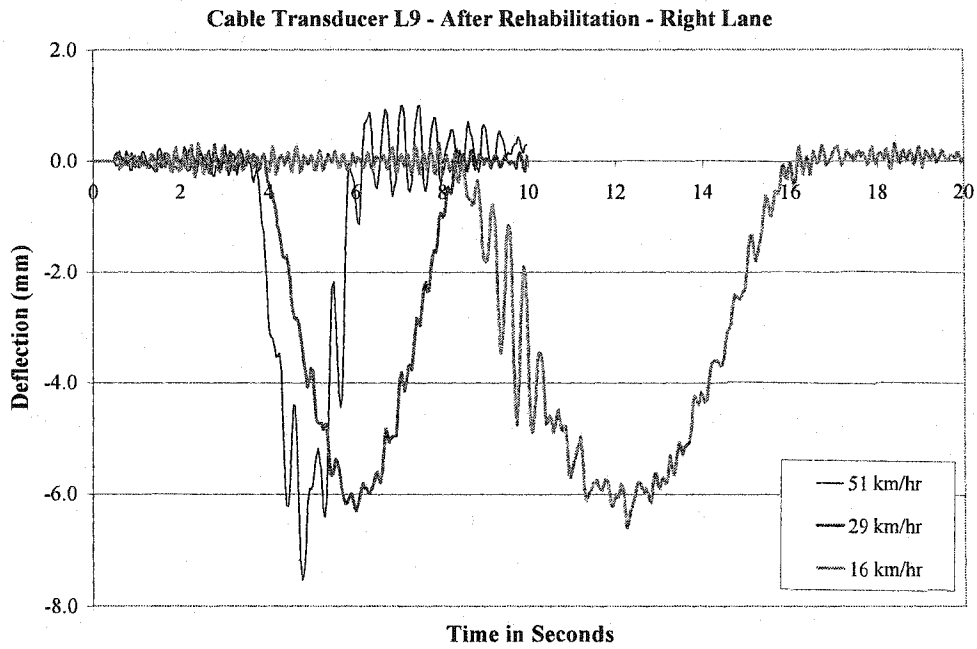
124

Cable Transducer L9 - After Rehabilitation - Right Lane

Figure 5.38: Dynamic response of cable transducer L9, truck on right lane

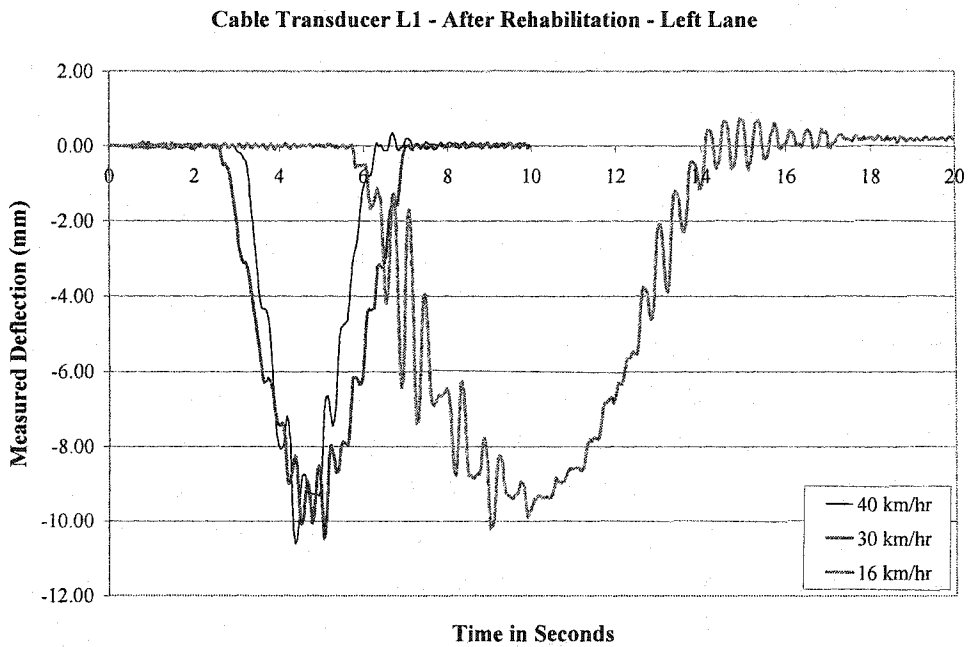Cable Transducer L1 - After Rehabilitation - Left Lane

Figure 5.39: Dynamic response of cable transducer L1, truck on left lane
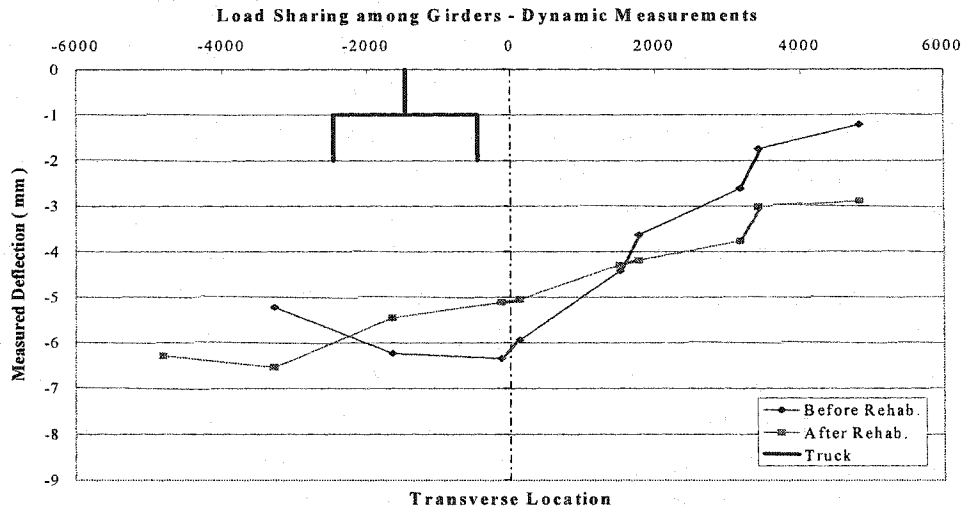
125

Figure 5.40: Load sharing based on deflections, Dynamic test, truck in right lane
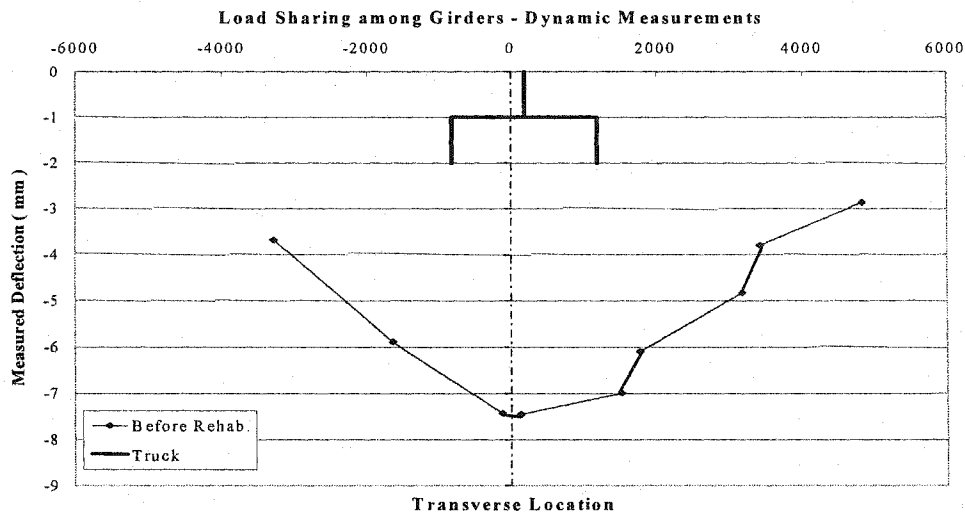

Figure 5.41: Load sharing based on deflections, Dynamic test, truck on centre mark
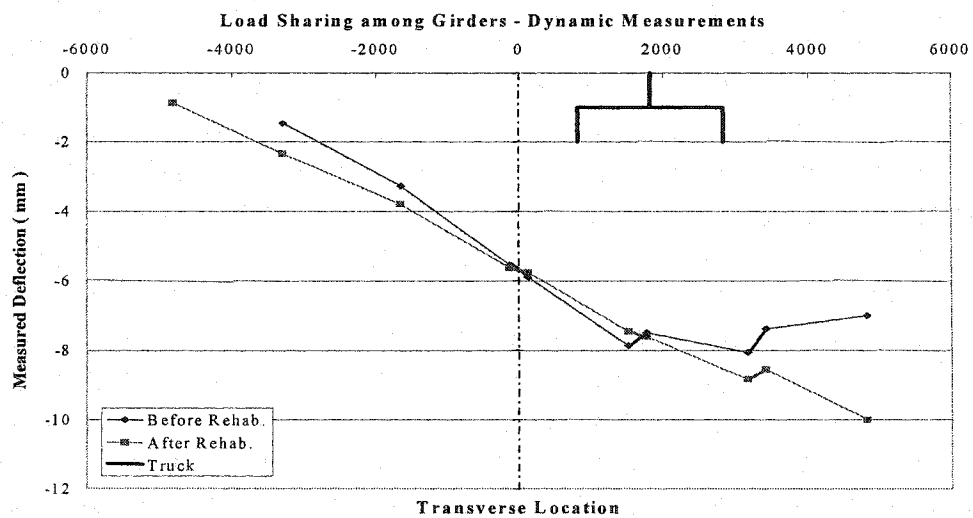

Figure 5.42: Load sharing based on deflections, Dynamic test, truck in left lane
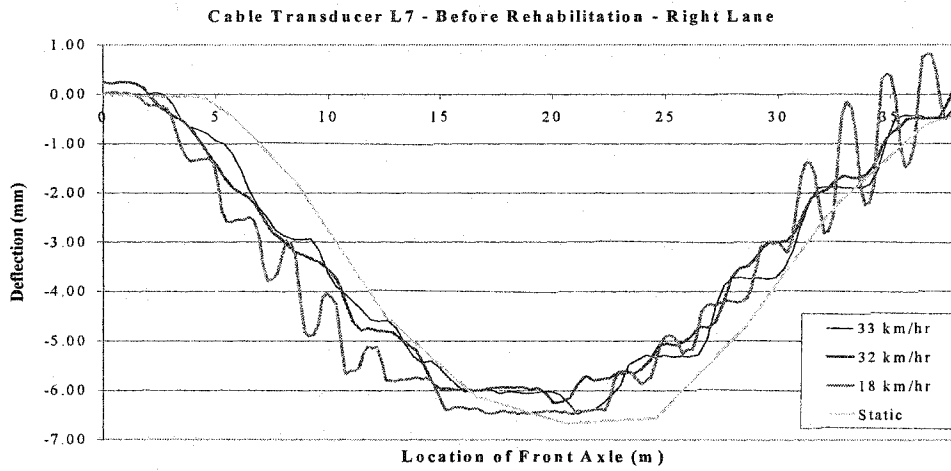
126

Figure 5.43: Deflection in static and dynamic tests, truck in right lane, before rehabilitation
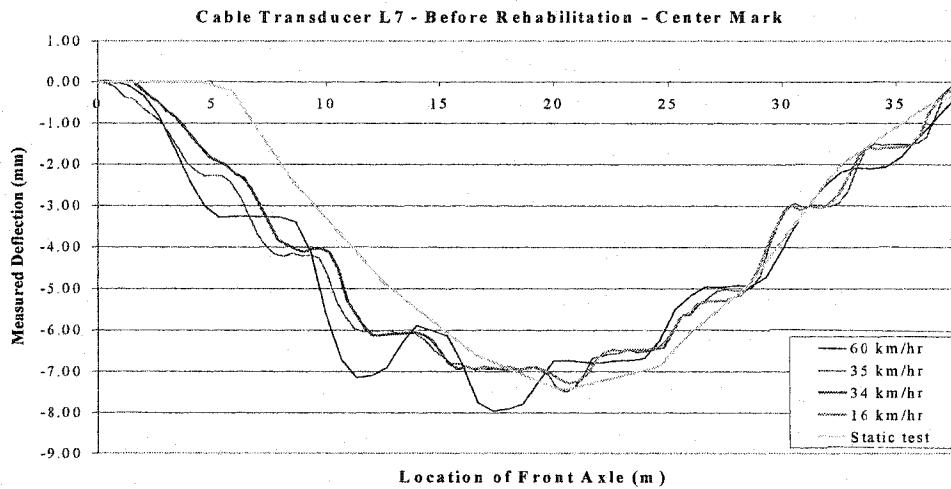

Figure 5.44: Deflection in static and dynamic tests, truck on centre mark, before rehabilitation
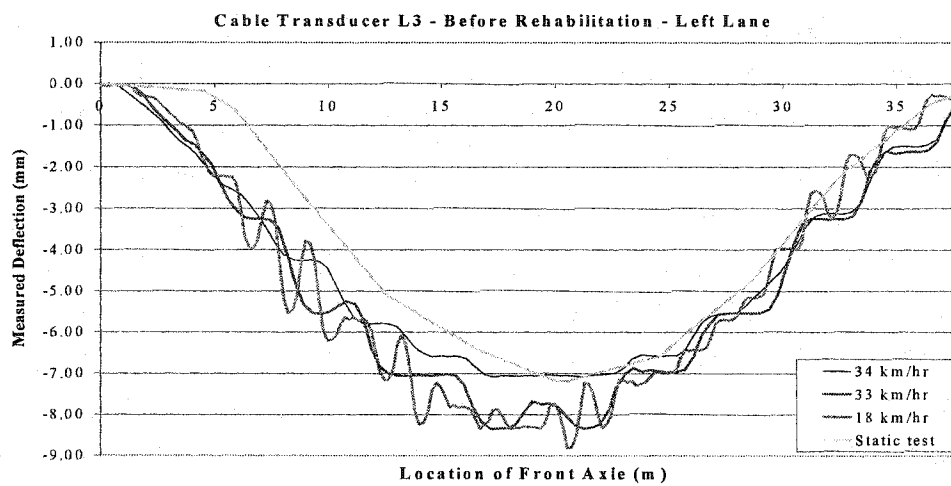
Figure 5.45: Deflection in static and dynamic tests, truck in left lane, before rehabilitation

127

Cable Transducer L9 - After Rehabilitation - Right Lane
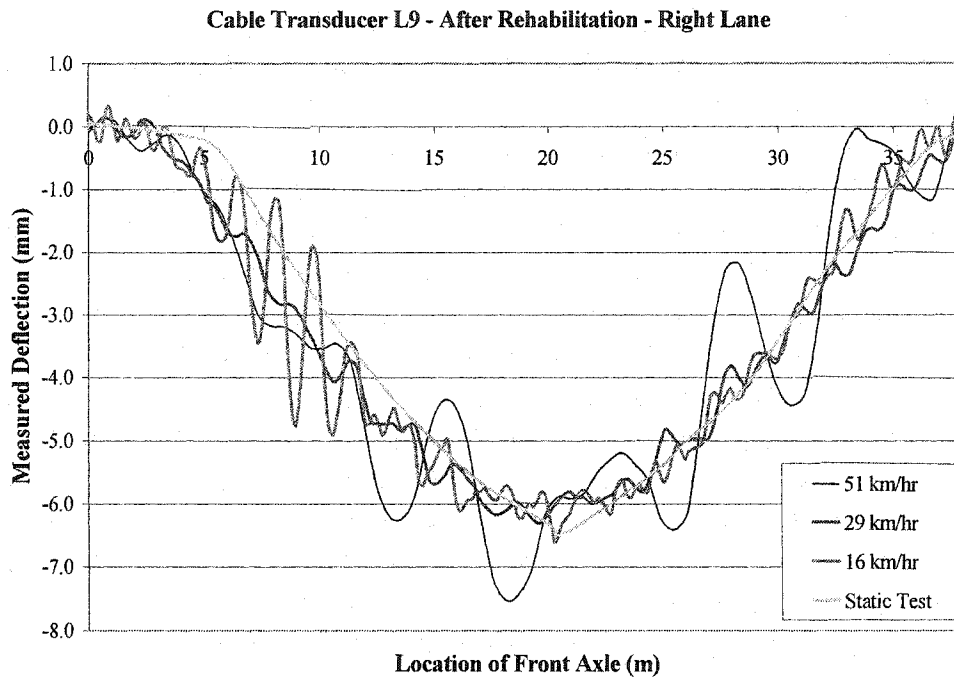
Figure 5.46: Deflection in static and dynamic tests, truck in right lane, after rehabilitation

Cable Transducer L1 - After Rehabilitation - Left Lane
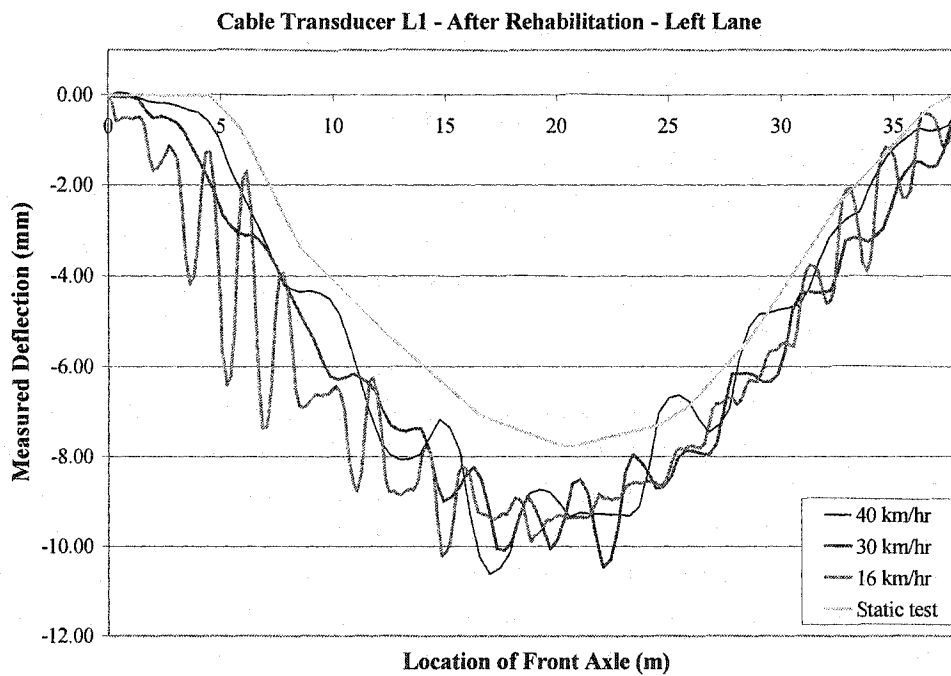
Figure 5.47: Deflection in static and dynamic tests, truck in left lane, after rehabilitation

128

Strain Gage G4 - Before Rehabilitation - Right Lane

Figure 5.48: Dynamic response of strain gauge G4 to truck in left lane, before rehabilitation

Strain Gage G8 - Before Rehabilitation - Center Mark

Figure 5.49: Dynamic response of strain gauge G8 to truck on centre mark, before rehabilitation

Strain Gage G10 - Before Rehabilitation - Left Lane
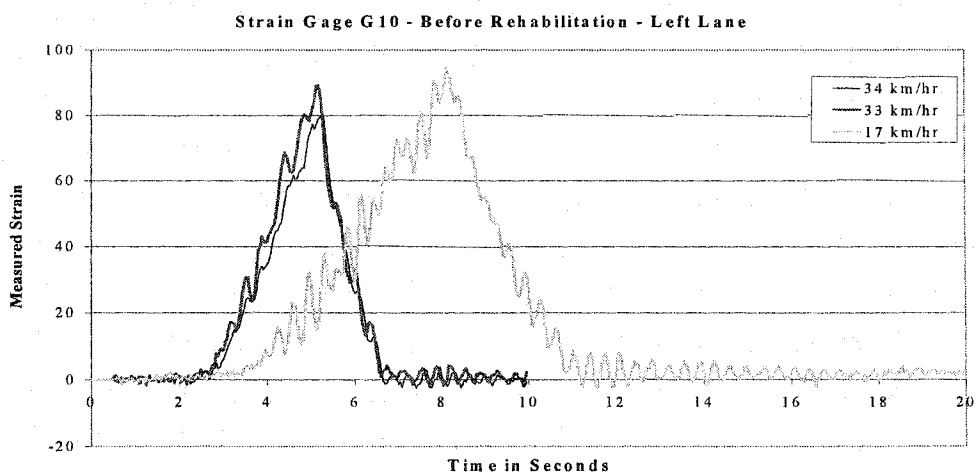
Figure 5.50: Dynamic response of strain gauge G10 to truck in left lane, before rehabilitation
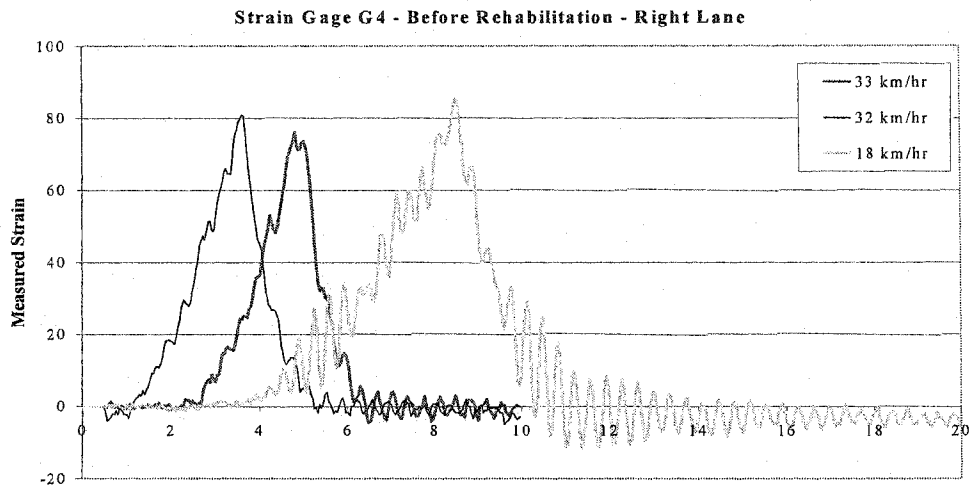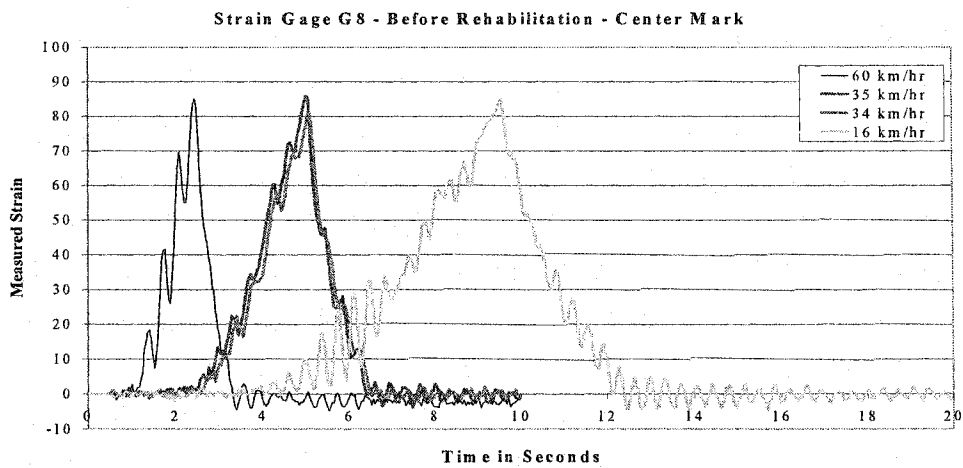
129
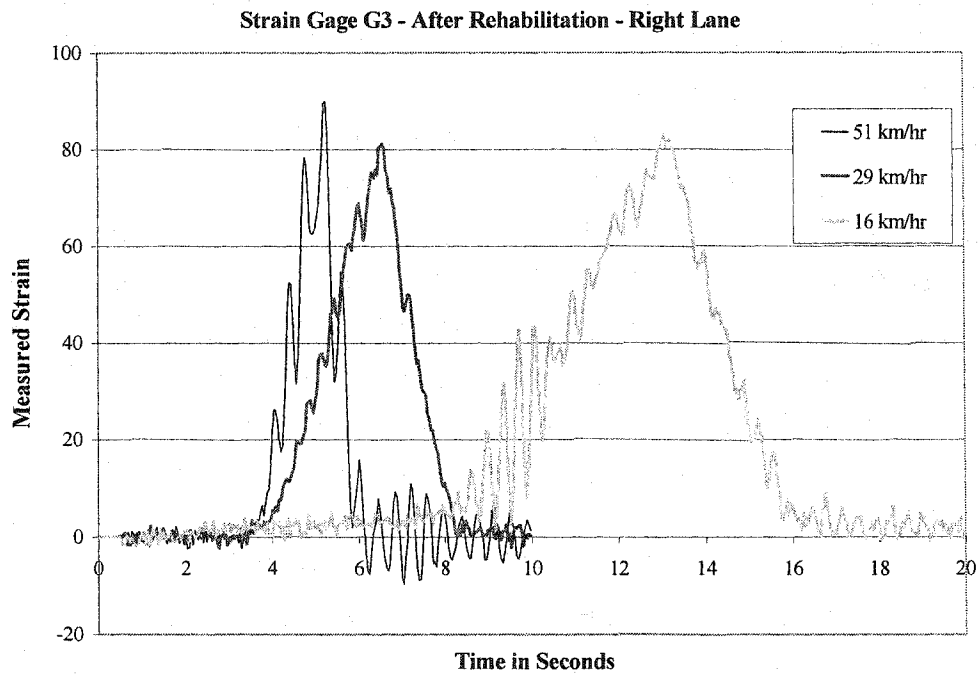
Figure 5.51: Dynamic response of strain gauge G3 to truck in right lane, after rehabilitation
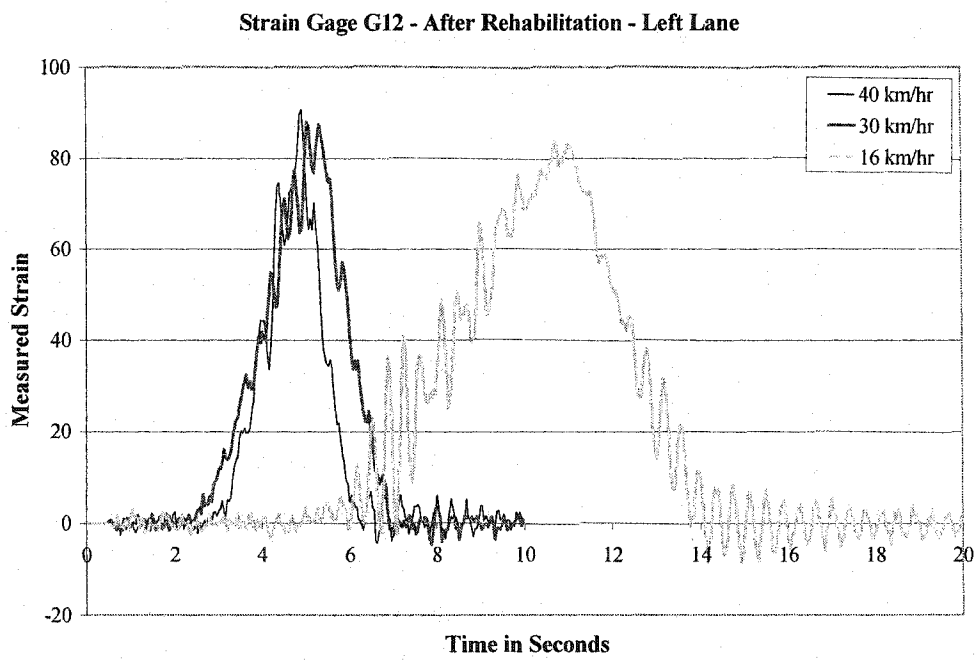
Figure 5.52: Dynamic response of strain gauge G12 to truck in left lane, after rehabilitation

130

Load Sharing among Girders - Dynamic Measurements
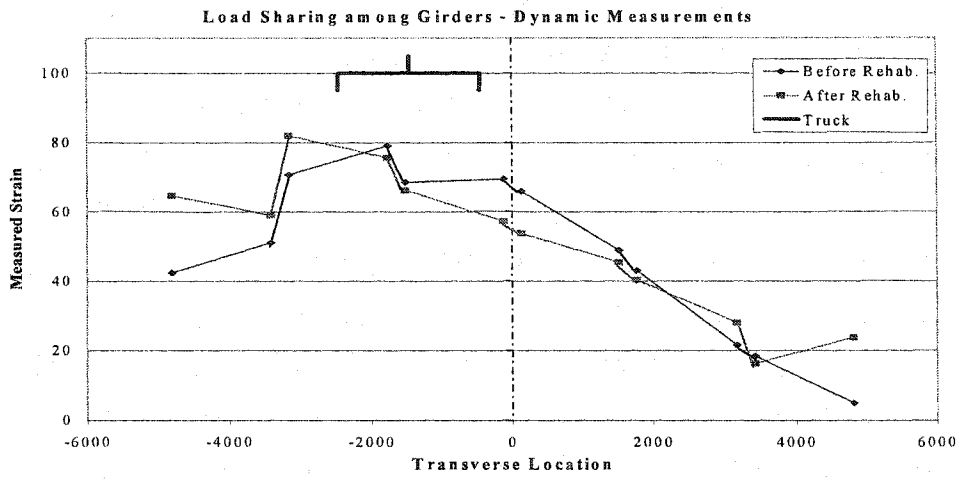
Figure 5.53: Load sharing in dynamic test based on strains, truck in right lane

Load Sharing among Girders - Dynamic Measurements
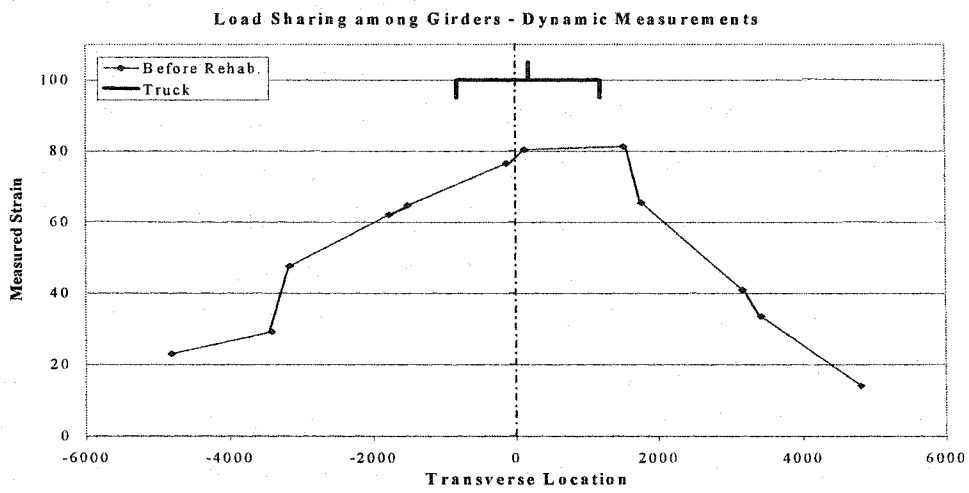
Figure 5.54: Load sharing in dynamic test based on strains, truck on centre mark

Load Sharing among Girders - Dynamic Measurements
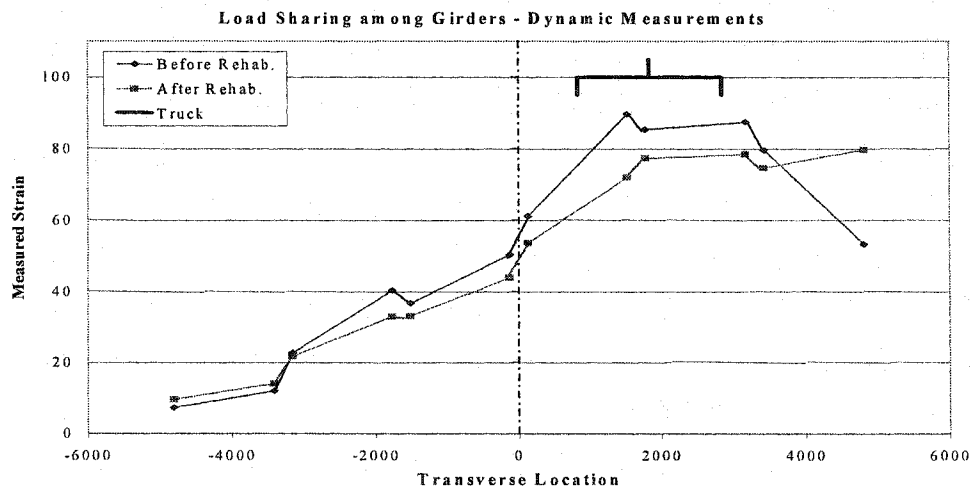
Figure 5.55 Load sharing in dynamic test based on strains, truck in left lane

131
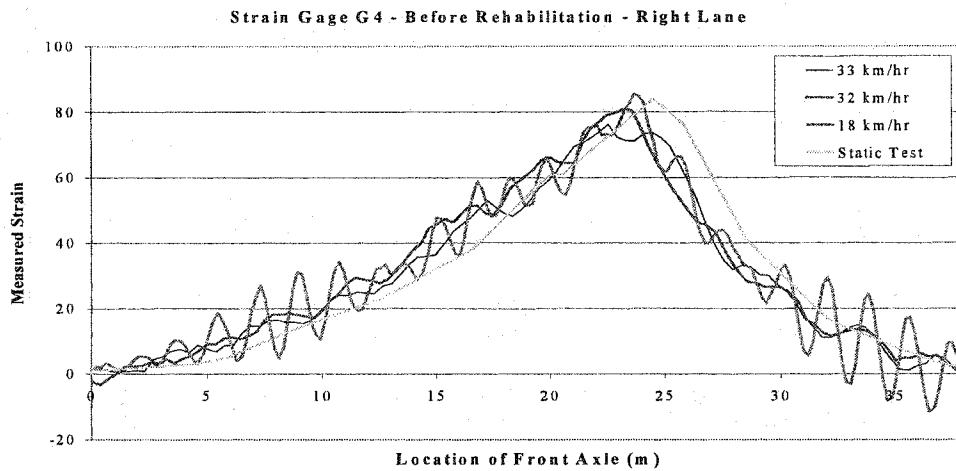
Figure 5.56: Strains in static and dynamic tests, truck on right lane, before rehabilitation
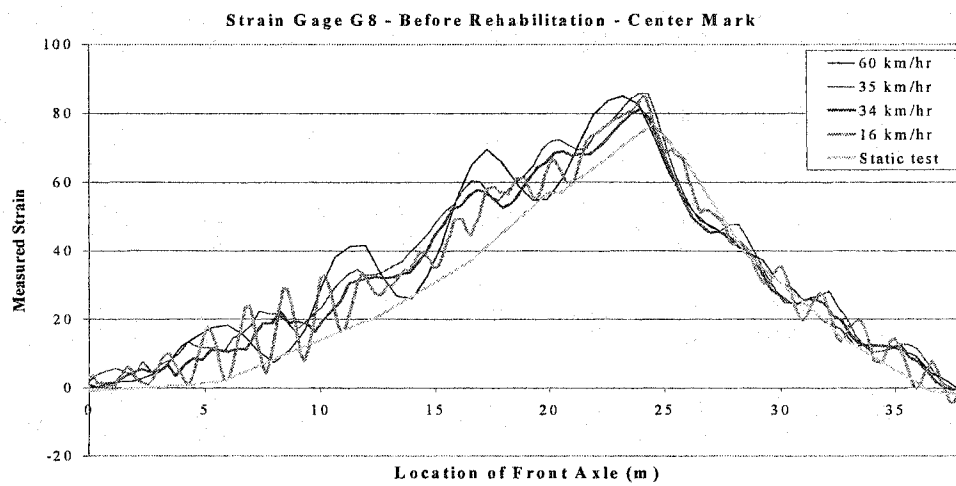
Figure 5.57: Strains in static and dynamic tests, truck on centre mark, before rehabilitation
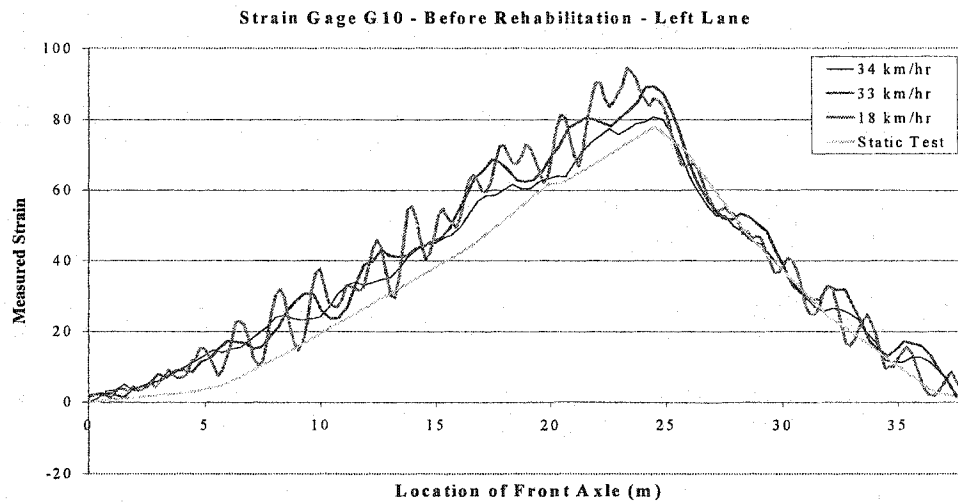
Figure 5.58: Strains in static and dynamic tests, truck on left lane, before rehabilitation

132

Strain Gage G3 - After Rehabilitation - Right Lane
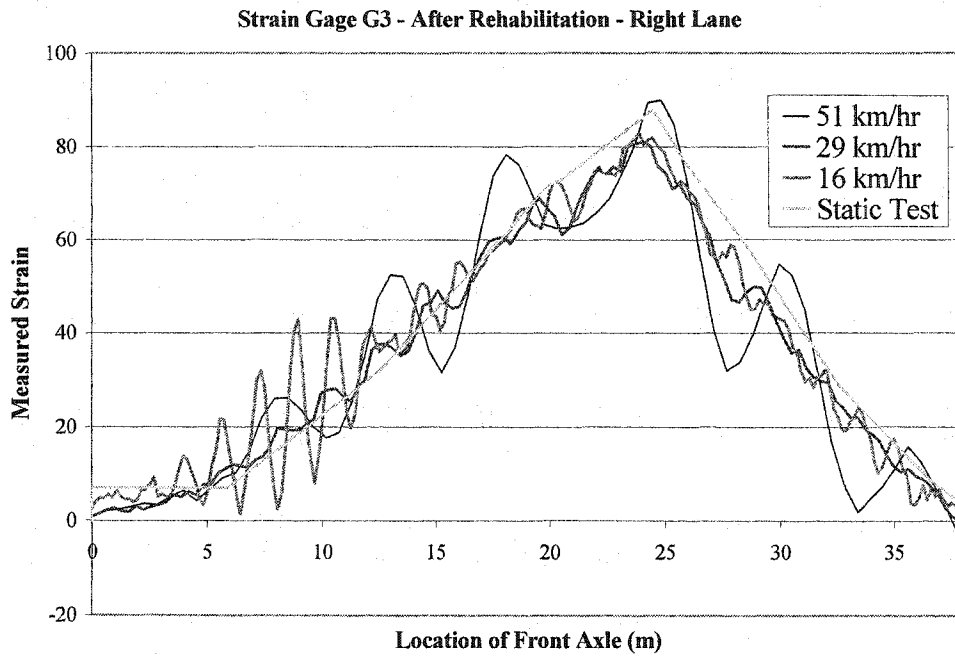
Figure 5.59: Strains in static and dynamic tests, truck on right lane, after rehabilitation

Strain Gage G12 - After Rehabilitation - Left Lane
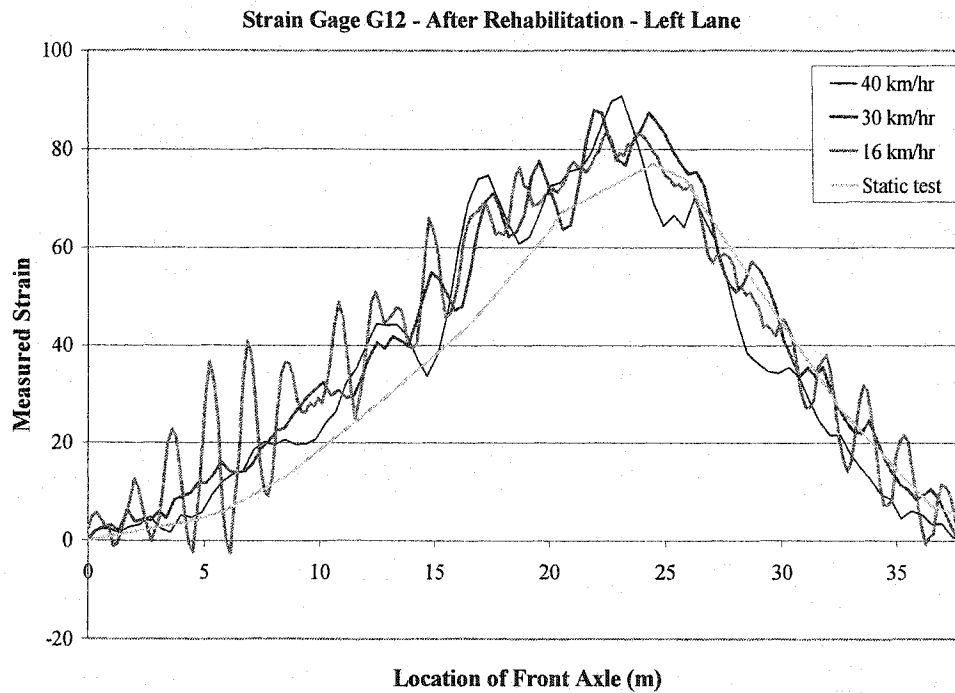
Figure 5.60: Strains in static and dynamic tests, truck on left lane, after rehabilitation

133

Strain Gage G4 - Before Rehabilitation - Right Lane - 18 km/hr
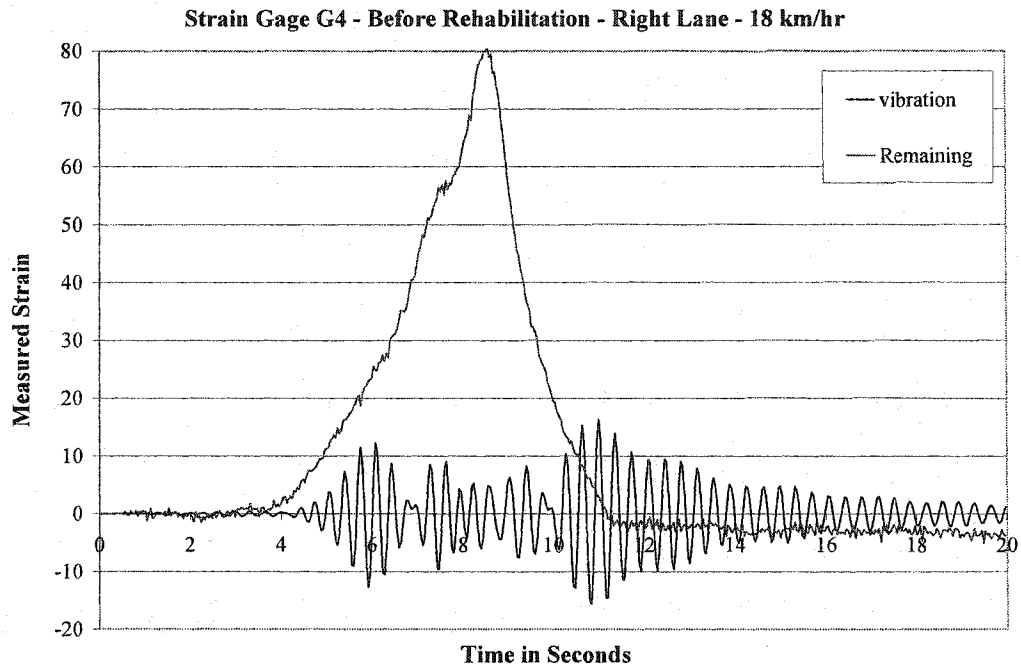
Figure 5.61: Vibration of the bridge in dynamic test, truck on right lane, before rehabilitation

Strain Gage G12 - After Rehabilitation - Left Lane - 16 km/hr
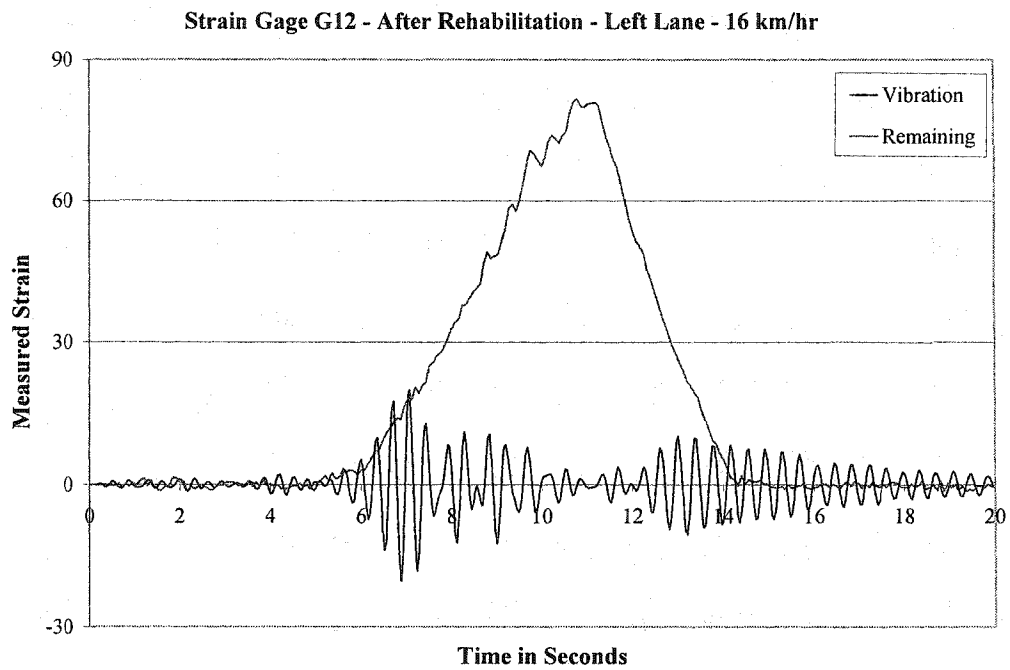
Figure 5.62: Vibration of the bridge in dynamic test, truck on left lane, after rehabilitation

134

Before Rehabilitation
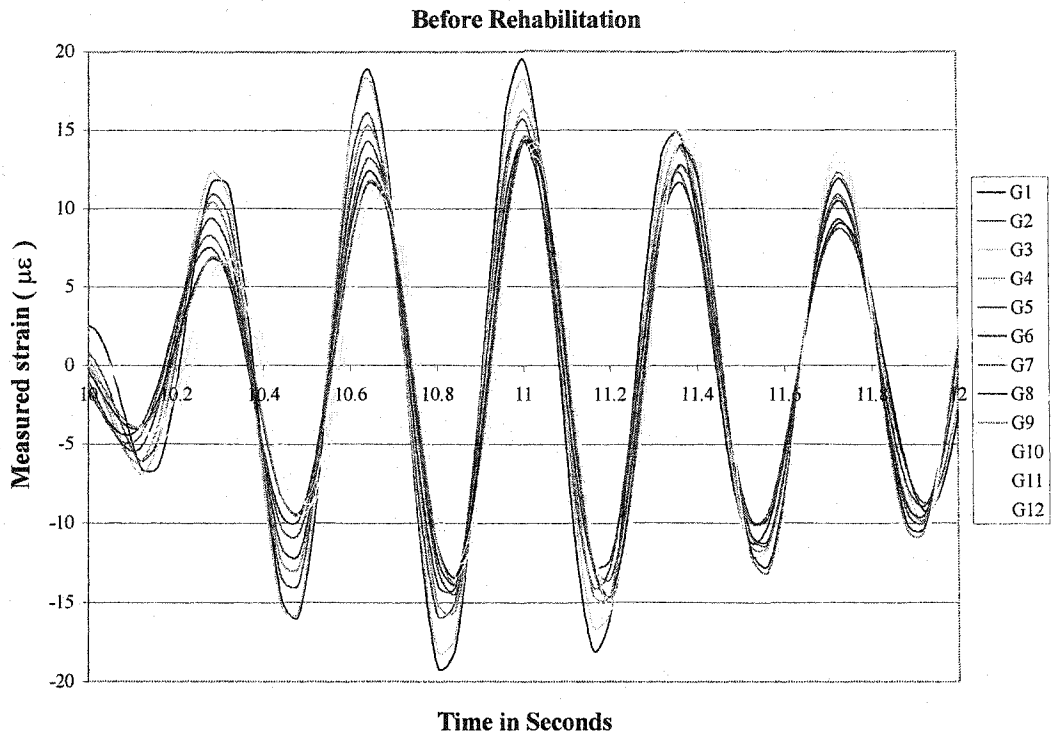
Figure 5.63: Two seconds of vibration of the girders caused by the truck at 18 km/hr.
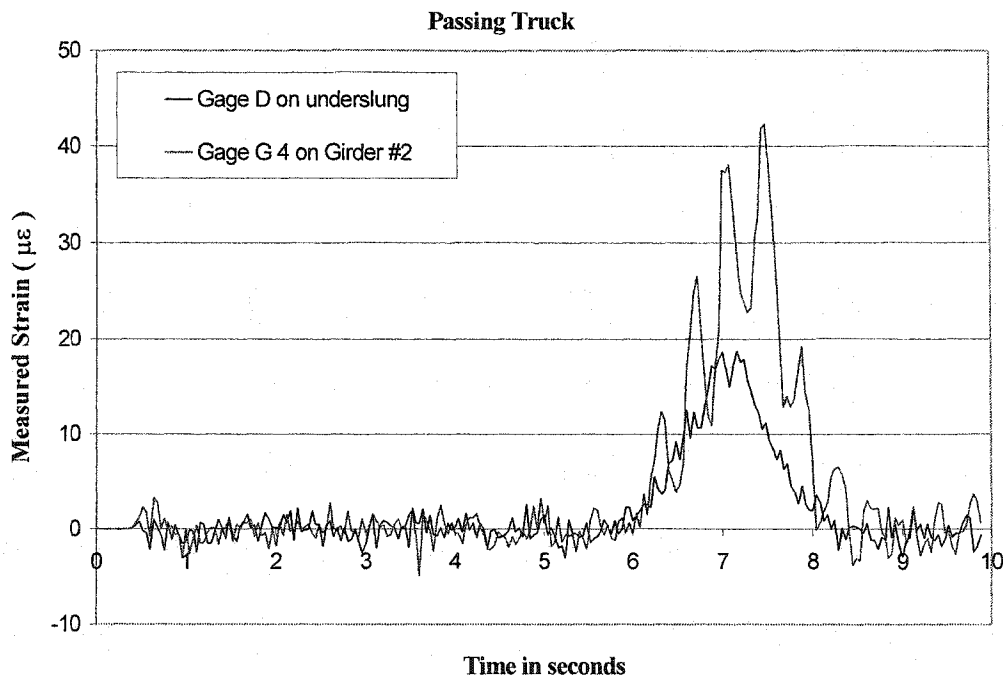
Passing Truck

Figure 5.64: Measured strain in the underslung assembly caused by passing truck load

135
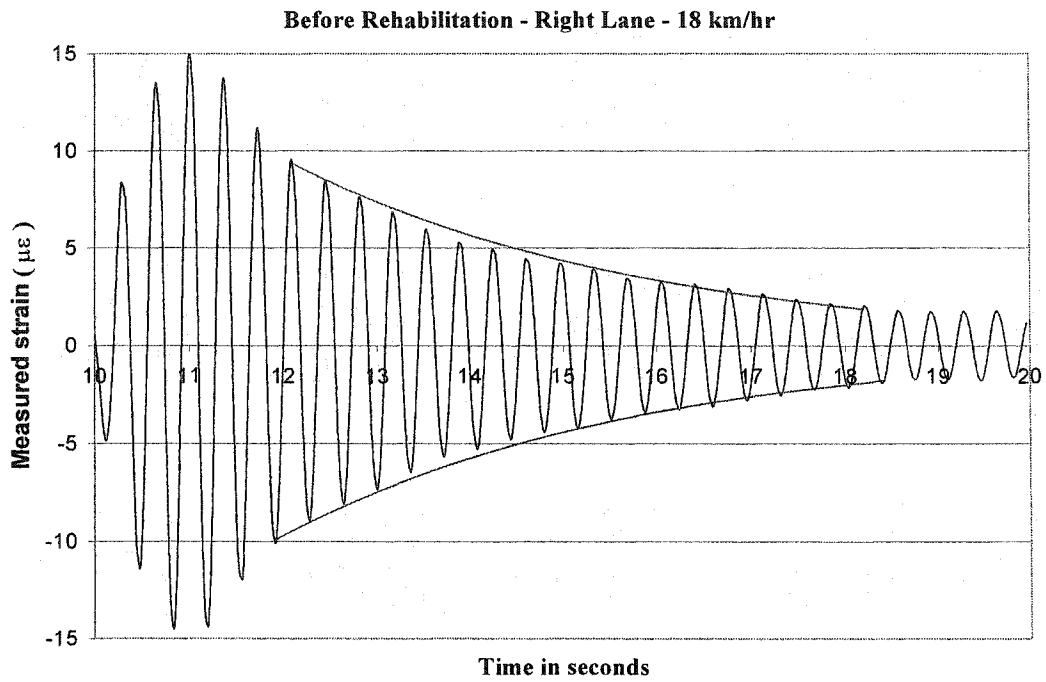
Figure 5.65: Free vibration of the bridge and its damping, before rehabilitation
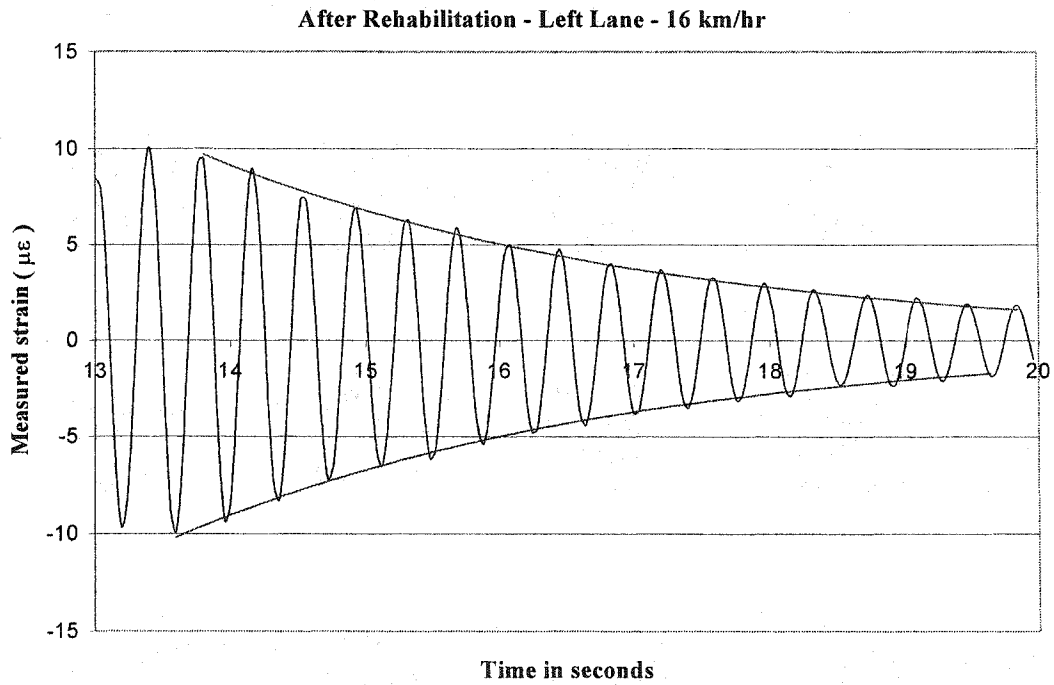
Figure 5.66: Free vibration of the bridge and its damping, after rehabilitation

136
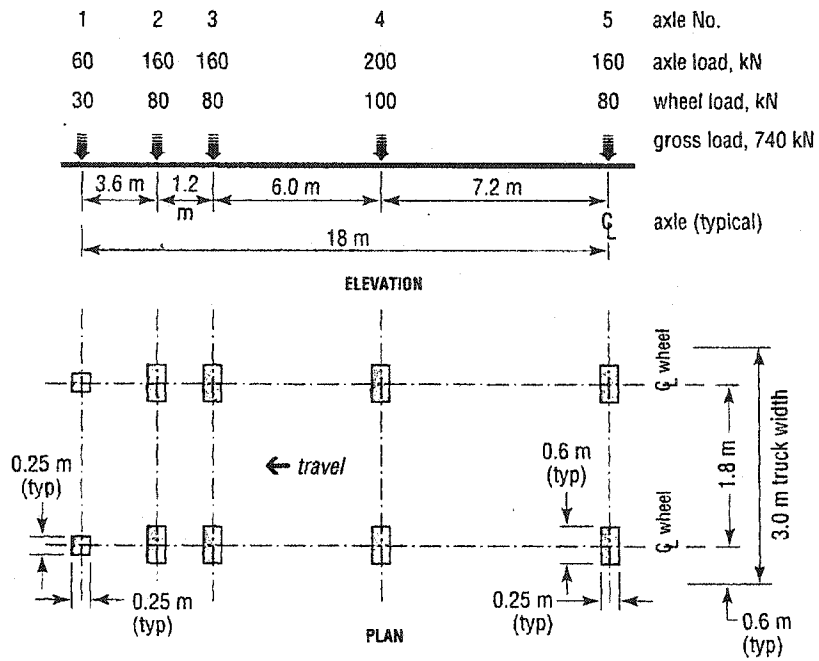
Figure 5.67: Truck information OHBD Code
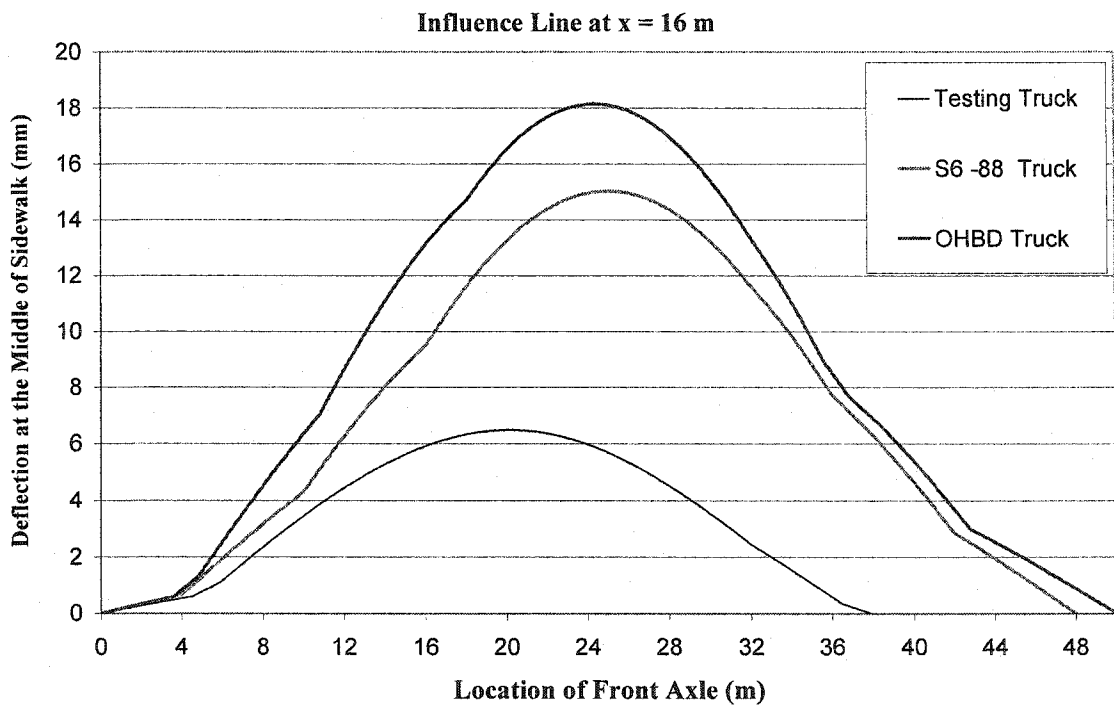
Figure 5.68: Influence line for deflection at the middle
of sidewalk for different trucks

137
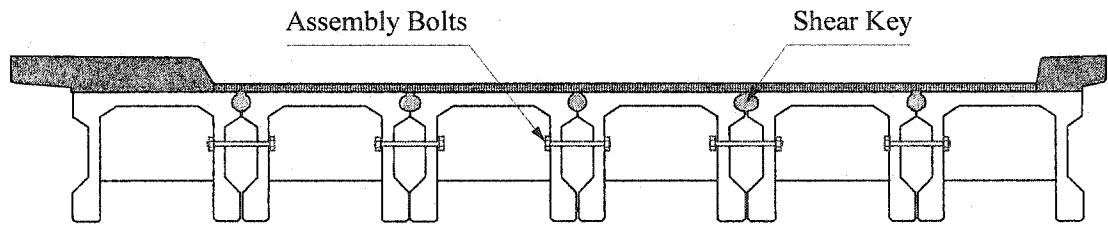
a) Undeformed Shape of the Bridge
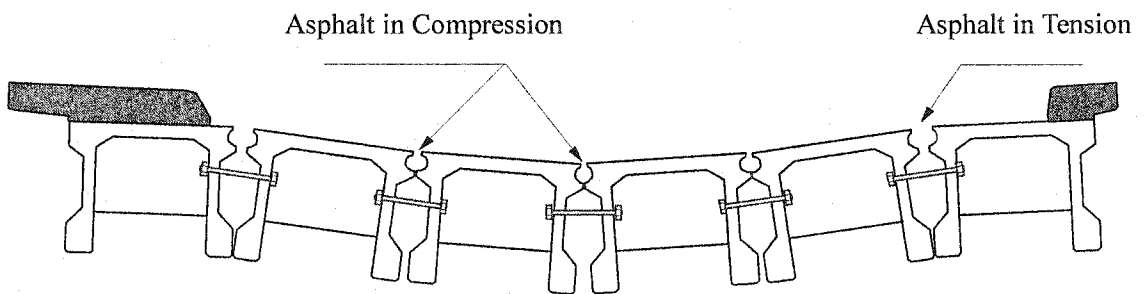
b) Deformation of the Bridge due to Vertical Loads
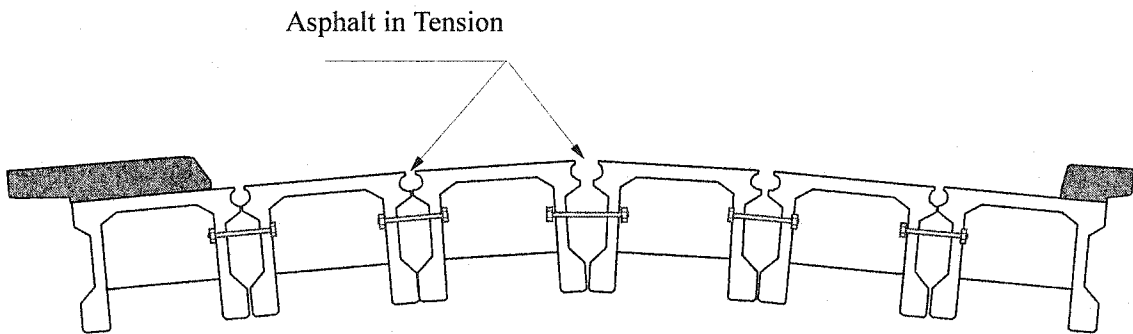
c) Vibration of the Bridge at the Frequency of 5.43 Hz

Figure 5.69: Transverse deformation and vibration profile of the bridge

138
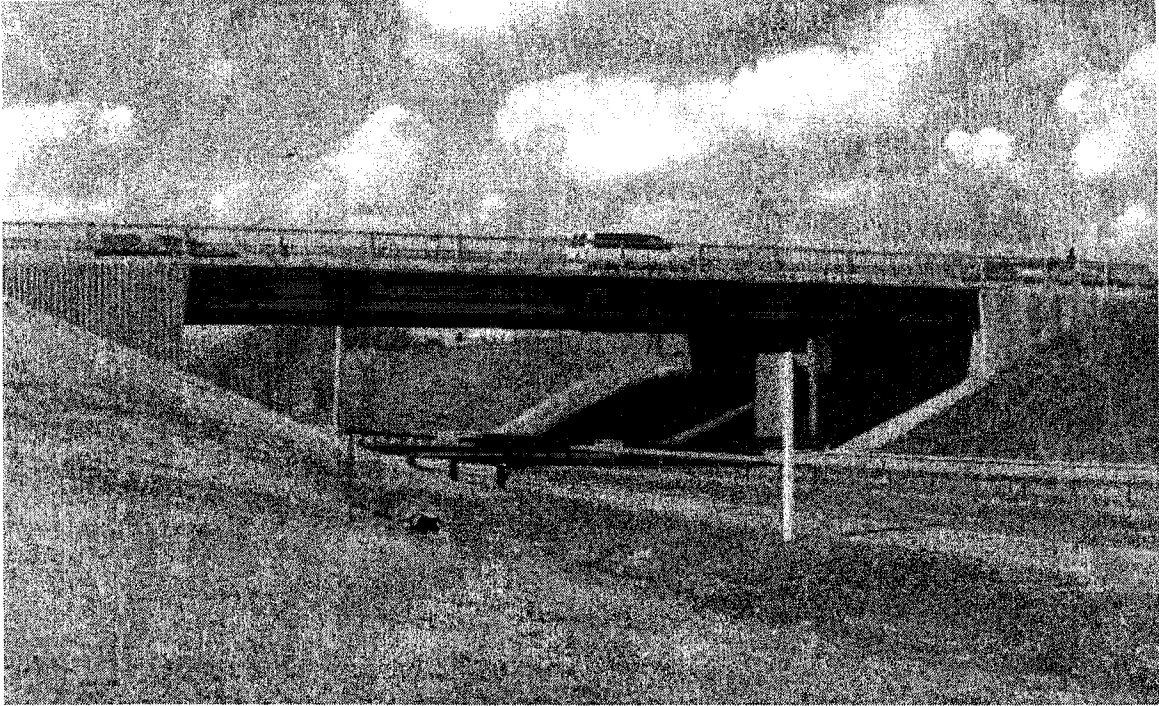
Figure 5.70: View of the 99th Ave. Fort Saskatchewan bridge

Figure 5.71: View of underside of the bridge

139
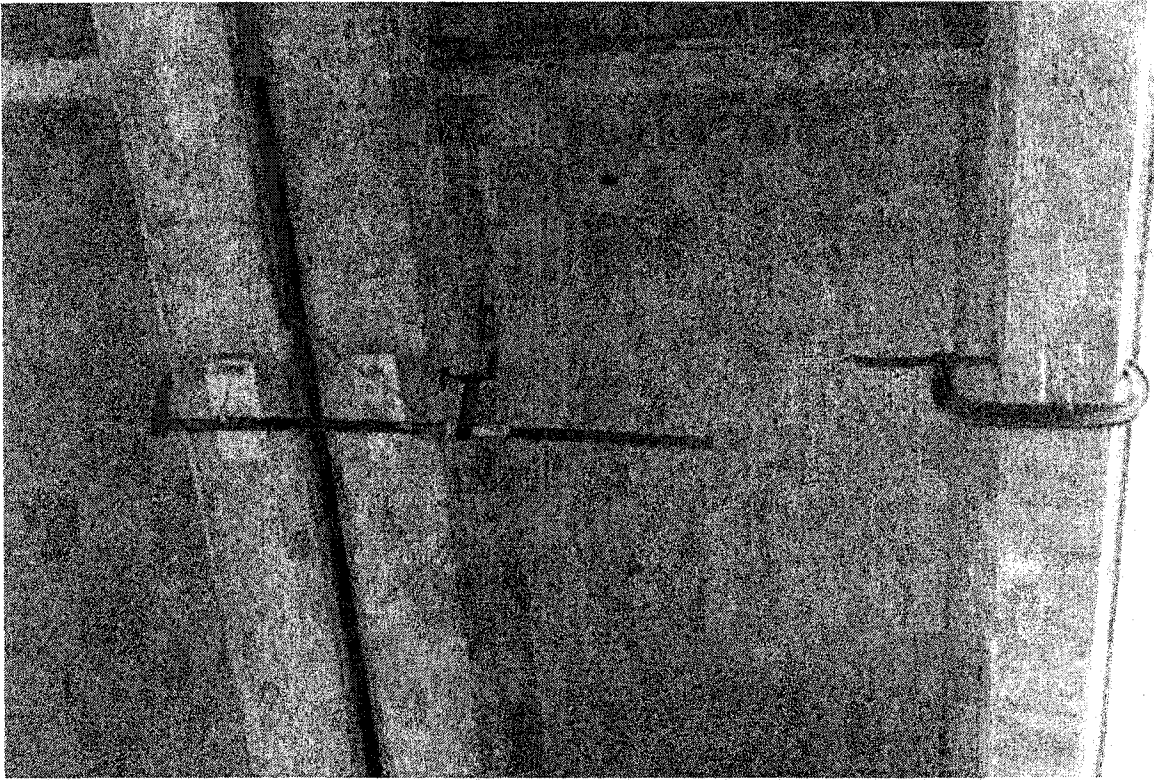
Figure 5.72: Installation of strain gauges in progress

Figure 5.73: Soldering strain gauge ends to wires

140
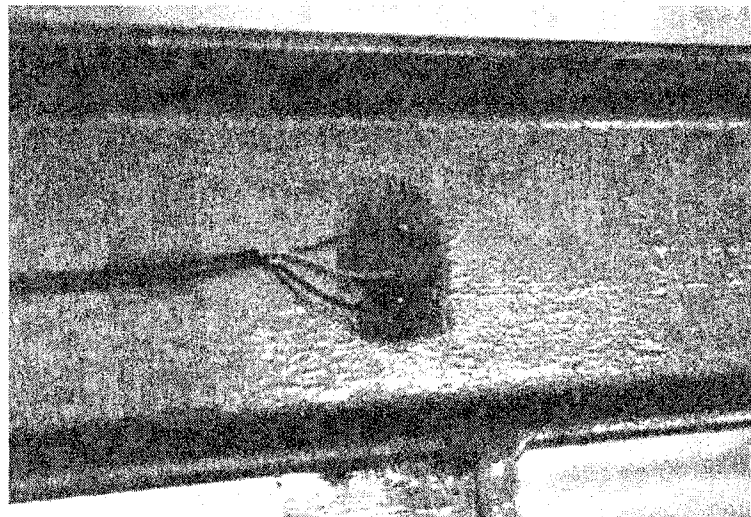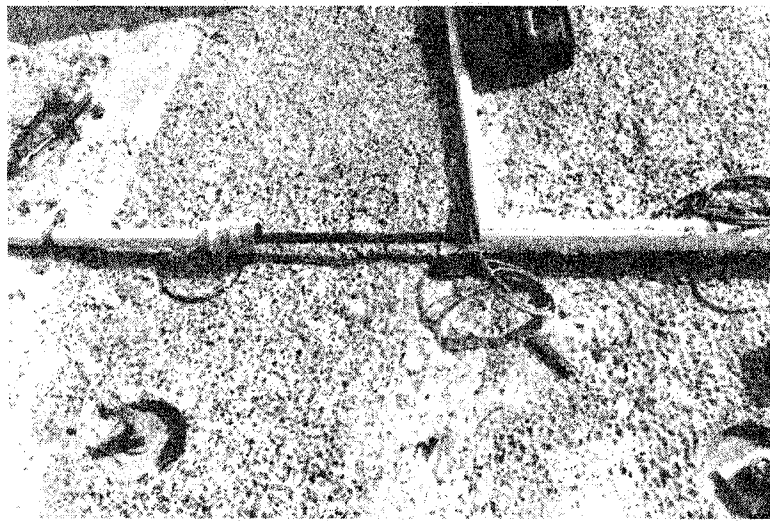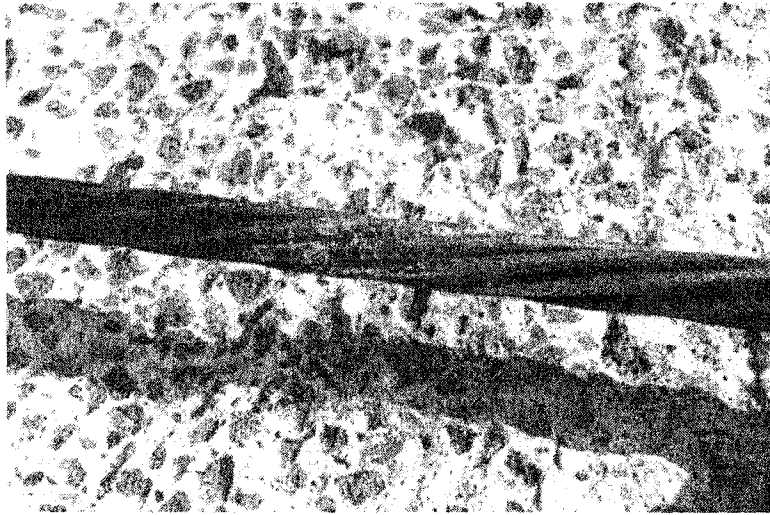
Figure 5.74: Strain gauging tendons and underslung diaphragm
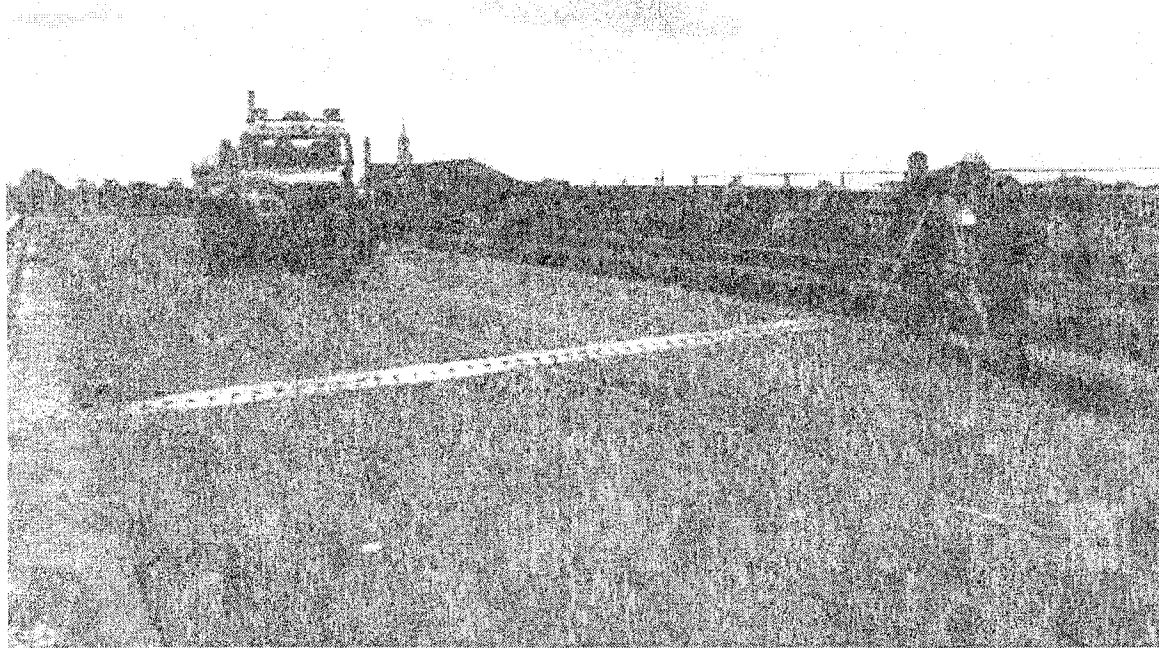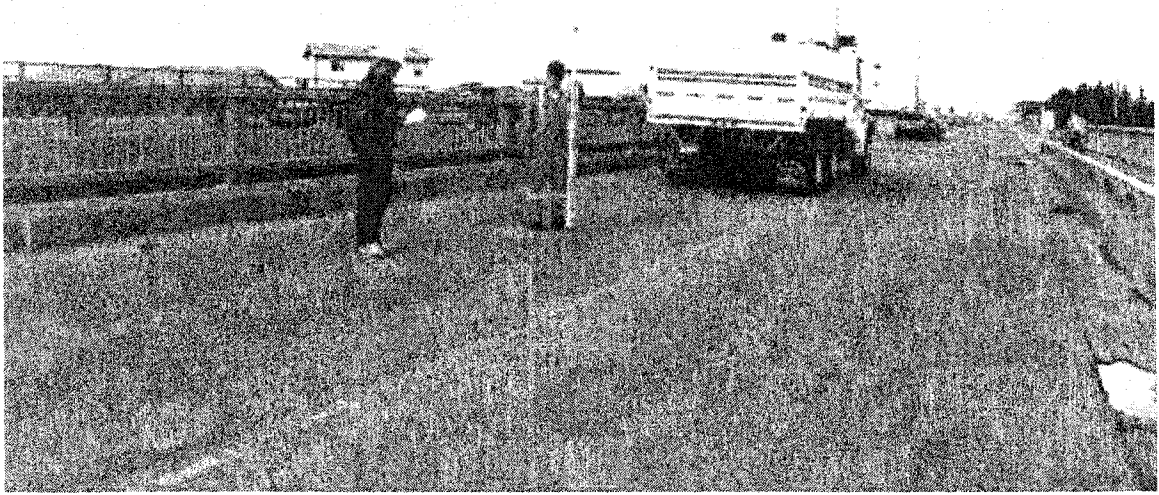
Figure 5.75: Level surveying to verify deflection measurements from cable transducers

142
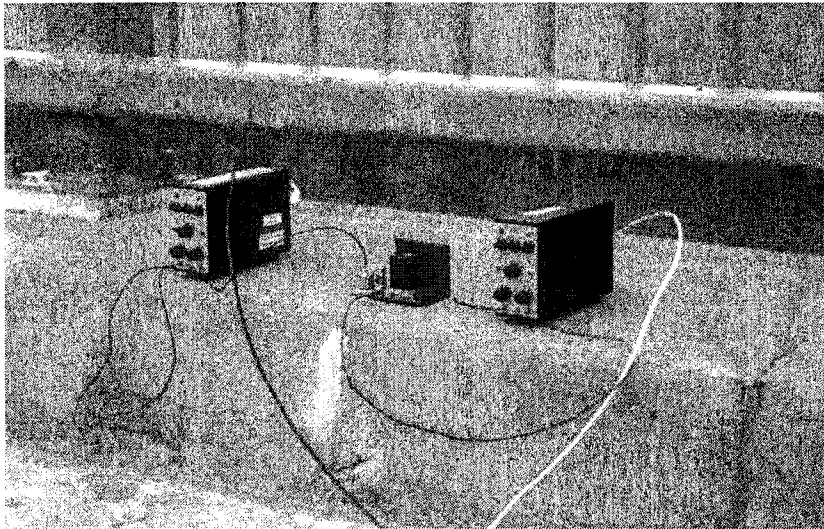
Figure 5.76:
Signal
conditioners
and
accelerometers
for ambient
vibration test

Figure 5.77:
Cable
transducers
installed on
guard rail,
under the bridge

143
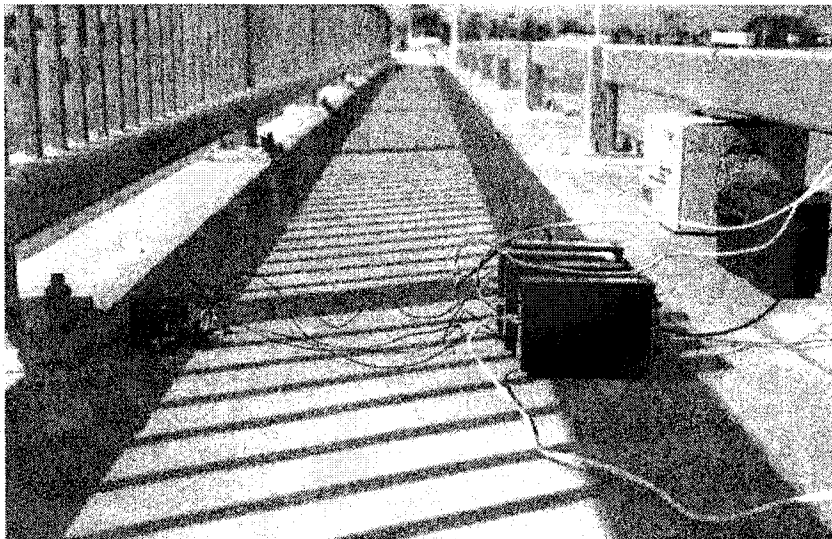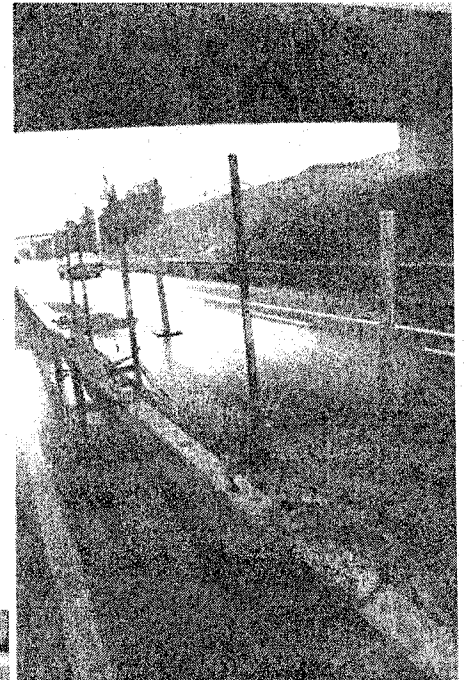
Figure 5.78: Static & Dynamic load tests with truck load
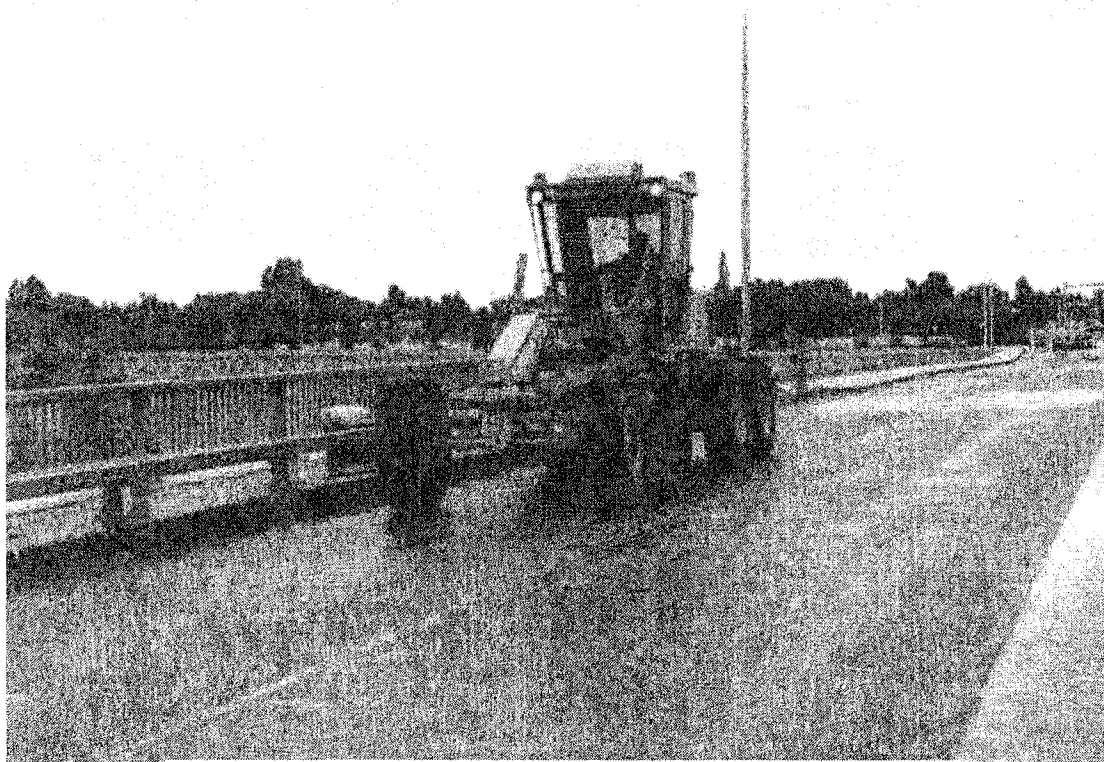
Figure 5.79: Static & Dynamic load tests using a grader

144
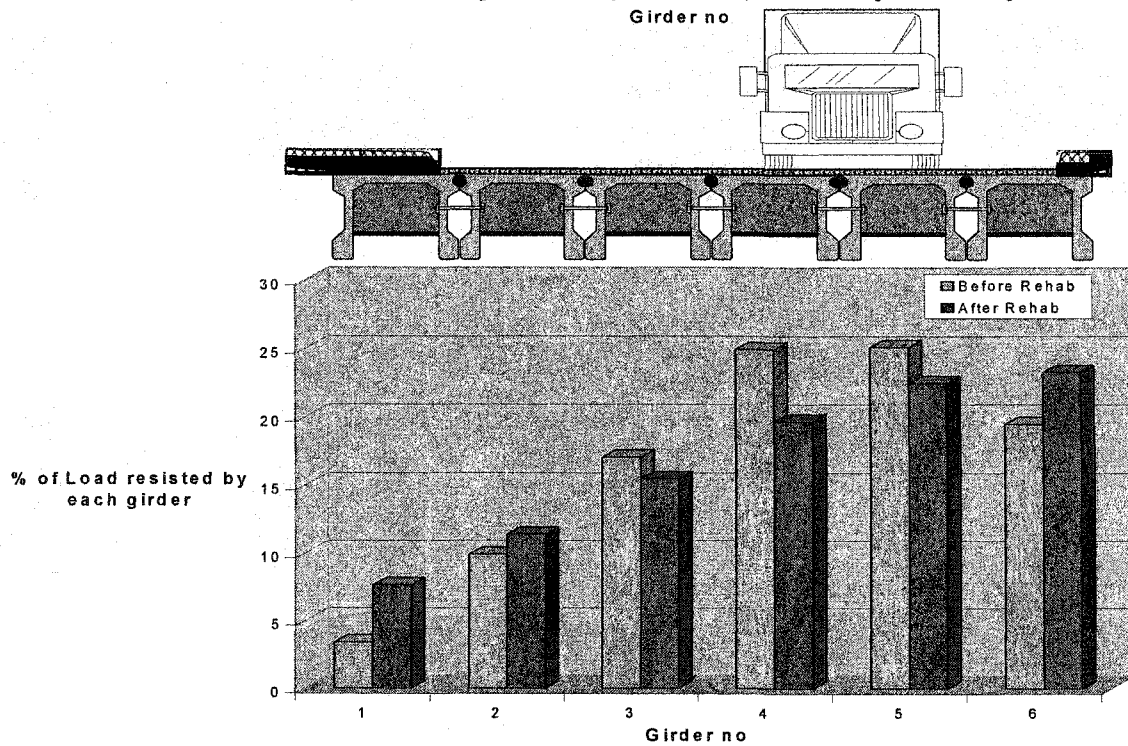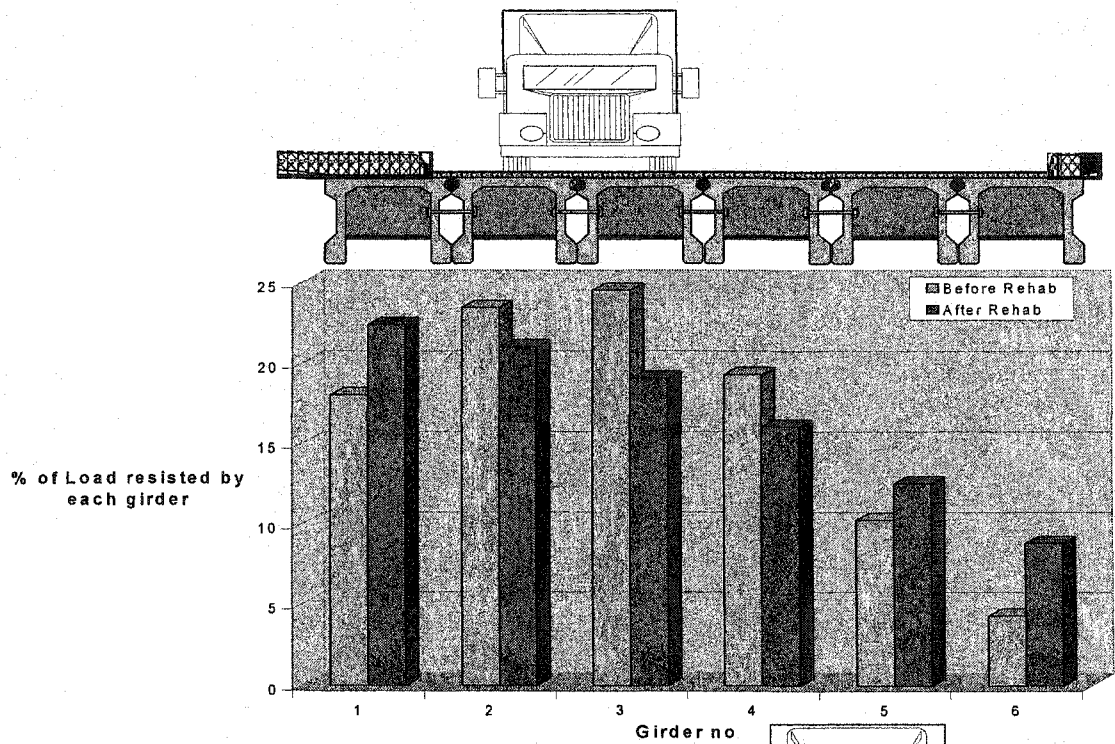
Figure 5.80: Lateral live load distribution factors (LLDF) based on measured test deflections

145

6.0 FINITE ELEMENT MODELLING OF THE BRIDGE REHABILITATION IN FORT SASKATCHEWAN, ALBERTA

6.1 Introduction

The 99th Ave. bridge in Fort Saskatchewan, Alberta, is a two lane, single span overpass, composed of six precast prestressed inverted U shaped FC girders, joined together by field grouted shear keys and connector bolts. The bridge deck had an asphalt overlay. Due to extensive longitudinal and transverse cracking of the asphalt and to accommodate increased traffic loads, a rehabilitation program was designed to improve the load sharing among the girders and increase the transverse stiffness of the bridge.

Historically, FC girder bridges in Alberta have developed load sharing and leakage problems due to shear key deterioration. This degradation often appears in these bridges in the form of longitudinal cracks in the bridge deck, directly over the shear key locations. Once a crack is formed in the shear key, water and de-icing salts from the road surface penetrate the wearing surface and weaken the shear key grout[1]. The loss of the shear keys not only eliminates the load sharing between the girders but also gives rise to corrosion of the prestressing tendons and the girder steel, after the salt laden water starts to deposit on the underside of the FC girders and eventually migrate towards the girder steel.

In 1998, it was decided to rehabilitate the 99th Ave. Fort Saskatchewan Bridge because of extensive longitudinal and transverse cracking as well as increased traffic loads on the overpass. The rehabilitation program mainly targeted the transverse stiffness of the bridge, which goes down once the shear keys deteriorate and the individual girders start acting independently. The main components of the rehabilitation scheme consisted of continuous underslung diaphragms, which limit the relative movement of adjacent girders and a 100 mm laterally post-tensioned, cast in place, fibre reinforced silica fume concrete

146

deck, to better distribute the load to the underlying girders. The concrete overlay had no longitudinal reinforcement and was laterally stressed by 12.7 mm strands.

To assess the effectiveness of the rehabilitation program and to develop a basic understanding of the behaviour of FC girder bridges a two-fold research program was conducted on the 99th Avenue bridge in Fort Saskatchewan, Alberta. The first half consisted of field testing and assessment of the FC girder bridge under service loads and the second half is the finite element modeling and simulation of the bridge, meant to evaluate the contribution of the different rehabilitation components on the resulting behaviour of the bridge.

With the development of electronic data acquisition and storage systems it has become easier now to apply periodic or continuous monitoring to structures. The main idea is to replace visual, undependable inspections by health monitoring systems, which periodically or continuously acquire and analyze response data and indicate damage when it is not too late. Several methods have been proposed in the research literature for interpreting changes in the key characteristics of a structure. However the case study given in this chapter makes use of the model based method, using a finite element model refined with information from field monitoring of the bridge. It will be shown by three independent measurements that the finite element model of the bridge proved to be a reasonably good indicator in simulating the behaviour of the actual FC Girder Bridge.

6.2 The Field Monitoring Program

Most of the remedial measures applied in the past have been based on visual site inspections and previous experiences. Different rehabilitation schemes are usually tried and improvements and modifications are refined over the years, based on response to previous schemes. This approach may not always yield the best results and valuable time and finances can be spent on using a particular strategy and studying its response on a particular structure. Due to the complexity of a real life structure and its real operating conditions, numerical models may not always prove to be accurate, unless they are calibrated with, in service, structure data. Hence the conventional means of rehabilitating

147

essentially reduce to hit and trial methods where design formulates on the degree of success achieved.

To be able to periodically monitor the Fort Saskatchewan Bridge, twenty eight strain gauges were installed on the FC girders, post-tensioning tendons and the underslung diaphragms. During load tests, ten cable transducers were attached to the girders to measure deflections and four accelerometers were used to perform the ambient vibration tests. Three types of tests were conducted on the bridge with the help of a 23 Ton truck load, i.e. a static load test, a dynamic load test and an ambient vibrations test, and three independent measurements, i.e. deflections, strains and natural frequencies and mode shapes were obtained from these tests[2].

The load tests and the ambient vibrations tests were conducted before and after rehabilitation to compare and assess the effect of the rehabilitation scheme on the behaviour of the bridge. For complete details on the experimental program of Fort Saskatchewan Bridge, please refer to Chapter 5 of this thesis.

6.2.1 Confidence limits of the test data

Before building the finite element model, it was felt necessary to evaluate the statistical dispersion of the data and hence investigate the confidence limits of the test results. The standard deviation of a data set is a good measure of the dispersion of the data because it is expressed in the same units as the data itself. The mean and standard deviation of the test deflections and strains, read by all the cable transducers and strain gauges were calculated and have been tabulated in Tables 6.1 and 6.2. The column n, indicates the number of readings taken by each cable transducer. One reading for each of the displacement transducers came from the static load test whereas three came from the pseudo-static portion of the dynamic load test.

148

Table 6.1: Data dispersion in measured test deflections

Cable Transducer	Number of Readings (n)	Before Rehabilitation		After Rehabilitation	
		Mean (mm)	Standard Deviation (mm)	Mean (mm)	Standard Deviation (mm)
L1	4	0.89	0.05	2.09	0.20
L2	4	1.63	0.24	2.62	0.28
L3	4	2.40	0.08	3.17	0.16
L4	4	3.55	0.16	3.74	0.21
L5	4	4.34	0.18	3.97	0.17
L6	4	6.00	0.17	4.85	0.21
L7	4	6.39	0.18	5.13	**0.31**
L8	4	6.38	0.46	5.61	0.27
L9	4	5.34	**0.48**	6.31	0.20

It can be seen from Table 6.1 above that the largest standard deviation before rehabilitation comes from the cable transducer L9 and is 0.48. Similarly the largest standard deviation after rehabilitation, from the cable transducer L7 was 0.31. According to normal probability distribution characteristics, 95.44% of the time, a normal random variable assumes a value within plus or minus two standard deviations of its mean[3]. Two standard deviations for L9 comes out to be 0.96 mm, and for L7 it is 0.62 mm. It may be noted here that the sample size only consists of four readings (i.e. n). Generally, the standard deviations go down as the sample size increases and hence we can comment that the standard deviation would have been a lower value, had we taken more readings in the same test. Moreover, it can be observed from Table 6.1 that only L7, L8 and L9 gave standard deviations higher than 0.3, whereas all the other cable transducers had standard deviations around 0.2 mm. Two standard deviations of 0.2 would amount to 0.4 mm, which can be considered as a very reasonable dispersion figure.

149

Table 6.2: Data dispersion in measured test strains

Strain Gauge	Number of Readings (n)	Before Rehabilitation		After Rehabilitation	
		Mean ($\mu\epsilon$)	Standard Deviation ($\mu\epsilon$)	Mean ($\mu\epsilon$)	Standard Deviation ($\mu\epsilon$)
G1	4	45.2	3.3	63.0	2.0
G2	4	53.1	**4.6**	58.6	3.9
G3	4	71.6	4.5	81.0	**5.6**
G4	4	79.3	4.1	73.2	5.1
G5	4	68.0	2.7	63.0	4.2
G6	4	67.8	3.2	53.4	2.8
G7	4	63.2	2.1	50.2	1.2
G8	4	45.8	1.0	42.3	2.9
G9	4	39.9	1.4	36.8	0.8
G10	4	18.4	1.0	23.0	2.7
G11	4	14.9	0.7	13.3	0.8
G12	4	0.9	0.6	20.3	1.3

Similarly Table 6.2 shows the dispersion of strains recorded in the static and dynamic load tests on the bridge. It can be seen that the strain gauges G2 and G3 give the largest standard deviations of 4.6 and 5.6 $\mu\epsilon$ respectively, which again represent reasonable scatter in the strain test data.

To conduct periodic monitoring and to test the reproducibility of the earlier data, a series of dynamic load tests were again carried out in 1999, using the same set of gauges, which have been permanently installed to the bridge. A comparison of the 1998 after rehabilitation results and the 1999 results showed that no significant change has occurred in the structural behaviour of the bridge. Moreover excellent agreement between the results of the two years confirmed the reliability of the testing methods and the apparatus used. Figure 6.1 shows the strain comparison, measured in the load tests from the two years. The slight difference between results from the two years can be attributed to the

small change in weights of the two trucks used for the tests in different years. The 1998 test was conducted with a 23-ton truck whereas the 1999 test was carried out with a 22-ton truck.

6.3 Finite Element Analysis

The main objective of the finite element analysis was to develop a model that would predict the behaviour of the FC girder bridge under traffic loads. The predicted deflections, strains and modal parameters from the model were compared to those obtained from the field tests on the bridge, to test the validity of the model. A validated finite element model provides a useful tool for evaluating the effect of various parameters and rehabilitation components that were not, or could not be specifically investigated in the test program.

Many FC girder bridges utilize a combination of rehabilitation schemes and it is difficult to identify and quantify the contribution of each of these schemes from the test information. The finite element model can be particularly useful in studying the effect of using each of the rehabilitation schemes separately.

6.3.1 Description of the model

A three dimensional finite element model was prepared for the bridge using the professional version of the finite element analysis software S-Frame (Version 5.1). The choice of the program was based on its simplicity of use, efficiency in computational time, user-friendly graphical interface, and a wide acceptance in the industry. A three dimensional model was selected instead of a two dimensional one because torsional and transverse mode shapes of vibration could not be identified in a two dimensional model.

The quadrilateral shell element was selected as the main building block for the model. This element in S-Frame has both out-of-plane (bending) and in-plane (membrane) capabilities and permits both in plane and out of plane loading. It can be used for bending only, membrane only or combined bending-membrane problems. The element has six degrees of freedom at each node, i.e. three translations in the element x, y and z

151

directions and rotations about the element x, y, and z-axes. The finite-element formulation of these shell elements uses a linear polynomial for the in-plane action, and a third order polynomial for the out-of-plane actions[4]. The material properties and thickness are assumed to be constant over the area of the element.

The element connectivity of the four-node shell element is described by connecting the four joints, I-J-K and L in counter-clockwise direction around the element. The element coordinate system is at the centre of the element where the lines joining the mid points of sides IJ to LK and IL to JK intersect. The element forces are computed at the centre of the element and are the membrane stresses and bending moments[4]. The aspect ratio defined as length to width, should not be large to skew the element (preferably less than 4). The interior angles should not be much greater than 90 degrees.

A large number of shell elements (4800) were used to model the girders, precast transverse concrete diaphragms, field grouted shear keys and the concrete overlay. Figures 6.2 and 6.3 show the cross sectional views of the actual single girder and the finite element model of the girder. Each FC girder is 1.62 m. wide and 1.27 m deep. Six precast transverse concrete diaphragms have been provided at longitudinal distances of 0-3-12-20-29-32 metres. These diaphragms are not continuous in a transverse cross section of the bridge and only span within the transverse cross section of the girder. Connector bolts (12.5 mm diameter) tie the legs of the girders at a longitudinal interval of 3 metres, as shown in Figure 6.4 and are placed at a depth of 0.53 metres from the top surface of the top flange. As visible from Figures 6.2 and 6.3, the finite element model was made to resemble the actual girder, in the closest possible shape. The shell elements forming the cross section of the model girders were adjusted in the following manner:

- The height of the bottom most elements of both the legs, running in the plane normal to the plane of the paper, were selected so as to align with the thicker portions of the actual girder legs.
- The precast transverse concrete diaphragm of the actual girder was modeled by a set of four transverse shell elements. The rationale behind breaking the diaphragm into

152

four pieces was to obtain a node or joint at the correct location of the connector bolts in the girder legs.

While, shell elements were used to model the longitudinally running field grouted shear keys, beam elements were used to model the connector bolts, as can be seen in figure 6.5.

6.3.2 Adjusting the shell element thickness

The thicknesses of the shell elements in the cross section of the girder model were adjusted by equating the bending stiffness and the position of the neutral axis of an actual single girder to that of the finite element model[1]. A transformed area approach was used to model the prestressing tendons in the girder legs. Five different girder cross sectional cases were identified, owing to the differences in the cross sectional shape as well as the internal reinforcement, i.e.:

i)	Exterior girder at support
ii)	Exterior girder at midspan
iii)	Interior girder at support
iv)	Interior girder at midspan
v)	Exterior or interior girder at ribs

Figure 6.6 shows cross sectional views of a single girder when looking at the actual geometry of the girder as well as the finite element model. It may be noted here that the length of the girder, according to this figure, is in the direction perpendicular to the plane of the paper, whereas the transverse girder diaphragms run in the plane of the paper. Hence the shell elements of the girder legs C, D, E, F, G, H and I are shown in the thickness dimension so as to illustrate the change in the thickness of the shell elements due to the change in the thickness of the actual girder geometry or the change in tendon profile. Another reason to present the model cross section in this way is to illustrate the geometry and the element connectivity that the finite element program will see and analyze. Elements J, K, L and M show the transverse girder diaphragm, and elements A and B show the prestressing tendons inside the concrete girder. Though the

153

accompanying table in Figure 6.6 shows different cross sectional cases for interior and exterior girders, owing to small differences in the girder tendons, the final model girder was generalized over the whole bridge by taking the average of the interior and exterior shape dimensions. Since all the other dimensions for the interior and exterior model girders were similar, an average of 318 mm and 312 mm for the bottom most elements of the girder legs was taken as 315 mm and used for every girder in the bridge at mid span.

The girder cross section has solid straight edged webs at the supports and haunched webs at mid span. Every three metres on the longitudinal span, the solid straight edged cross section has been used in the actual girder and is referred to as a rib. The ribs have been inserted in the actual girder to confine the connector bolts, which are used every three metres to tie adjacent girders together. To simulate the actual girder ribs, intermediate finite element model cross sectional dimensions were worked out, which would be cases between those of the support and the mid span. This is because the ribs were solid cross sections but the position of the tendon profile changed with the longitudinal span. This emphasis on precision and the effort to incorporate a number of different cross sectional thicknesses along the span of the bridge was necessary to obtain the best possible simulation of the distribution of mass of the actual geometry. Accuracy in the distribution of mass would come into play when we are dealing with the investigation of the vibrational characteristics of the bridge.

Reproduced here as a sample for the cross sectional shape of the exterior girder at mid span, Tables 6.3, 6.4, 6.5 and 6.6 shows the tabulated procedure of comparing the neutral axis and the moment of inertia of the actual geometry of the girder with that of the finite element model. Please refer to Figure 6.6 for dimensions of the girder elements. Approximating corners however with straight edges and incorporating transformed concrete areas for the steel tendons produced a resulting mass increase of about 16 %, which was adjusted uniformly over the bridge by reducing the material weights accordingly.

154

Table 6.3: Calculating position of the centroid for the actual girder geometry

	Top deck	Upper triangular elements	Vertical uniform thickness legs	Lower triangular elements	Lower portion of legs	Steel strands (nA_s)	Total
Area (mm^2)	206000	31000	150000	23200	206000	37200	654000
Moment of Areas (mm^3)	118×10^6	14.7×10^6	20.9×10^6	-4.13×10^6	-89.1×10^6	-18.9×10^6	41.3×10^6
Position of Centroid (mm)	= Total Moment / Total Area = 63.2 mm from the assumed position of the centroid which was 1270/2 = 635 mm. Since the result is positive therefore the resulting centroid is above the assumed centroid. Hence the position of the centroid from the top of the cross section = 635-63.2 = 571.8 mm						

Table 6.4: Calculating position of the centroid for the model geometry

Element	Length (mm)	Width (mm)	Area (mm^2)	Lever Arm (mm)	Moment (mm^3)
C	406.4	318.0	129200	-431.8	-55805000
D	406.4	318.0	129200	-431.8	-55805000
E	330.2	166	54800	-63.5	-3480000
F	330.2	166	54800	-63.5	-3480000
G	469.9	207.8	97600	336.6	32862000
H	469.9	207.8	97600	336.6	32862000
I	1371	127	174100	571.5	99508000
Position of Centroid (mm)	Total Area = 737510.74 (mm^2) Total Moment = 46661000 (mm^3) Position of Centroid = Moment / Area =63.3 mm Centroid from top of cross section = 635 – 63.3 = 571.7 mm				

155

Table 6.5: Calculating the moment of inertia for the actual girder geometry

Using the Parallel Axis Theorem, I.e. $I = I_i + A_i d^2$						
Rectangular Elements	**b (mm)**	**h (mm)**	**I_i (mm^4)**	**A_i (mm^2)**	**d (mm)**	**I (mm^4)**
Top Deck	1625	127	277×10^6	206000	508	53.6×10^9
Vertical legs	101.6	736.6	3383×10^6	74800	76.5	7.64×10^9
Wide leg part	254	406.4	1420×10^6	103000	495.0	53.4×10^9
Triangular Elements						
E2	101.6	152.4	9.99×10^6	7740	410.9	5.27×10^9
E4	152.4	152.4	15.0×10^6	11600	241.0	1.38×10^9
Steel strands				37200	571.2	12.2×10^9
Total moment of inertia of the X-section, I = 133.5×10^9						

Table 6.6: Calculating the moment of inertia for the model geometry

Using the Parallel Axis Theorem, I.e. $I = I_i + A_i d^2$						
Elements	**b (mm)**	**h (mm)**	**I_i (mm^4)**	**A_i (mm^2)**	**d (mm)**	**I (mm^4)**
C and D	318.0	406.4	1779×10^6	129200	495.1	66.9×10^9
E and F	166	330.2	498×10^6	54800	126.8	2.76×10^9
G and H	207.8	469.9	1797×10^6	97600	273.3	18.2×10^9
I	1371	127	234×10^6	174100	508.2	45.3×10^9
Total moment of inertia of the X-section, I = 133.1×10^9						

Two basic assumptions were made with the finite element model, i.e. the material properties of the bridge deck were the same in all directions and at all locations and the abutments were infinitely stiff and hence had no impact on the behaviour of the bridge deck. At least the first assumption regarding the stiffness of the girders had a tendency to vary in the field but it was felt that working out different stiffnesses of the girders for test to model calibration would give rise to a huge number of combinations which would only complicate matters.

6.3.3 Model parameters

156

Four parameters were identified to have a marked influence on the behaviour of the bridge and a base value for each of these parameters was established for the model. Those parameters were:

i)   The stiffness of the neoprene bearing pads

ii)   The thickness of the shear key elements

iii)   The modulus of elasticity of concrete girders

iv)   The mass of the different materials used

6.3.3.1 Stiffness of the neoprene bearings

The neoprene bearings below the girder legs were modelled as linear translational springs in the system x direction or in the direction of the longitudinal span of the bridge. 24 horizontal translational springs were used to model these neoprene bearings under each leg of the FC girders The system x, y and z directions can be seen in figure 6.7 which shows an isometric view of the finite element model.

The effective stiffness of these springs was calculated by taking into account the shearing rigidity GA of the neoprene pads, where G is the Shear Modulus of the material and A represents the area of the pad. The force required to cause a deflection Δ, on the volume shown in Figure 6.8 is given by:

$$F = (\frac{GA}{L})\Delta$$

Hence the value GA/L can be taken as the stiffness of the springs that were used to model the elastomeric bearings.

For this particular neoprene bearing;

A = (203 x 356) = 72268 mm^2

L = 32 mm

G = 2 MPa (Usual hardness of neoprene bearings used in Alberta = 60 Duro)

Hence stiffness of the translational springs = $\dfrac{2 \times 72268}{31.75}$ = 4552 N/mm

6.3.3.2 Thickness of the shear key elements

157

The longitudinal shear keys in the actual bridge seem to transfer load in the transverse direction by both bending and shear. However, Figure 6.9 shows that moving traffic over the bridge may cause it to go through vibrating cycles of the transverse cross section, in which the shear keys could easily undergo axial tension or compression. Since the bridge exhibited longitudinal cracking on the deck surface, it was assumed that the shear keys had deteriorated and the cracked concrete was not very helpful in contributing in axial tension. A relationship between the axial stiffness of the shear key elements of the model and the actual field key was worked out in the following way:

$$\text{Axial stiffness} = \frac{AE}{L} = \frac{(w \times t)E}{L}$$

Please refer to Figure 6.10 for use with the above expression.

For the actual shear key:

w = 1000 mm (constant for both the shear key & the shell element)

t = 150 mm (or 6")

L = 150 mm (or 6")

E = 4500(35)$^{0.5}$ = 26600 MPa (constant for both key & element)

$$\text{Therefore Axial stiffness, k} = \frac{(1000 \times 150) \times 26622}{150} = 26622359 \text{ N/mm}$$

Or, k = 26600 kN/mm

When the shear key cracks we assume that the whole tension is taken by the candy cane steel bars embedded in the shear keys. Hence we do another calculation for the cracked shear key stiffness as follows:

As = Area of Steel

The candy cane bars are 10mm diameter bars @ 190 mm on centres

Since we took an arbitrary longitudinal length of 1m for the shear key, therefore the number of bars crossing this distance will be $\frac{1000}{190} = 5.2$, say 6

158

Though two bars overlap, one coming from each side, we will ignore the contribution of one of these bars because of insufficient overlap for anchorage purposes and consider only one bar from each overlap. Therefore, total number of steel bars within the 1m strip would be 6.

Total Area of steel in the 1 m strip = $(\frac{\pi \times d^2}{4}) \times 6$ = 471 mm^2

$E_t = E_s = 200,000$ MPa

$L = 150$ mm

Therefore,

$$\frac{A_s E}{L} = \frac{471 \times 200000}{150} = 628000 \text{ N/mm}$$

In other words the stiffness of the cracked shear key, $k_{cracked\,shear\,key} = 628$ kN/mm. Now the axial stiffness of the plate element with a thickness of 15 mm will be evaluated and compared with the stiffness of the deteriorated shear key. The 15 mm thickness of the model has compared well with the test results.

$K_{shell\,element} = \dfrac{AE}{L}$ where A = (1000mm x 15mm) = 15000 mm^2

$E = E_c = 26622$ MPa

$L = 268$ mm

$K_{shell\,element} = (\dfrac{15000 \times 26622}{268}) = 1490037$ N/mm

Or, $K_{shell\,element} = 1490$ kN/mm, which is twice as large as the stiffness of the deteriorated shear key, i.e. 628 kN/mm.

It may be noted here that 628 kN/mm was calculated by totally neglecting the stiffness of the concrete in tension as well as the contribution coming from the overlapping hooked ends. Those contributions may be responsible for the difference here between the axial stiffness of deteriorated shear key and the shell element.

159

6.3.3.3 Modulus of elasticity of concrete girders

The modulus of elasticity of Canadian concrete varies considerably as a function of the concrete strength, the density of the concrete and of the type of coarse aggregate used. Two new equations have been introduced in the CSA standard A23.3-94 to allow the ten to twenty percent reduction due to experience with relatively lightweight Canadian concretes[5]. At the same time, the modulus of elasticity of concrete would increase with age as a result of increasing concrete strengths. Hence, the increase in fc′ and thus E due to age, over the specified value, seems to be offset due to the reduction in weight of the aggregate. Therefore the simplified expression for E, given by equation (8-7) of the CSA standard A23.3-94 was used to estimate the modulus of elasticity of concrete for the girders, i.e.;

$$E_c = 4500\sqrt{f_c'} = 26622 \text{ MPa for 35 MPa concretes}$$

6.3.3.4 Mass of materials

Values for the masses of the different materials used were taken from the original drawings of the Fort Saskatchewan Bridge[6]. The FC girders used in this bridge were of the type LF, which indicates the use of lightweight concrete. The specifications ask for the use of lightweight aggregates to conform to the requirements of A.S.T.M. Spec. C330 with maximum aggregate size of ¾". The unit weight of concrete was specified to be 120 lbs. per cubic foot.

6.3.4 Calibrating the finite element model

The model was calibrated with the test results to demonstrate that it was in fact a good representation of the actual behaviour of the real bridge. Three independent test measurements of deflections, natural frequencies of vibration and strains were used to calibrate the finite element model with the test. Monitored test deflections from load tests and natural frequencies and mode shapes from ambient vibrations tests were used to calibrate the model, and strain measurements were used to verify the validity of the model without changing any parameters.

160

6.3.4.1 Model optimization

Changes in the four parameters mentioned earlier, i.e. horizontal spring stiffness, shear key thickness, modulus of elasticity and mass were found to affect the behaviour of the bridge. A parametric study of each of the above parameters was conducted to study their influence on the model results in terms of deflections and natural frequencies as well as to assess the best match with the test. While a reasonable amount of information could be obtained for three of these parameters from the bridge project drawings and other product data, the shear key condition was a parameter that involved a great degree of uncertainty in the amount of deterioration and damage that it may have accumulated over the years of service.

It was observed that the spring stiffness parameter was not sensitive to small changes within the acceptable range for both the deflection and natural frequency indicator. While the mass and stiffness parameters had a uniform influence on the vibrational characteristics of the bridge, changes in the mass parameter did not have a relation with the deflection indicator. Similarly the shear key thickness was a good measure of the health of the shear keys and demonstrated a direct relationship with the transverse bending frequencies and mode shapes and an inverse relationship with the deflection indicator. Table 6.7 shows the change in the natural frequencies of different modes with the change in shear key thickness, whereas Figure 6.11 shows the change in the mid span deflections of the bridge with the change in shear key thickness of the shell elements in the finite element model. Changes in the shear key thickness, though, did not influence the first longitudinal flexural natural frequency. The optimized values for these four parameters, as a result of the parametric study, which produced the best model to test match are as follows:

- Horizontal spring stiffness (for the neoprene bearings) = 5000 KN/m

- Shear key thickness = 15 mm

- Modulus of Elasticity = 26427 MPa (based on fc' of 34.49 MPa or 5000 psi)

- Mass of concrete = 0.000018 N/mm^3 (lightweight concrete)

161

Table 6.7: Change in natural frequencies with change in shear key thickness

Mode shape	Shear key thickness (mm)						Test
	6	12	15	25	50	101	
Vertical	2.78	2.79	**2.79**	2.79	2.79	2.79	**2.82**
Torsional	2.98	3.21	**3.25**	3.31	3.33	3.33	**3.25**
Transverse Bending	3.81	5.19	**5.52**	5.90	6.05	6.32	**5.43**

6.3.4.2 Test to model comparison for the bridge before rehabilitation

Figure 6.12 gives the informational plan of the truckload that was used on the bridge for the load tests before and after rehabilitation. The same axle loads along with the same axle distances were applied on the finite element model and the truckload placed in three different adjacent locations. It may be noted here that the cable transducers were placed one metre off the center in the actual test, to align it with the guardrail of the under-passing highway and to avoid the highway lane traffic under the bridge. The same longitudinal location of 17 metres from one end was selected to read the results in the finite element model.

Figure 6.13 shows the comparison of model and test deflections, measured in load tests before rehabilitation, with the truckload stationed in the three different transverse positions on the bridge deck. The cross section of the bridge deck along with the truck load is shown on top of the plot to illustrate the alignment of the plotted points with the girder legs, where both the cable transducers and the strain gauges were installed for the field tests.

It can be seen from these plots that the model was able to predict the behaviour of the bridge with reasonable accuracy in all the three different placements of the truck load.

162

However, although the model generally follows the same trend as the test, it does not exactly map the test plot, which can be attributed to a number of reasons. The finite element model is based on simplified assumptions of considering the same value of the modulus of elasticity for all girders and another value for all shear keys. This may not be the case in the real bridge where different girders as well as different shear keys may have different stiffnesses. Since cracking in the shear keys may not be uniform, the stiffness can vary between different shear keys and various portions of even the same shear key. Many attempts were made to calibrate the model with the test by using a combination of different stiffnesses in the shear keys. Figure 6.14 illustrates the comparison of the test deflections, measured in load tests before rehabilitation, with the finite element model using the best combination of shear key stiffnesses. The best possible combination of shear key thicknesses of 25-10-22-15-15 mm (from left to right) across the bridge cross section was used in Figure 6.14. To obtain the best calibration, the jumps in the shear keys as well as the slope of the bridge deck or the individual girder flanges in the model, should match that of the test. The combination of the shear key stiffnesses were again not able to achieve exact mapping of the test profile, as shown in Figure 6.14, due to the complicated nature of the actual shear keys. The shear keys, after cracking behave in a non-linear fashion and would deflect differently to different loading situations. Moreover, most of the measurements in the test were quite small and subject to at least some percentage of error. However, since the model was able to predict the global behaviour of the bridge reasonably well therefore the need to further refine the model, or the mesh was not felt.

The natural frequencies for the first three modes of vibration, and their mode shapes, obtained from the ambient vibrations test are shown in Figure 6.15. Of particular interest is the transverse bending mode shape, which produces vertical movements in alternate sets of girders hence, inducing distress in the shear keys.

After the initial calibration of the model results, in terms of deflections and natural frequencies and mode shapes, the results were then verified by comparing the strains measured in the test to those of the model. It was observed that without the need of

163

changing any further parameters, the model matched well with the test results. Figure 6.16 shows the strain comparison of the model and the test.

6.3.4.3 Test to model comparison for the bridge after rehabilitation

The actual bridge was strengthened by a combination of two rehabilitation schemes. The asphalt on the original bridge was replaced by a 100 mm transversely prestressed, fibre reinforced, silica fume concrete overlay without any reinforcement, and transversely running steel underslung diaphragms, as can be seen in Figure 6.17. The steel underslung diaphragms were modeled by using the beam element whereas the concrete overlay was modeled with the help of shell elements of the program. To maintain the vertical distance between the horizontal centroidal planes of the girder top flange and the concrete overlay shell planes, vertical rigid elements were used in the model. Figure 6.18 shows the model cross-section illustrating the girder flange plane; the concrete overlay plane and the rigid element connecting the two planes. The beam elements used for underslung diaphragms are also visible in this figure. Table 6.7 below gives the material and section properties used for the concrete overlay and the underslung diaphragm in the model after rehabilitation.

Table 6.8: Material and Section properties of different materials used

	E (N/mm^2)	G (N/mm^2)	γ (N/mm^3)	I strong axis (mm^4)	I weak axis (mm^4)	J (mm^4)	A (mm^2)
Concrete Overlay	22500.0	9375.0	0.000024	-	-	-	-
Underslung Diaphragms	200000	75000	0.000076	51.4×10^6	17.9×10^6	516×10^3	7740.0

Where:

E = Young's Modulus

G = Shear Modulus

164

γ = Density of material

$I_{\text{strong axis}}$ = Moment of Inertia about the strong axis

$I_{\text{weak axis}}$ = Moment of Inertia about the weak axis

J = Torsion Constant

A = Gross Area

The transverse prestressing in the actual bridge was modeled as transverse concentrated load cases, applied at the same longitudinal and vertical locations on both sides of the model as in the actual bridge. These rehabilitation techniques were now incorporated in the model as discussed above, and the model results re-compared with the test results, again using the same deflection, strain and natural frequency of vibration indicators.

The comparison showed the model to be stiffer than the real test with respect to all the three parameters. Figure 6.19 shows the comparison of the test and model deflections while Table 6.9 gives the comparison of the test and model natural frequencies of vibration. The same trend is repeated in the strain information and is illustrated in Figure 6.20

Table 6.9: Model - test comparison, using natural frequency indicator, after rehabilitation

Mode Shape	Test (Hz.)	Model (Hz.)	% Error
1st Vertical	2.77	2.82	1.8
1st Torsional	3.38	3.66	6.3

As the rehabilitation process consisted of the addition of a laterally stressed fiber reinforced concrete overlay and transverse underslung diaphragms therefore it was assumed that any artificial stiffening effect in the model would be coming from the addition of any of these two schemes. It may be noted here that the model gave a reasonable match with the test before rehabilitation and since the incorporation of the rehabilitation strategies was only an extension of the model work, therefore it was not irrational to conclude that the discrepancy in the comparison was a result of the malfunctioning of one or both of the rehabilitation schemes.

165

To isolate the effect of each of the rehabilitation strategies, a comparative analysis on the model was conducted, by using one scheme at a time. The results indicated that the test matched with the "underslung diaphragm only" scheme reasonably well but was softer when compared with the "concrete deck only" scheme. This effect can be seen in Figure 6.21 where the deflections obtained for the test, with the truck in both the lanes, were greater than the model with the concrete deck only, and were relatively closer to the model with the underslung diaphragms only.

This has posed an interesting question on the contribution of the concrete deck to the stiffness of the whole system. The model assumes that the overlying deck and the underlying girders are fully composite in action, which, in the absence of any significant shear connection between the two surfaces, may not be the case in real life. Though, it is not very simple to predict the real behaviour of the concrete deck since factors like an imperfect bond between the girder flange and the concrete deck or some possible cracking in the deck due to shrinkage, or a combination of both may easily tarnish the performance of the concrete overlay.

6.4 Discussion

Most of the researches in the past have shown that in the presence of a rough interface, shear transfer can rely on aggregate interlock to transfer the horizontal shear under service loads[7]. However there will be some small movement between the planes initially until the grooves in the aggregates bear against each other and activate the aggregate interlock. Hanson[8] has shown from his series of girder tests on different types of girder-slab interface that girders with roughness but without bond, deflect more from early load to failure, than the monolithic or rough bonded beams. This indicates a partial composite action rather than full composite action. He also concluded that in the development of precast prestressed bridges, it seems advisable to continue work only with horizontal shear connections effected by a combination of a rough, bonded contact surface and stirrups extending from the precast girders into the situ-cast deck slab. Saemann and Washa[9] have also shown the effect of roughness on shear stress versus deflection.

166

The tremendous amounts of shrinkage in the concrete deck could also have cracked the concrete, eventually reducing the overall stiffness of the deck to a small value. Immediately after pouring the deck, due to adhesion between the top flange of the girder and the concrete overlay, the concrete deck goes into tension due to shrinkage. This happens because the concrete deck wants to shrink but the underlying girder restrains it from doing so.

Using the ACI Committee 209 guidelines[10], the shrinkage strain and consequently the stress due to shrinkage was calculated, which came out to be 11.08 MPa. The calculation has been reproduced as follows:

$$\varepsilon_{sh} = \frac{t}{C_s + t} \varepsilon_{shu} P_{sh}$$

where:

t = Time in days starting immediately after the initial wet curing = 60 days (i.e. from August 5th 1998 to October 5th 1998)

C_s = 35 if concrete is moist cured for 7 days

ε_{shu} = Ultimate shrinkage strain. In the absence of specific data for local conditions, the average value of ε_{shu} suggested for use is 0.00078 mm/mm

P_{sh} = Correction factor for conditions other than standard conditions

$\quad = P_c P_h P_f P_r P_s P_v$

$\qquad$ where: P_c = Factor for cement content

$\qquad\qquad P_h$ = Factor for relative humidity

$\qquad\qquad P_f$ = Factor for ratio of fine to total aggregate

$\qquad\qquad P_r$ = Factor for volume surface ratio

$\qquad\qquad P_s$ = Factor for slump of concrete

$\qquad\qquad P_v$ = Factor for % air

However, standard conditions produce modification or correction factors of 1.0. Since detail information on all of these factors was not available therefore a correction factor (P_{sh}) of 1 was adopted for the calculation purposes.

$$\varepsilon_{sh} = \frac{60}{(35 + 60)} \times 0.00078 \times 1.0$$

ε_{sh} = 0.000493 mm/mm

Accompanying stress = strain x modulus of elasticity

Since fc´ = 25 MPa

Therefore $E = 4500\sqrt{fc'} = 4500\sqrt{25} = 22500$ MPa

Stress = 0.000493 x 22500 = 11.08 MPa

Hence tensile stress in the concrete deck due to shrinkage = 11.08 MPa

Compressive stress in the concrete deck due to the prestressing strands = 0.39 MPa (as a result of a tendon force of 130 KN per tendon, spaced at 2 metres on centers)

Since shrinkage is putting tension in the concrete, therefore net stress in concrete

= 11.08-0.39 = 10.69 MPa (in tension)

Now, the Modulus of rupture of concrete[11] $f_r = 0.6\lambda\sqrt{fc'}$

Taking fc´ = 25 MPa, f_r works out to be 3 MPa.

Since the earlier calculated net stress of 10.69 MPa > 3 MPa, therefore the deck will crack under the effect of the shrinkage stresses. The absence of any longitudinal reinforcement and the appearance of minor hair line cracks in the concrete deck seem to confirm the issue of concrete cracking due to shrinkage.

6.5 Conclusions

The results of the field-monitoring program on the Fort Saskatchewan Bridge had shown that the rehabilitation program was able to increase the torsional and transverse stiffness of the bridge significantly. However the longitudinal stiffness did not change much and the contribution of the concrete deck to the whole system was questionable and requires further research. Issues like concrete cracking due to shrinkage or insufficient bond between the deck and the underlying girders or a combination of both could be responsible for the deficient contribution of the concrete overlay to the overall stiffness of the whole system. From the deflection profiles of the bridge cross section it can be seen that both the concrete deck and the underslung diaphragm assembly provide similar load distribution characteristics to the bridge.

168

It was seen that the monitoring program provided useful information on the structural behaviour of the bridge and its accuracy limits were dependable. The finite element model, having been calibrated with test data, was a reasonable approximation of the actual structure and can be used to extensively investigate the effects of using various rehabilitation schemes and to incorporate different scenarios and situations, which might be hard to reproduce under test conditions.
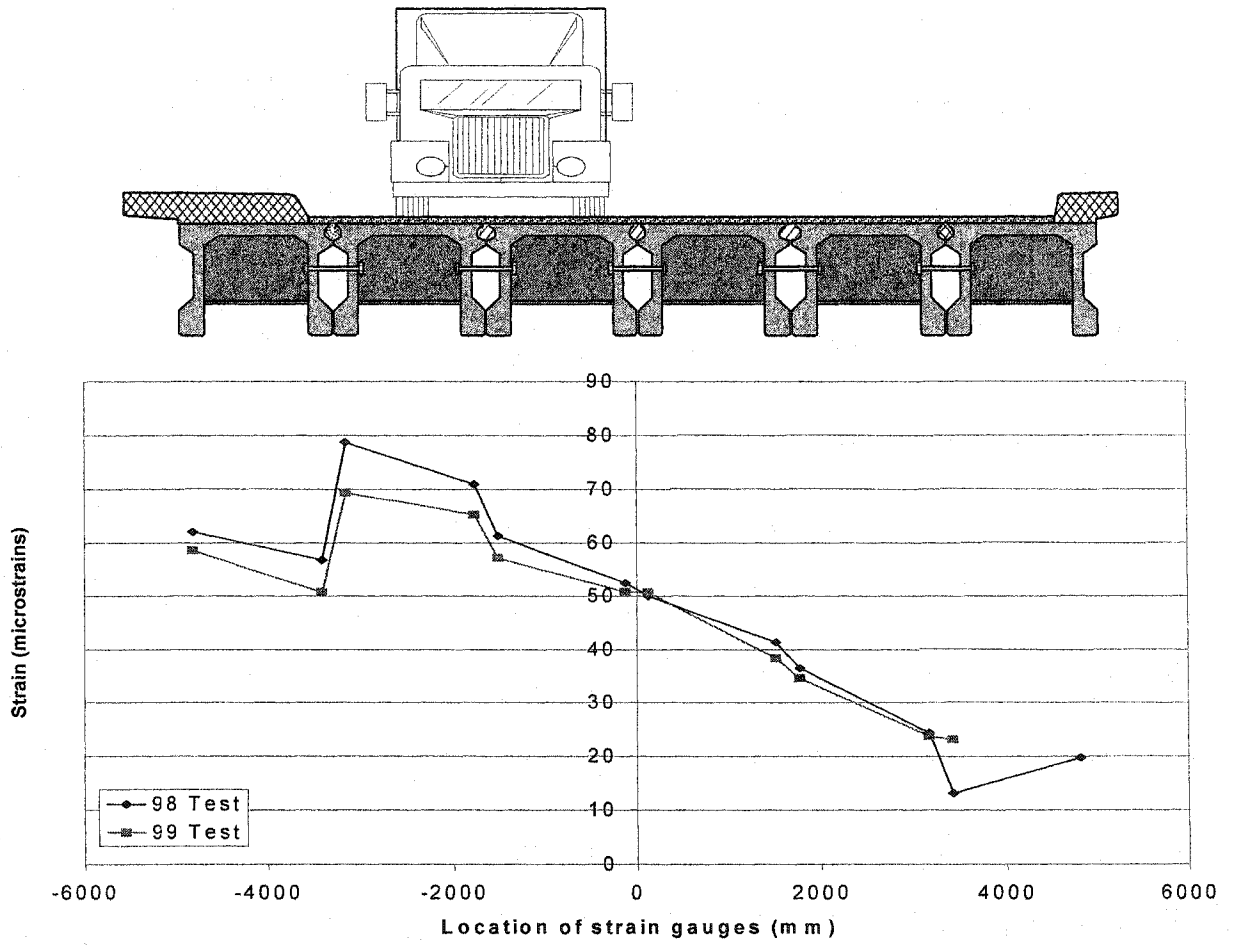
169

Figure 6.1: Comparison of 1998 and 1999 test results in terms of Strain
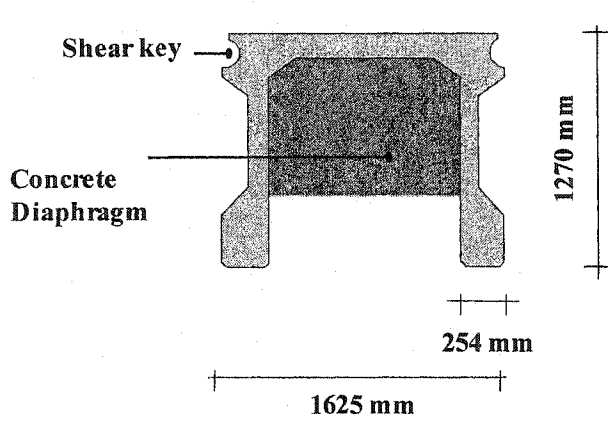
Figure 6.2: Cross section of a typical FC girder
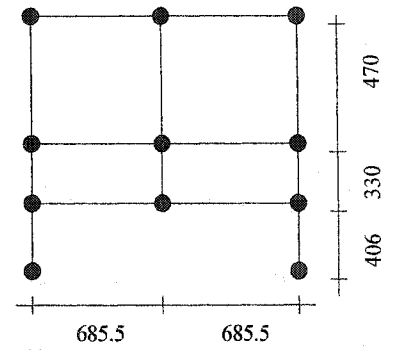
Figure 6.3: Finite element model of a single girder, cross sectional view
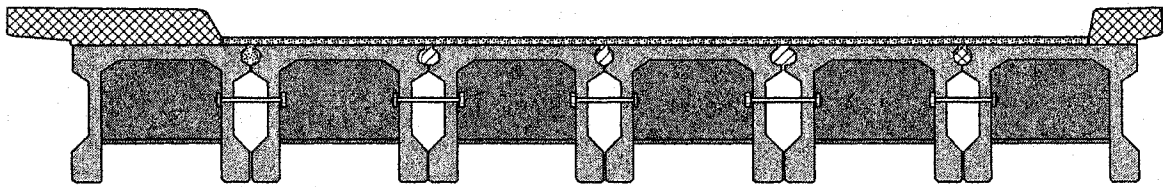
Figure 6.4: Cross sectional view of the full bridge
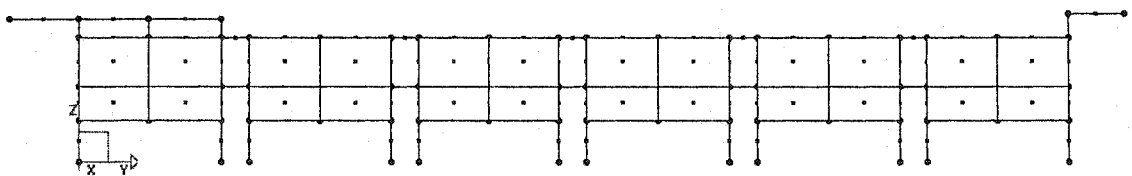
Figure 6.5: Finite element model of the whole bridge, cross sectional view

171
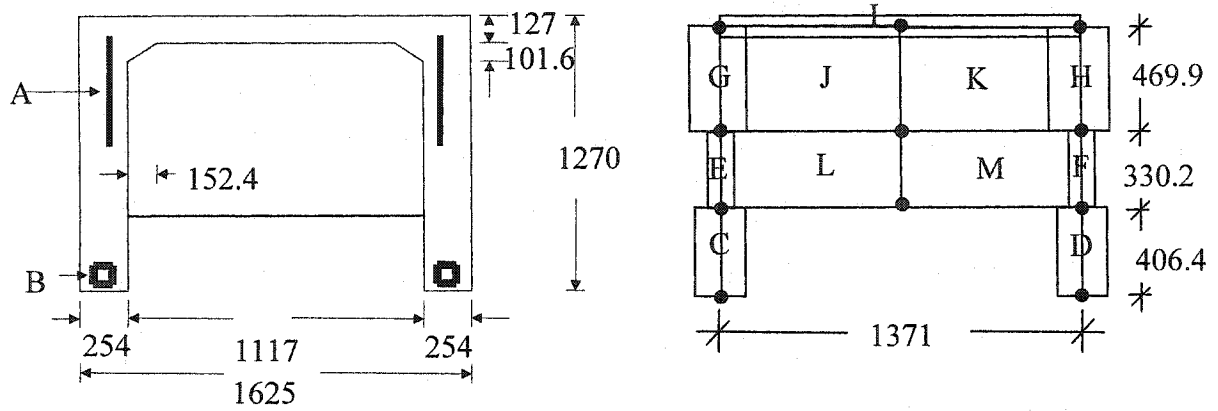
Single girder cross section at support – Actual girder vs. Finite Element Model
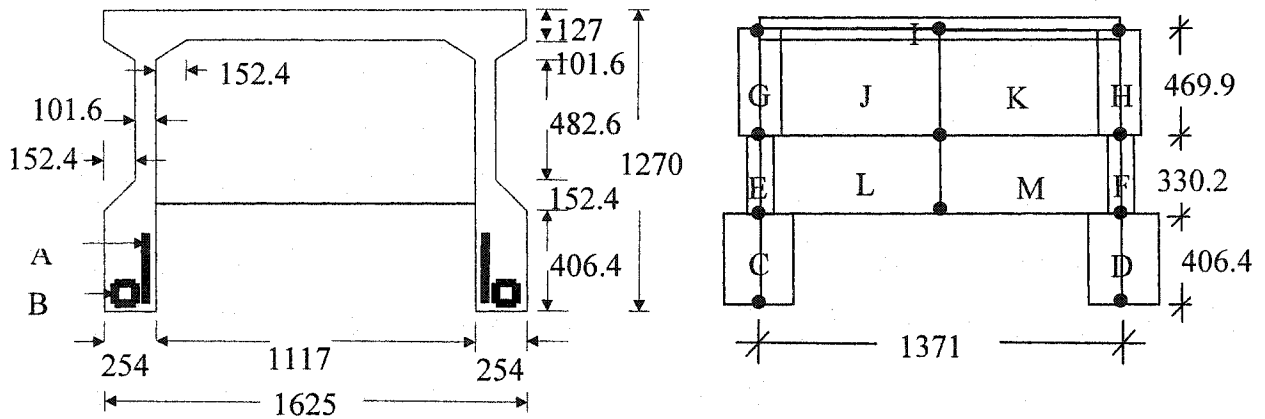
Single girder cross section at mid span – Actual girder vs. Finite Element Model

	Exterior Girders		Interior Girders	
	At Support	At mid span	At Support	At mid span
Strands Steel A	12-12.7 mm/leg	12-12.7 mm/leg	10-12.7 mm/leg	10-12.7 mm/leg
Strands Steel B	9-12.7 mm/leg	9-12.7 mm/leg	9-12.7 mm/leg	9-12.7 mm/leg
Element thickness C	278 mm	318 mm	278 mm	312 mm
Element thickness D	278 mm	318 mm	278 mm	312 mm
Element thickness E	265 mm	166 mm	265 mm	166 mm
Element thickness F	265 mm	166 mm	265 mm	166 mm
Element thickness G	314 mm	207.8 mm	314 mm	207 mm
Element thickness H	314 mm	207.8 mm	314 mm	207 mm
Element thickness I	127 mm	127 mm	127 mm	127 mm
Element thickness J,K,L,M	203.2 mm	203.2 mm	203.2 mm	203.2 mm

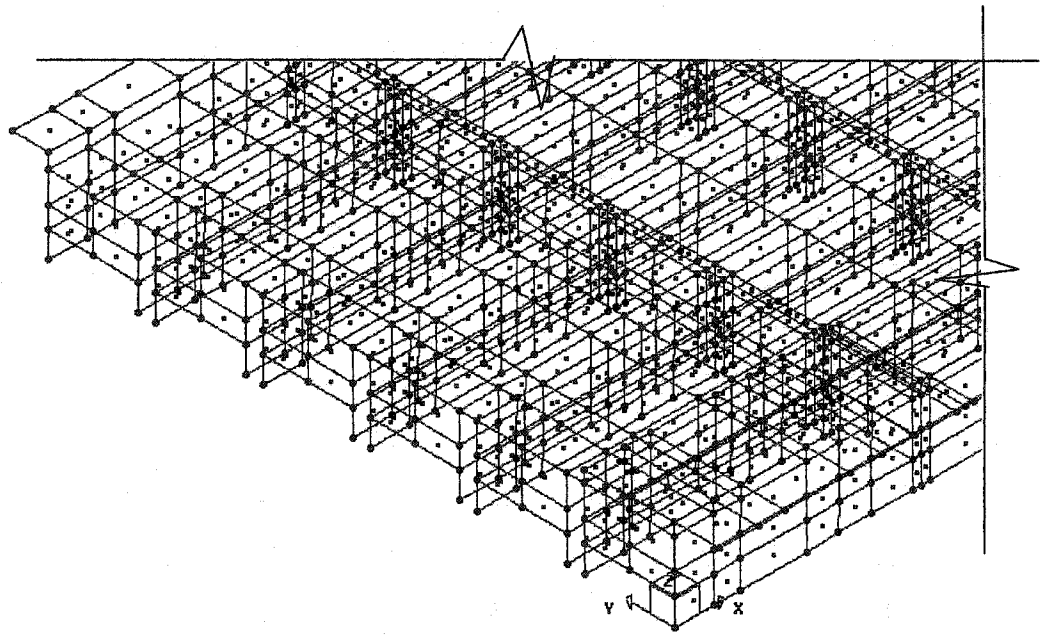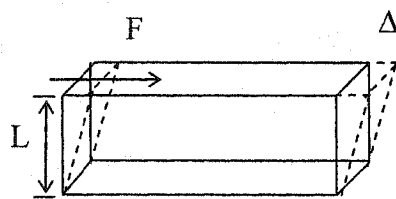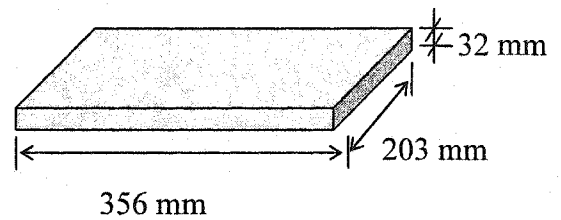Figure 6.6: Single girder cross section – Actual vs. Model

172

Figure 6.7: Isometric view of the finite element model

F   Δ

L

Calculating the effective stiffness of the
neoprene bearings

32 mm

203 mm

356 mm

Dimensions of the neoprene bearing pads
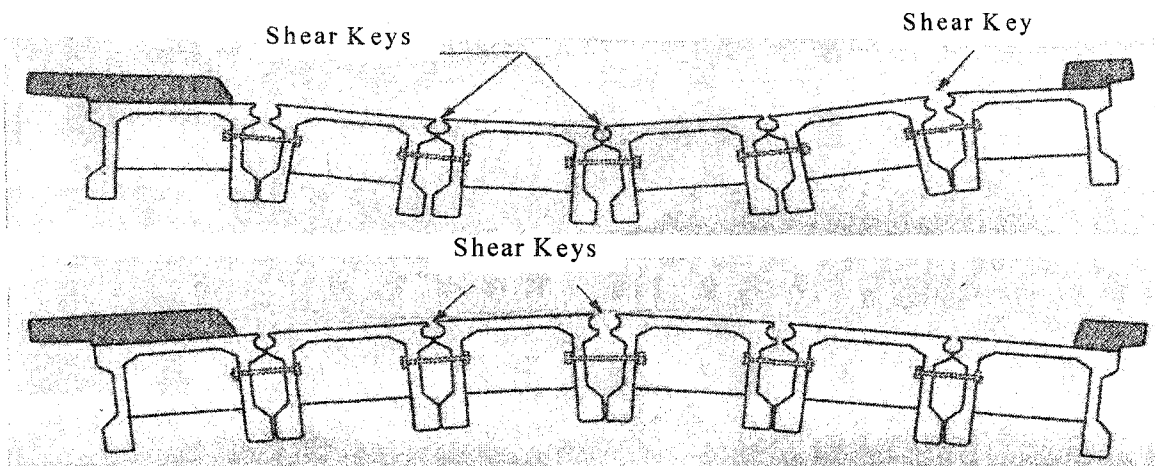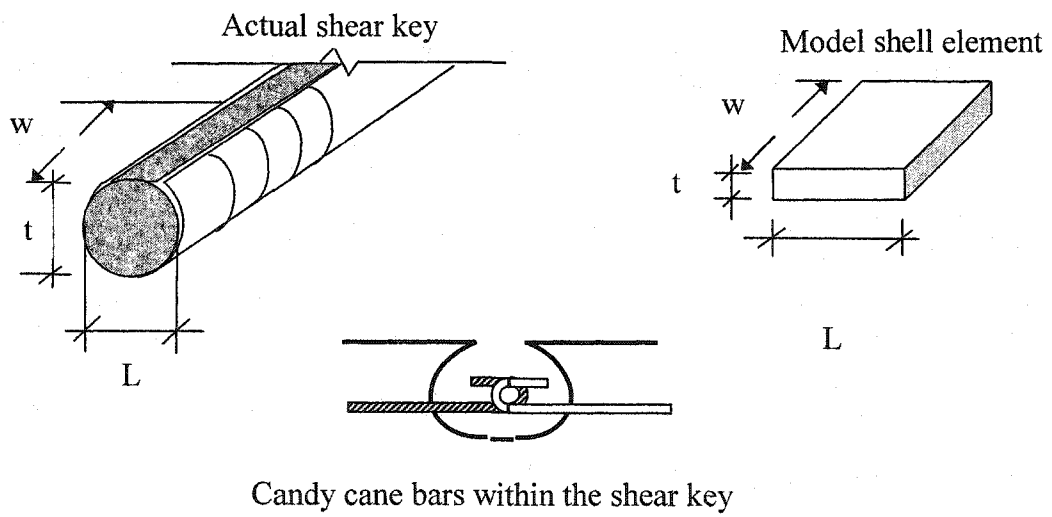
Figure 6.8: Details for the girder support bearings

173

Figure 6.9: Transverse vibrating cross section of the bridge

Actual shear key

Model shell element

Candy cane bars within the shear key

Figure 6.10: Shear key details

174
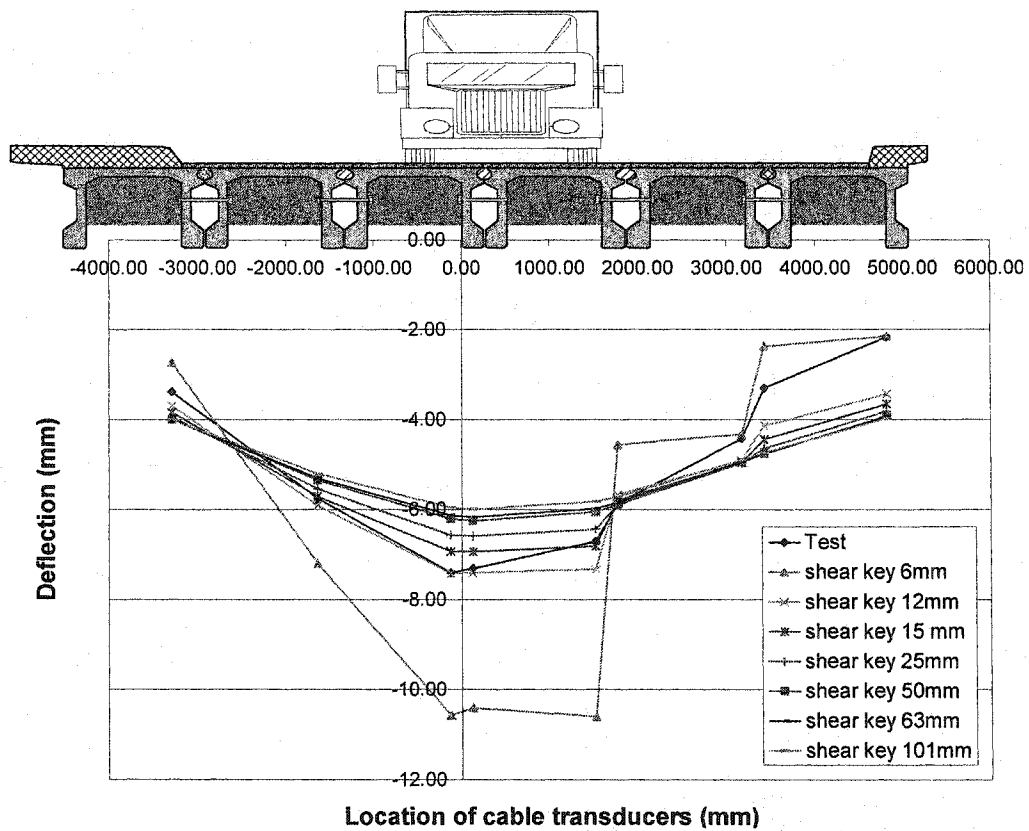
Figure 6.11: Variation of mid span deflections with changes in shear key thickness

(a) Truck
information, before
rehabilitation

(b) Truck
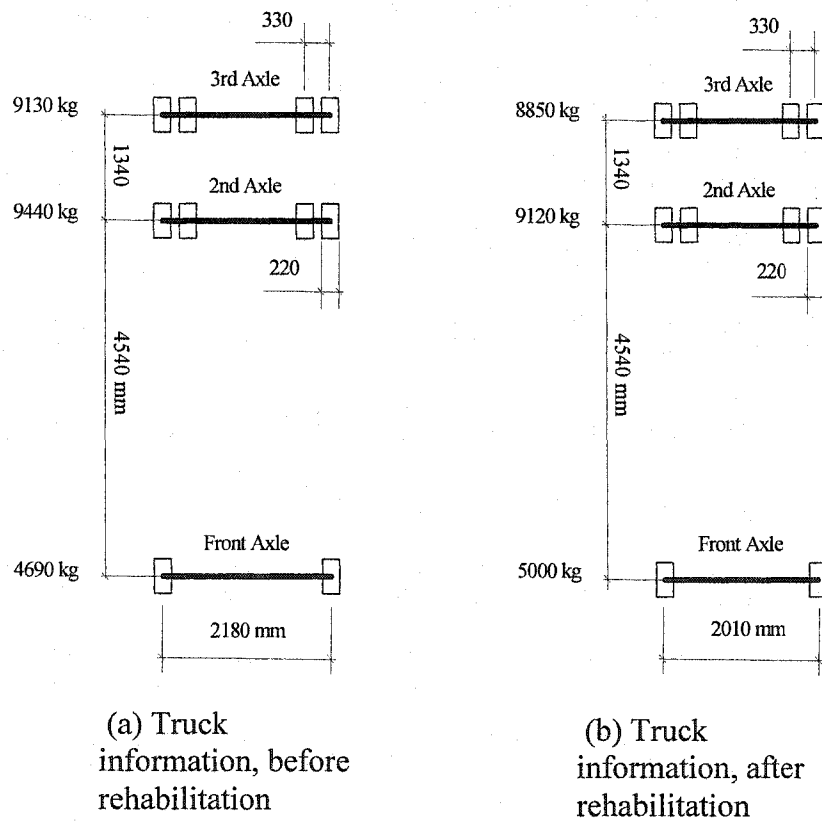information, after
rehabilitation

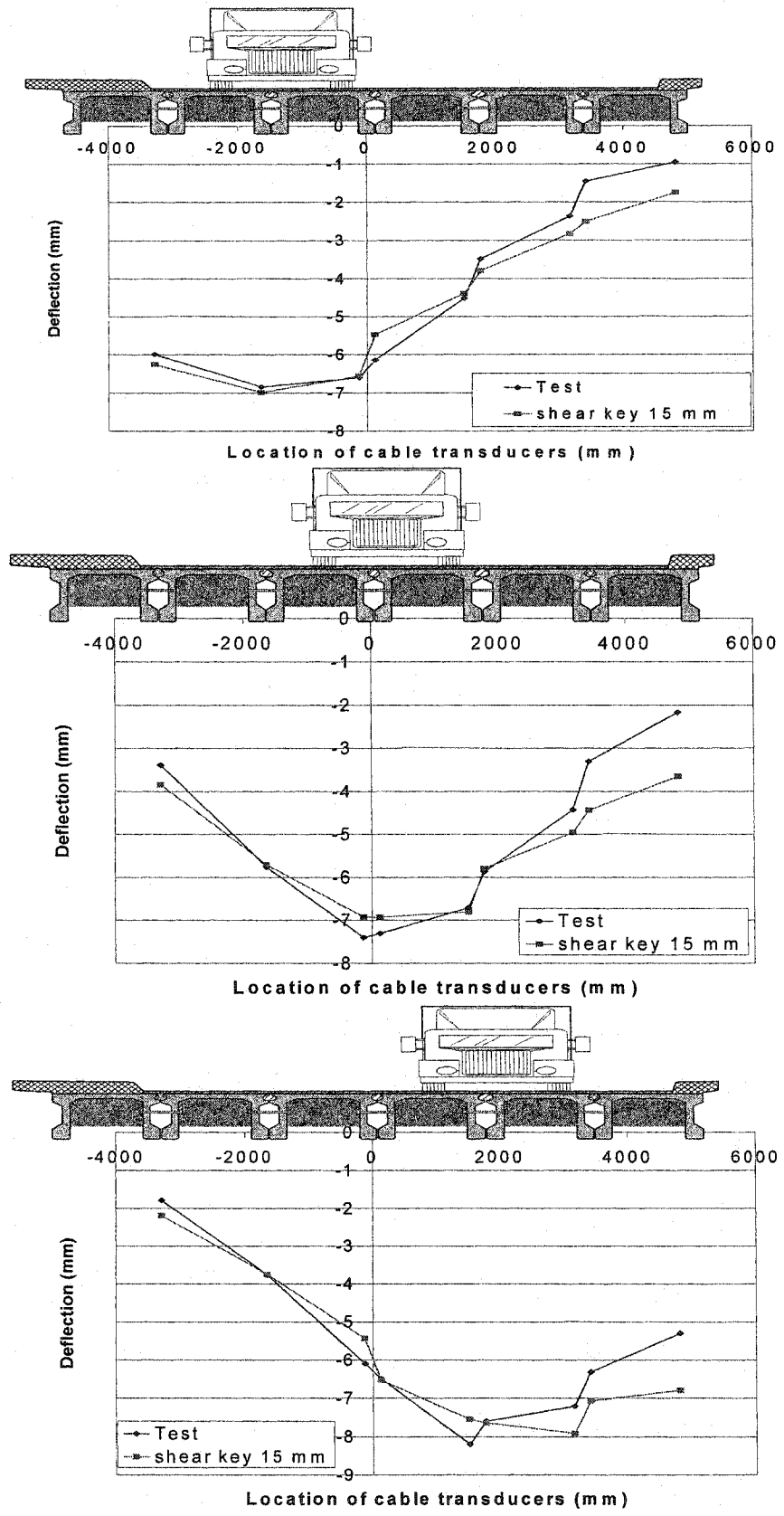Figure 6.12: Truck load information used in load tests

175

Figure 6.13: Model to test comparison using the deflection indicator, before rehabilitation
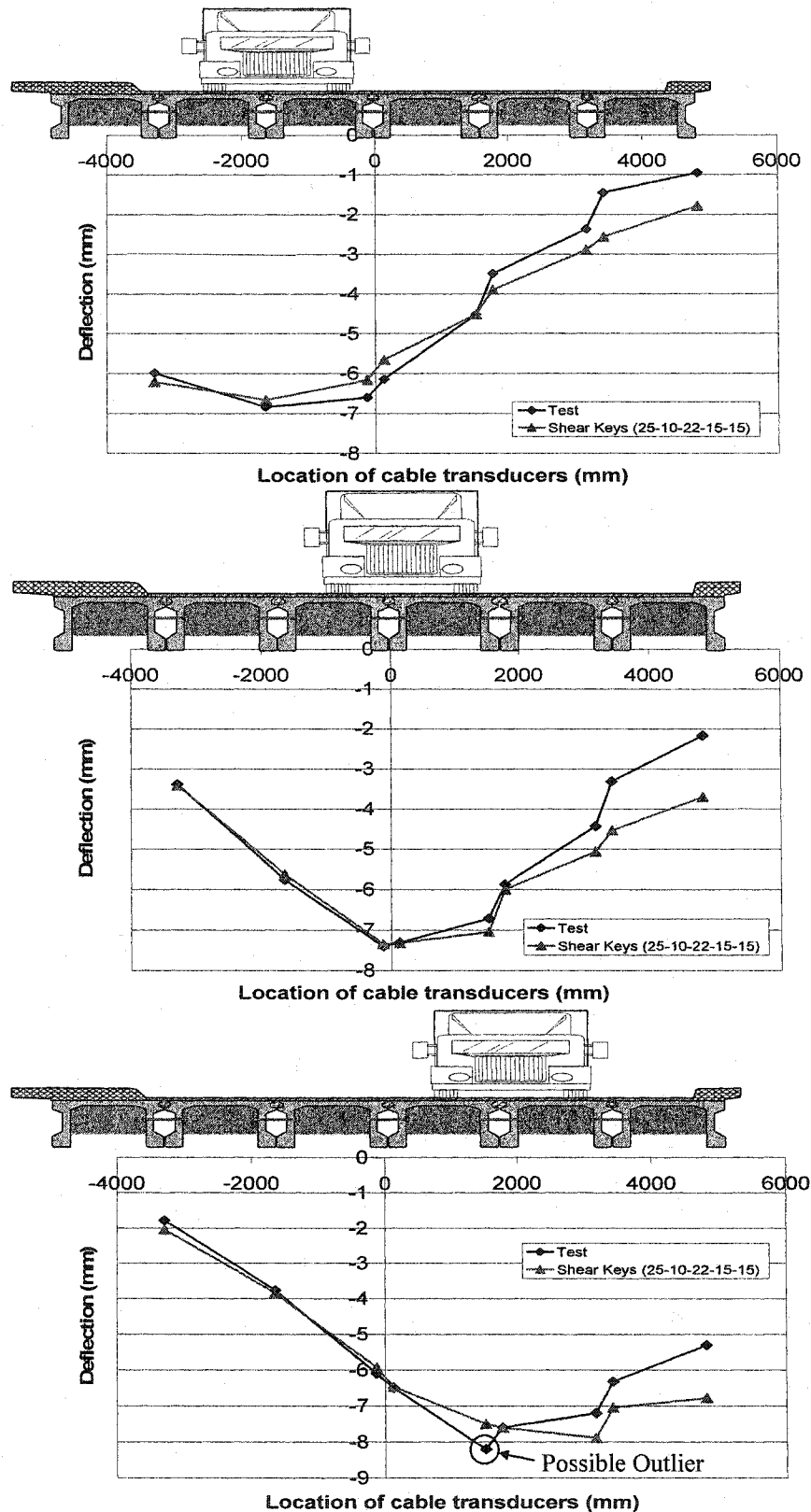
176

Figure 6.14: Model to test comparison using the deflection indicator and stiffness combination shear keys (25-10-22-15-15)
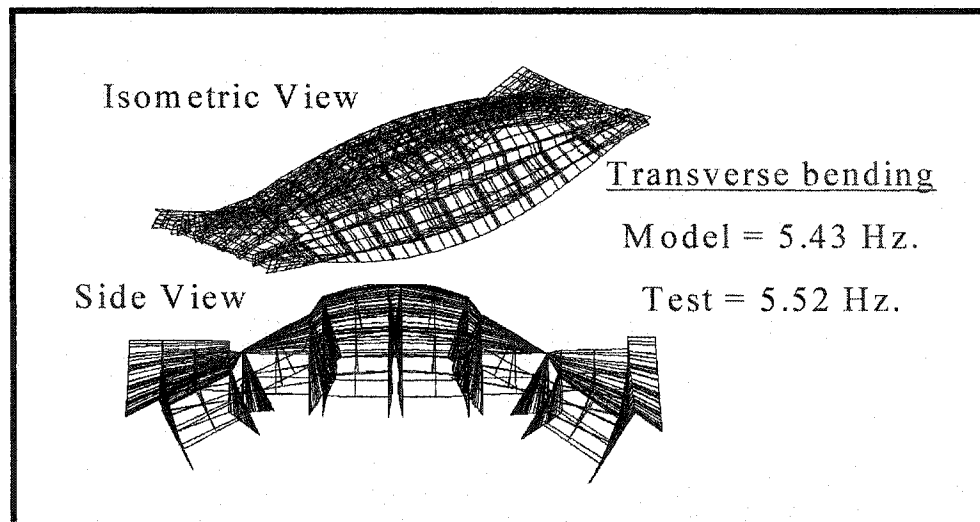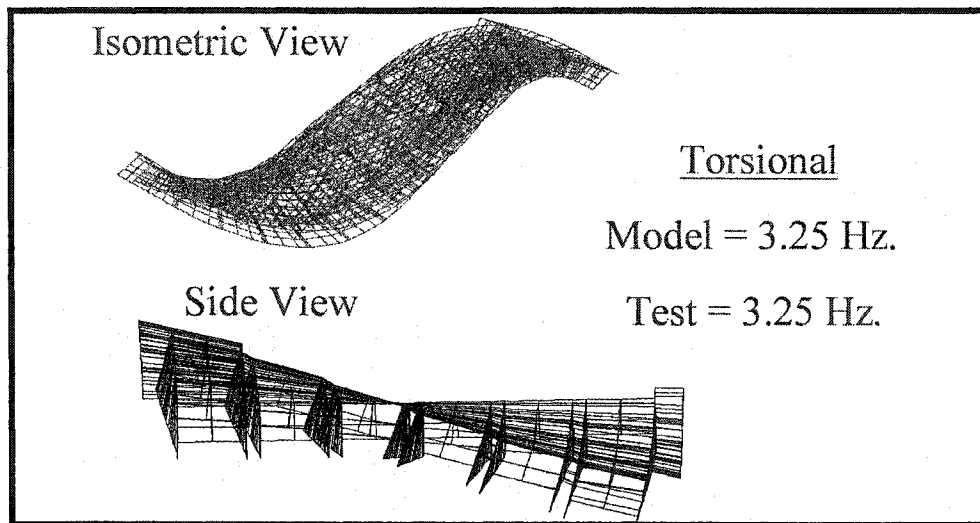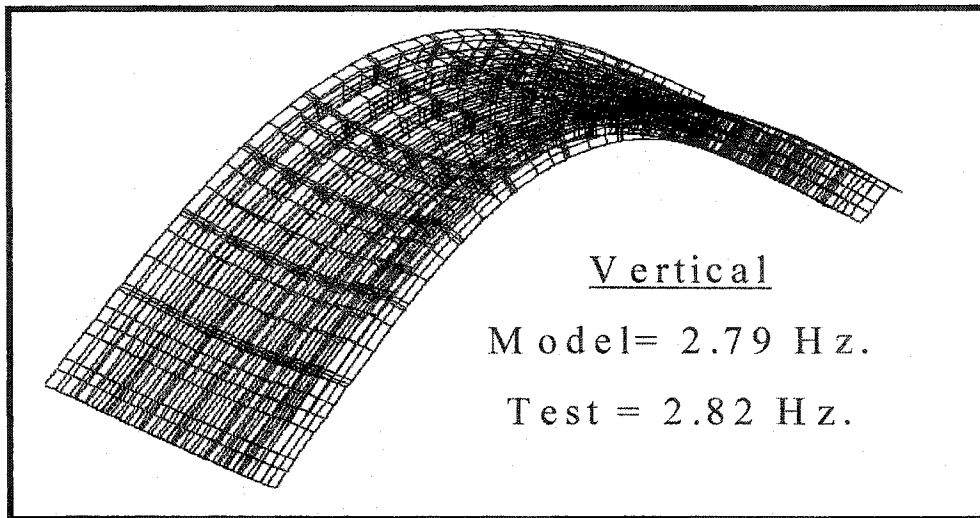
177

Figure 6.15: Model to test comparison using the natural frequency & mode shape indicator, before rehabilitation
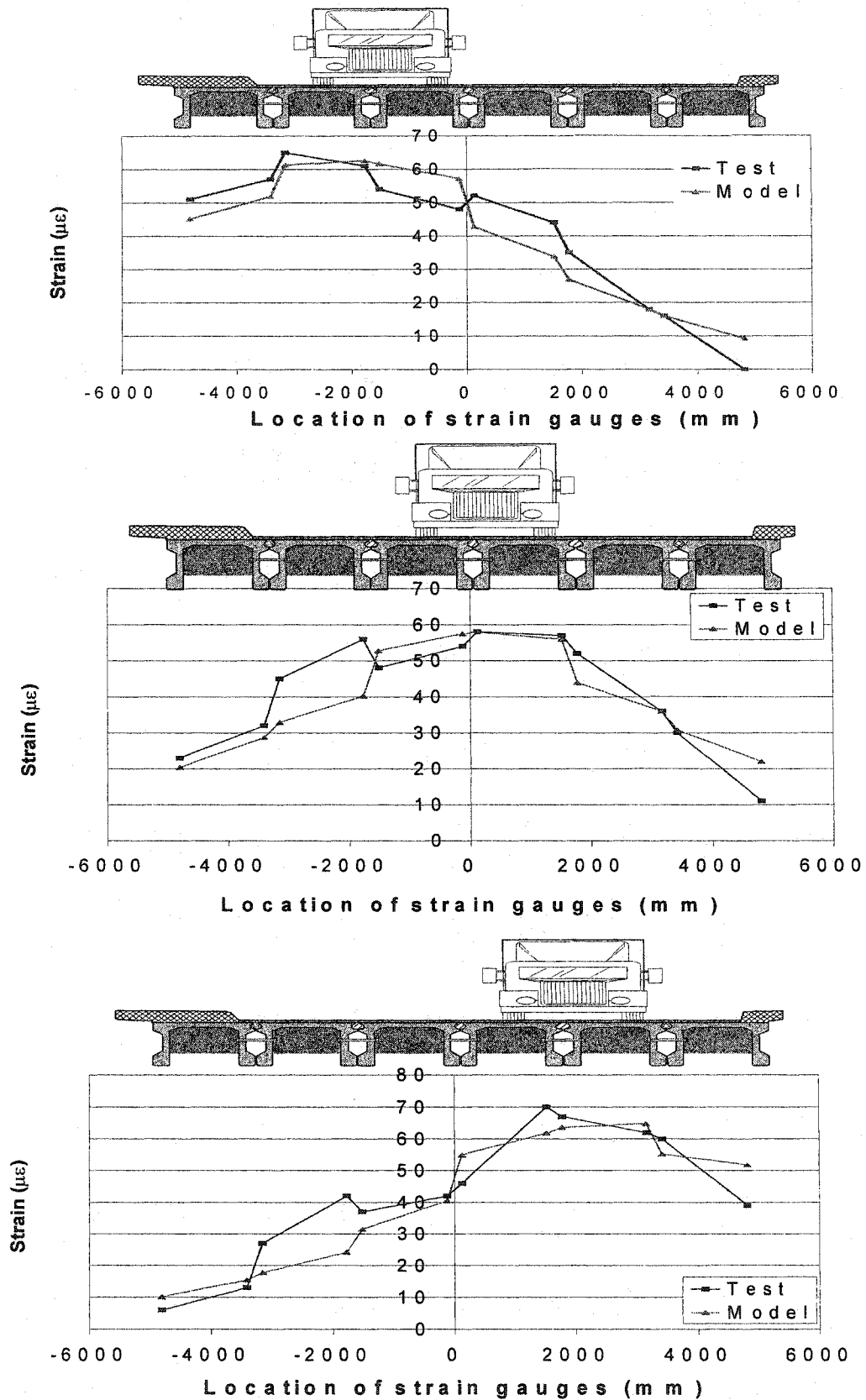
Figure 6.16: Model to test comparison using the strain indicator, before rehabilitation

Figure 6.17: Cross section of the actual bridge showing combination of rehabilitation schemes

Figure 6.18: Model cross section of the bridge with rehabilitation schemes incorporated

180

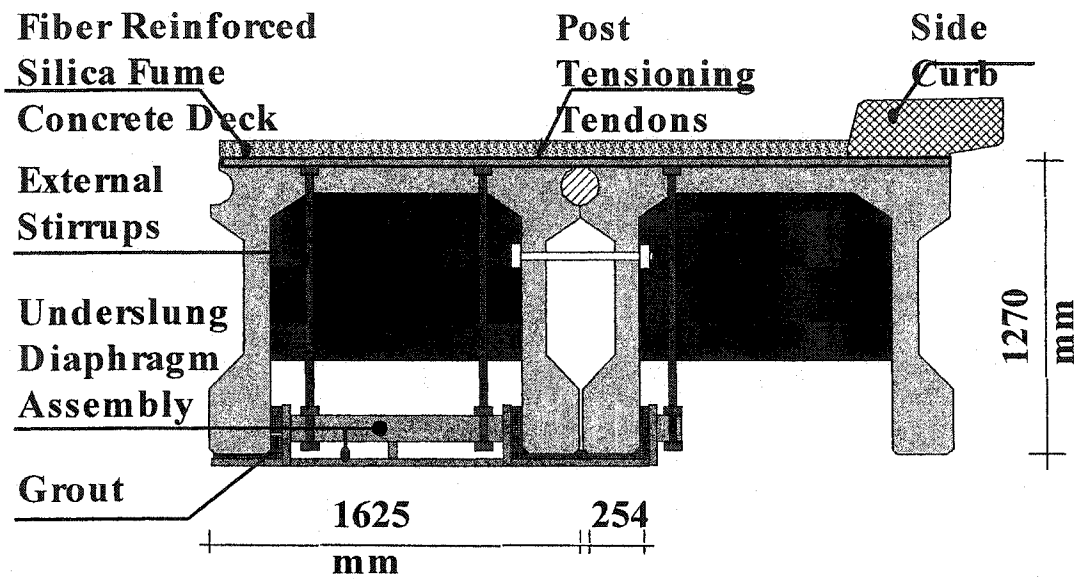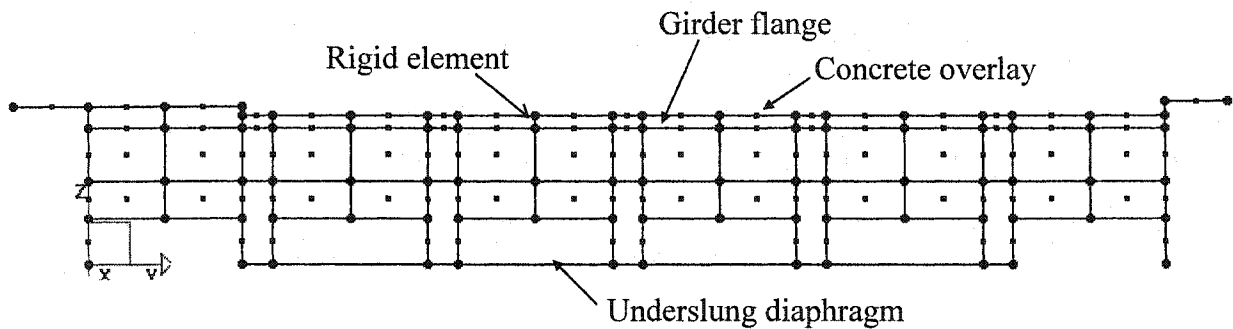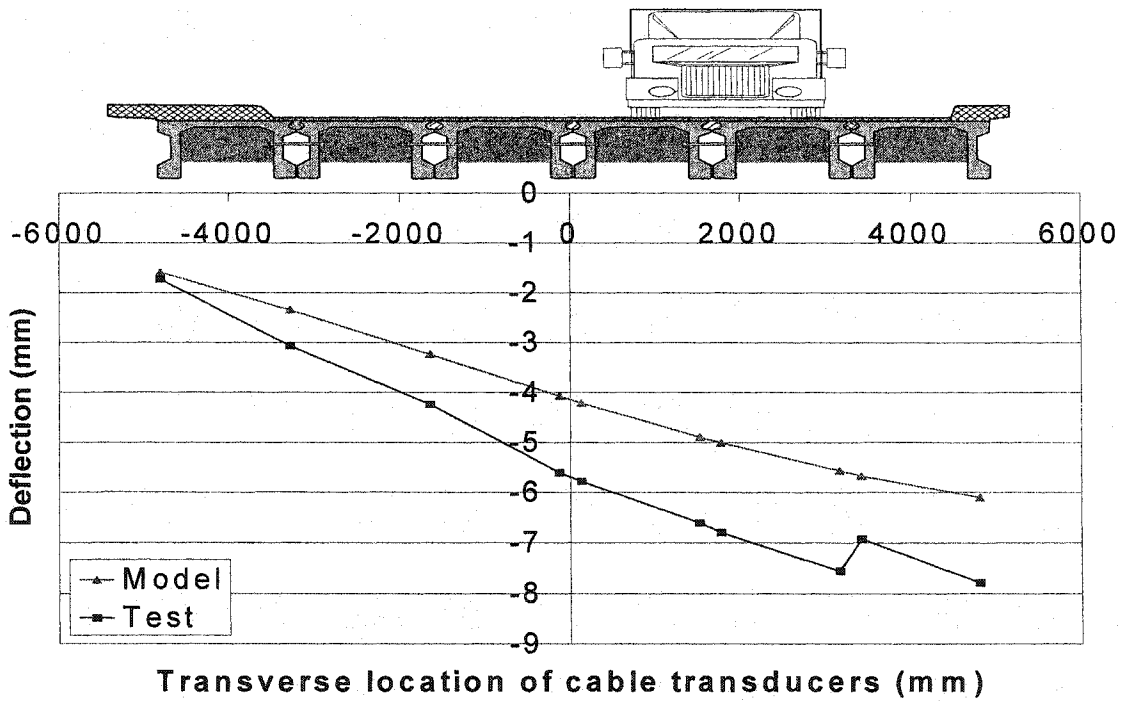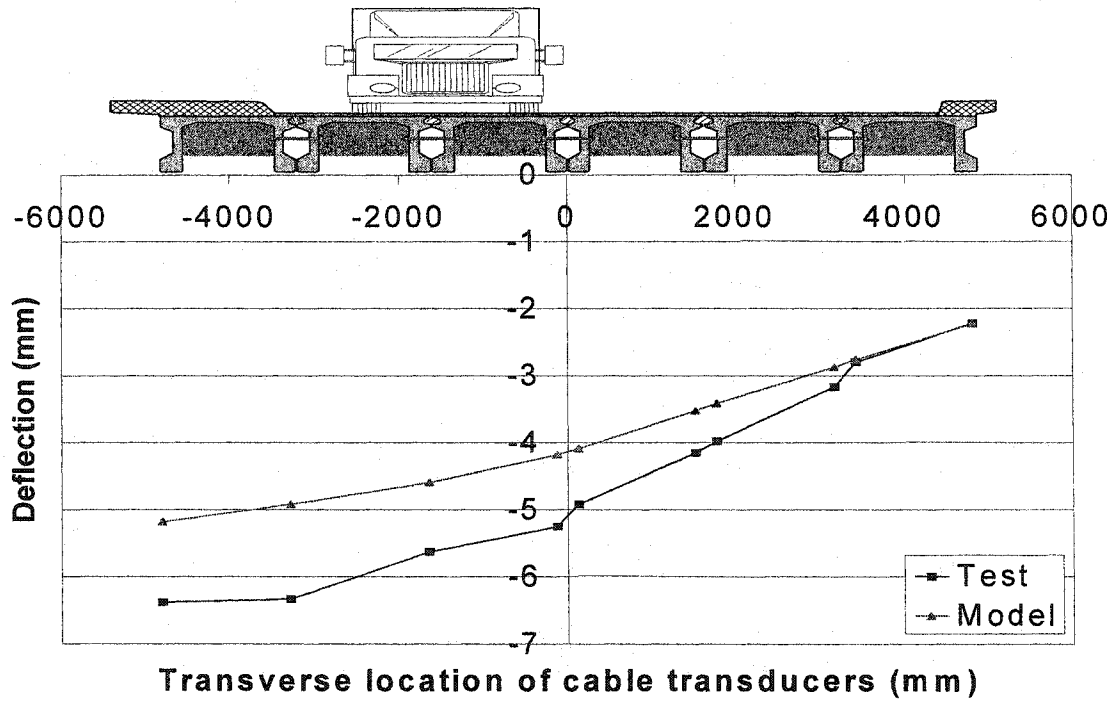Figure 6.19: Model to test comparison using the deflection indicator, after rehabilitation
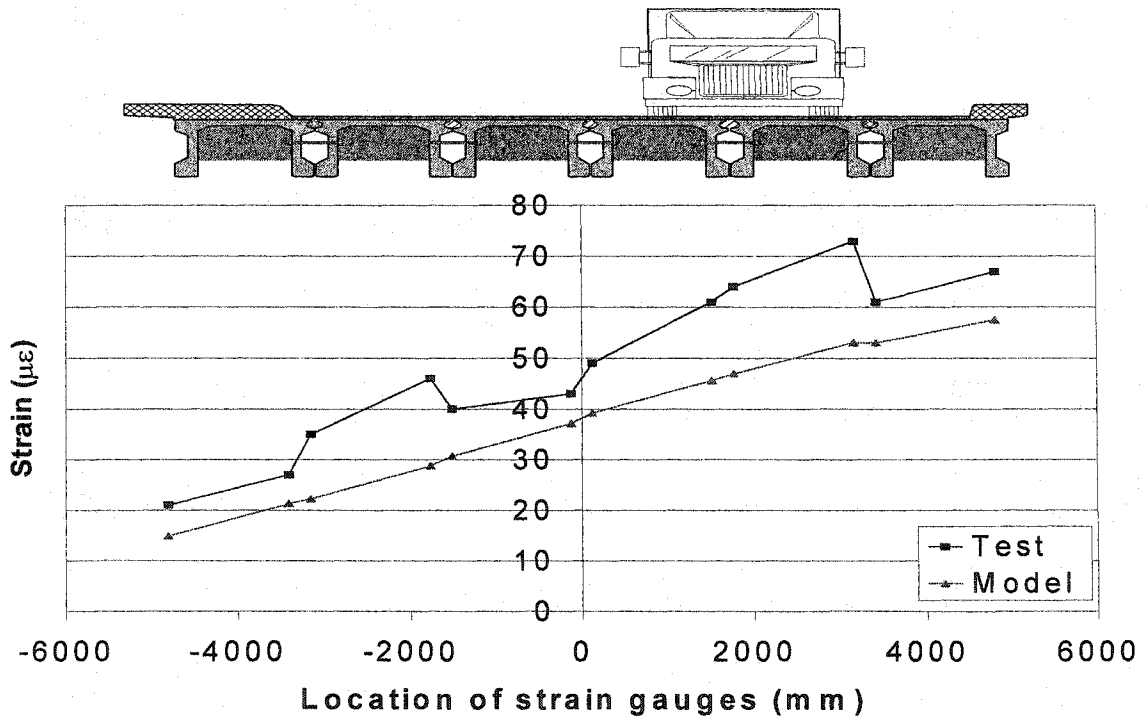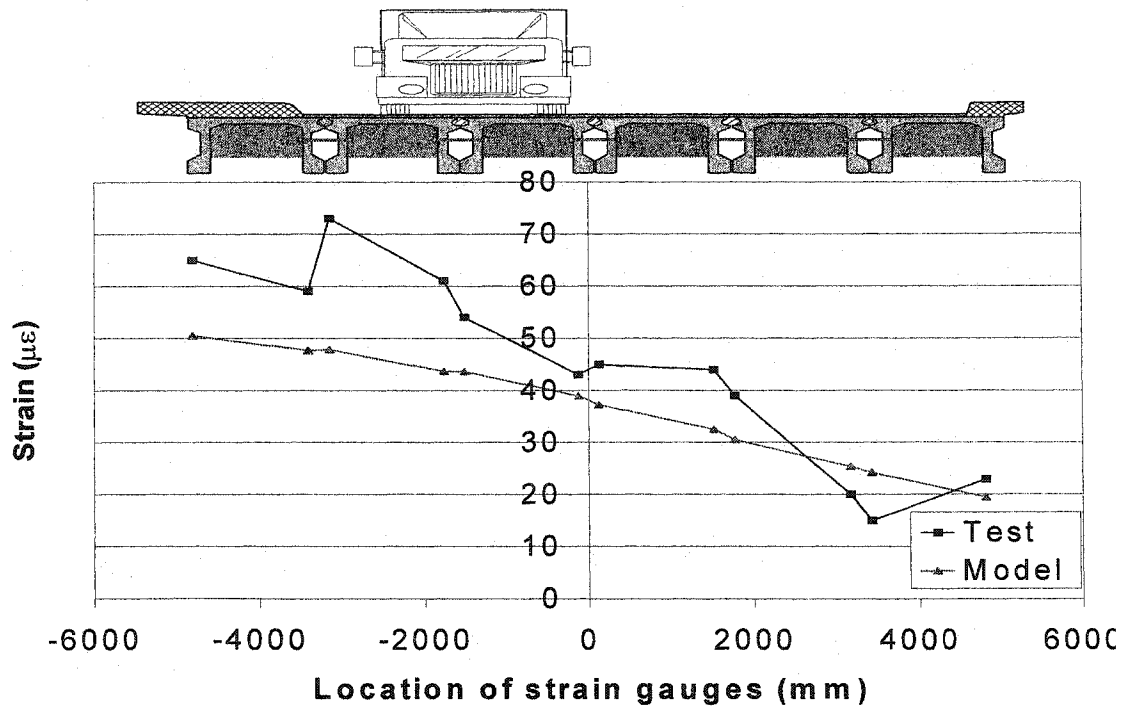
Figure 6.20: Model to test comparison using the strain indicator, after rehabilitation

182
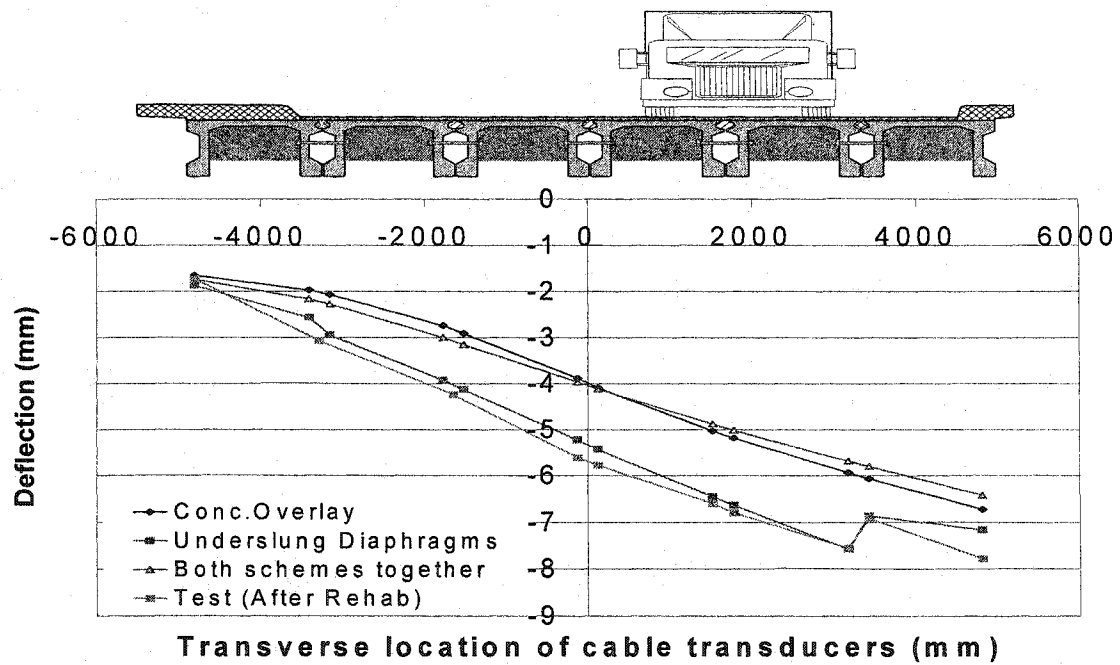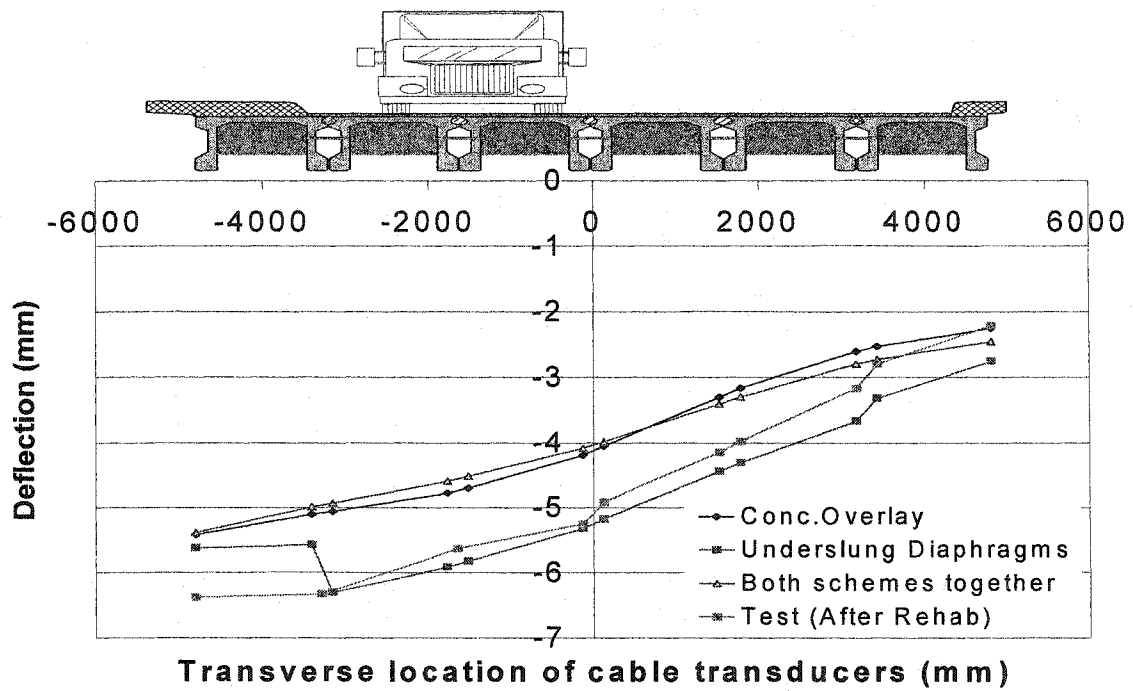
Figure 6.21: Rehabilitation schemes compared

183

6.6 References

1. Hrudey, T.M. and Serink, D., "Finite Element Analysis of shear key behaviour in FC girder bridges", 1st Structural Specialty Conference, CSCE, 1996, pp. 263-272.

2. Afhami, Shahab, Khattak, Nadeem and Cheng, J.J.R., "Field Assessment of the Bridge Rehabilitation in Fort Saskatchewan, Alberta". City of Fort Saskatchewan Report, March 1999

3. Anderson, Sweeney and Williams, "Introduction to Statistics - Concepts and Applications", 3rd Edition, 1991, pp. 204-207.

4. S-Frame for Windows, Reference Manual, SOFTEK Services Ltd.

5. CSA standard A23.3-94, Clause 8.6.2 and N8.6.2, Page 29

6. City of Fort Saskatchewan, Alberta, Project Drawing Set No. 44-00-60, " Railway Avenue – Highway 15 Overpass", July 1973, AESL Consulting Engineers.

7. Mattock and Hawkins, "Shear Transfer in Reinforced Concrete – Recent Research", PCI Journal, Vol. 17, No.2, March-April 1972, pp. 55

8. Norman W. Hanson, "Precast Prestressed Concrete Bridges – Horizontal Shear Connections," Journal of the Research and Development Laboratories, Portland Cement Association, Vol.2, No.2, May 1960, pp. 38-58.

9. Saemann and Washa, "Horizontal Shear Connections between Precast Beams and Cast in Place Slabs," ACI Journal, Vol 61, No.11, November 1964, pp.1383-1409

10. CSA standard A23.3-94, Part II, "Concrete Design Information", Equation (1.10), Pages 1-5 to 1-7.

11. CSA standard A23.3-94, Part I, Clause 8.6.4 and N8.6.5, Page 21

7.0 Ambient Vibration Test on four FC Girder Bridges[*]

7.1 Introduction

To study the behaviour of bridge structures with respect to traffic, wind, seismic activity and other dynamic influences, it is important to have knowledge of the key dynamic characteristics of the bridges, such as natural frequencies and mode shapes of vibration. These dynamic properties, if experimentally measured, can also serve as an important means of characterizing the global structural behaviour of the bridges.

The repeated application of traffic loads on highway bridges cause deterioration in the form of surface wear, fatigue and cracking leading to further corrosion problems. All these slow acting and sometimes subtle phenomena continuously degrade the bridges and reduce their service life. Shutting traffic on account of testing or repairs can sometimes be close to impossible. Most transportation departments in North America would accumulate huge costs in alternate commuter arrangements, if a bridge on a major highway was closed for even a few days. An effective solution to such problems is the use of a periodic or continuous testing and monitoring system, which can be applied quickly and used efficiently to assess the condition of the bridge without interrupting on going traffic.

Presently, most departments of transportation across North America rate and monitor their bridge structures through biennial inspections using visual inspection techniques[1].
It is quite possible that damage could go undetected during such an inspection or grow to critical levels between inspection intervals. Hence, a continuous mechanism of bridge condition assessment is a definite requirement for certain types of bridges, specifically, those bridges which have no redundant structural members. Such a system could be expected to detect sudden significant damage and give the maintenance departments ample notice to activate remedies.

---

[*] Essentials of this chapter appear as a paper in the proceedings of the sixth international conference on short and medium span bridges held in Vancouver BC, 2002

185

Vibration testing has been used successfully in the past to obtain the dynamic characteristics of the bridge in the form of its natural frequencies and mode shapes of vibration. The ambient vibration test is one such method that can be conveniently used for the evaluation of modal response and is becoming increasing popular due to its simplicity of use and cost effectiveness. The test can be conducted without interrupting bridge traffic and does not require forced excitation from an artificial source[2]. The vibration signatures obtained from the test are a required ingredient for the various damage detection algorithms, which may be used to detect and quantify accumulated damage in a bridge structure.

The same vibration characteristics can also be used to calibrate a finite element model of the bridge. The manual method of model refinement usually consists of manipulating key parameters such as the mass and stiffness values of major members of the numerical model until a satisfactory correlation is achieved between the numerical and experimental characteristics. The calibrated model can now be utilized to study the response of the bridge to various external influences and load types[3].

This chapter will present the details of the Ambient Vibration Test conducted on several single span prestressed concrete bridges in the province of Alberta. The major objective in conducting these tests was to authenticate the findings of the ambient vibration test conducted on the Fort Saskatchewan bridge before and after rehabilitation[4] and to test the precision and accuracy of the testing procedure, developed by the authors for this experimental program. With the help of three-dimensional finite element models of each of these bridges, a comparison between the experimental and numerical modal parameters will be presented. This will be followed by a discussion on the accumulated damage in those bridges and its assessment with the help of the dynamic response parameters.

7.2 Bridges Tested

Four single span concrete bridges in Alberta were selected for conducting the ambient vibration test. Two of the bridges were located on local unpaved roads that saw very little traffic while the other two were located on main highways. This selection of the bridges undergoing different use conditions was intentional, to observe the changes in the resulting modal parameters due to differences in bridge conditions.

All four bridges had similar multi-girder decks comprising of pre-cast prestressed channel shaped (FC) concrete girders, as shown in Figure 7.1, but the wearing surface was different in each case. Table 7.1 shows a comparison of the different shape parameters of the four bridges. While the Meanook and Pibroch bridges were located on unpaved gravel roads, the Devon and Gwynne bridges were located on main highways and had asphalt pavements. The Devon Bridge had a chip seal coat on top of the FC girders whereas the Gwynne Bridge had a layer of high density concrete.

While the Meanook and Pibroch Bridges were in their original state since erected, the Devon bridge was one of the series of FC girder bridges which were assembled with transverse prestressing with the help of prestressing tendons, embedded inside the transverse precast concrete diaphragms. Since the prestressing was in the bridge from its first day of service, therefore the shear keys in this bridge could actually have been in relatively better shape than the other bridges. The Gwynne Bridge had been rehabilitated with the help of a combination of steel underslung diaphragms and transverse prestressing, just under the girder flanges with Dywidag bars. Both the Devon and Gwynne bridges had field placed concrete between the girders at diaphragm locations, as shown in Figure 7.1.

The ambient vibration test was used as the field test to determine the natural frequencies and mode shapes of vibration of these bridges.

187

7.3 Ambient Vibration Test

Ambient vibration test, as the name suggests, uses ambient sources of vibration like wind, traffic and ground motions to excite a structure. During ambient excitation, the input is often non-stationary and not directly measured[5]. Field measurements during the test are usually taken for a long time to ensure that multiple modes of vibration are excited and captured. For large bridge structures, ambient excitation is the only practical way of exciting the structure. This method can also be used for smaller bridges when it is not possible to take the structure out of service.

Table 7.1: Comparison of the four bridges tested

	Bridge 1	**Bridge 2**	**Bridge 3**	**Bridge 4**
Name of Town	Meanook	Pibroch	Devon	Gwynne
Over stream or highway	Tawatinaw river	Wabash creek	White mud creek	Pipestone creek
Wearing surface	None	None	Chip seal treatment	High density concrete overlay
Span length	32 meters	38 meters	34 meters	32 meters
Deck Width	10 meters	10 meters	13.7 meters	15.1 meters
Number of adjacent girders	6	6	8	9
Year construc.	1981	1980	1981	1977
Type of road	Local road	Local road	Main Highway	Main Highway
AADT	70	130	7000	4000

188

The natural frequencies of a structure can be estimated using the Fourier transforms of the ambient vibration acceleration records[6]. The natural frequencies are determined from the peaks of the power spectral density of an ambient vibration acceleration record. The mode shapes can be determined experimentally using the ratios of the Fourier amplitudes at the natural frequencies.

However it is important to keep in mind that this estimate can only be successfully made if the natural frequencies are well separated and lightly damped, such that the response at a natural frequency is dominated by the corresponding mode shape[5]. Moreover, it is difficult to obtain good vibration records when the ambient excitation is very small or the structure is very stiff. In these cases it is important to use transducers that are very sensitive.

Earlier researchers have shown that damping cannot be reliably estimated using ambient vibration techniques[6,7]. Brownjohn[8] presented a discussion on the errors in damping estimation and showed that damping estimates from the same ambient vibration study could differ on a large scale if different analysis techniques were used. Okauchi[9] (1992) indicated that damping could not be correctly estimated using the ambient vibration test data because damping values were dependent on the amplitude of excitation. Based on their study on three suspension bridges in Japan, Okauchi et al. demonstrated that damping values were not constant and increased with an increase in the excitation amplitude. At small amplitudes associated with ambient vibration testing, all of the damping estimates showed significant amplitude dependence.

7.4 Test Vibration Measurements

Ambient vibration test on Meanook bridge was conducted on the 2nd of August, 2001. The test was started at around 9:00 am and continued till around 2:00 pm. The temperature during that testing period was about 20 degrees Celsius, with clear sky conditions and a moderate wind. Vibration excitation to the bridge was mainly provided by wind and human activity on the bridge, in addition to light water currents under the bridge. The test on Pibroch bridge was also conducted on the 2nd of August, 2001 and

189

continued from around 2:30 pm to 8:00 pm. Same sources of excitation were used for the Pibroch bridge. The Devon bridge was tested on the 16th of September, 2001 whereas the Gwynne bridge was tested on 25th September, 2001. The temperature in Devon was 15 degrees Celsius whereas the temperature in Gwynne was around 12 degrees during the test. In addition to the sources of excitation earlier mentioned, light traffic was also used to excite the Gwynne Bridge. Figure 7.30 shows pictures of the ambient vibration test conducted on the four bridges

7.5 Instrumentation

Four low g, high sensitivity, Uni-Gain type accelerometers were used for recording the ambient vibration signals. These accelerometers are appropriate for the measurement of very low level vibrations and with a narrow band filter included in the measuring arrangement, measurement of vibration levels down to 0.00002 ms^{-2} is possible[10]. These accelerometers have built-in preamplifiers that can be powered from an external DC. Because of the low output impedance of the accelerometers, the use of relatively long output cables was allowed without introducing any voltage sensitivity losses.

A charge-conditioning amplifier was used with each accelerometer to amplify, improve and filter the range of signals, which were of interest to us. The signal conditioners were powered from internal batteries and their output was routed to the data acquisition connector. The analog signals from the DAQ connector were converted to digital data through the 12-bit multifunction data acquisition card, giving interface with the portable laptop PC. The field data was then stored and analyzed by a LabView program in the time and frequency domains. The whole set up was extremely portable and very convenient for a quick field test.

Figure 7.2 shows the plan view of the bridge deck, indicating positions of accelerometers on top of the girders. While one accelerometer kept its position as the reference, the other three were moved about at different pre-selected locations and the test was completed in several instrument set-ups. A reference indicator was important to connect the vibration information from different set ups.

190

Accelerometer positions were selected in such a way so as to capture as many mode shapes as possible. The positioning of the accelerometers was important because if the sensors were wrongly placed at locations, which do not move significantly, as compared to other points on the bridge, not much useful information would be obtained. The placement of four accelerometers on the four corners at quarter span from both ends (Figure 7.2), on the bridge deck, was particularly useful at recognizing the second torsional mode shape, which often gets mixed up with some other mode shapes. Figures 7.31 and 7.32 show the longitudinal and transverse placement of accelerometers on the bridge deck. All vibration measurements were done in the vertical direction, which were suitable for extracting the vertical, torsional and transverse bending mode shapes. For each set of measurement, 200 seconds of data was collected at the scan rate of 200 Hz, resulting in a resolution of 0.005 Hz for the frequencies.

Table 7.2 shows a comparison of the number of measurement locations and instrument set ups required to complete the test.

Table 7.2: Comparison of the four bridge test set up

	Meanook	Pibroch	Devon	Gwynne
Span length L	32 meters	38 meters	34 meters	32 meters
Accelerometer Spacing, S	4 meters	4.75 meters	4.25 meters	4 meters
Span Width, W	10 meters	10 meters	13.7 meters	15.1 meters
Number of adjacent girders, G	6	6	8	9
Number of sensor locations	22	22	28	31
Number of set-ups	9	9	12	13

191

7.6 Natural Frequencies and Modes Shapes of Vibration

The power spectral densities of the measurements were plotted with the help of a power spectrum, to identify the peaks corresponding to the natural frequencies of vibration, in the frequency domain. Frequencies up to 20 Hz. were selected to be plotted in the power spectrum. The data was carefully examined manually, to make sure that a certain peak did represent a natural frequency of the bridge. Such a frequency may sometimes not lie on the peak but only in the vicinity of it[11].

Figures 7.3 to 7.6 show the power spectrums of the four bridges in the frequency domain. Where as Figures 7.3 to 7.5 show the power spectrum plots for bridges using wind and under passing water currents only, Figure 7.6 shows the Gwynne Bridge case, which took into account excitation from traffic as well. While the x-axis on these plots shows the frequency, the y-axis shows the magnitude of the spectral density function[12]. After the natural frequencies were identified in the frequency domain, a narrow range for each frequency was filtered to assess the mode shape of vibration linked with that particular frequency. A band-pass filter was used to isolate each frequency of interest. Figure 7.7 shows that filtered response for the four accelerometers for a sample test reading. Plots in the time domain can be magnified, by examining a one second window of the time data. That is, the x-axis time scale is magnified into a one second window at time instants, which show peaks of vibrating cycles. The mode shape at a particular vibrating frequency was assessed by looking at the magnitude and direction of accelerometer movements for each frequency of interest. The vibration measurements were normalized with respect to the reference sensors and the phase difference between the reference sensors and other sensors was utilized to predict the mode shape[12]. Figure 7.8 shows plots demonstrating the phase difference between the sensors in the time domain. The first of these plots show all accelerometers moving up and down together, while the other plot shows one of the accelerometers moving out of phase from the other three. Hence it can be concluded from the second plot that while three of the girders (and hence the three accelerometers) were moving up, the fourth one was moving down.

192

Six mode shapes were conveniently extracted from the field test. Some higher frequencies were also observed but the mode shapes representing those frequencies would be difficult to predict without the aid of a finite element model. To understand the higher mode shapes, the accelerometers should be placed with a fairly extensive arrangement on the bridge deck, so that the change in girder movement directions can be seen.

The mode shapes were placed in three primary categories: "Vertical mode shapes" where the girders all move up and down together, "Torsional mode shapes" where the girders on either side of a longitudinal centre of the bridge move up and down alternately, or in other words the bridge deck goes into a torsional motion and "Transverse Bending mode shapes" where pairs of girders move up and down alternately or in other words the deck goes into bending when looking at a transverse cross section of the bridge. Hence all these mode shapes for the bridge deck are produced due to the first and second flexural modes of the individual girder. Table 7.3 shows the six natural frequencies for each of these primary categories for the four bridges tested. Higher modes were generally combinations of these primary categories and could be described as secondary categories. However, those secondary combinations are not being reported or discussed in this chapter.

Bridges, which are very stiff, may yield natural frequencies, which are very high and hence difficult to identify. A similar effect was observed in the Gwynne Bridge where the structure had been rehabilitated for lack of transverse stiffness and hence the test did not yield the torsional and transverse bending frequencies which probably were increased after the rehabilitation process imparted the needed transverse stiffness. Figures 7.9 to 7.28 show the six two-dimensional mode shapes plotted for the four bridges. It may be noted here that the x-axis in these plots shows the longitudinal span of the bridges for the vertical mode shapes, whereas it shows the transverse span of the bridges for the torsional and transverse bending mode shapes. The points on the plots actually indicate the normalized magnitudes of the vertical movements of the accelerometers. All other accelerometer movements were normalized with respect to the reference accelerometer. Since the reference accelerometer did not leave its position therefore it provided a means

193

to connect the data from different readings. It may be mentioned here that the shape of the mode is of interest here but the amplitude is not. Hence moving the accelerometers into a different set up to complete reading the full mode shape does not affect the accuracy of plotting the full mode shape. Figure 7.29 shows the three dimensional view of these six mode shapes, which were generated by the finite element model.

Table 7.3: A comparison of the natural frequencies of the four bridges tested in Hz.

	Meanook	Pibroch	Devon	Gwynne
1st Vertical	2.7	2.1	2.4	2.5
1st Torsional	3.1	2.5	2.9	2.9
1st Transverse Bending	5.4	4.9	8.4	10.3
2nd Torsional	-	8.0	9.2	10.8
2nd Vertical	10.2	7.6	12.9	-
2nd Transverse Bending	11.1	10.8	19.0	-

7.7 Finite Element Model

A three dimensional finite element model was prepared for the bridges and calibrated with the results of the ambient vibrations test in terms of the natural frequencies and mode shapes of vibration. The numerical model serves as the non-destructive tool to evaluate the performance of the bridges to various scenarios and loading conditions.

The commercial software S-FRAME was used to construct the model. Shell elements were used to model the precast girders, field grouted shear keys and transverse concrete diaphragms whereas beam elements were used to model the girder connector bolts and the underslung steel diaphragms. Horizontal translational springs were used to model the neoprene bearings.

Initial material and sectional properties have been taken from the original bridge drawings. These properties do not vary very much from bridge to bridge because the precast FC girders are standard units that go into the construction of these bridges. For full details on the model building process, please refer to Chapter 6 of this thesis. The

194

original finite element model, which was prepared for the single span FC Girder Bridge in Fort Saskatchewan, was modified and reused for the four bridges of Meanook, Pibroch, Devon and Gwynne.

Table 7.4 gives values of the material and sectional properties that were used for different components of the finite element models.

Table 7.4: Material and section properties of components of finite element models

	Modulus of Elasticity $(E_c = 4500\sqrt{fc'})$ (N/mm^2)	Unit weight or density of material (N/mm^3)	Gross Area (mm^2)	Moment of Inertia (mm^4)
Girders	26622 (fc' = 5000 psi, or 35 MPa)	0.00001885 (or 120 lbs/ft.^{3})	Not applicable for shell elements	Not applicable for shell elements
Transverse concrete diaphragms	26622 (fc' = 5000 psi, or 35 MPa)	0.00001885 (or 120 lbs/ft.^{3})	Not applicable for shell elements	Not applicable for shell elements
Field placed concrete, between girders at diaphragms	24647 (fc' = 30 MPa)	0.000024	Not applicable for shell elements	Not applicable for shell elements
Prestressing strands	200000	0.000076	126.67 (12.7 mm dia.)	1276.98
Dywi Dag bars	200000	0.000076	490.62 (25 mm dia.)	19165.04
Steel Underslung Diaphragms	200000	0.000076	7740.0	51387190.0

7.7.1 Using the Modal Assurance Criterion (MAC)

The numerical model was then validated by making a direct and objective comparison of the measured dynamic properties, i.e. the natural frequencies and mode shapes of vibration, with the predicted ones from the model. It is important to assess the modes of the experiment, which are to be compared to the modes of the numerical model. For example, the second mode of the experimental results may not be the same mode as the second mode of the numerical model. To make sure that the different modes had a one to one comparison, the numerical correlation technique MAC (Modal Assurance Criterion) was used to correlate the experimental mode shapes to the numerical mode shapes. The

MAC values provide a measure of the deviation or scatter of the points from the straight-line correlation.

This parameter is defined by:

$$MAC(A,X) = \frac{|\{\psi_x\}^T \{\psi_A\}|^2}{[\{\psi_x\}^T \{\psi_x\}][\{\psi_A\}^T \{\psi_A\}]} \quad \text{(Ewins 2000)}[3]$$

where $\{\psi_x\}$ = Experimentally measured mode shape vector

and $\{\psi_A\}$ = Theoretically predicted mode shape vector

The MAC is clearly a scalar quantity and generally a value greater than 0.9 (or 90%) indicates the presence of well-correlated modes whereas a value of less than 0.1 (or 10%) show uncorrelated modes. The accelerometer settings measuring the vertical movements, set out at predefined locations, as shown in Figure 7.2, gave the experimentally measured mode shape vector, $\{\psi_x\}$, while the numerical mode shape vector was obtained from a free vibration analysis of the finite element model. Table 7.5 shows the MAC values extracted for the four bridges. Most of the values are above 0.90, which indicate a high degree of correlation between the modes under consideration. The MAC analysis hence gave the positive identification of each measured mode with its predicted counterpart, to provide a set of Correlated Mode Pairs (CMPs).

Table 7.5: MAC values for six mode shapes for the four bridges

Mode Shape	Meanook	Pibroch	Devon	Gwynne
1st Vertical	0.99	0.99	0.99	0.99
2nd Vertical	0.99	0.95	0.97	_
1st Torsional	0.96	0.97	0.94	0.99
2nd Torsional	_	0.90	0.93	0.88
1st Transverse Bending	0.98	0.99	0.99	0.99
2nd Transverse Bending	0.86	0.98	0.93	_

7.7.2 Model updating
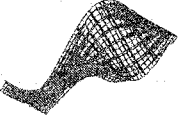
The most obvious comparison between the results of the experiment and the finite element model, in terms of modal properties, can be done by comparing the measured vs. the predicted natural frequencies of vibration. This is often done by a simple tabulation of the two sets of results. Table 7.6 provides such a comparison of the model and test natural frequencies of Meanook, Pibroch, Devon and Gwynne bridges. Most of the natural frequencies had a percentage difference of less than 10%.

However, a more useful format of this comparison is by plotting the experimental values against the predicted ones for each of the modes included in the comparison. That way, it is possible to see not only the degree of correlation, but also the nature of any discrepancies, which may exist between the two sets of results[3]. It is important to stress, however, that the points plotted in this way must be of the measured and predicted natural frequencies of the corresponding or correlated modes. Before plotting the natural frequencies, sets of Correlated Mode Pairs (CMPs) were obtained with the help of the Modal Assurance Criterion (MAC) and the modal frequencies, which showed a high degree of correlation, as shown in Table 7.5, were then plotted to show a comparison of the experimental and numerical results. The emphasis on using correlated mode pairs here is to make sure that we are plotting the 1st vertical mode shape of the test against the first vertical mode shape of the model and not the first torsional mode shape of the model.

Figure 7.33 shows these plots for the four bridges after the finite element models had been updated or calibrated with test results. The points on these plots should lie on or close to a straight line of slope 1. If they lie close to a line of a different slope then the cause of the discrepancy is an erroneous material property used in the predictions. If the points lie scattered widely about the 45 degree straight line then there is probably a serious failure of the model to represent the test structure and a fundamental re-evaluation may be required. If the scatter is small and randomly distributed about the 45° line, then this may be expected from a normal modelling and measurement process[3]. However, a case of particular interest is where the points deviate slightly from the ideal line but in a systematic rather than a random fashion. Such a situation may suggest that there is a

197

specific characteristic responsible for the deviation and that this cannot simply be attributed to experimental errors.

Table 7.6: Test to model comparison of natural frequencies and mode shapes

Mode Shape	Meanook		Pibroch		Devon		Gwynne	
	Test (Hz.)	Model (Hz.)	Test (Hz.)	Model (Hz.)	Test (Hz.)	Model (Hz.)	Test (Hz.)	Model (Hz.)
1st Vertical	2.7	2.8	2.1	2.0	2.4	2.40	2.5	2.66
1st Torsional	3.1	3.3	2.5	2.5	2.9	2.85	2.9	3.08
1st Transverse Bending (Side View)	5.4	5.6	4.9	4.9	8.4	7.72	10.3	9.89
2nd Torsional	_	11.3	8.0	8.1	9.2	9.90	10.8	10.91
2nd Vertical	10.2	10.8	7.6	7.6	12.9	9.28	_	10.29
2nd Transverse Bending (Side View)	11.1	9.9	10.8	8.9	19.0	17.12	_	21.00

198

A similar effect was observed in all the four models where both the first and second transverse bending mode shapes were quite off, whereas the other modes matched reasonably well. The source of discrepancies was identified and manual adjustments were made to the model to bring the two sets of results closer resulting in an updated model. The details of the model updating are given below:

Channel shape bridge cross sections like the ones tested often accumulate great degree of damage in the field grouted shear keys, as a result of years of service. This makes it difficult to correctly assess the stiffness of the shear keys to be used in the model. The test results were consequently used to arrive at a stiffness value for the shear keys, where the test best matched the model results. The Transverse Bending mode shape, which shows the up and down movement of girders, when seen at a transverse cross section, is a good indicator of the shear key condition. Comparing with the stiffness of the original shear keys, it became evident that the present shear keys were deteriorated. The Menook and Pibroch models calibrated nicely after having incorporated a low stiffness for the shear keys whereas the Devon and Gwynne models gave a good match, once lateral stiffness was increased in the system by introducing transverse elements to model the lateral prestressing and field grouted concrete between the girders at diaphragm locations.

Figure 7.33 also illustrates that the first four modes showed excellent agreement between the test and the model, but the last two modes often had errors. In most cases this had to do with the second vertical mode shape and the second torsional mode shape. Since both these mode shapes are a product of the second flexural mode shape of the individual girder therefore there could be chances of misreading the correct mode from the test data. Redundant sensor placements during the test could provide more options to differentiate the two modes from each other, but it would be difficult to guarantee good results if the natural frequencies were not well separated. It is also difficult to accurately plot the mode shapes when two or more natural frequencies are present in a close range, which was the case in some of the bridges.

7.8 Non-destructive Model Based Assessment

The Ambient Vibration Test – Finite Element Model combination is a simple and inexpensive tool for the periodic or continuous assessment of any bridge structure. The change in the key characteristics of the bridge can be monitored in this way and its effect on the response of the bridge can be studied. Accumulated damage in various ways can also be effectively monitored using this tool.

In our case, field-testing proved to be an effective tool in monitoring the FC Girder Bridge, shear key deterioration problem. The transverse bending mode shape demonstrated that a change in the stiffness of the shear key was directly proportional to a visible change in the natural frequency of that mode shape. Both the Devon and Gwynne bridges have used lateral prestressing as a measure to improve the load sharing and stiffen the shear keys. This effect is very clearly visible through the transverse bending mode shape where Table 7.3 shows that the Devon and Gwynne bridges have higher measured values for the transverse bending mode shape as compared to the other bridges, which did not use any means of increasing the shear key stiffness.

To illustrate the sensitivity of the natural frequencies to certain real life damage situations, artificial damage was induced in the finite element model of Pibroch Bridge in the following two ways:

1) Reduction of the flexural stiffness of the external girders, which can result due to corrosion of the prestressing tendons or the impact of high under-passing truck loads.

2) Reduction of the shear key stiffness as a result of accumulated damage from service over the years.

The effects of both these damage situations will alter the natural frequencies of the bridge, which have been shown in Tables 7.7 and 7.8. Table 7.7 illustrates the fact that a loss in the flexural stiffness of the external girders due to the loss of some of the prestress

Table 7.7: Natural frequencies with stiffness loss in external girders for Pibroch Bridge

Mode Shape	Base frequencies (Hz.)	At 25% Stiffness Loss	% Change in frequencies	At 50% Stiffness Loss	% Change in frequencies
1st Vertical	1.98	1.88	4.6	1.79	9.1
1st Torsional	2.50	2.35	6	2.21	11.6
1st Transv. Bending	4.90	4.81	1.8	4.66	4.8
2nd Vertical	7.60	7.26	4.7	6.77	11.2
2nd Torsional	8.12	7.59	6.3	6.92	14.5
2nd Transv. Bending	8.98	8.87	0.5	8.73	2.0

Table 7.8: Natural frequencies with stiffness loss in shear keys for Pibroch Bridge

Mode Shape	Shear key 268 mm	Shear key 100 mm	Shear key 50 mm	Shear key 25 mm	Shear key 15 mm	Shear key 5 mm
1st Vertical	1.95	1.96	1.96	1.97	1.98	1.97
1st Torsional	2.53	2.52	2.51	2.51	2.49	2.17
1st Transv. Bending	7.46	5.85	5.44	5.28	4.91	2.82
2nd Vertical	7.52	7.59	7.60	7.60	7.60	7.56
2nd Torsional	8.18	8.19	8.20	8.18	8.12	7.93
2nd Transv. Bending	16.88	12.31	10.97	10.37	8.98	3.46

tendons will lower the natural frequencies of almost all the modes of vibration. Though the vertical and torsional frequencies show a greater shift whereas the transverse bending frequency is only slightly affected. Similarly we can observe from Table 7.8 that with a stiffness loss in the shear keys, the modal frequency affected most was that coming from the transverse bending mode shape. Similar exercises with other damage scenarios can simulate and predict the bridge behaviour in those cases.

7.9 Conclusions

The Ambient Vibration Test is an effective tool to develop and calibrate a finite element model of any bridge structure, which can then be used to monitor the health of the bridge in the years to come. By closely examining the trend in the shift in the natural frequencies, it is possible to comment on the area affected by the damage.

However, a draw back with the system is the relatively small magnitude of the shifts involved with change in structural properties. This can sometimes be an issue, owing to the presence of noise and other extraneous data that can easily affect the test data. Moreover, it is difficult to obtain good results if the natural frequencies are not well separated. Also the manual method of data reduction that was used by the authors is sometimes dependent on personal judgement and can thus lead to errors in mode shape estimation.

From the Ambient Vibrations Tests conducted on the four prestressed concrete bridges, it was observed that the performance of the bridges, which were under different usage conditions, could be characterized in terms of their modal parameters. In our case, we saw that the transverse bending mode shape could be used as a parameter to comment on the condition of the shear key, or in other words, on the transverse stiffness of the bridge. The transverse bending mode frequencies of around 5hz. in the Meanook and Pibroch bridges and around 8 and 10 hz. in the Devon and Gwynne bridges showed that an increase in the transverse stiffness due to the prestressing tendons in the Devon bridge and rehabilitation in the Gwynne bridge did show up in the transverse bending mode parameter. In other words, this parameter can be used to comment on the transverse stiffness of the bridge.

The change in the modal frequencies with the change in length and width of the bridge deck were consistent with the expectations, which show credibility of the testing process. Similarly, the repeatability, reproducibility and consistency of the test results in the case of each bridge also indicated the successful implementation of the testing procedures. The ability of the finite element models to predict the test with reasonable accuracy was a useful feature towards non-destructive model based assessment of the structure.

The low values obtained for the transverse bending mode shape natural frequencies for Meanook and Pibroch bridges indicate some deterioration in the shear keys in those bridges. Though, cracks were not visible on the surface by the naked eye, the presence of micro cracking inside the shear key as well as hair line cracks on the surface which can easily get filled by dirt and dust, cannot be ruled out. De-bonding of the shear key grout from the edge of the girder shear key is another possibility.

Unfortunately we do not have a direct relation of the shear key cracking to the transverse bending mode shape. In other words we have no data to rely on and comment that if the transverse bending mode shape sinks low to some value, the shear keys would crack.

7.10 Acknowledgements

Field grouted shear keys

Field placed concrete in the case of Devon and Gwynne bridges
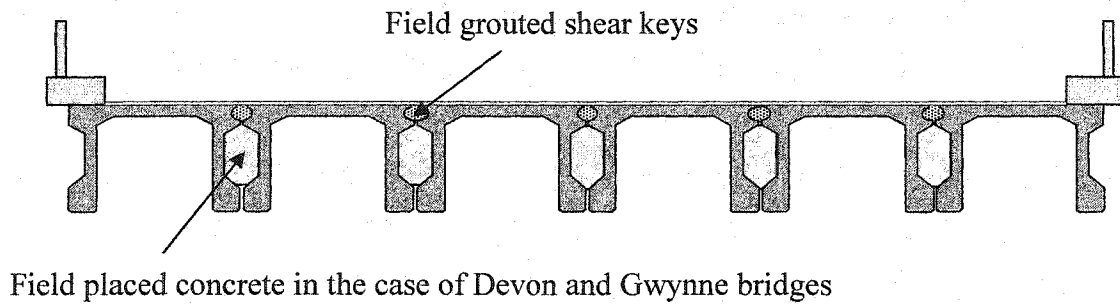
Figure 7.1: Typical cross section of an FC girder bridge

$S = L/8$

W

L
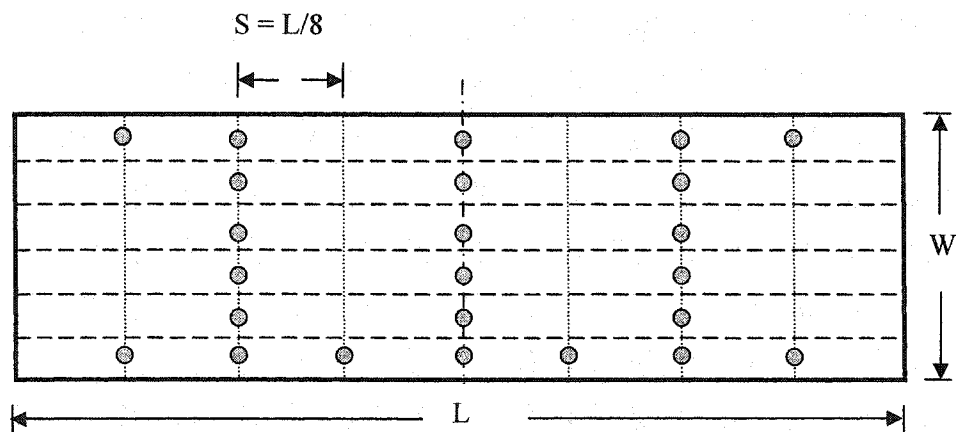
Figure 7.2: Plan of bridge deck showing accelerometer locations

204
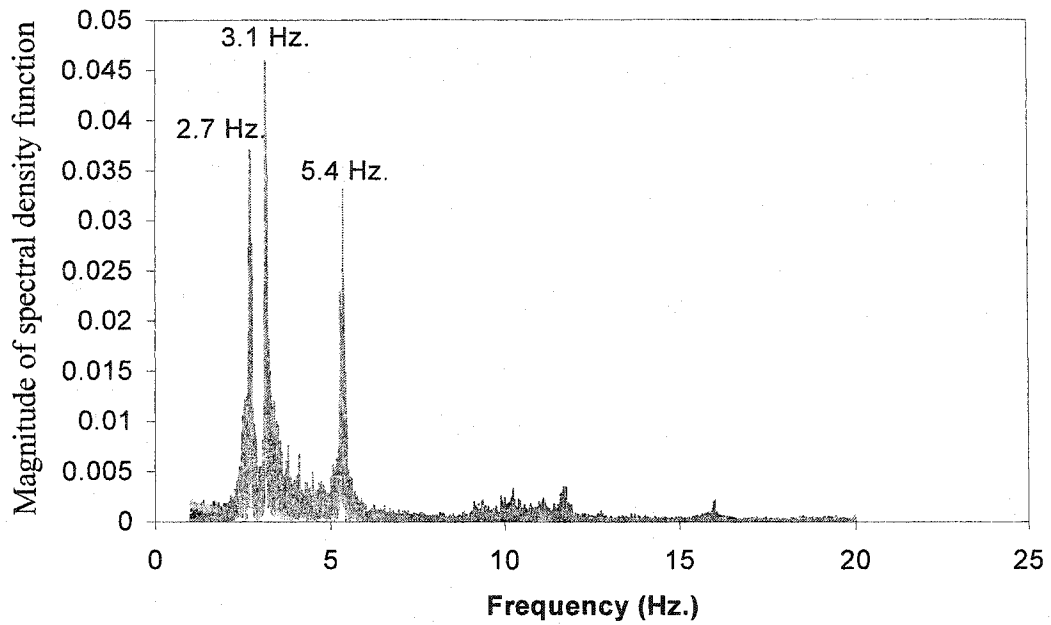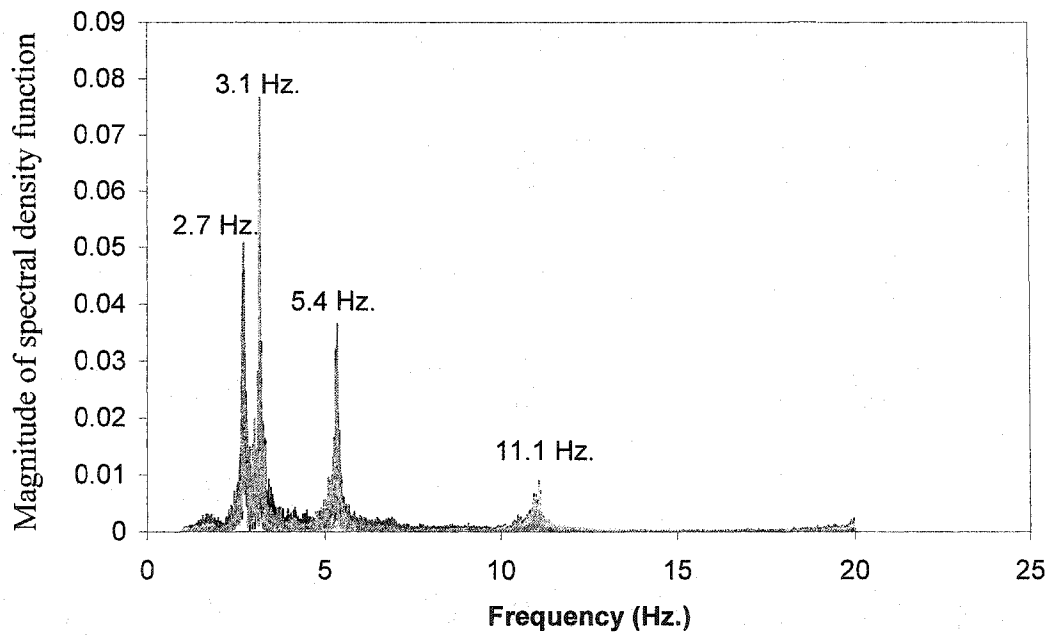
Figure 7.3: Power Spectrum in the frequency domain, Meanook Bridge

Longitudinal placement of the accelerometers
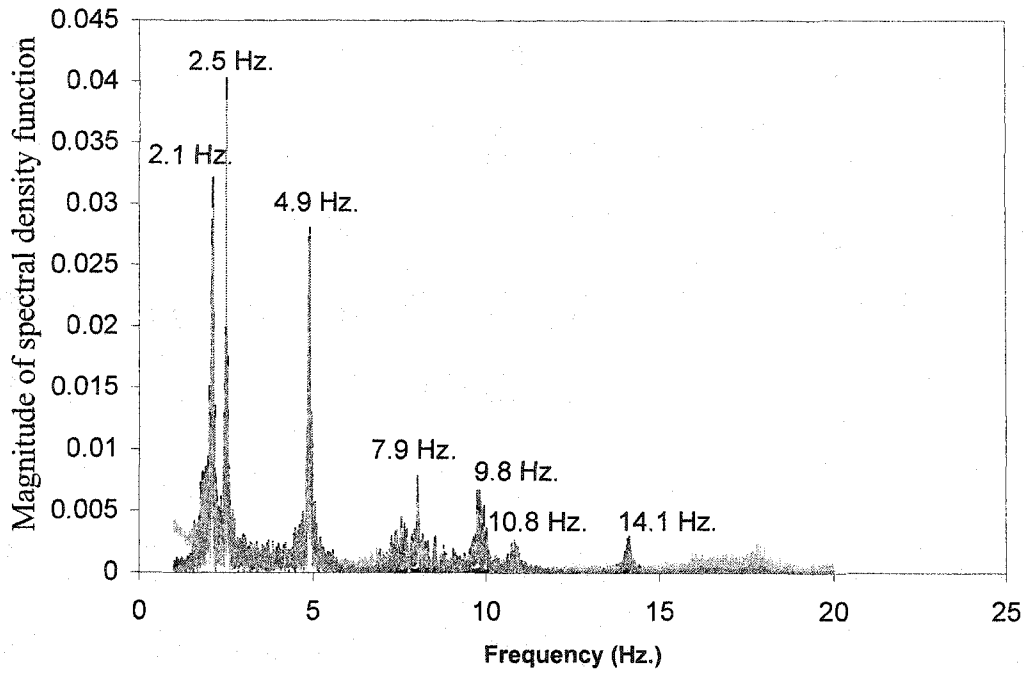
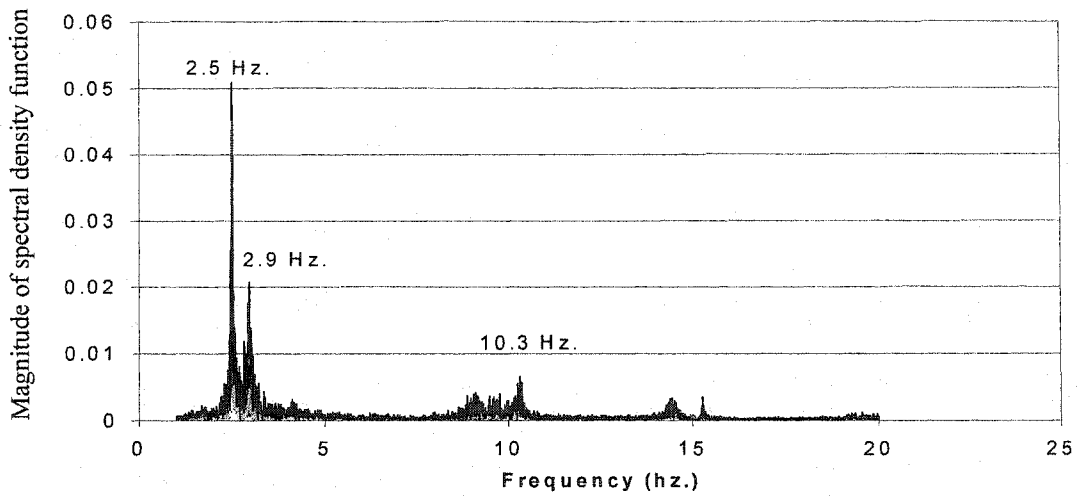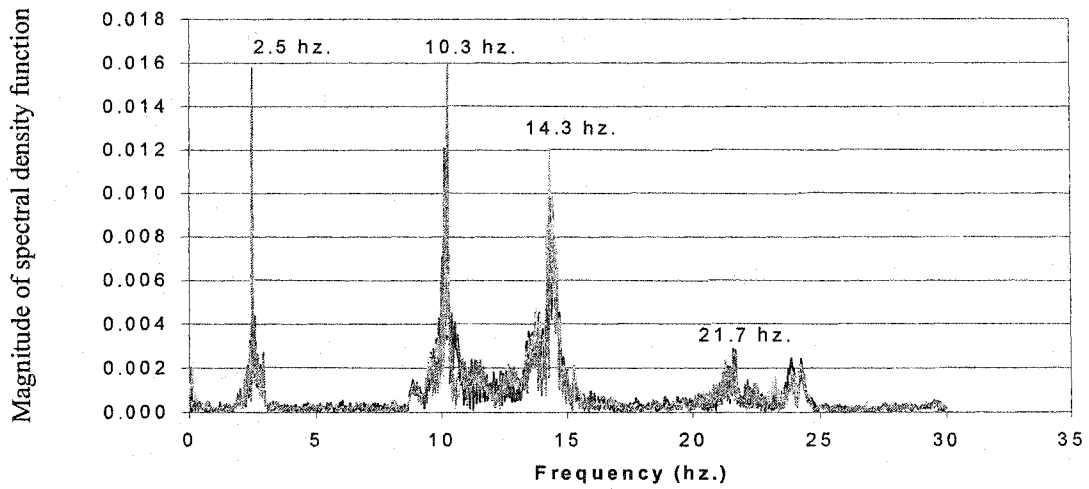Transverse placement of the accelerometers at mid span
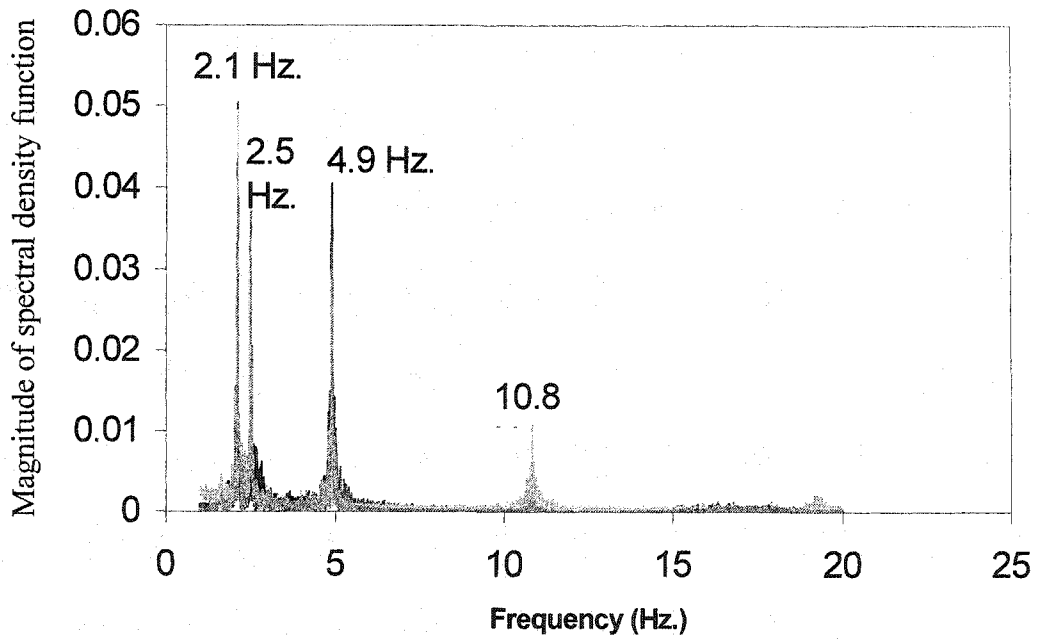
Figure 7.4: Power Spectrum in the frequency domain, Pibroch Bridge

206

Longitudinal placement of the accelerometers
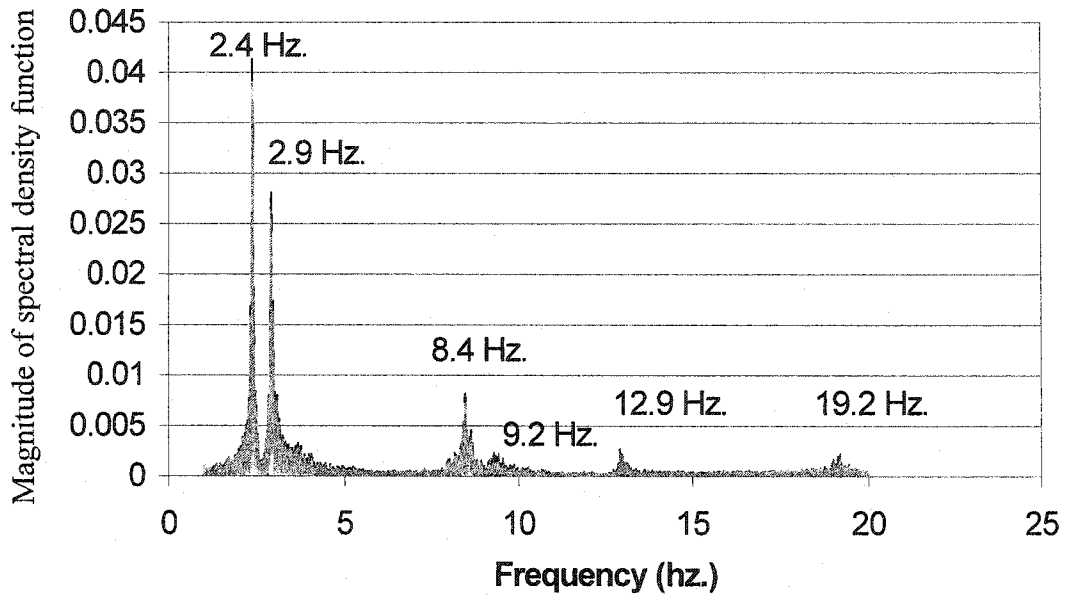
Transverse placement of the accelerometers at mid span
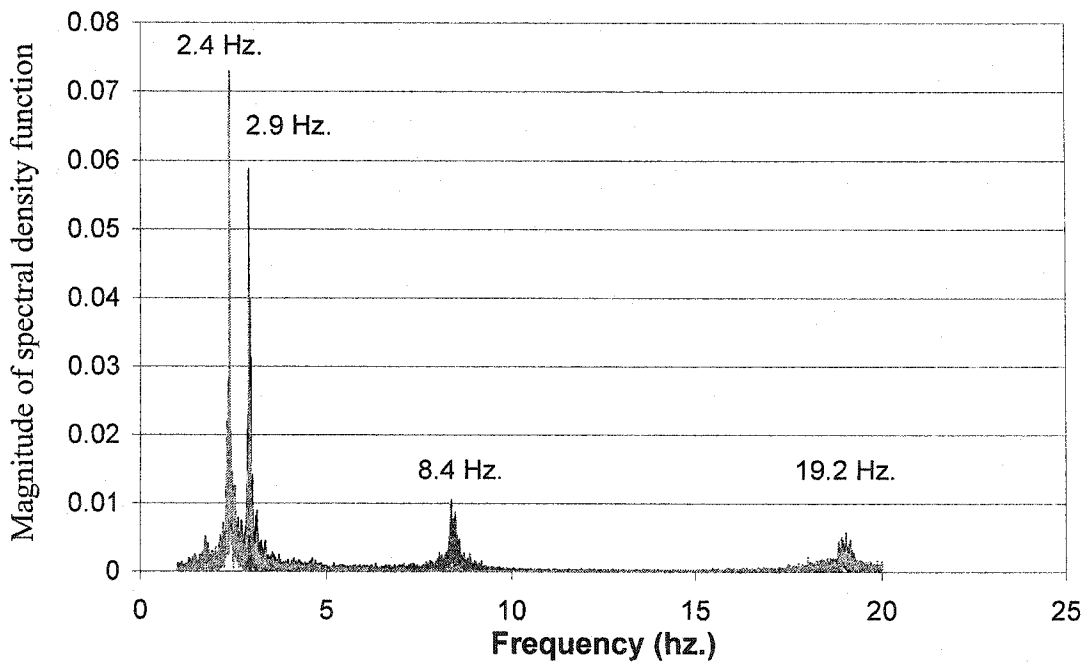
Figure 7.5: Power Spectrum in the frequency domain, Devon Bridge

Transverse placement of the accelerometers at quarter span with no traffic on bridge

Longitudinal placement of the accelerometers, under light traffic (small cars)

Longitudinal placement of the accelerometers, under heavy traffic (large truck)
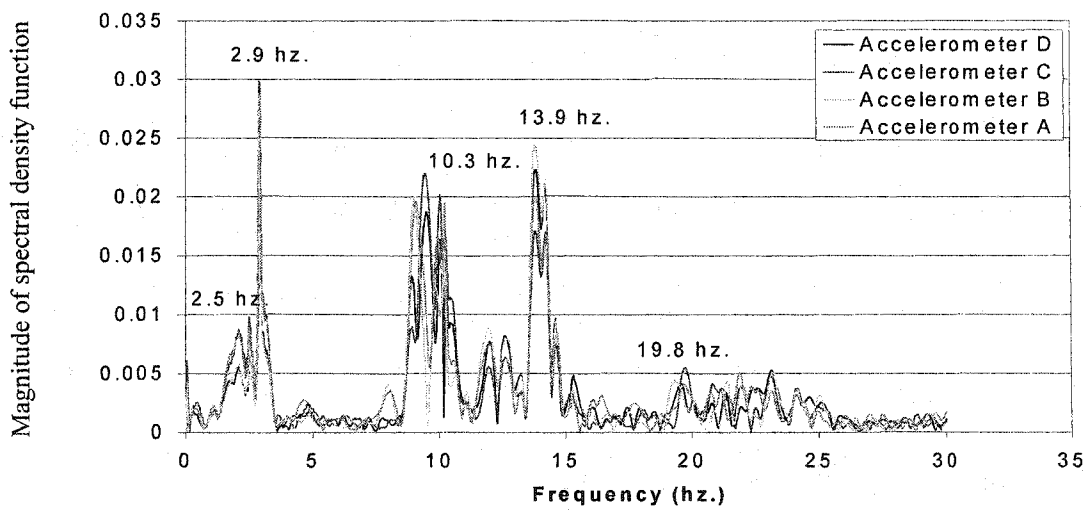
Figure 7.6: Power Spectrum in the frequency domain, Gwynne Bridge

208
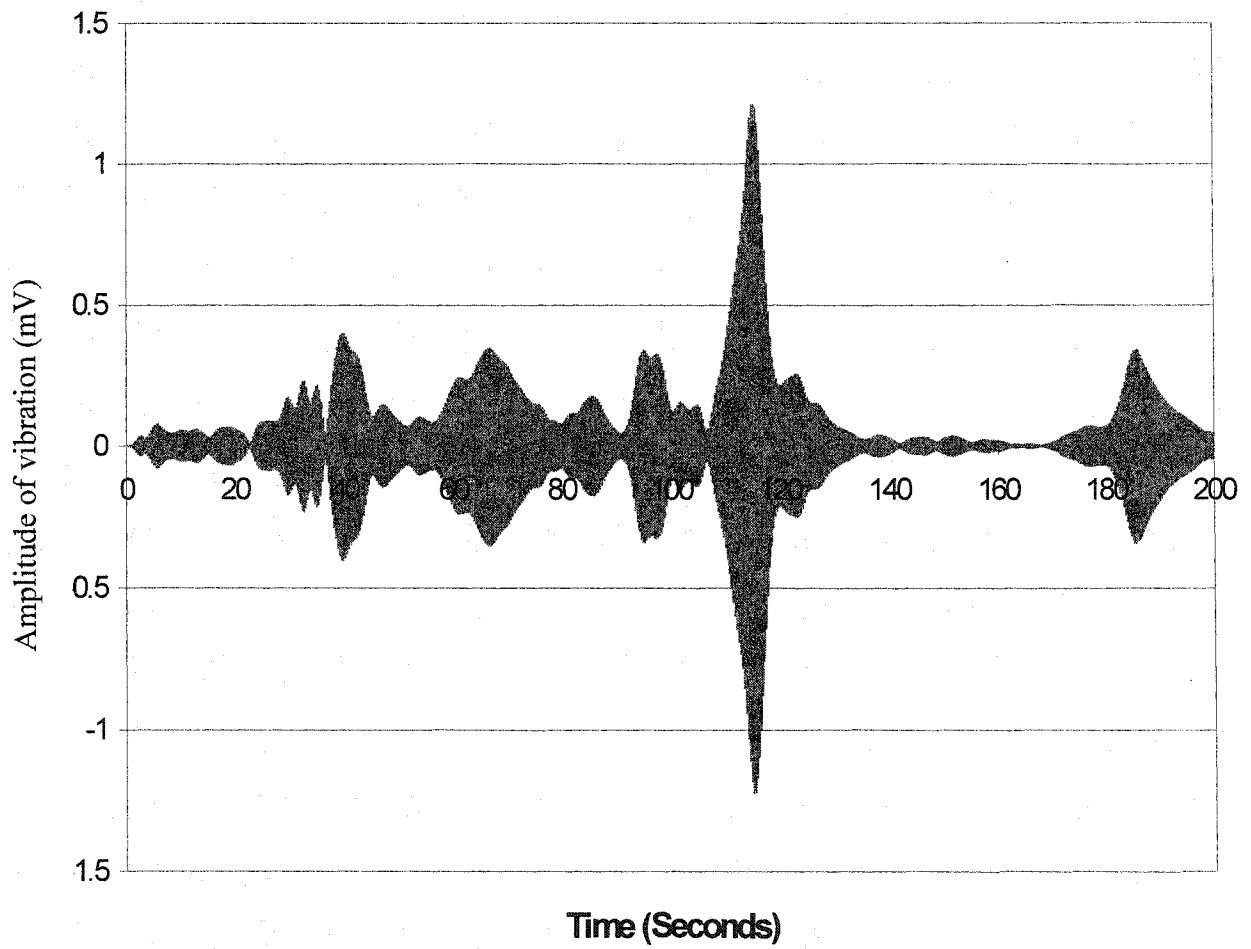
Figure 7.7: Filtered response for a single frequency of interest with a band pass filter

209
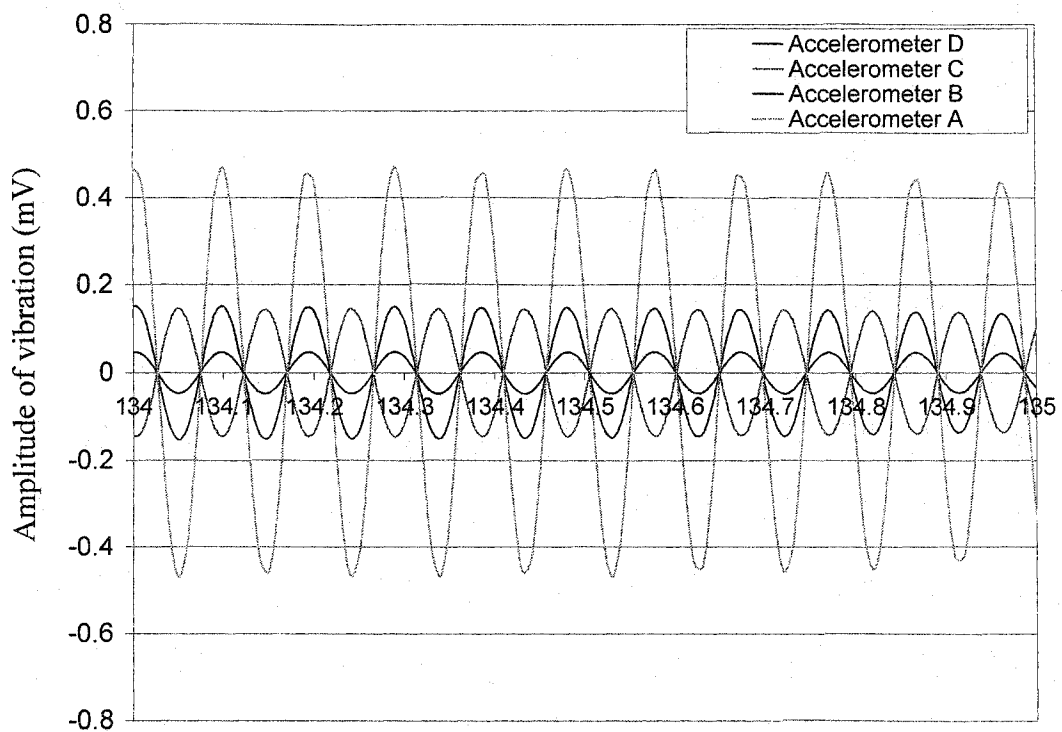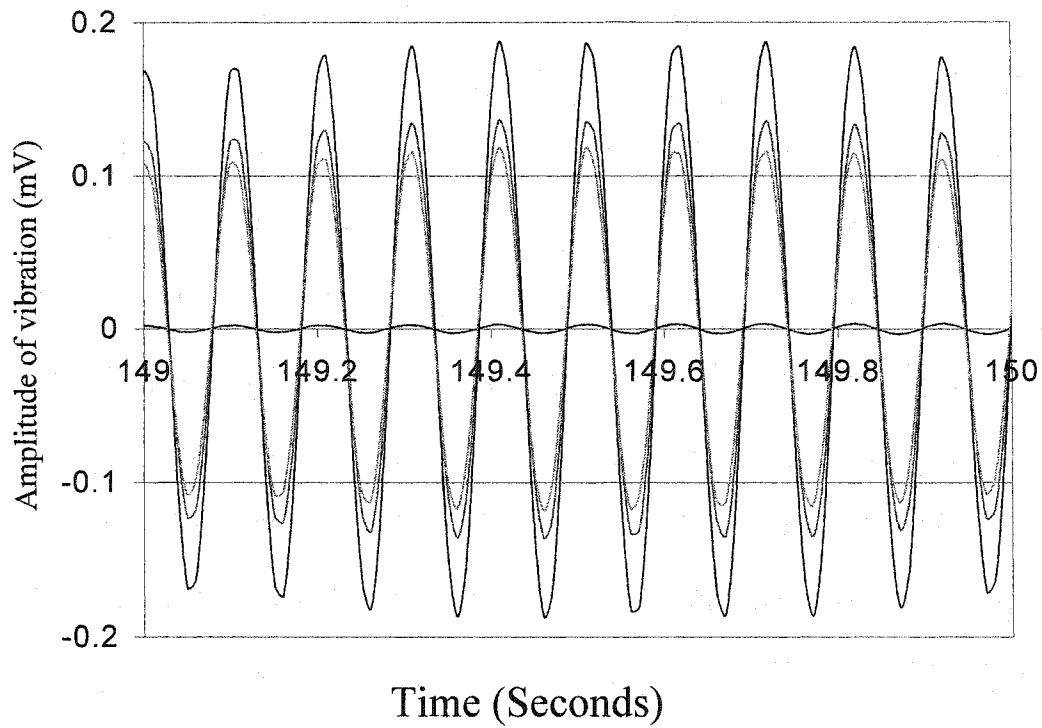
Figure 7.8: Phase difference of sensors in time domain
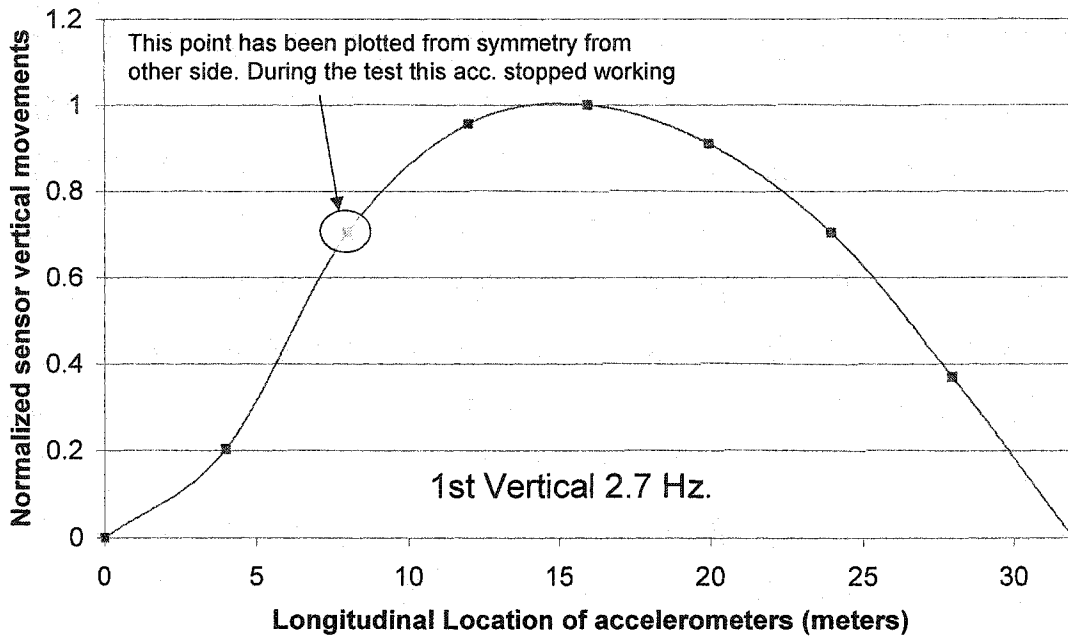
Figure 7.9: 1st vertical mode shape, plotted from field measurements for Meanook bridge
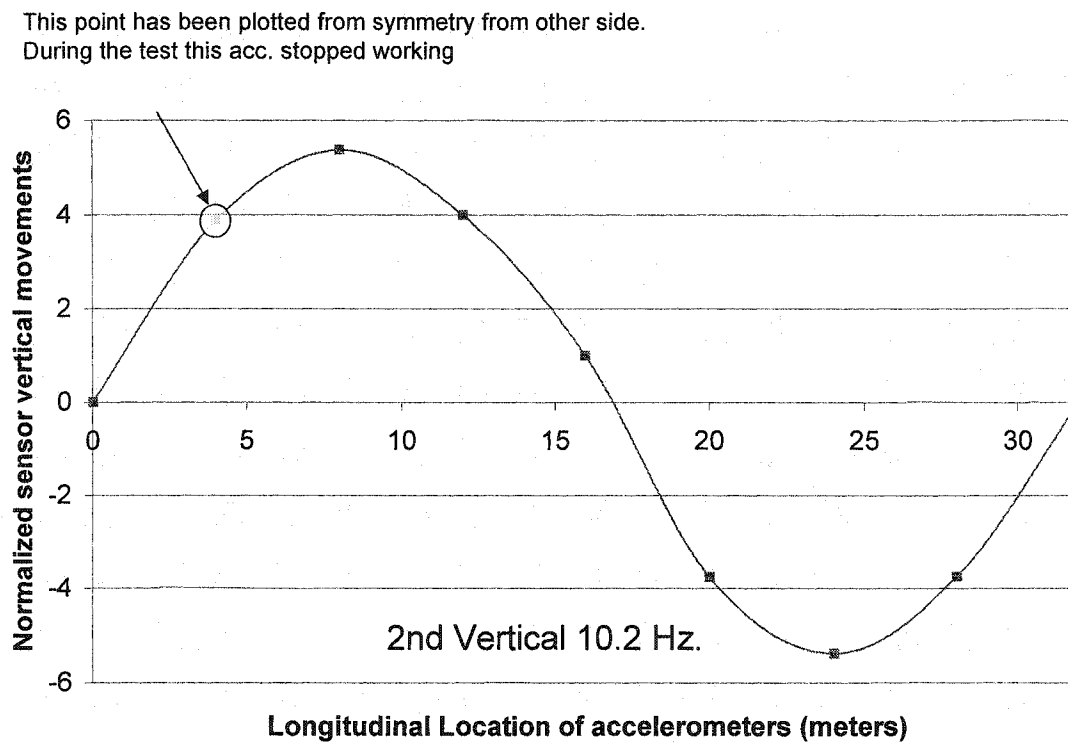
Figure 7.10: 2nd vertical mode shape, from field measurements for Meanook bridge

211
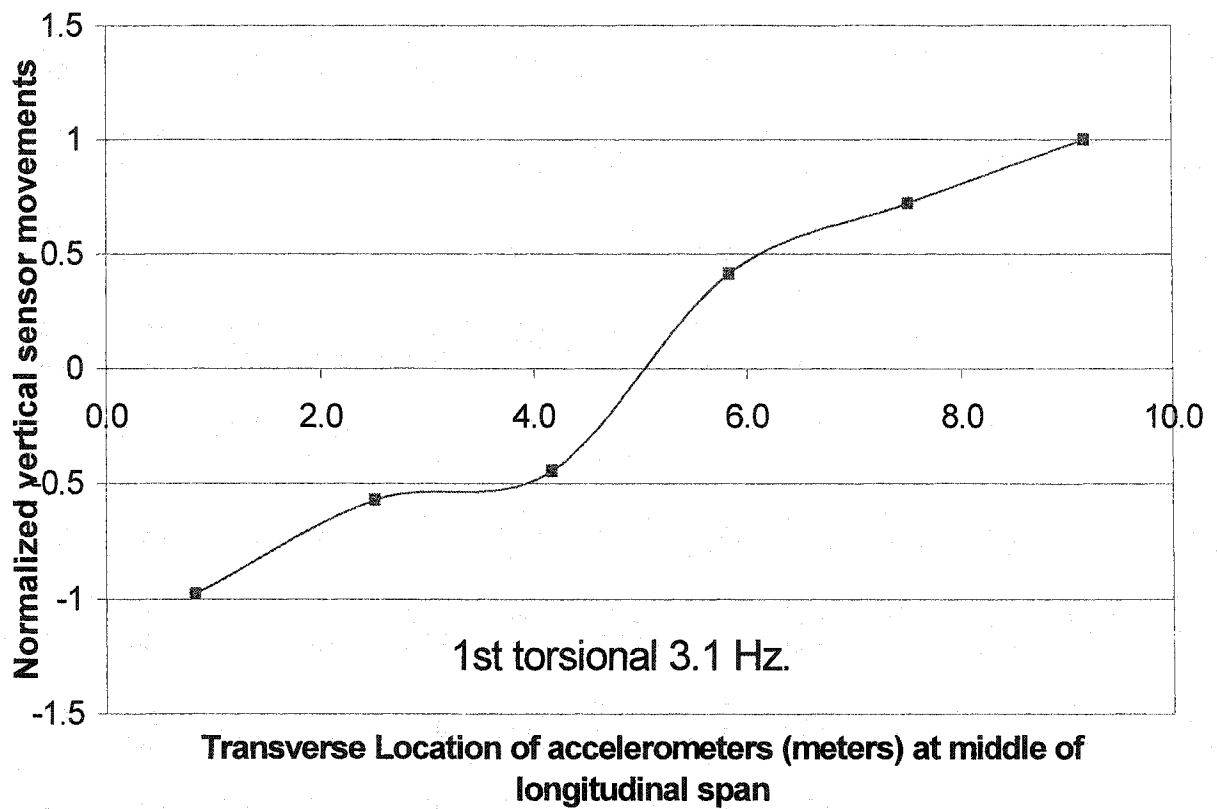
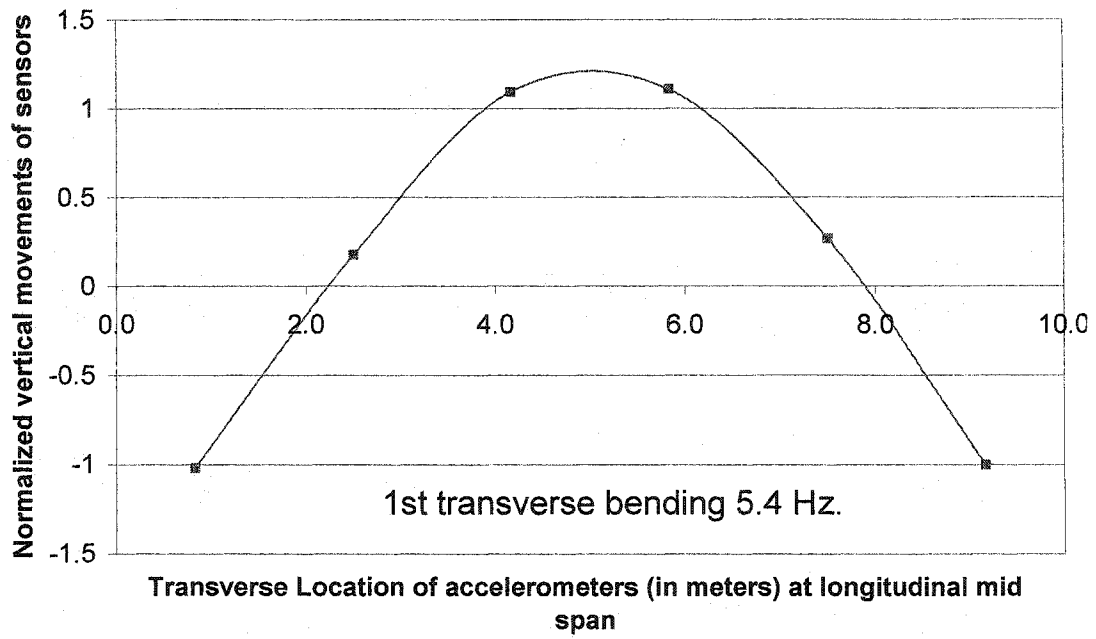Figure 7.11: 1st torsional mode shape, from field measurements for Meanook bridge

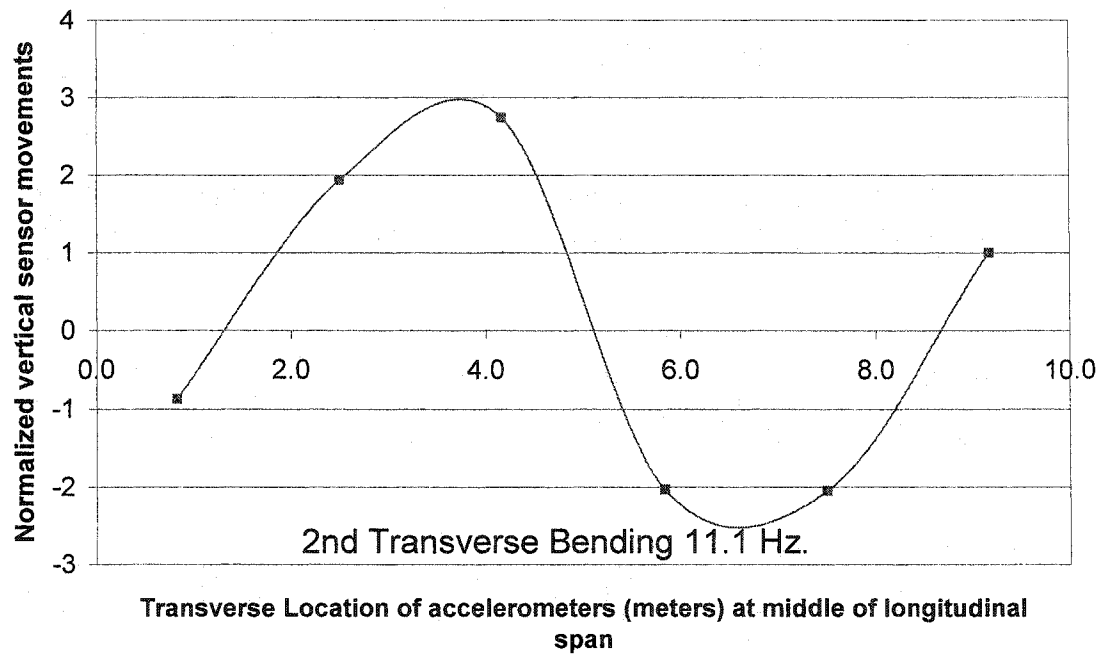Figure 7.12: 1st transverse bending mode shape, from field measurements for Meanook

Figure 7.13: 2nd transverse bending mode shape, from field measurements for Meanook
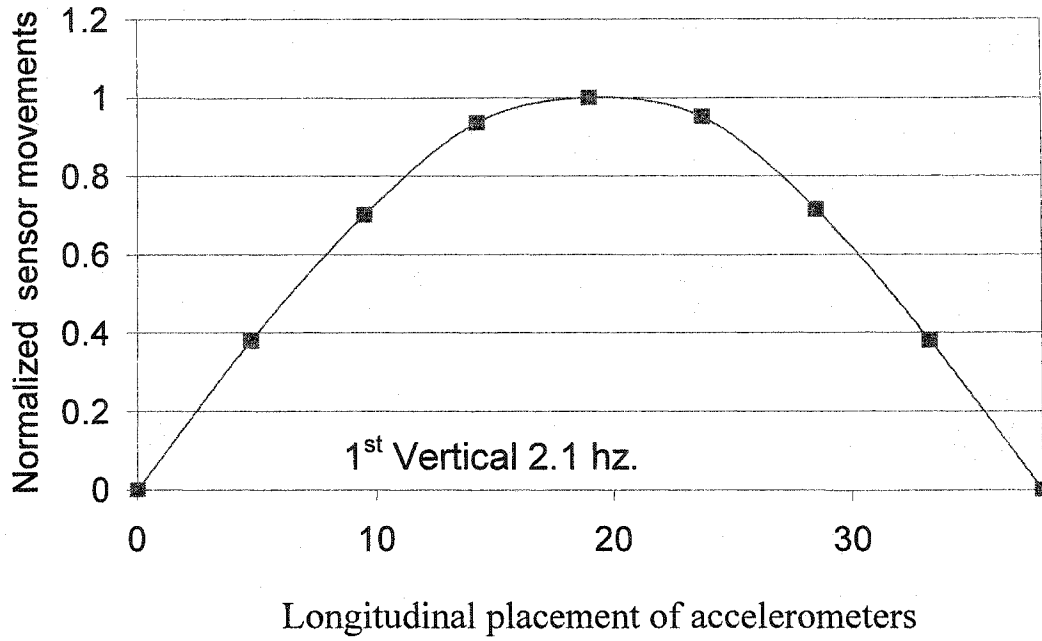
213

Figure 7.14: 1st vertical mode shape, plotted from field measurements for Pibroch bridge
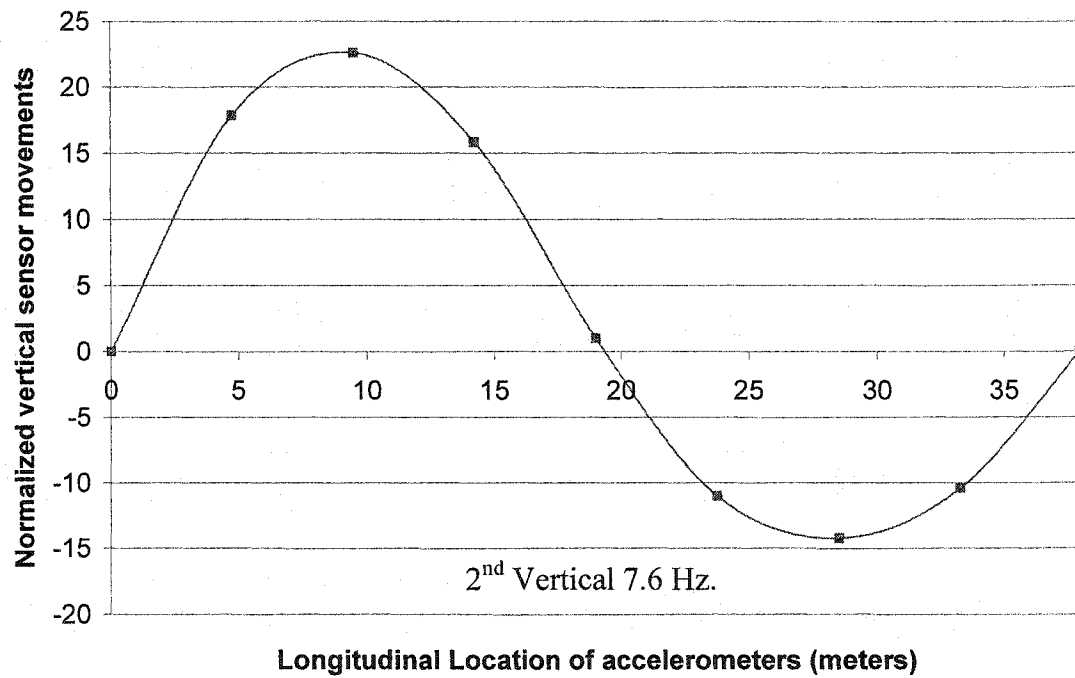

Figure 7.15: 2nd vertical mode shape, plotted from field measurements for Pibroch bridge
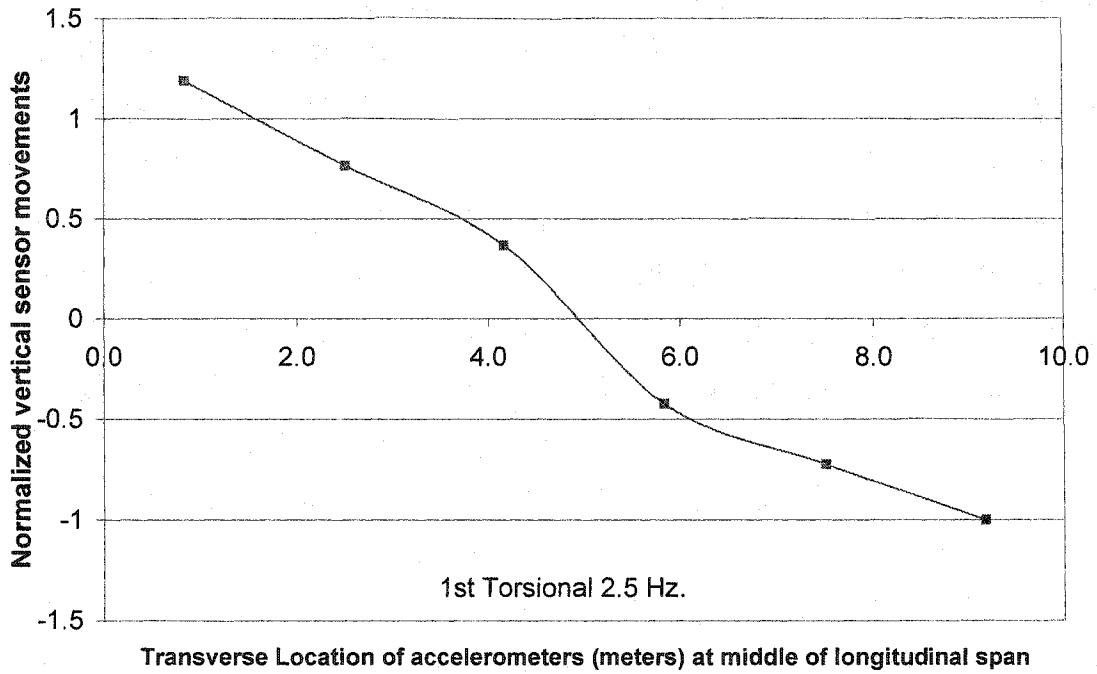
214

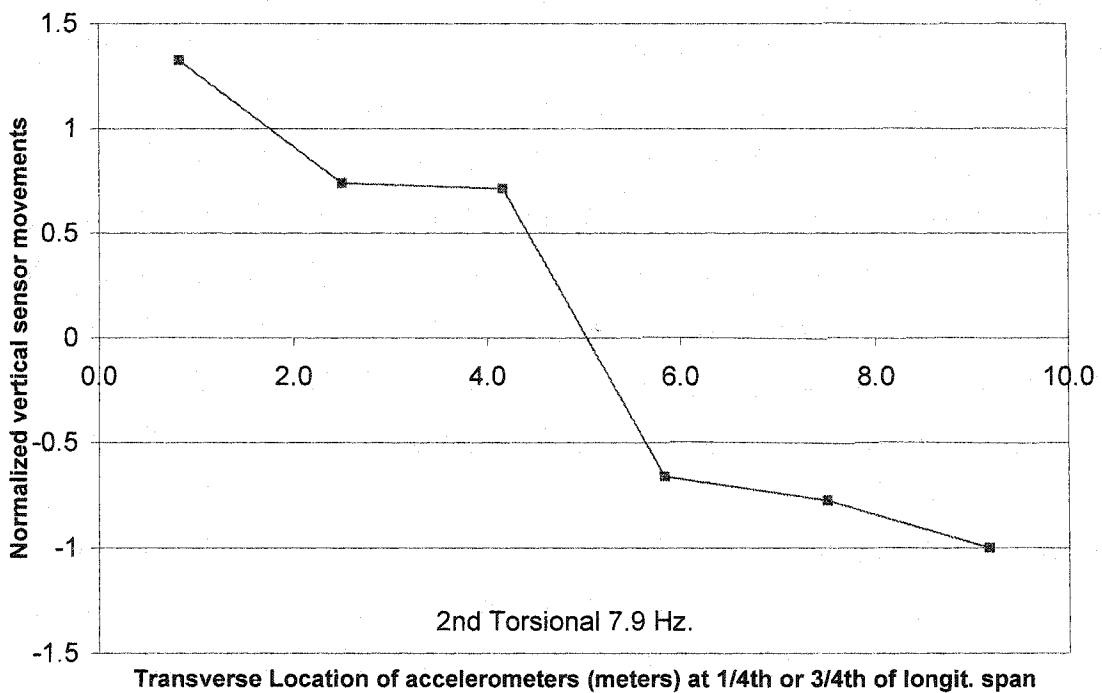Figure 7.16: 1st torsional mode shape, from field measurements of Pibroch Bridge

Figure 7.17: 2nd torsional mode shape, from field measurements of Pibroch Bridge
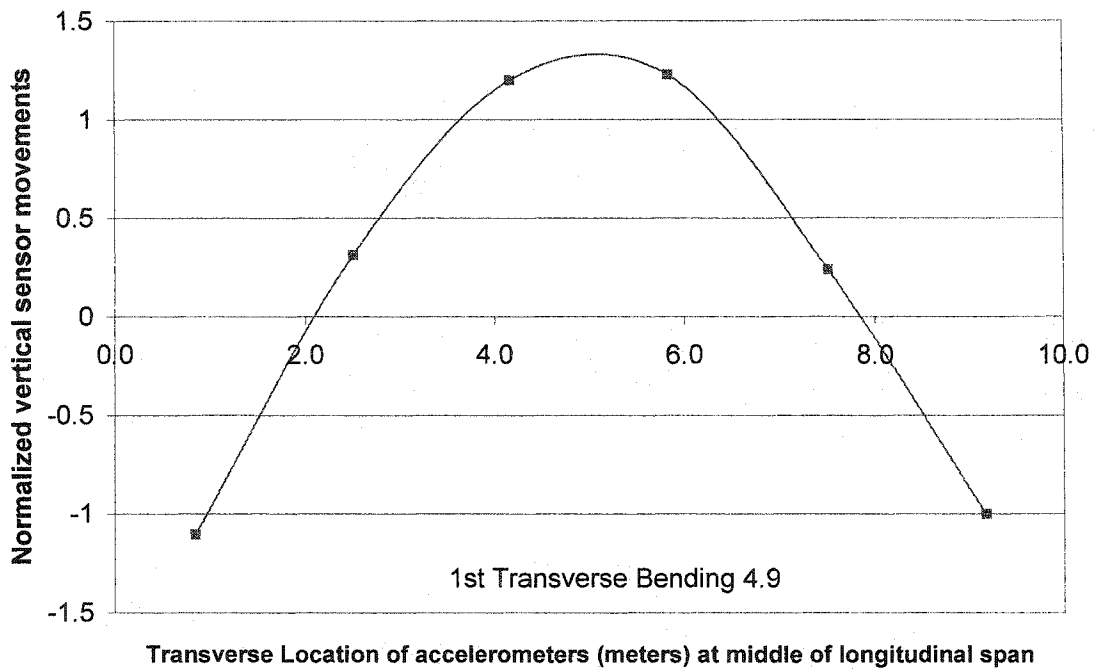
215

Figure 7.18: 1st Transverse Bending mode shape, from field measurements of Pibroch

Figure 7.19: 2nd Transverse Bending mode shape, from field measurements of Pibroch

216

Figure 7.20: 1st vertical mode shape, plotted from field measurements of Devon bridge

Figure 7.21: 2nd vertical mode shape, plotted from field measurements of Devon bridge

217
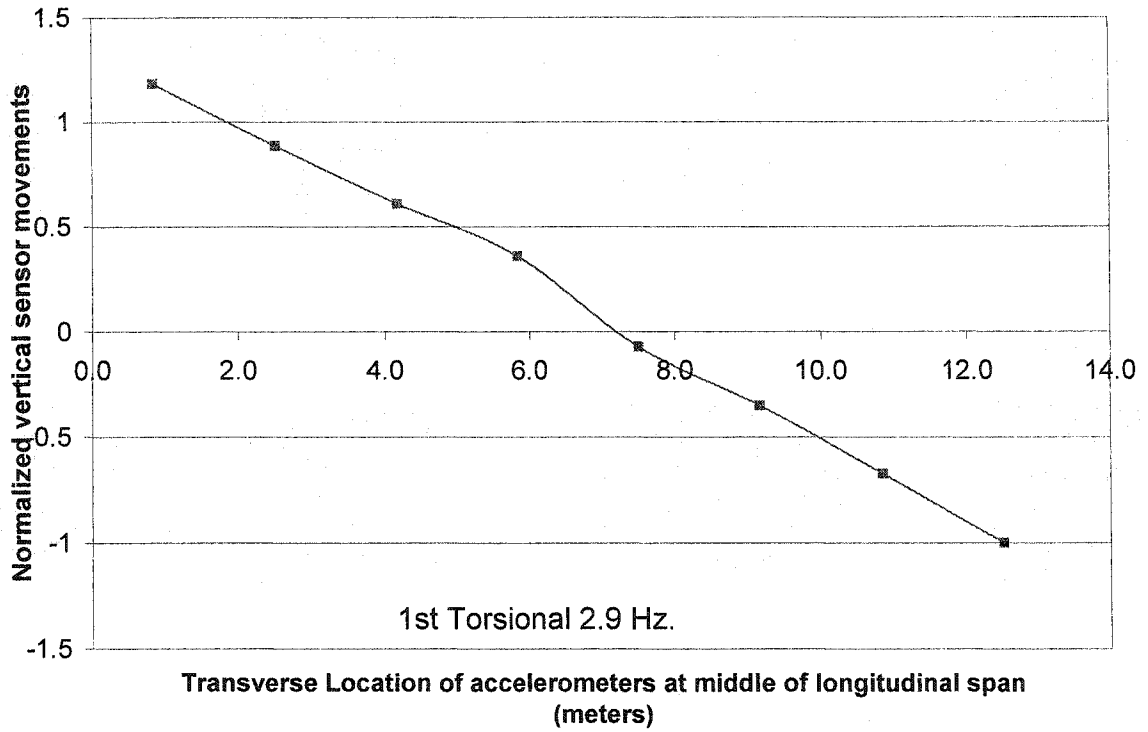
Figure 7.22: 1st Torsional mode shape, plotted from field measurements of Devon bridge
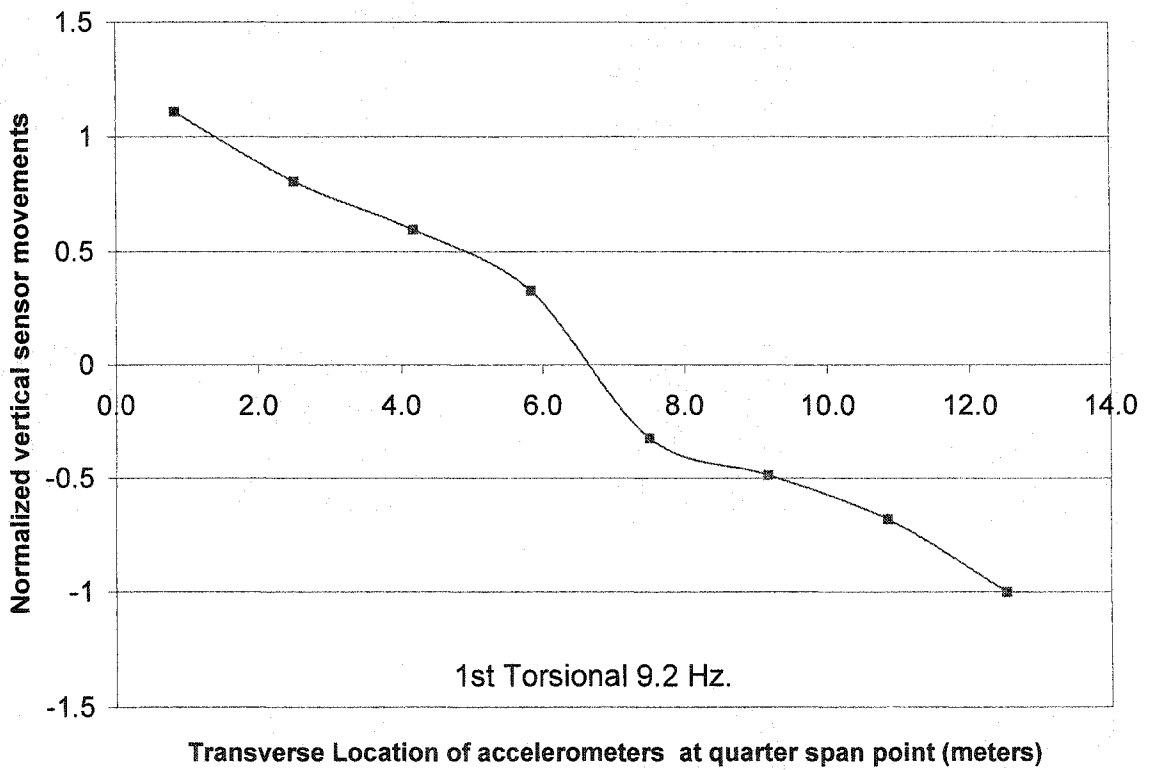
Figure 7.23: 2nd Torsional mode shape, plotted from field measurements of Devon

218
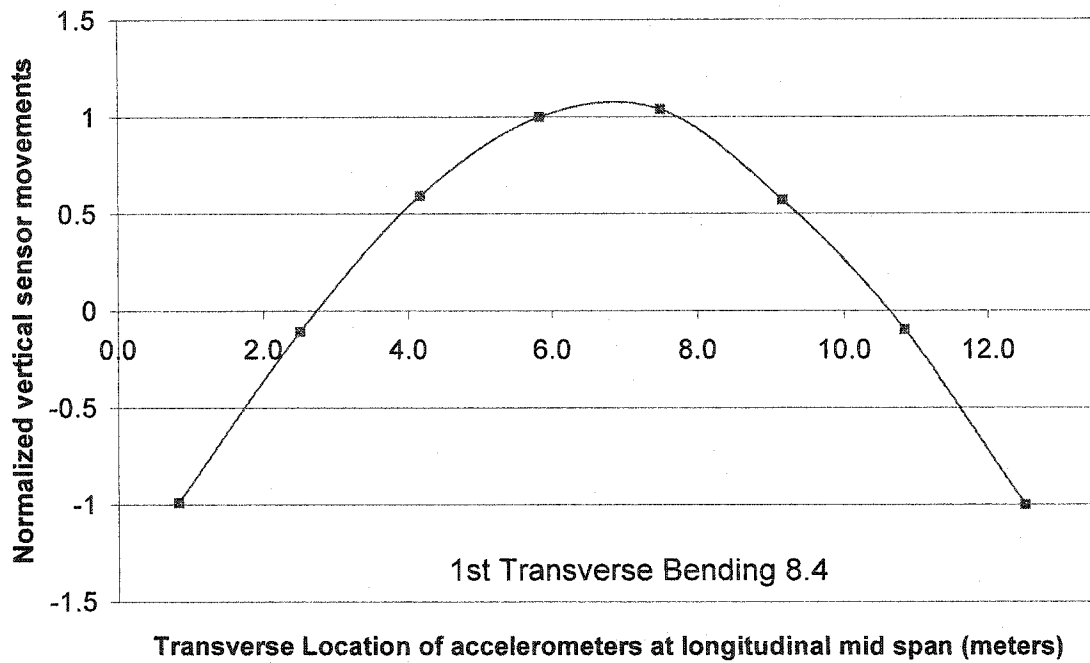
Figure 7.24: 1st Transverse Bending mode shape, from field measurements of Devon
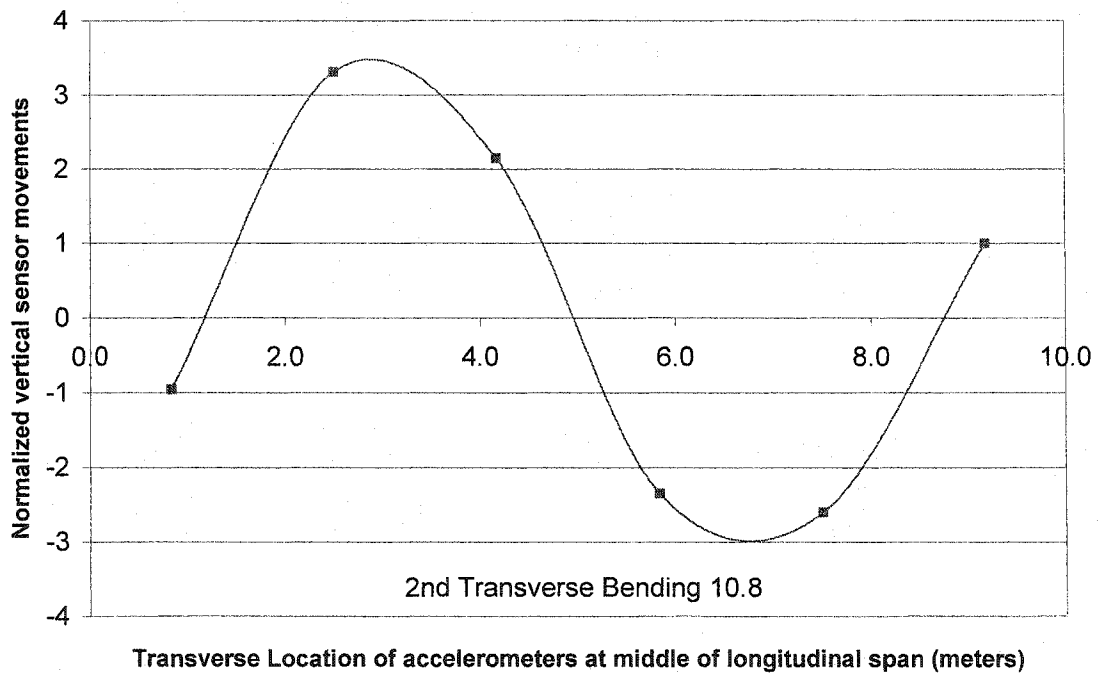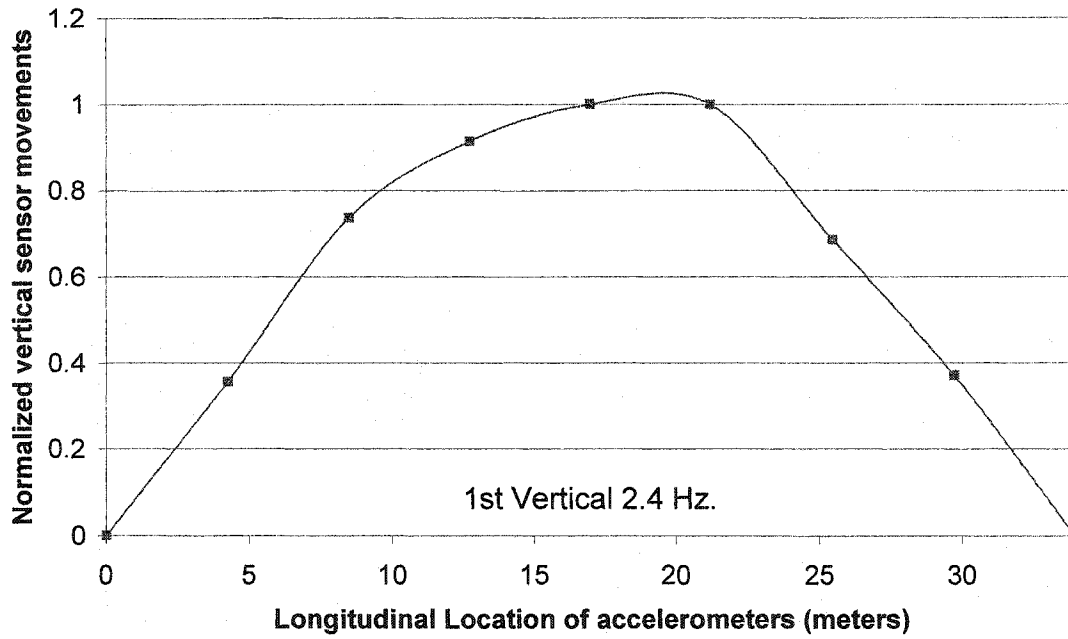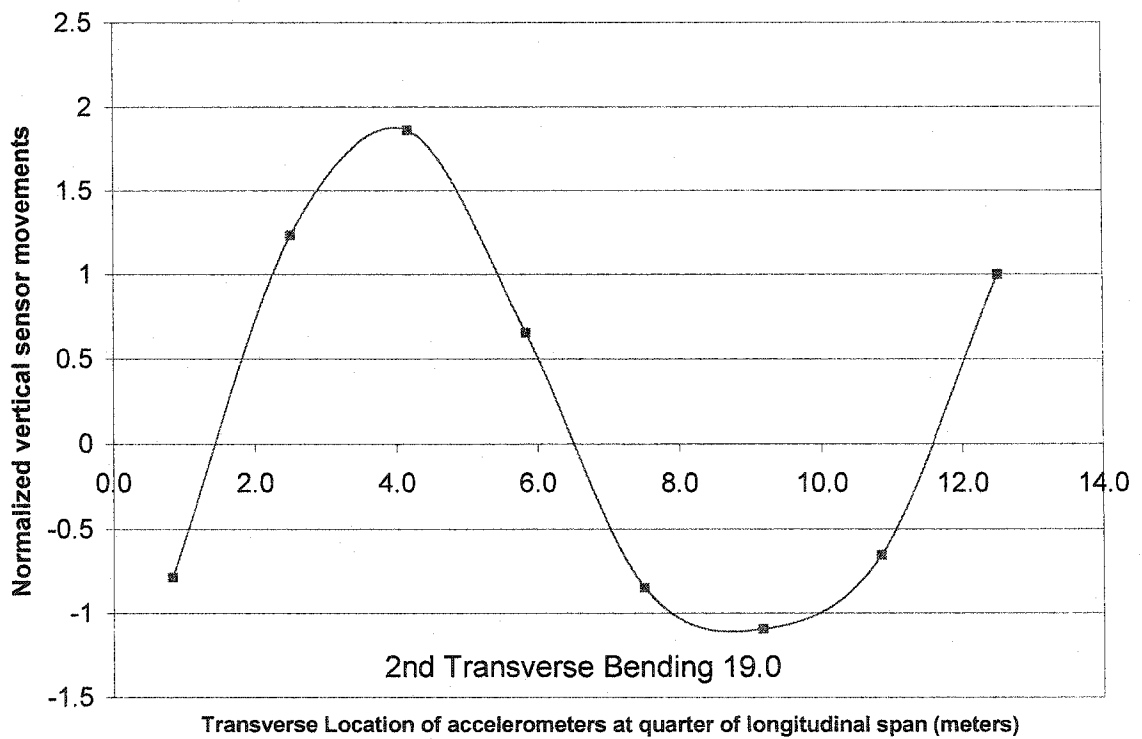

Figure 7.25: 2nd Transverse Bending mode shape, from field measurements of Devon

219
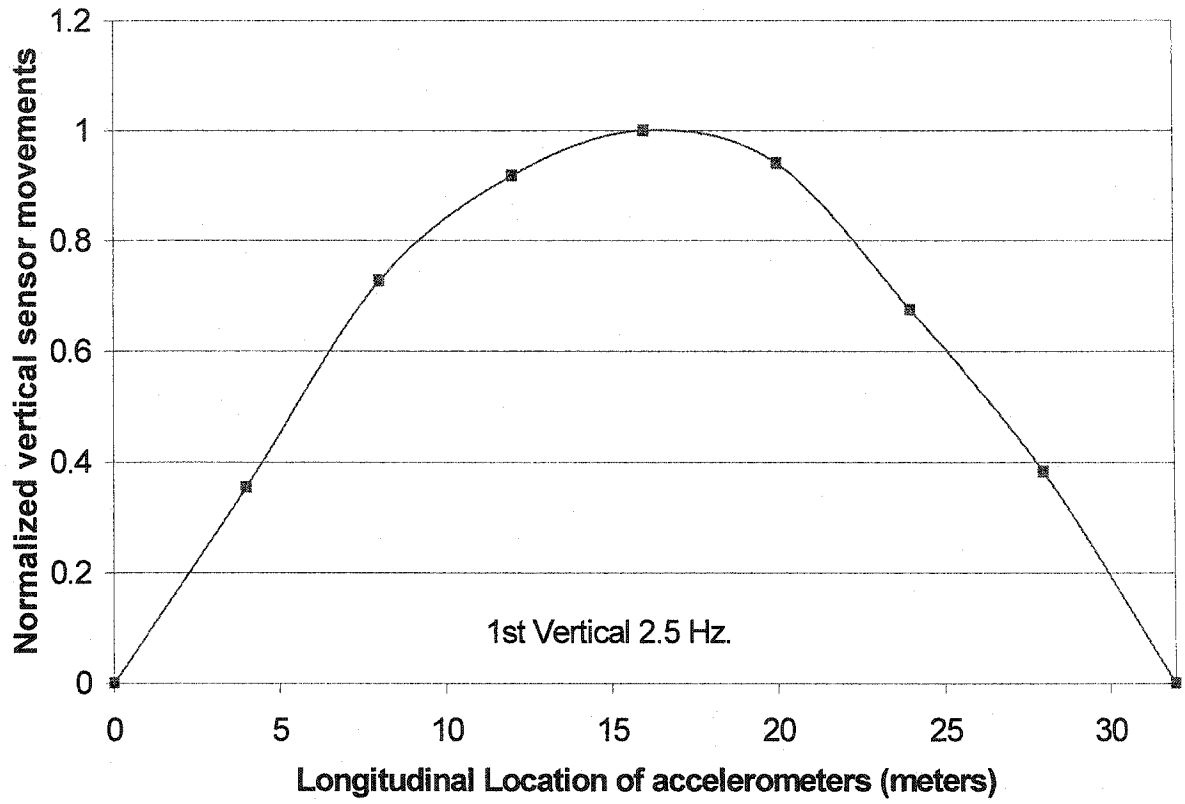
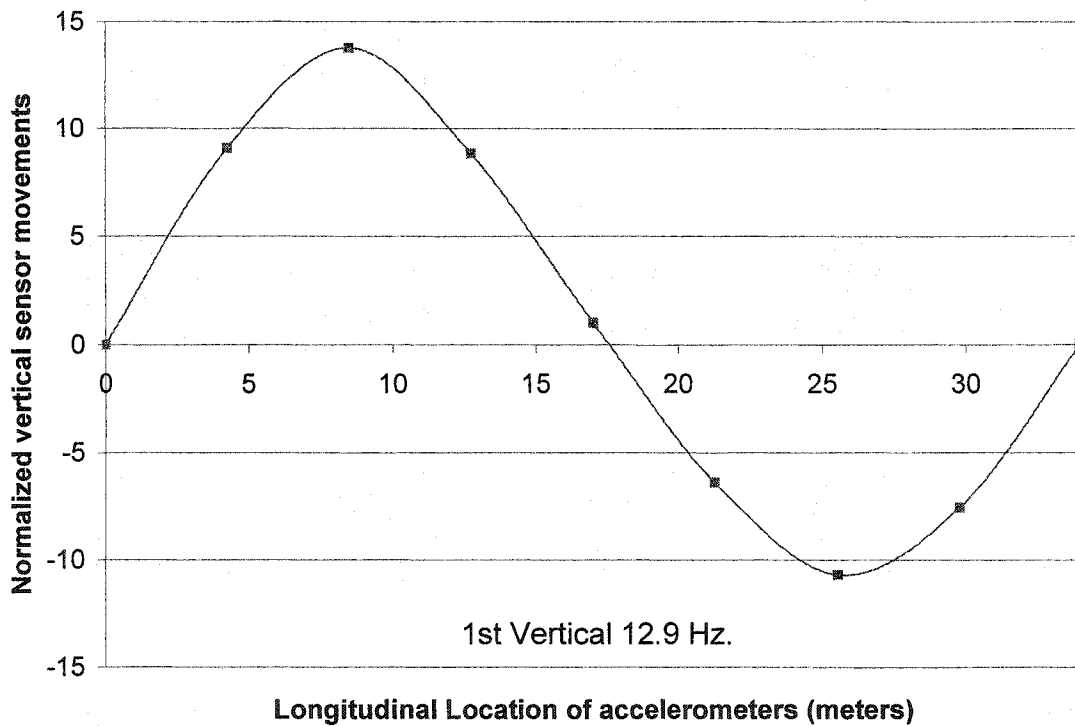Figure 7.26: 1st vertical mode shape, plotted from field measurements of Gwynne bridge

220

1st Torsional 2.9 Hz.

Transverse Location of accelerometers (meters) at middle of
longitudinal span
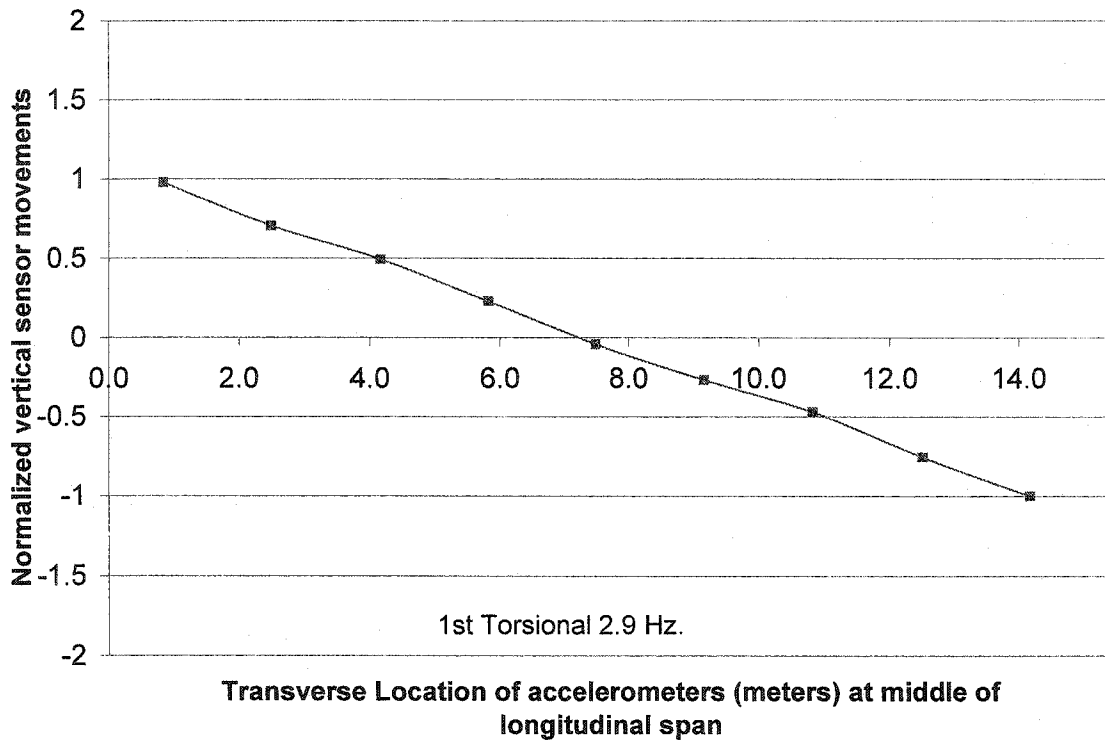
Figure 7.27: 1st Torsional mode shape, plotted from field measurements of Gwynne

1st Transverse Bending 10.3 Hz.

Transverse Location of accelerometers (meters) at longitudinal mid span
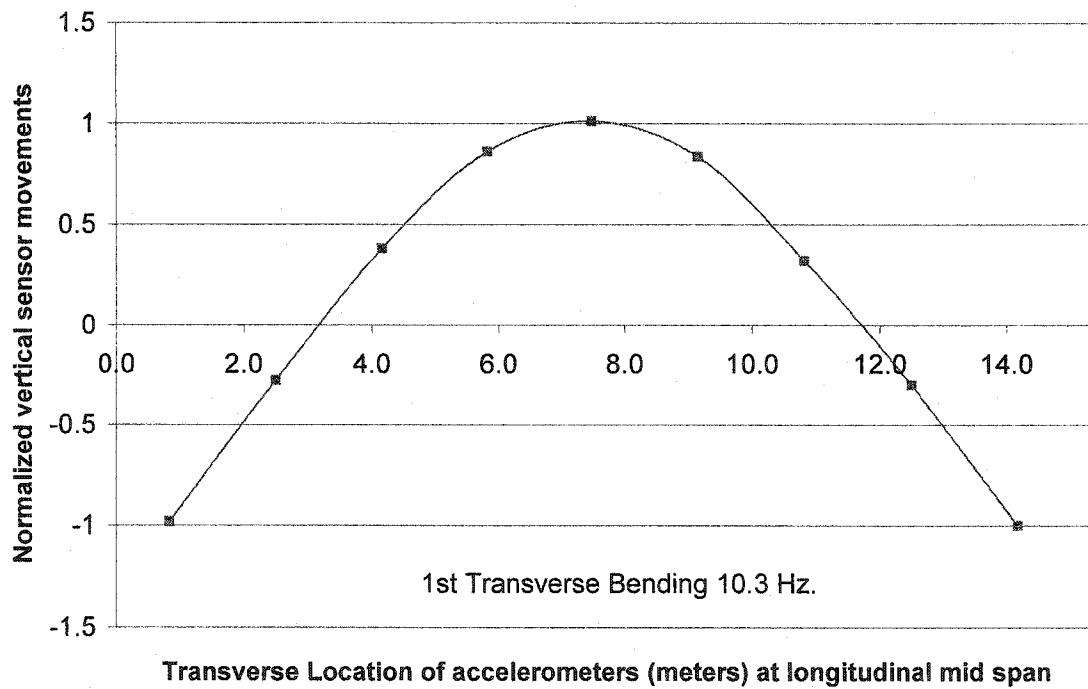
Figure 7.28: 1st Transverse Bending mode shape, from field measurements of Gwynne

221

1st Vertical

2nd Vertical

1st Torsional

2nd Torsional

1st Transverse Bending
(Side View)

2nd Transverse Bending
(Side View)
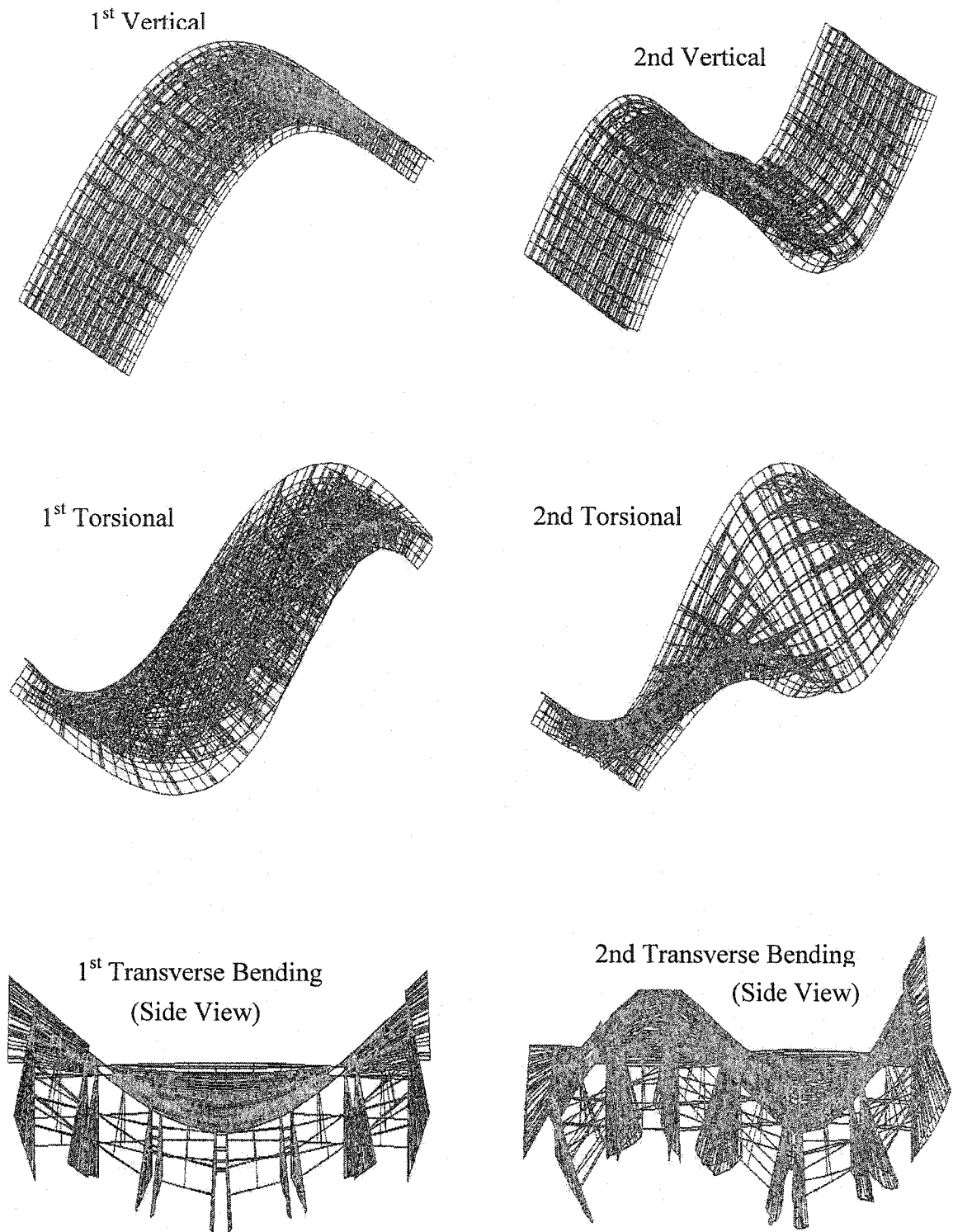
Figure 7.29: Three dimensional mode shapes generated by the finite element model
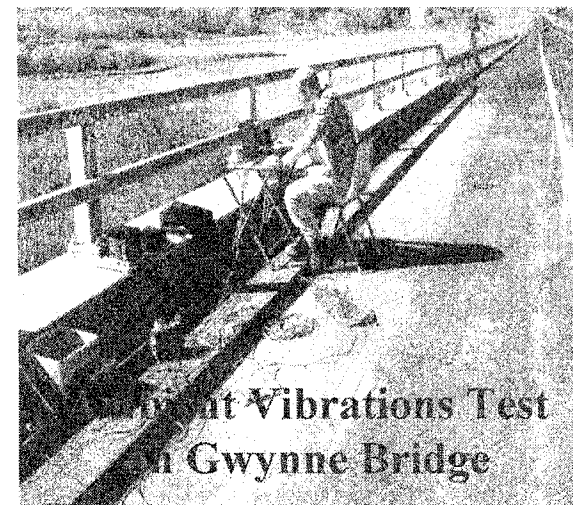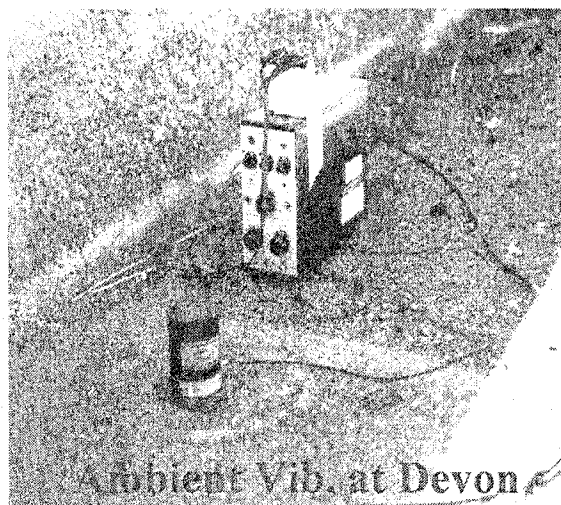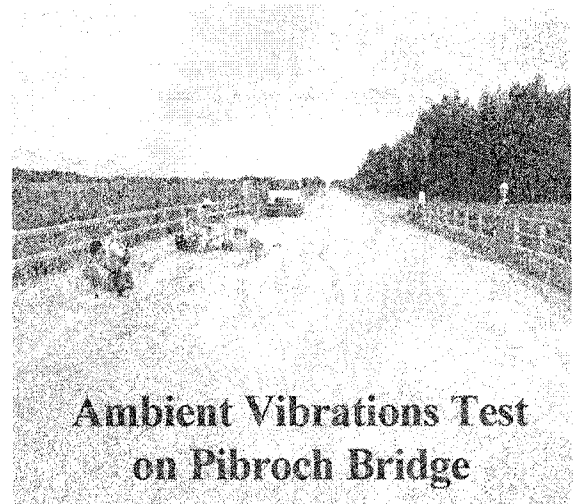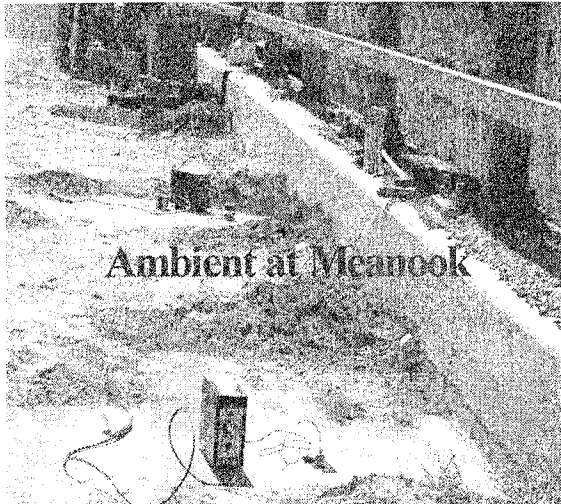
Figure 7.30: Ambient Vibration Test in progress on four bridges

223
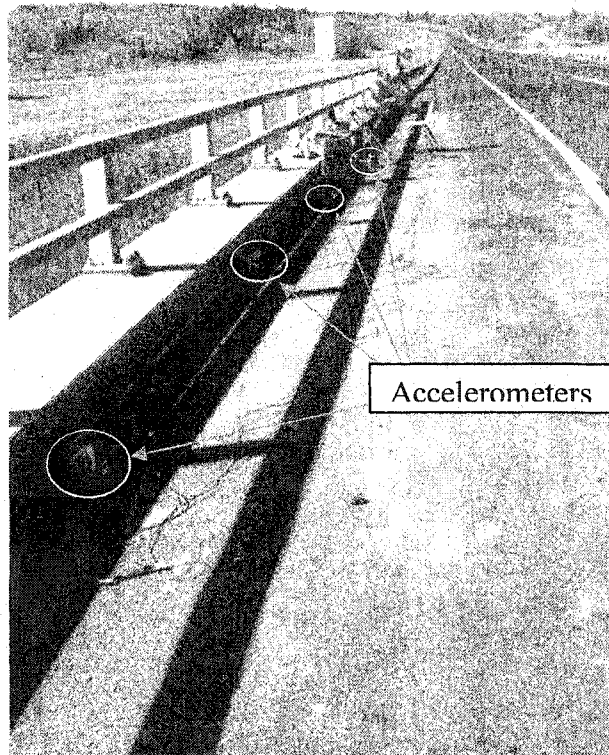
Figure 7.31: Longitudinal placement of accelerometers during ambient vibration test
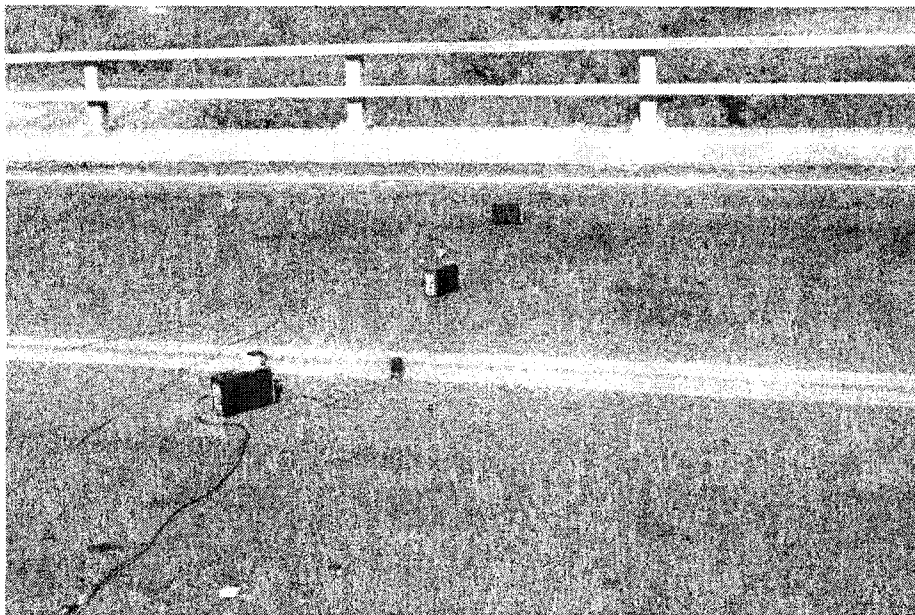
Figure 7.32: Transverse placement of accelerometers during ambient vibration test

224
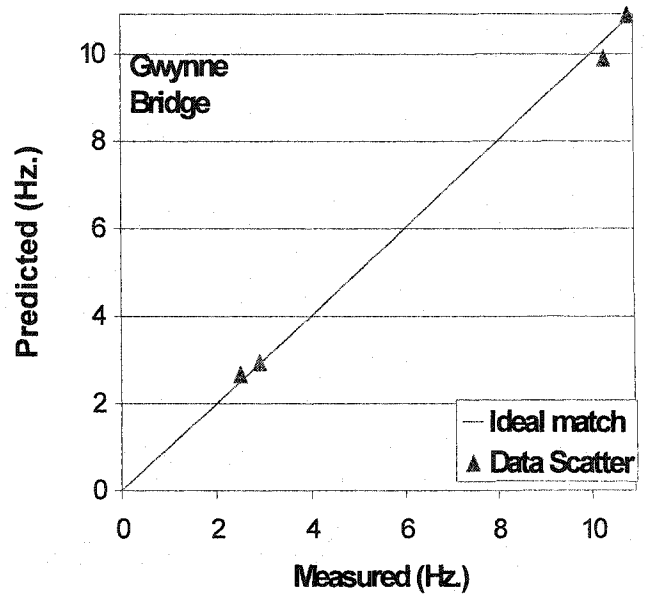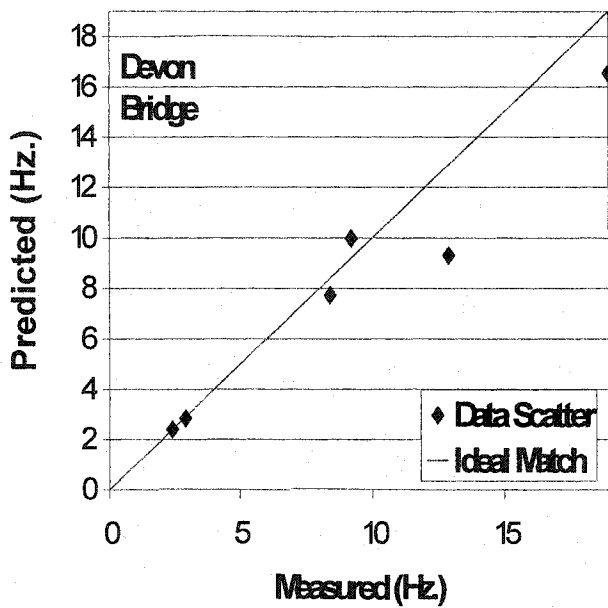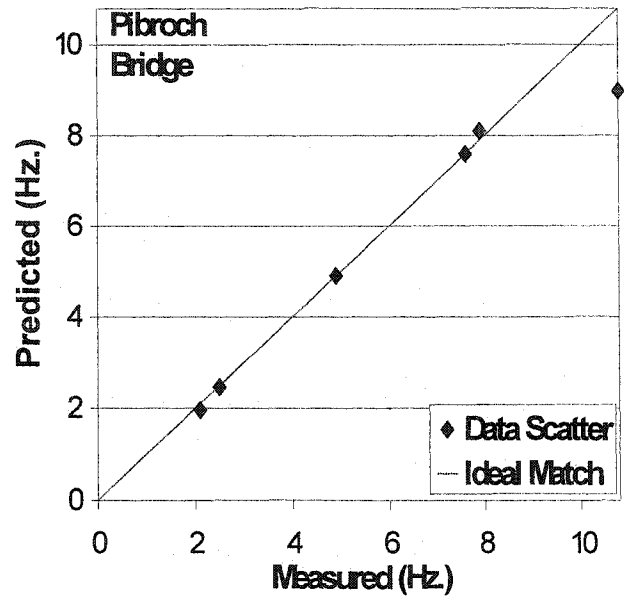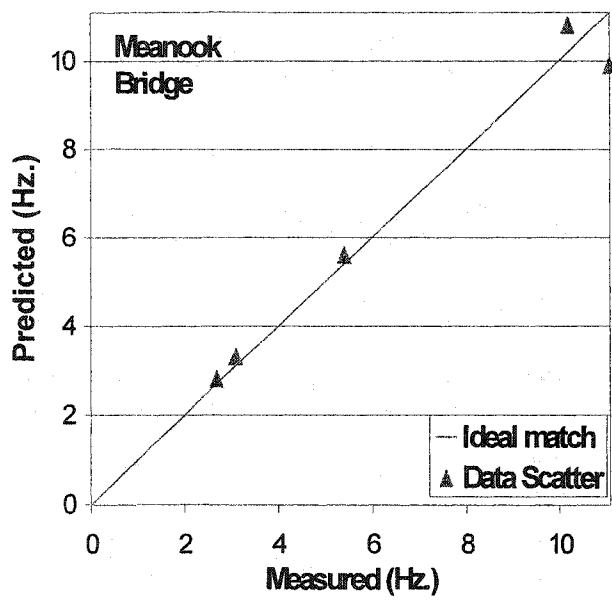
Figure 7.33: Measured natural frequencies in test vs. predicted natural frequencies from Finite Element Model

7.11 References

1. Doebling Scott W., Farrar Charles R., Prime Michael B., Shevitz Daniel W., 1996, "Damage Identification and Health Monitoring of Structural and Mechanical Systems from Changes in Their Vibration Characteristics: A Literature Review" Los Alamos National Laboratory Report No. LA-13070-MS

2. O.S. Salawu & C. Williams, 1995 "Review of Full scale dynamic testing of bridge structures", Engineering Structures, Vol. 17, #2

3. Ewins, D. J. 2000, "Modal Testing: Theory, Practice and Application", Second Edition, Research Studies Press Ltd., Baldock, Hertfordshire, England

4. Afhami S., Cheng JJR, Khattak N., Alexander J., 2000, "Field Assessment of the Bridge Rehabilitation in Fort Saskatchewan, Alberta", Report prepared by the University of Alberta Structures Group for the City of Fort Saskatchewan.

5. Farrar Charles R., Duffey Thomas A., Cornwell Phillip J., Doebling Scott W., 1999, "Excitation methods for bridge structures", Proceedings of the 17th Modal Analysis Conference, Kissimmee, Florida, pp. 1063 – 1068

6. Felber, A.J., 1993 "Development of the Hybrid Bridge Evaluation System", PhD. Thesis, University of British Columbia

7. Brownjohn, J.M.W., Dumanaoglu A.A., & Blakeborough A. 1989. "Ambient Vibration Survey of the Bosporus Suspension Bridge", Earthquake Engineering and Structural Dynamics 18, (pp. 263-283)

8. Brownjohn, J.M.W. 1988, "Assessment of Structural Integrity by Dynamic Measurements" PhD. Thesis, University of Bristol, United Kingdom

226

9. Okauchi, L, Miyata, T, Tatsumi, M., & Kiyota, R. 1992, "Dynamic Field Tests and Studies on Vibration Characteristics of Long Span Suspension Bridges", JSCE Journal of Structural Engineering and Earthquake Engineering, Vol.9. (pp.89-100)

10. Bruel & Kjaer Electronic instruments, 1980, Master Catalogue, pp.161-167, Bruel & Kjaer Denmark

11. Black C., Tsai, P.C., and Ventura C., October 1997, "Ambient Vibration Measurements of the University Drive /Crowchild Trail Bridge in Calgary, Alberta" Report No. 97-005, prepared for ISIS Canada, by U.B.C. Earthquake Engineering Research.

12. Taing, K.K., Cheng, JJR, Afhami S., January 2000, "Field Assessment of Crowchild Trail Bridge in Calgary, Alberta" Structural Engineering Report No. 231, University of Alberta.

227

8.0 A MODELLING APPROACH TO THE ASSESSMENT OF REHABILITATED FC GIRDER BRIDGES

8.1 Introduction

A review of the Alberta Transportation FC girder bridge maintenance and evaluation reports (BIM and BMRs) and databases[1] indicate that almost 50 % of these bridges have undergone rehabilitation. The main reason for this rehabilitation has been the progressive deterioration of the field grouted longitudinal shear keys between the girders, which eliminates the load sharing between the girders and hence subjects the girders to possible overloads.

A number of rehabilitation schemes and their combinations have been designed and applied on these bridges by different consultants[2,3,4] for Alberta Transportation. However, there doesn't seem to be a consensus on a particular favourable strategy for this kind of a bridge system and most consultants have conducted their own finite element studies, which have not been calibrated with the actual structural response in the field.

To get a better understanding of the FC girder bridge behaviour and to obtain information on the performance of different rehabilitation schemes used in the past, a detailed finite element study was undertaken, and is being presented in this chapter. The finite element model was calibrated with the help of a number of field tests, using load and vibration testing and the success of a particular rehabilitation scheme was measured on the basis of its response to certain assessment parameters. In other words, this group of assessment parameters was used to compare the performance of the rehabilitation schemes and comment on its ability to effectively rehabilitate the shear key deterioration in FC girder bridges.

8.2 The Finite Element Model

A three dimensional finite element model for a single span, 32 metres, six adjacent girders bridge was prepared using the professional version of the finite element analysis software S-Frame (Version 5.1). The span and geometry considerations of the finite

228

element model were kept consistent with most of the bridges that have been tested in the field. This was done to first calibrate the model with the various test results, before undertaking a study of the performance of the different rehabilitation schemes. Intricate details of the basic finite element model have already been described in Chapter 6 of this thesis. However, a brief description of the finite element model is presented as follows:

- The cross sectional views of the actual single girder and the finite element model are shown in Figures 8.1 and 8.2. Each FC girder is 1.62 m wide and 1.27 m deep. Seven precast transverse concrete diaphragms exist within the interior FC girders at longitudinal distances of 0-5-11-16-21-27-32 meters. These diaphragms are not continuous in a transverse cross section of the bridge and only provide torsional rigidity to the individual girder.

- The four-node quadrilateral shell element serves as the main building block for the model. The shell element was used to model the inverted U shape of the girder, which is particularly advantageous when observing the mode shapes of vibration of the bridge. 3800 shell elements were used to model the girders, precast transverse concrete diaphragms and field grouted shear keys.

- Connector bolts (12.5 mm diameter) tie the legs of the girders at a longitudinal interval of 3 meters, as shown in Figures 8.3 and 8.4, and are placed at a depth of 0.53 meters from the top surface of the top flange. Beam elements were used to model the connector bolts.

- Shell elements and beam elements were used in different modelling scenarios to model the field grouted shear keys. These modelling scenarios will be explained in detail in the next few articles.

- To best predict the behaviour of the actual bridge, the finite element model was compared to the actual bridge in three different ways. The centroid and the moment

of inertia of the actual girder were made coincident with those of the model and the behaviour of the model coincided with that of the test.

8.3 Modelling of the Shear Key

The shear key has been modelled in two different ways in this study. In the first case, the shear key was modelled as a series of longitudinally running continuous line of elements as can be seen in Figures 8.5 and 8.6. In the second case the longitudinal shear key was modelled by a series of short transverse beam elements and this modelling scenario is visible in Figures 8.5 and 8.7.

8.3.1 Using shell elements as shear keys

The advantage of using shell elements as shear keys was that they provided a continuous set of elements joining the two adjacent girders together, just as in the case of the real bridge. The response of the structure, by using this modelling scenario, with respect to the total deflection profile of the bridge, was compared with a set of field load tests. Since the shear keys in the actual bridge are cracked, therefore jumps were visible at the shear key locations, in the deflection profile of a transverse cross section of the bridge. This is visible in Figure 8.8 of this chapter. With respect to this same figure, it may be mentioned here that cable transducers were attached to measure the deflections at the bottom of each leg of the girders for the four girders on the right hand side, whereas the transducers were used in the middle of adjacent legs, for the next two girders. No deflections have been plotted for the extreme girder on the left hand side because the cable transducer stopped functioning in the middle of the test. To calibrate the model to the field test results, thickness of the shear keys was reduced. This lowers the stiffness of the shell elements and gives the desired jumps at the shear key locations, giving a good match with the test. This effect of varying the shear key thickness on the transverse deflection profile of the bridge is shown in Figure 8.8. The wheel spacing and axle loads of the truck load used in the load tests is given in Figure 8.9.

8.3.2 Using beam elements as shear keys

Since adjacent girders transfer load by transverse shear, beam elements were incorporated as the shear key elements in the model, in place of the shell elements. The shear key action can then be shown by looking at the fixed end actions caused by end displacements, as shown in Figure 8.10. Since the shear keys are assumed to be cracked, therefore the girders would rotate about the centre of the shear key and hence release any moment there. Figure 8.10 shows that the moment at the centre would be zero anyways but a hinge was still provided in the centre to release any moments which may arise due to some unbalance in the fixed end moments in the actual structure.

Figures 8.11 and 8.12 show modelling of the shear key as a beam element with a hinge in the middle. Since the middle hinge in the shear key would still allow load sharing, therefore two hinges were incorporated in the shear key to obtain a no load sharing case. These two hinges were first provided at the ends of the shear key and then close to the middle of the shear key. However both of these placements yielded the same results. Figure 8.13 shows load sharing based on deflections, compared for the test, shear key with one hinge and shear key with two hinges cases. The plot clearly shows that the test case is located somewhere in between the "load sharing" and the "no load sharing" cases. Hence we can conclude that there was partial load sharing observed in the field tests on the bridge being tested.

The same effect is observed by looking at a completely different test measurement parameter, i.e. the changes to the transverse bending mode shape parameter. The natural frequency for this mode shape was measured to be 5.4 Hz. in the test. With the one hinge shear key model, this frequency come out as 6.2 Hz. while with the two hinges shear key model, the frequency drops down to 4.1 Hz. Again, we observe that the test case provides a condition of partial load sharing since the mode shape frequency falls in between the two load sharing and non load sharing cases. Figure 8.14 shows the isometric and side views of the transverse bending mode shape, generated by the finite element model.

231

Having established the observation that the test results provided a case of partial load sharing, the moment of inertia of the one hinge shear key beam element was lowered to reduce the stiffness of the beam element, until a reasonable match with the test was obtained. Partial load sharing results in the test case because of cracking of the shear keys which reduce the stiffness of the shear keys hence giving rise to differential deflections and hence a deeper total transverse deflection profile. A comparison of the beam shear key element and the shell shear key element cases shows that the response is almost identical for the two cases and both represent the actual structure with reasonable accuracy. Figure 8.15 shows this comparison based on load sharing with respect to the deflection measurements. The same effect was obtained by considering the natural frequencies of the transverse bending mode shape. The frequencies were as follows:

Test Structure   =   5.43 Hz.

Shell element shear key (thickness 15 mm) =   5.5 Hz.

Beam element shear key (depth 15 mm)   =   5.40 Hz.

The finite element model with the beam element used as shear key has subsequently been used as the model for the detailed study of the rehabilitation schemes.

8.4 Parameters Used for Rehabilitation Scheme Comparison

Five different rehabilitation schemes were compared with the help of the finite element model, on the basis of results of two parameters:

- Differential deflections at shear key locations;
- Natural frequencies of the transverse bending mode shapes.

Both these parameters are easily testable in the field and characterize the performance of the shear keys. An intact shear key must not permit differential movement at the shear keys joints and should distribute the load laterally to the adjacent girders. Thus an estimate of the differential deflections at shear key joints can give an indication of the health of the shear keys. Similarly, a change in the shear key stiffness would alter the frequency of the transverse bending mode shape without affecting frequencies of most other mode shapes. Hence the shift in the natural frequency of the transverse bending mode shape can be taken as a viable indicator of the health of the shear key or the

effectiveness of the rehabilitation process in restoring or even improving the transverse load sharing among the girders.

8.5 Truck Load Information

The static truckload of the Canadian Highway Bridge Design Code, CAN/CSA-S6-2000[5] was used to conduct the finite element study. CSA/S-6[5] clauses 3.8.3 and 14.4 recommend the use of both the five-axle CL-625 single truckload and the CL-W lane load, for design or evaluation purposes. The number 625 signifies the total axle weight of the truck in kN. A dynamic load allowance of 0.4 was used with the CL-625 truckload, in accordance with the chart in figure C3.8.4.5 (page 66) of the CSA/S-6 Commentary which relates the first flexural frequency of the bridge to a dynamic load allowance value. The dynamic load allowance is meant to increase the truckload by the proportion of the load specified. In other words the static truckload used for the finite element study was actually, $625 + (625 \times 0.4) = 875$ kN. Since the lane load is a uniformly distributed load representing a continuous train of vehicles on the bridge, therefore the code does not require the lane load to be amplified by the dynamic load allowance.

It was observed that the CL-625 truckload gave higher deflections as compared to the CL-W lane load in all cases. Hence the single truck load was then considered the governing load for this study and only the analysis runs with the CL-625 truckload will be reported in this chapter. Figure 8.16 shows axle weight and spacing details of the CSA/S-6-2000, CL-625 truckload and CL-W lane load.

8.6 Rehabilitation Schemes Applied

Five rehabilitation schemes were selected for comparison by applying them on the finite element model. They are outlined as follows:

i)   Using bolts to tie adjacent girders;

ii) Laying a non reinforced, fully composite concrete deck over the girders;

iii) Transverse prestressing of the bridge cross section;

iv) Transverse stiffening of the bridge cross section;

v)   A combination scheme.

233

8.6.1 Improving lateral girder connections by bolts

The original design of the FC girder bridge uses 12.7 mm diameter bolts provided at 3 metres on centres longitudinally and positioned at half a metre below the top flange of the girder. These bolts provide lateral connections between the girders and are shown in Figures 8.3 and 8.4. The different arrangements of bolts that were applied on the model are described below. Their short forms given in brackets have been used as legend in the plots. However, only three of these variations have been plotted in the graphs for clarity.

- Using no bolts. (No bolts)
- Using standard bolts, i.e. @ 3 m. on centres and 469 mm. below the girder flange. (Standard 3m o.c.)
- Using bolts @ 1.5 m. on centres and 469 mm. below the girder flange. (1.5m o.c.)
- Using two layers of bolts @ 3 m. on centres, the first layer at 469 mm. below the flange and the second layer at 799 mm. below the flange. (Double layer)
- Same as above except moving the second layer down to the bottom of the girder web. (Double layer down)
- Same as above except staggering the two layers with respect to each other. (Double down & staggered)
- Using two layers of bolts @ 1.5 m. on centres, the first layer at 469 mm. below the flange and the second layer at 799 mm. below the flange. (On 1.5 o.c. & double layer)

Beam elements were used to model the bolts in the finite element study. Figure 8.17 shows a longitudinal section at one shear key. The plot illustrates the effect of variation of this scheme on differential deflections along a longitudinal section at this particular shear key. To observe the differential deflections at other shear keys, a cross section at a longitudinal distance of 20m is shown in Figure 8.18, which displays differential deflections at each shear key, with the use of various rehabilitation scheme combinations and placed in the form of a column graph on top of each shear key. The longitudinal location selected for the cross sectional plot was based on the maximum differential deflection value in the longitudinal section plot. The truck is shown positioned on the plot to show its actual location during the finite element analysis run.

234

The plots show significant differential deflections if bolts were not used in the original design. Moreover, increasing the number and layers of connecting bolts would reduce the differential deflections. Perhaps the worst disadvantage with using a large number of connecting bolts, to bring differential movement between the girders down, would be the need to drill several holes through the girder webs, which is not only a cumbersome but a non desirable process to go through. There is a high probability of cutting through the girder steel and hence this kind of an exercise would not be recommendable.

Table 8.1 gives the natural frequencies of the 1st, 2nd and 3rd transverse bending mode shapes for the three cases of "no bolts", "standard bolts" and "On 1.5 m. o.c. & double layer bolts". The trend of frequency shifts in this table confirms the behaviour of the model with respect to the differential deflection parameter.

Table 8.1: Natural frequencies of the transverse bending mode shapes for use of bolts

Mode Shape	No bolts	Standard 3m. o.c.	On 1.5m. o.c. & double layer
1st Transverse Bending (Hz.)	4.62	5.44	8.61
2nd Transverse Bending (Hz.)	5.88	10.00	18.74
3rd Transverse Bending (Hz.)	6.96	16.82	31.98

8.6.2 Laying a non reinforced, fully composite concrete deck over the girders

Many FC girder bridges have been rehabilitated by providing a non-reinforced 100 mm concrete deck, cast on site, over the girders. The idea is that the concrete deck will act as a rigid layer and improve transverse distribution of the live loads. All the concrete overlays on FC girder bridges in Alberta have been cast non-composite and rely only on horizontal shear friction to provide the bond between the girders and the deck. However, the concrete deck in the model was incorporated as fully composite with the girders and it

235

was thought that if the fully composite deck allowed differential movement at the shear keys, then a non-composite overlay would be worse.

The performance of the concrete deck with respect to the two selected parameters, i.e. differential deflections and natural frequencies were investigated for comparison with the other rehabilitation schemes. Figure 8.19 shows the differential deflections at a longitudinal section whereas Figure 8.20 shows differential deflections at a transverse cross section at a longitudinal distance of 20 metres. Table 8.2 shows the natural frequencies of the 1st, 2nd and 3rd transverse bending mode shapes with the concrete overlay applied on top of the girders.

Table 8.2: Natural frequencies of the transverse bending mode shapes for concrete overlay

Mode Shape	With Concrete Deck
1st Transverse Bending (Hz.)	7.62
2nd Transverse Bending (Hz.)	15.98
3rd Transverse Bending (Hz.)	27.1

8.6.3 Transverse prestressing of the bridge cross section

Transverse prestressing may be applied to the bridge with the help of either Dywidag bars or prestressing tendons. These forces were incorporated in the finite element model as concentrated loads. The analysis consisted of three distinct steps. First of all, the vertical location of the prestressing forces was varied on the girder web to observe the change in the differential deflection parameter. Secondly, the magnitude of the prestressing forces was varied to observe the resulting effect and thirdly, the spacing of the prestressing was decreased to determine any further improvement in the differential deflections at the shear key lines. However these steps were combined in the sense that the vertical positioning of the prestressing was investigated with each variable. The prestressing force magnitude used per point of application was 2x100 kN and 2x350 kN, i.e. a set of two forces each of 100 kN applied on either side of the concrete diaphragm, represented the low prestressing magnitude case and a set of two forces each of 350 kN and applied on

236

each side of the transverse precast concrete diaphragm, represented the high prestressing magnitude case. Similarly the vertical positioning investigated during the analysis was:

- At deck level
- 165 mm below deck
- 216 mm below deck
- 317 mm below deck
- 368 mm below deck
- 419 mm below deck
- 470 mm below deck
- 724 mm below deck
- Total force equally distributed and applied at 317 mm and 724 mm below deck
- Total force equally distributed and applied at 140 mm and 724 mm below deck

Moving too low would sometimes result in negative bending of the cross section, which would induce tension in the shear keys. Hence, for clarity, only those of the above runs will be shown in the plots, which produced positive bending of the transverse cross section of the bridge (concave up). Initially, spacing of the force application in the longitudinal span was kept constant at the interior girder precast diaphragm locations, i.e. at 6 metres on centres.

8.6.3.1 The additional shear key

The longitudinal hollow spaces between adjacent FC girders are filled with concrete grout at the locations where transverse prestressing is to be applied. This grout serves as an additional shear key and mobilizes the transverse prestressing compressive force between the girders. The concrete grout between the girders was modelled by a series of closely spaced beam elements. This scenario is illustrated in Figure 8.21.

For each prestressing force run, in addition to the differential deflections, the axial force in the grout connectors between girder legs was also observed because this field cast grout in the girders is not intended to take tension. If the concrete grout goes in tension, it will either debond from one side of the girder or crack, and lose its stiffness and qualities

237

as an effective additional shear key. Hence, the number of these connectors that were in tension in each run were then observed and recorded.

Figure 8.22 shows the variation in differential settlements at one longitudinal shear key with a change in the vertical positioning of the prestressing force of 2x100 kN. It was observed from both the Figures 8.22 and 8.23 that relative deflections were best reduced by placing the force of 200 kN at 724 mm below the deck level. However Table 8.3 indicates that even placing the prestressing force at 724 mm below deck would still put 13 grout connectors from the bottom in tension. Similarly, this table illustrates that almost all the vertical variations of the prestressing force showed almost half of the grout connectors to be in tension. Since the concrete grout will lose its stiffness if it cracks because of tension, therefore its additional load distributing qualities can then not be relied upon.

Hence it was concluded that this prestressing force magnitude was not sufficient to utilize the concrete grout between the girders as the additional shear key. Analysis runs with the grout connectors in tension removed, showed that the differential deflections increased significantly without the aid of these grout connectors. To investigate the performance of this rehabilitation scheme with an increase in the magnitude of the prestressing force, similar analysis runs were conducted, now with a prestressing force of 2x350 kN and applied at identical vertical locations as before.

Figures 8.24 and 8.25 show the differential displacements on a longitudinal and a transverse cross section respectively when the prestressing force was increased to 2x350 kN. This force is generally applied in the field with the help of two Dywidag bars or a set of prestressing tendons, each carrying a force of 350 kN and applied on each side of the transverse concrete diaphragms. Table 8.4 shows the number of grout connectors in tension or compression during this second part of the prestressing force analysis.

Table 8.3: Effect of varying the application of the prestressing force of 2x100 kN on the number of grout connectors in tension or compression.

Prestressing force location	Number of grout connectors in compression	Number of grout connectors in tension
At deck level	8	17
317 mm below deck	9	16
470 mm below deck	10	15
724 mm below deck	12	13
At 140 mm and 724 mm below deck level (100 kN each)	10	15
At 140 mm and 724 mm below deck level (100 kN each)	10	15

Table 8.4: Effect of varying the vertical location of the prestressing force of 2x350 kN on the number of grout connectors in tension or compression.

Prestressing force location	Number of grout connectors in compression	Number of grout connectors in tension
At deck level	12	13
165 mm below deck	15	10
216 mm below deck	16	9
267 mm below deck	18	7

Finally, as the third and last step, the effect of reducing the longitudinal spacing of the prestressing force of 700 kN, was investigated by considering the prestressing forces applied at 3 metres on centres. Figures 8.24, 8.25, 8.26 and 8.27 show that the optimum vertical location changes from 267 mm to 190 mm below deck level when the longitudinal spacing of prestressing is reduced from 6 metres to 3 metres on centres. Hence as the magnitude or spacing of prestressing will increase, the optimum vertical location of prestressing on the girder web will continue to move upwards.

239

Reducing the spacing is equivalent to increasing the magnitude and hence we see that these results are highly sensitive to the placement of the prestressing forces with respect to the deck level.

The natural frequencies of the 1st, 2nd and 3rd transverse bending mode shapes are shown in Table 8.5 which take into consideration the prestressing force of 700 kN placed at 6 metres and 3 metres on centres. These values of the natural frequencies were compared with test results from actual bridges, which used the same rehabilitation scheme[6]. The model results agree very well with the test results, which verify the use of various arrangements used within the finite element model to simulate the prestressing and concrete grout between the girders.

Table 8.5: Variation of natural frequencies of the transverse bending mode shapes with change in prestressing longitudinal spacing

Mode Shapes	Prestressing applied at 6 metres on centres	Prestressing applied at 3 metres on centres
1st Transverse Bending (Hz.)	12.25	12.46
2nd Transverse Bending (Hz.)	27.66	28.17
3rd Transverse Bending (Hz.)	44.5	45.64

8.6.4 Transverse stiffening of the bridge cross section

Transverse stiffening of the bridge cross section is achieved with the help of continuous steel underslung diaphragms. These diaphragms are basically a built up section made out of steel plates and wide flange or channel sections. The total continuous assembly from one end of the cross section to the other end can be broken down into two sub assemblies with different cross sectional areas and properties. The cross sectional shape of this continuous underslung diaphragm at a section between the two webs of the same girder is shown in Figure 8.28. This part of the underslung diaphragm serves as the stiff lateral

240

brace, which prevents any lateral movement of the girders. Similarly, the cross sectional shape of the diaphragm at a section between the adjacent webs of the two adjacent girders is also shown in the same figure. This portion of the diaphragm firmly locks the two adjacent webs together and prohibits any differential movement of the two adjacent webs relative to each other. The portion locking the adjacent girder webs is filled with a non shrink cementitious grout (SIKA 212). A picture of this rehabilitation scheme can be seen in Figure 8.29 of this chapter.

The underslung diaphragm rehabilitation scheme was applied as a two-step variation, i.e.:

i)   Changing the spacing of the underslung diaphragms keeping the sectional properties constant

ii)   Selecting an optimum spacing and changing the stiffness of the underslung diaphragms at that optimum spacing.

The different spacing values that were used for the application of the underslung diaphragms on the finite element model were as follows:

- At 6 metres on centres which results in 5 diaphragms. This is the most common spacing used.
- At 3 metres on centres, resulting in 9 diaphragms.
- At 1.5 metres on centres, resulting in 19 diaphragms.

Even though, underslung diaphragms at 1.5 metres reduce the differential deflections to a lowest value, 3 metres on centres was selected as the optimum spacing, to account for economy and the fact that the drop from 6 metres spacing to 3 metres spacing was larger than the drop from 3 metres spacing to 1.5 metres.

Having selected 3-metre spacing as the optimum, the stiffness of the underslung diaphragm assembly was now varied as the second step, by varying the moment of inertias of the underslung diaphragm. Since the underslung diaphragm is a combination of a lateral brace (between the same girder webs) and a web stiffener (that locks the

241

adjacent girder webs together), therefore a study was conducted to observe the effect of changing the flexural stiffness of each of these components, on the differential deflections at one shear key at the centre. This was done by changing the moment of inertia of one component while keeping the other one constant and vice versa. It was observed that the stiffness change of the leg locking arrangement had a much larger effect on the differential deflections as compared to the stiffness change of the lateral brace between the legs. Figure 8.30 shows this rate of change of the differential deflections with the change in moment of inertia of the underslung diaphragm components plotted on the same graph for comparative purposes.

Hence it was concluded that the sectional properties of the web brace used with 1I were already close to the optimum value and would not yield big changes in the results if the moment of inertia was increased to a large number. Hence, the stiffness of the web stiffener was then varied by increasing its moment of inertia and to observe the corresponding change in the differential deflections. The variations used were:

- 1 times I (moment of inertia)
- 2 times I
- 5 times I
- 10 times I
- 20 times I

Figures 8.31 and 8.32 show the effect of changing the underslung diaphragm spacing on differential deflections between the girders at shear key lines while Figures 8.33 and 8.34 show the effect of changing the moment of inertia of the web locking arrangement while keeping the spacing of the diaphragms constant. Table 8.6 presents the natural frequencies of the 1st, 2nd and 3rd transverse bending mode shapes with changing sectional properties, when an optimum spacing of 3 metres was used as spacing.

242

Table 8.6: Variation of natural frequencies of the transverse bending mode shapes

Mode Shapes	1 x times I	2 x times I	5 x times I	10 x times I	20 x times I
1st Transverse Bending (Hz.)	18.88	20.10	20.66	20.96	21.23
2nd Transverse Bending (Hz.)	33.23	36.17	37.41	38.05	38.62
3rd Transverse Bending (Hz.)	45.58	49.29	50.73	51.50	52.23

8.6.5 Scheme Combination

It was observed in the prestressing scheme case that the results of the differential deflection parameter were highly sensitive to the prestressing force placement, measured vertically from the deck level. However, if the bottom of the girder webs can get restrained against transverse rotation, compression can be induced into the bridge cross section by transverse prestressing which will put compression into the shear keys as well as improve load sharing between the girders. Hence the idea of combining the underslung diaphragms with transverse prestressing was born.

From both the prestressing and underslung diaphragm cases, it was observed that the optimum spacing of both these schemes when applied separately was 3 metres on centres. Hence the same spacing was selected to be applied for the combination scheme along with the 2x350 kN as the prestressing force magnitude. The vertical distance from the top of the girder deck was once again investigated with this combination scheme to arrive at the optimum location in the case of the combination scheme. Since the underslung diaphragms now restrain the lateral movement of the FC girders therefore the sensitivity of the placement of the prestressing force from the deck level is greatly reduced. This can be seen in Figures 8.35 and 8.36 which show that the difference in differential displacements at shear keys with the change in placement of the prestressing forces is negligible (< 0.04mm).

243

Since the placement of prestressing forces at any distance from the deck level is not an issue now, the question arises on what would be the best location for the prestressing forces, given that the combination scheme was to be used. As the laterally continuous underslung diaphragms prevent the girder webs from transverse rotation, therefore the whole cross section of the bridge now acts as one stiff plate and the full depth of the field placed grout remains in compression. Hence it would be beneficial to place the prestressing close to the bridge deck. The post-tensioning tendons can either be used right on top of the girder flange, embedded inside the wearing surface or immediately under the girder flange, cored through the girder webs.

There are merits and demerits for both these installations. The deck wearing surface is generally cast in two longitudinal halves. When one longitudinal half has been laid, traffic is generally opened to that half, while the other one is prepared for paving. This is shown in Figure 8.37 in a highly exaggerated profile, just to get the point across. In the case of prestressing on top of the girder flanges, the post-tensioning cannot be mobilized till the full deck is ready and hardened. Hence, when traffic runs on half of the road, while the other longitudinal half has had freshly placed concrete, the transverse cross section would be in double curvature with the new concrete deck experiencing transverse tensile stresses. Since no transverse prestressing has been placed as yet, this continuous transverse tension could result in longitudinal cracks at the shear key locations in the concrete deck. However the distinct advantage of this technique is the absence of any concrete coring or cutting through the FC girders.

Placing prestressing immediately under the girder flange is advantageous and will be proposed here as the preferred placement location because it has no relation to the wearing surface. Hence all the rehabilitation work can be completed before laying the new wearing surface which can easily avoid the double curvature situation in the new concrete deck. However, one disadvantage with placing prestressing under the girder flange is the need to core holes through the girder webs for the passage of the prestressing tendons.

The increase in lateral stiffness of the bridge can also be seen in Tables 8.7 and 8.8. Table 8.7 shows the natural frequencies of the 1st, 2nd and 3rd transverse bending mode shapes at two different longitudinal spacings under the combination scheme, whereas Table 8.8 gives a comparison of the transverse bending frequencies for all the rehabilitation schemes discussed in this chapter. From this table we can easily see that the prestressing-underslung diaphragm combination improves the lateral stiffness of the cross section to the best level.

Table 8.7: Variation of natural frequencies of the transverse bending mode shapes with change in combination scheme spacing

Mode Shapes	Underslung diaphragms and Prestressing applied at 6 metres on centres	Underslung diaphragms and Prestressing applied at 3 metres on centres
1st Transverse Bending (Hz.)	18.66	22.88
2nd Transverse Bending (Hz.)	37.29	45.00
3rd Transverse Bending (Hz.)	52.19	62.3

Table 8.8: Comparison of natural frequencies of the transverse bending mode shapes for different rehabilitation schemes

Mode Shapes	Concrete Deck	Bolts	Prestressing (P/S)	Underslung Diaphragms (USD)	PS & USD Combination
1st Transverse Bending (Hz.)	7.62	8.61	12.46	18.88	22.88
2nd Transverse Bending (Hz.)	15.98	18.74	28.17	33.23	45.00
3rd Transverse Bending (Hz.)	27.1	31.98	45.64	45.58	62.3

8.7 Changes in Load Positions

To investigate the worst positioning of the truck load on the bridge deck, the load was moved to different transverse and longitudinal positions. Three transverse truck positions are shown in Figures 8.38, 8.39 and 8.40 and a comparison of the relative deflections, measured on a longitudinal axis of shear key 2, because of these three transverse load positions is shown in Figure 8.41. Even though under load positions P1 and P2, the shear key differential deflections appear to have increased with reference to the results under load position P1, this apparent increase is due to the geometric deformation of the transverse profile.

This effect is clearly visible in Figure 8.42, which illustrates a comparison of the transverse bridge profiles under load positions P1, P2 and P3. Hence, we can see that the bridge top deck rotates as a rigid layer eliminating any differential movement at the girder joints or shear keys. This can be seen in more detail in Figure 8.43, which shows a highly exaggerated deflected shape of the cross section of two girders under load position P1. A slope comparison of the shear key only and the two adjacent girders demonstrates that there was no differential rotation of the girders with respect to each other because the angles of rotation of the shear key and the girders included, both turn out to be 0.1 degrees.

Hence the whole transverse cross section is now acting as one big plate eliminating any differential deflection or rotation between the girders. The differences in rotations between the two end joints of the shear key are shown in Figures 8.44 and 8.45. From both these figures it can be seen that the differential rotations fell below 0.0002 radians (0.02 degrees) which indicate that there was no differential rotation or deflection between the girders, when the combination scheme was used.

8.8 Overall Assessment

Under vehicular load, the bridge deck can deflect as well as rotate. To getter a better idea of the improvement in transverse stiffness of the bridge cross section, differential deflections as well as rotations were measured in the finite element model which was

246

subjected to a static truck load. A comparison of the performance of the different rehabilitation schemes with respect to these parameters is shown in Figures 8.46 and 8.47. These figures show differential deflections and rotations measured on a longitudinal cross section at shear key 2 of the bridge deck, with the truck load placed at position 1, i.e. at one side of the transverse cross section. In addition, Figure 8.48 shows the transverse deflected profile of the bridge under side load placement, for the different rehabilitation schemes. This figure was used to evaluate the individual slopes of the girders and the shear keys on a transverse cross section at mid span, which are then shown in Figures 8.49 to 8.53, for the different rehabilitation schemes. For the cross section of the bridge to act like a stiff plate, the slopes of the individual units, i.e. the girders and shear keys should be the same. Hence the column graphs shown in the plots of Figures 8.49 to 8.53 should have been all equal (i.e. of equal slope) in an ideal condition. The best match to that condition has been achieved by the combination scheme which shows all columns in the plot as bearing equal magnitudes or individual units having almost the same slopes.

Figure 8.48 was also used to evaluate curvature in the shear keys due to the rotation of the girders. Again, it was assumed that the best rehabilitation scheme would transform the deck cross section into a stiff plate and hence minimize curvature in the shear keys. Figure 8.54 shows a comparison of the largest shear key curvatures obtained by using different rehabilitation schemes. From this figure it can be seen that the combination scheme gave the best results and the smallest curvature, which is hence the closest approximation to a stiff plate case and the best possible scheme to rehabilitate this family of bridges.

8.9 Conclusions

Load and vibration testing was conducted on a number of FC Girder Bridges to investigate load sharing concerns as well as the dynamic response. Test results from these bridges were used to calibrate a finite element model of a single span 32 metre, six adjacent girder, straight bridge. The need of a representative model was felt to overcome

247

the difficulties in the field assessment of innumerable variations and combinations of the rehabilitation schemes applied on these bridges.

Three independent test measurements of deflections, strains and natural frequencies were used to compare the model to the test. All the three measurements, which came from entirely different instruments, i.e. cable transducers, accelerometers and strain gauges, demonstrated excellent agreement with the results of the finite element model. Hence there was a high level of confidence that the finite element model was successfully predicting the behaviour of the real bridge.

To isolate the effect of different rehabilitation schemes used on the bridge, each rehabilitation strategy was applied separately on the model, and its optimum variation observed on the basis of two performance parameters. These two parameters were differential deflections at the shear keys and natural frequencies of the transverse bending mode shape. Finally, the best rehabilitation scheme was verified against a third performance parameter of differential rotations at shear key locations.

Five different rehabilitation strategy groups were investigated in this finite element study. Those were the use of additional bolts, a composite non-reinforced concrete overlay, transverse prestressing, steel underslung diaphragms and a combination scheme consisting of transverse prestressing and steel underslung diaphragms. While most of these schemes have been applied on actual bridges in the past, very little performance comparison data from the field exists that will place one scheme better than the other in the order of its field performance. Moreover, the presence of an optimum arrangement in each scheme by considering variations of that scheme, make field comparisons quite misleading just because the two rehabilitation strategies being compared might not be at their optimum arrangements. Hence the finite element model proved to be a useful tool in generating the optimum arrangement of each rehabilitation scheme and making optimum to optimum comparison possible, based on the two deformation and stiffness criteria of differential deflections and natural frequencies.

The field calibrated finite element model when used with a healthy (undamaged) shear key and a centrally placed truck load demonstrated a maximum differential deflection of 0.1 mm at the shear key locations and gave a transverse bending mode shape frequency of 7.1 Hz. With the use of different rehabilitation schemes, it was desired that these schemes would better these two parameters in question.

The use of additional bolts was rejected on two grounds. Firstly it would require a number of holes to be drilled through the girder webs, which is not only a cumbersome but dangerous process. Secondly, a very high number of bolts were required to arrest differential deflections to a low value and to raise the transverse bending mode shape to a reasonably high value.

The failure of the concrete deck in improving the torsional rigidity of the girders and the flexural stiffness of the transverse cross section of the bridge resulted in its differential deflection values that were greater than some other rehabilitation schemes. Moreover, the concrete overlay was incorporated as a composite layer above the girder flange to avoid uncertainty in the degree of the bond between the two surfaces. Since all concrete overlays over FC Girder Bridges have been applied as non-composite toppings therefore it can easily be concluded that such surfacing would result in differential deflections that would be greater than 0.28 mm observed in the case of the composite overlay.

The use of transverse post-tensioning was a useful alternative but depended heavily on its positioning on the webs of the girders. A high placement at deck level or close to it would result in positive bending of the transverse cross section, which will increase differential deflections, while a low placement on the girder webs would cause a negative bending of the transverse cross section that will put the shear keys in tension. Hence the ideal position to place the prestressing was to be close to the centroid, but it varied with the magnitude of the prestressing force. The finite element study showed a prestressing force of 2 x 350 kN, applied equally distributed between two adjacent points on each side of the transverse concrete diaphragms of the girder, will yield the lowest differential deflections at the shear keys. However, many FC Girder bridges, which had been,

rehabilitated with transverse prestressing have shown signs of recracking after some years of use. One possible reason for this outcome has been the fact that most of the prestressing has been rather low in magnitude and applied immediately below the girder flange, which aggravates the transverse rotation of the cross section.

Our study assumes perfect connection between the grout connectors (representing the concrete grout in the hollow spaces between the girders) and the girder webs. In the absence of the right force magnitude or location placement, this concrete grout may go into tension and crack or debond from the girders. Once this happens, differential movement at the shear key lines would increase hence giving rise to shear key recracking. Besides, prestressing force losses are another enemy to the prestressing rehabilitation system.

The use of continuous steel underslung diaphragms from the finite element model study showed that by decreasing the spacing and increasing the sectional properties of these diaphragms, differential deflections at the shear keys could be successfully arrested. This rehabilitation scheme does not depend on uncertain connections like the prestressing scheme and greatly enhances the flexural stiffness of the transverse cross section. This is clearly visible in the transverse bending mode shape frequencies, which jump up significantly with the use of the steel underslung diaphragms.

Finally, the recommended rehabilitation scheme was the combination scheme consisting of using the steel underslung diaphragms in combination with transverse prestressing. The combination scheme extracts the benefits of both the schemes, provides an element of redundancy in the system and allows the use of less conservative variations of the individual schemes, when they are to be used together. The finite element study showed that the combination scheme would control the differential deflections to almost 0.03mm when the truck load was placed centrally or at load position P3. When the load position was changed to P1 or P2, the differential deflections jumped up to approximately 0.4 mm. However it was shown from the transverse deflected geometric profile of the girders that this differential deflection of 0.4 mm was actually produced as a result of girder

250

rotation rather than girder settlement. In other words, there was absolutely no settlement of one girder with respect to another girder. Movement at shear key locations was then investigated with the help of another parameter of differential rotations which showed that the two end joints of the shear keys rotated exactly the same amount hence eliminating any type of differential movement at the shear keys.

Hence we can conclude that the combination of prestressing applied under the flange of the girders and continuous steel underslung diaphragms provide the best solution to the shear key cracking and load sharing problems. This conclusion is consistent to some of the early proposals by researchers[2] whose models were not calibrated with the test results and provide further evidence that the transverse prestressing – underslung diaphragm combination is the most appropriate rehabilitation scheme for this type of bridges.

251
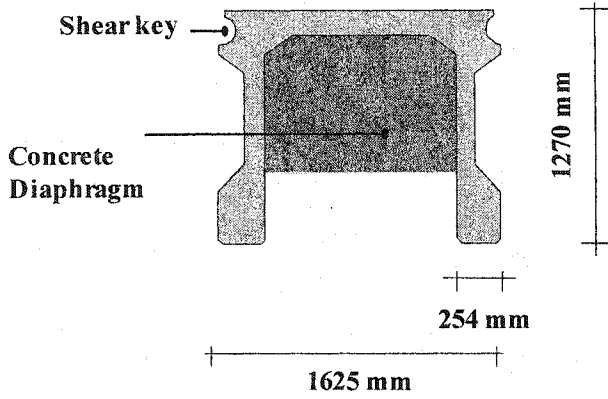
Figure 8.1: Cross section of a typical FC girder
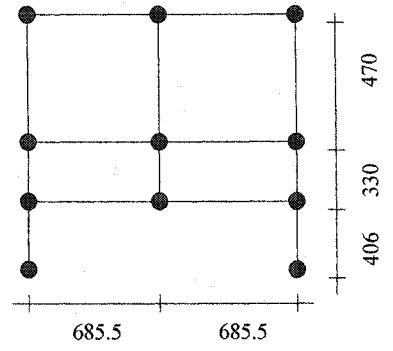
Figure 8.2: Finite element model of a single girder, cross sectional view
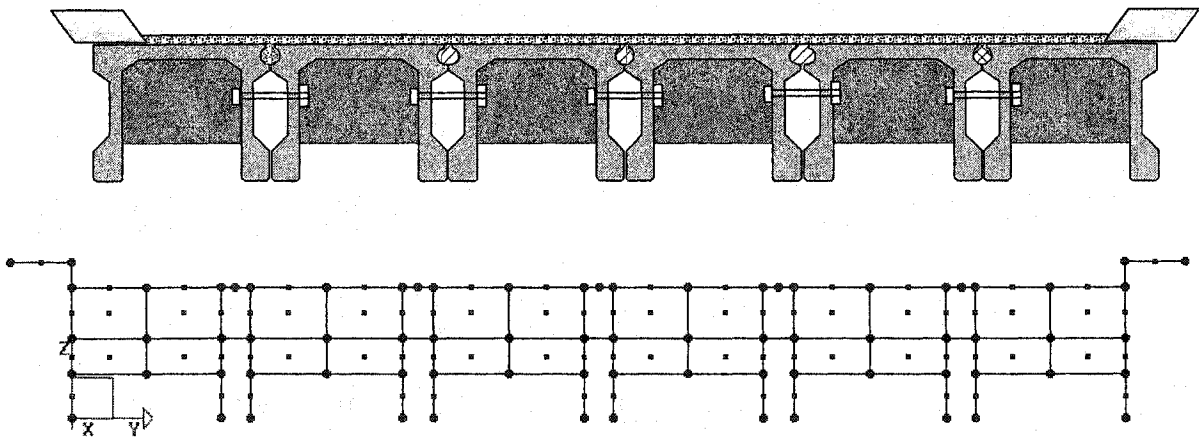
Figure 8.4: Finite element model of the whole bridge, cross sectional view
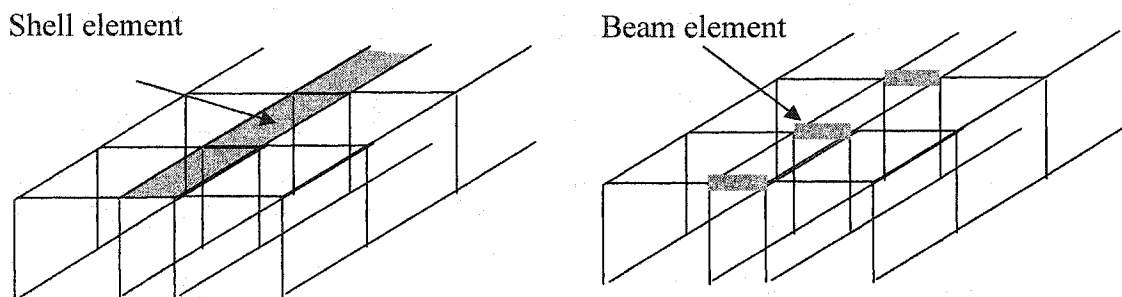
Figure 8.5: Modelling of the shear key, shell element vs. beam element
(Note: The figures are not to scale)

252
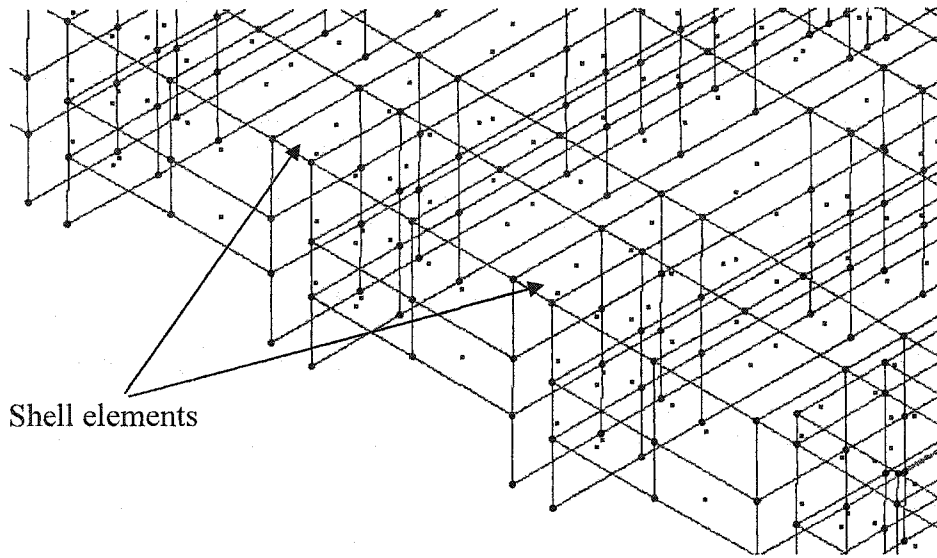
Figure 8.6: View of the finite element model, using shell element as shear key
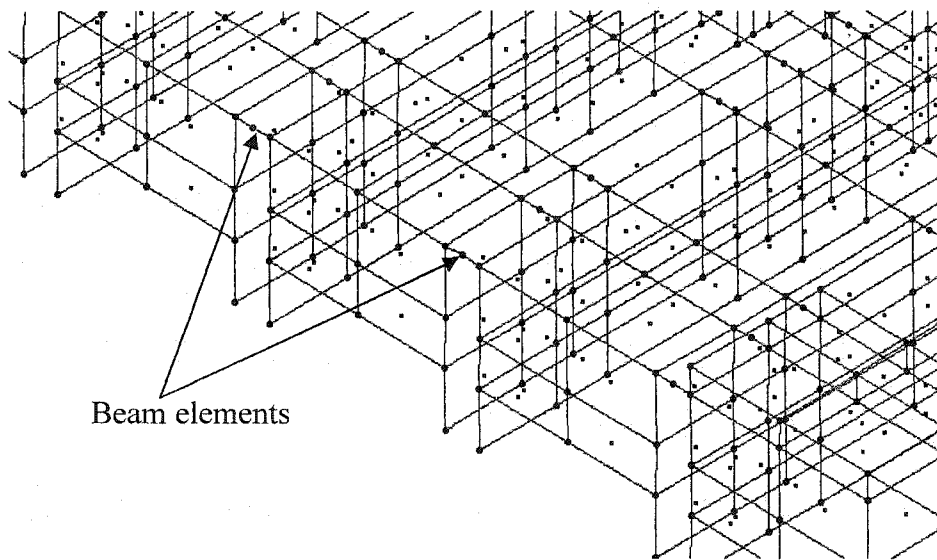
Figure 8.7: View of the finite element model, using beam element as shear key

253
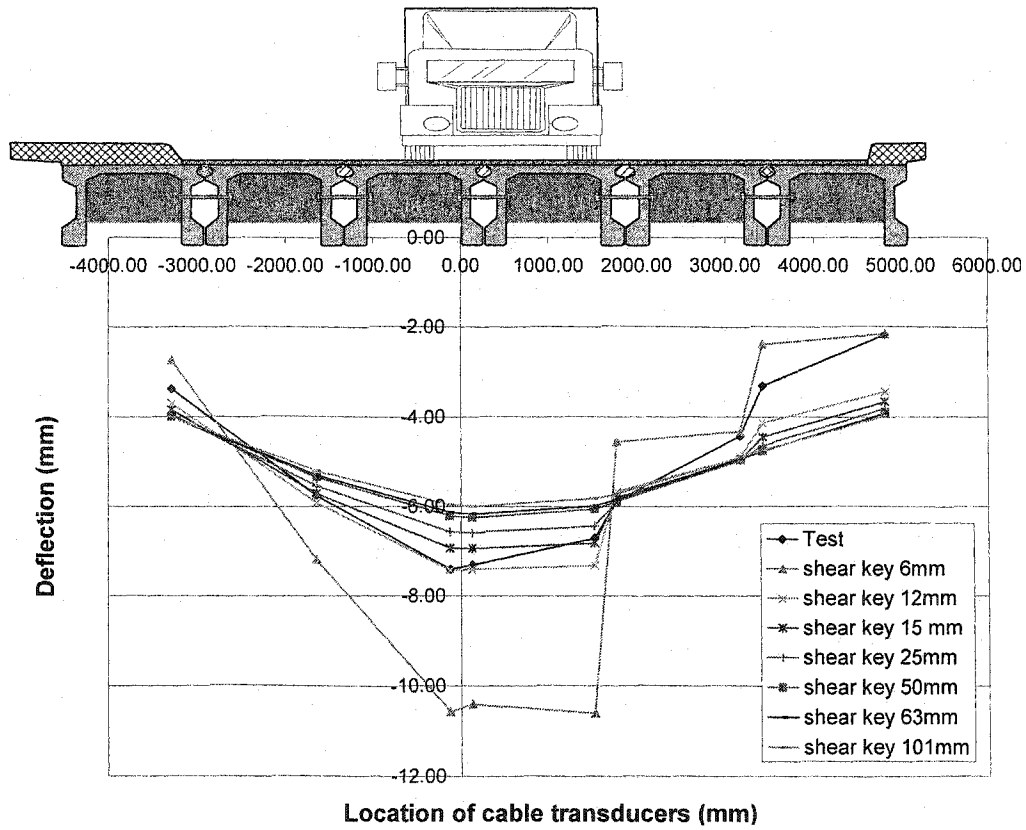
Figure 8.8: Variation of mid span deflections with shear key thickness
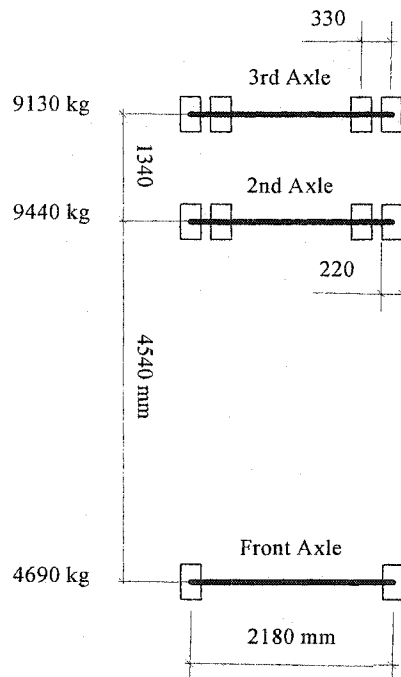
Figure 8.9: Truck Information for bridge load tests

254

$$M_A = M_B = 6EI \, \Delta/L^2 \qquad\qquad R = 12EI \, \Delta/L^3$$
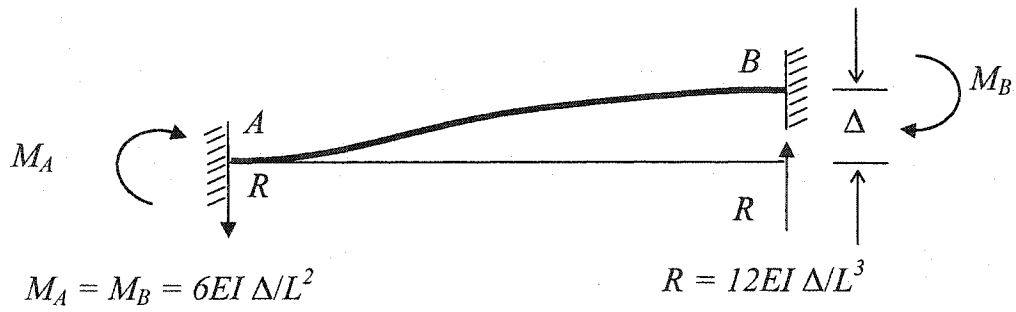
Figure 8.10: Fixed end actions caused by end displacements

130 mm   130 mm
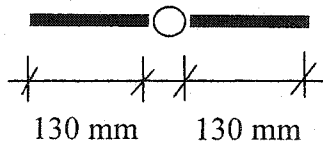
Figure 8.11: Shear key with a
hinge in the middle
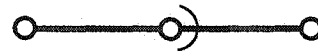
Figure 8.12: Beam element in the finite
element model as shear key
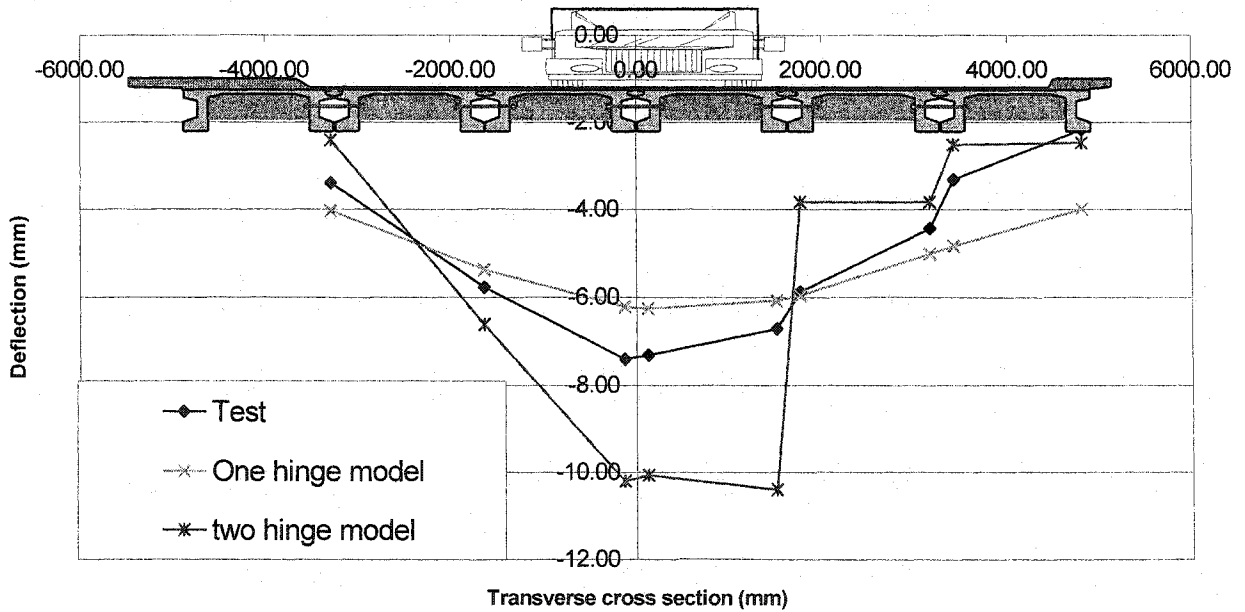
Figure 8.13: Test to model comparison with respect to the transverse deflection
profile, using beam element as shear key
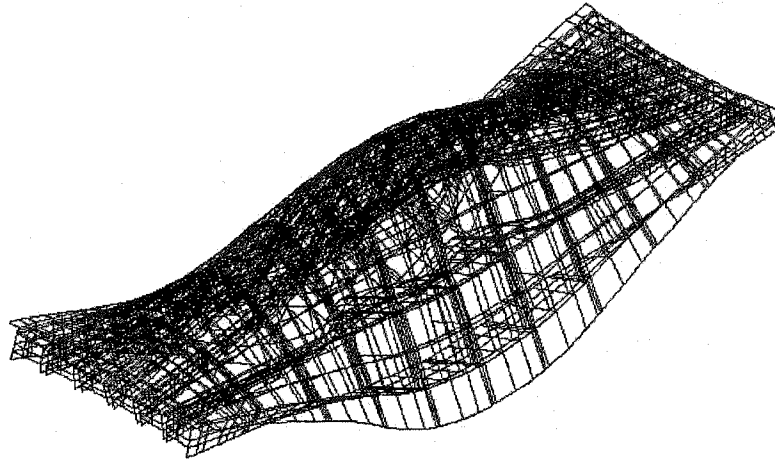
Transverse bending mode shape
Isometric View
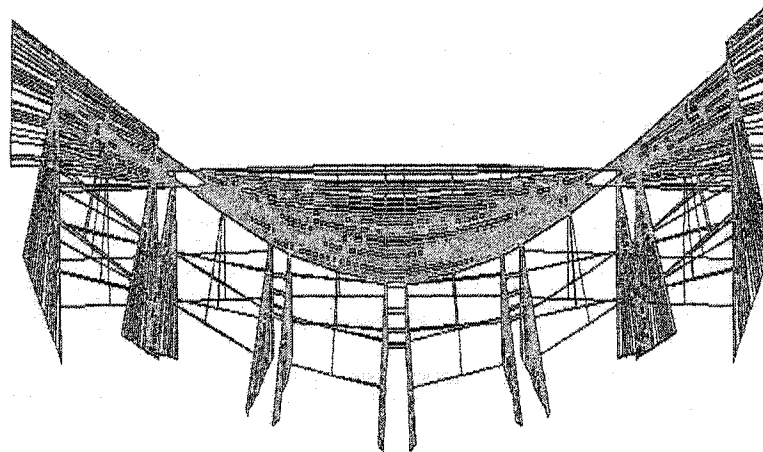
Transverse bending mode shape
Side View

Figure 8.14: Isometric and side views of the transverse bending mode shape

256
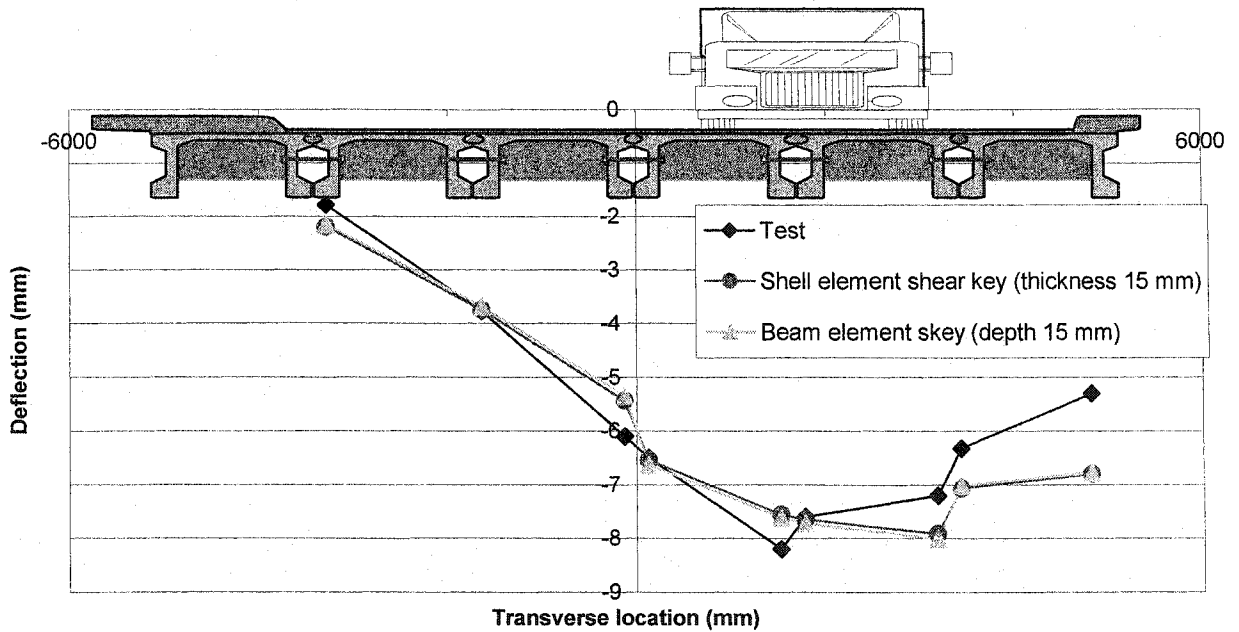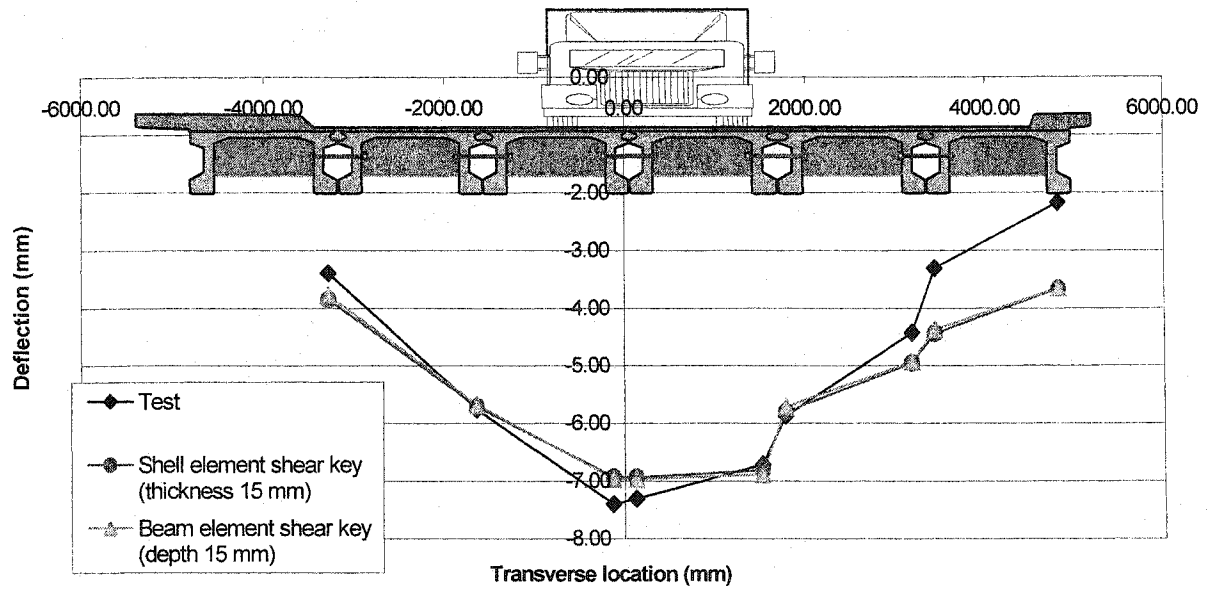
Figure 8.15: Test to model comparison using both shell and beam shear key element cases

257
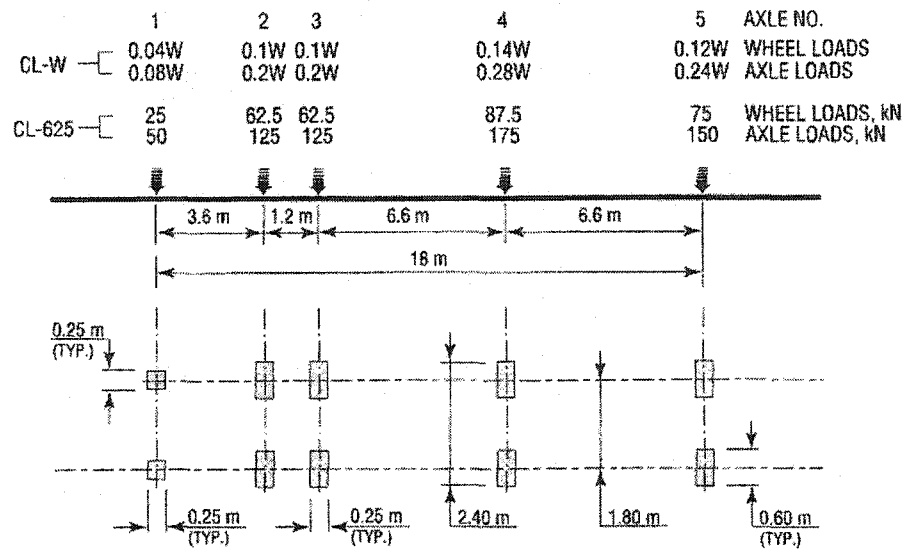
CL-625 Truck from CSA/S-6 (2000)

CL-W Lane Load from CSA/S-6 (2000)
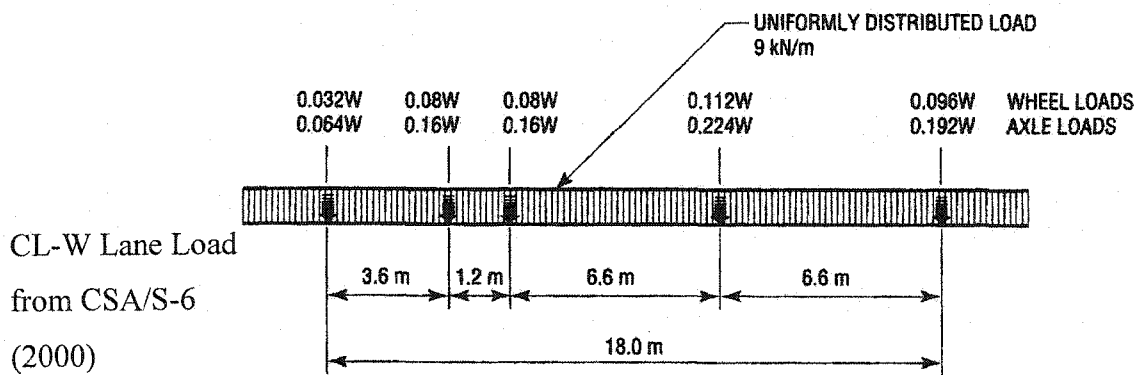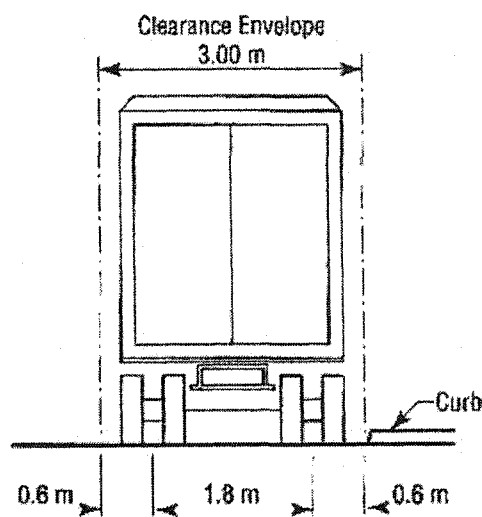
Figure 8.16: Load information for truck and lane loads used on the model

258
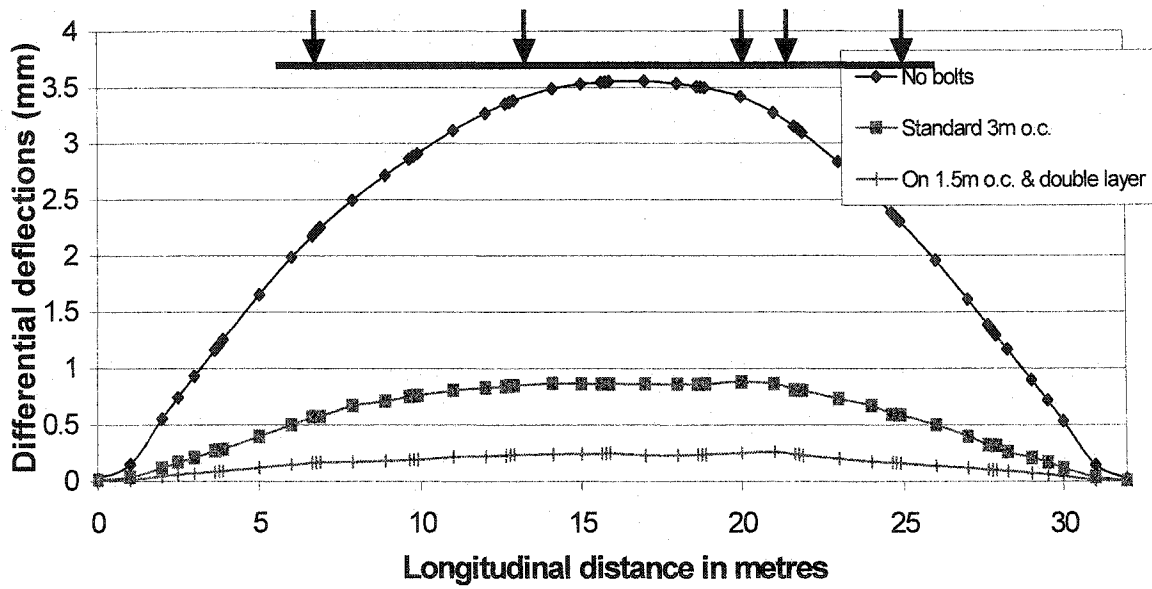
Figure 8.17: Differential deflections at one shear key at a longitudinal section
Rehabilitation Scheme = Bolts
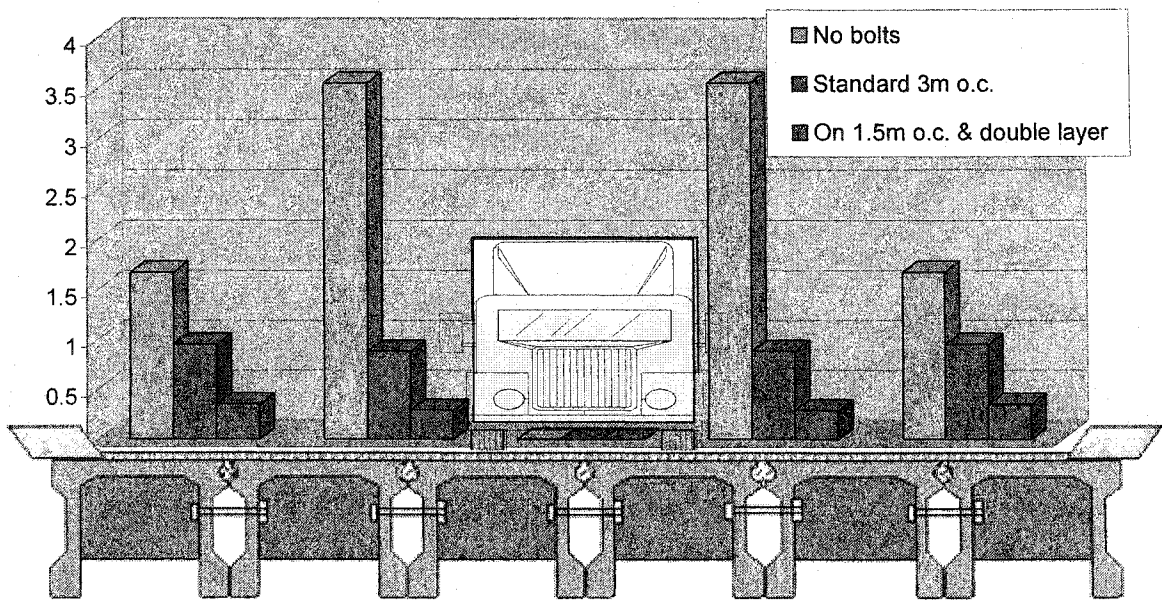
Figure 8.18: Differential deflections at shear keys in mm., shown at a
transverse cross section at 20 m.

259
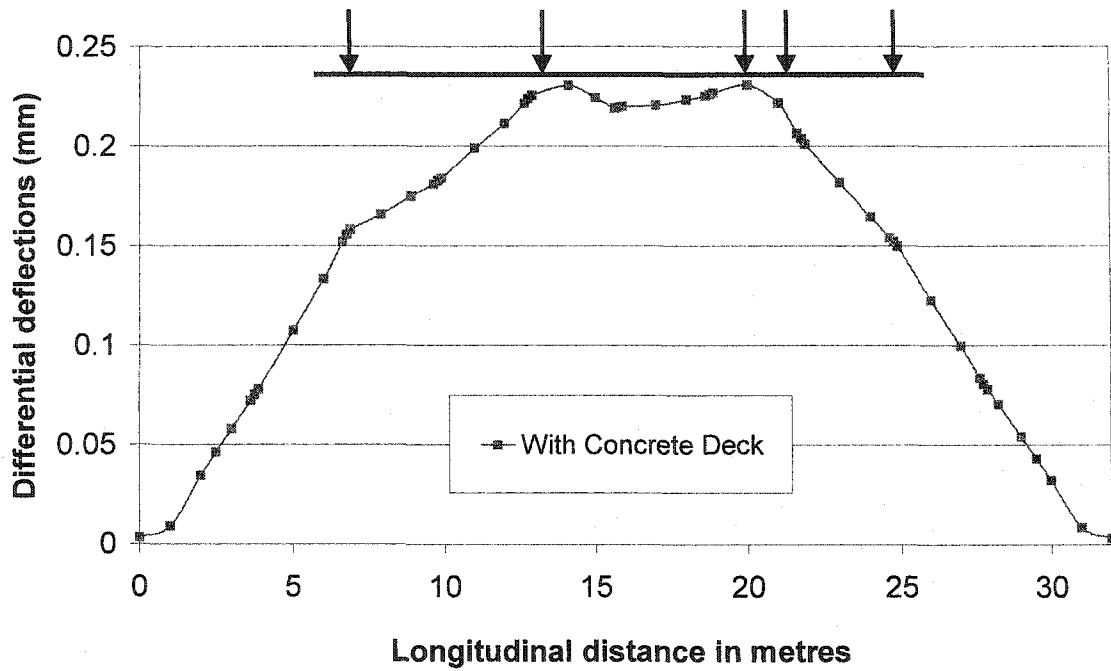
Figure 8.19: Differential deflections at one shear key at a longitudinal section
Rehabilitation Scheme = Concrete Overlay
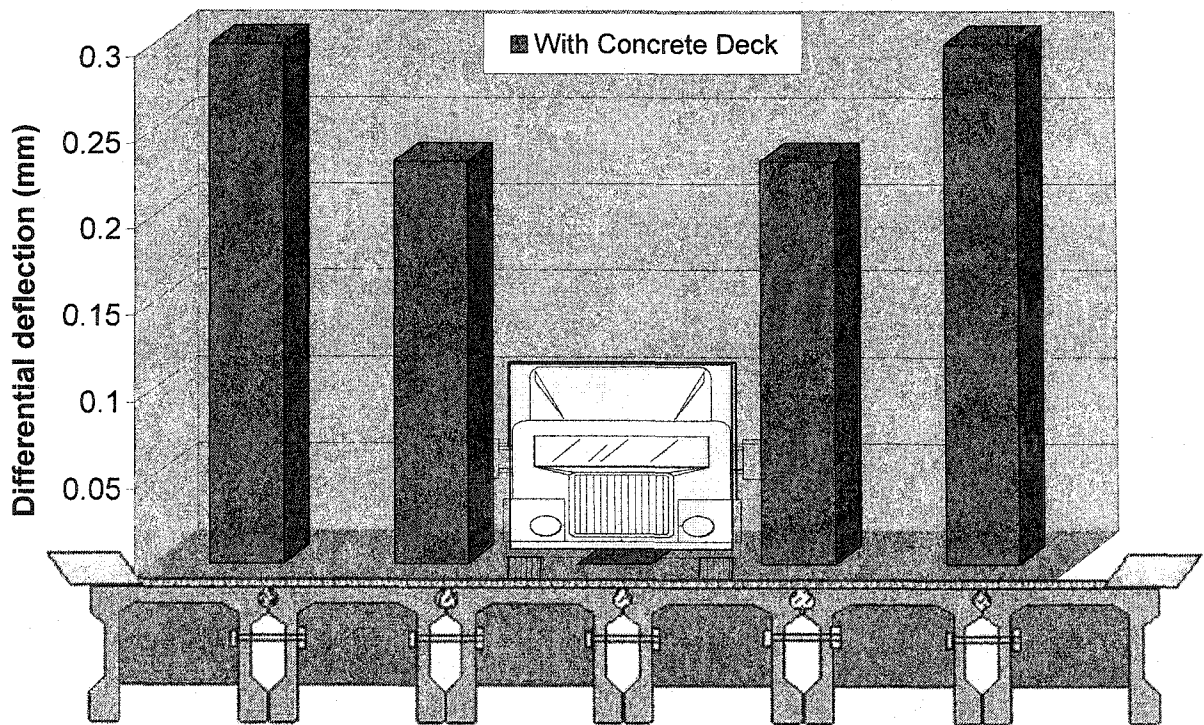
Figure 8.20: Differential deflections at shear keys in mm., shown at a
transverse cross section at 20 m.

260

The Actual girders   The finite element model
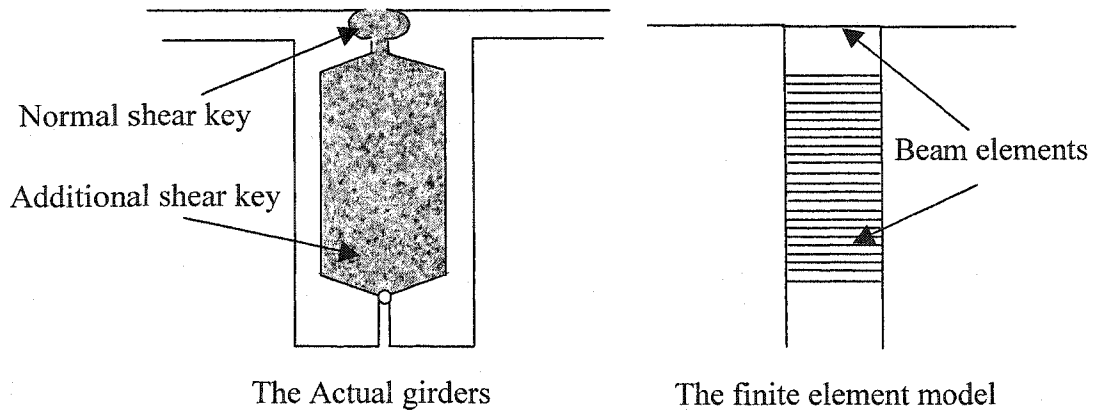
Figure 8.21: The normal and additional shear key, actual girder vs. the model
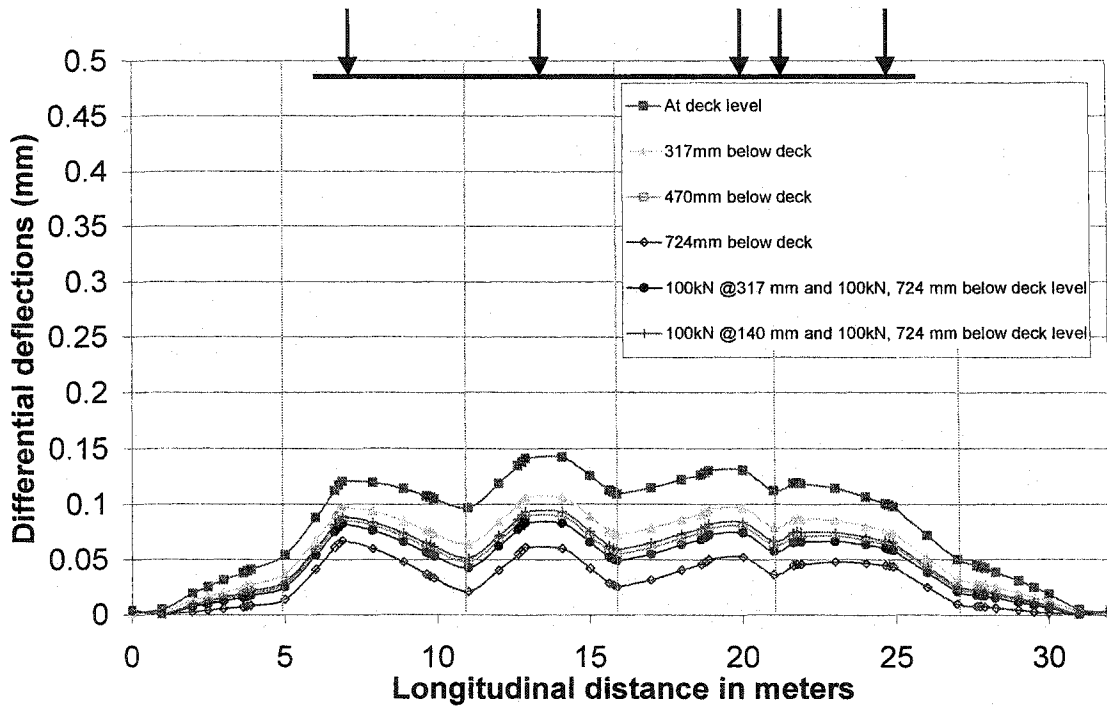
Figure 8.22: Differential deflections at one shear key at a longitudinal section
Rehabilitation Scheme = Prestressing (keeping force at 2x100 kN,
spaced at diaphragm locations and changing vertical location)
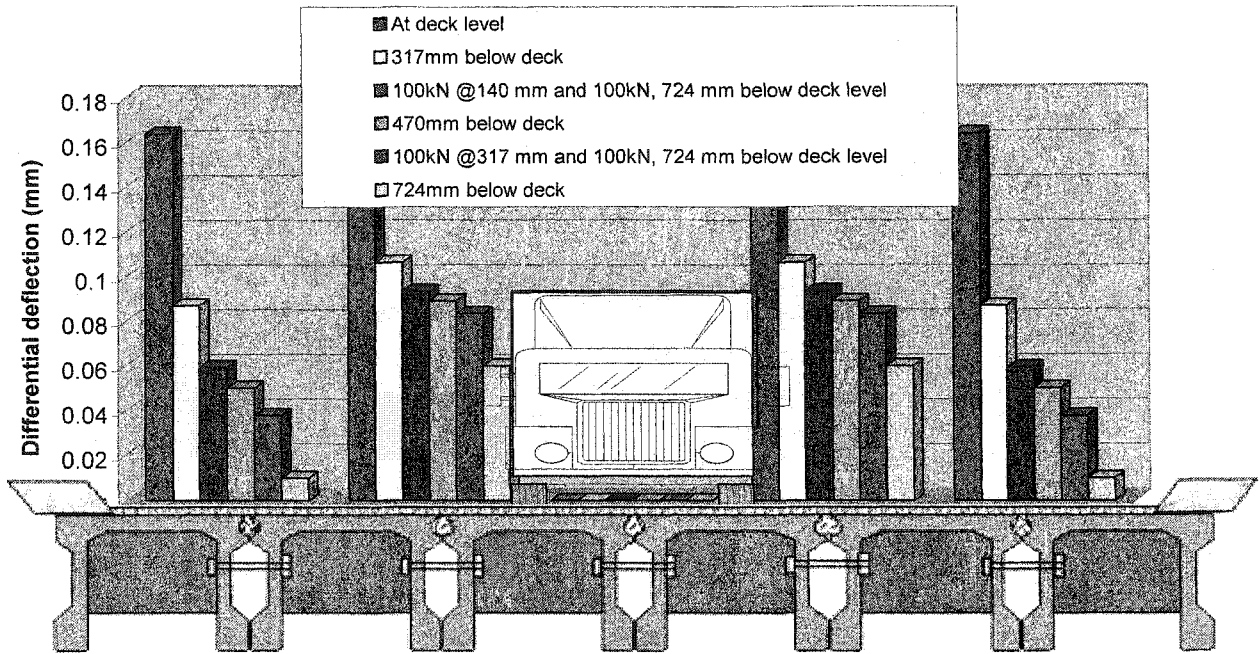
Figure 8.23: Differential deflections at shear keys in mm., shown at a
transverse cross section at 14 m.
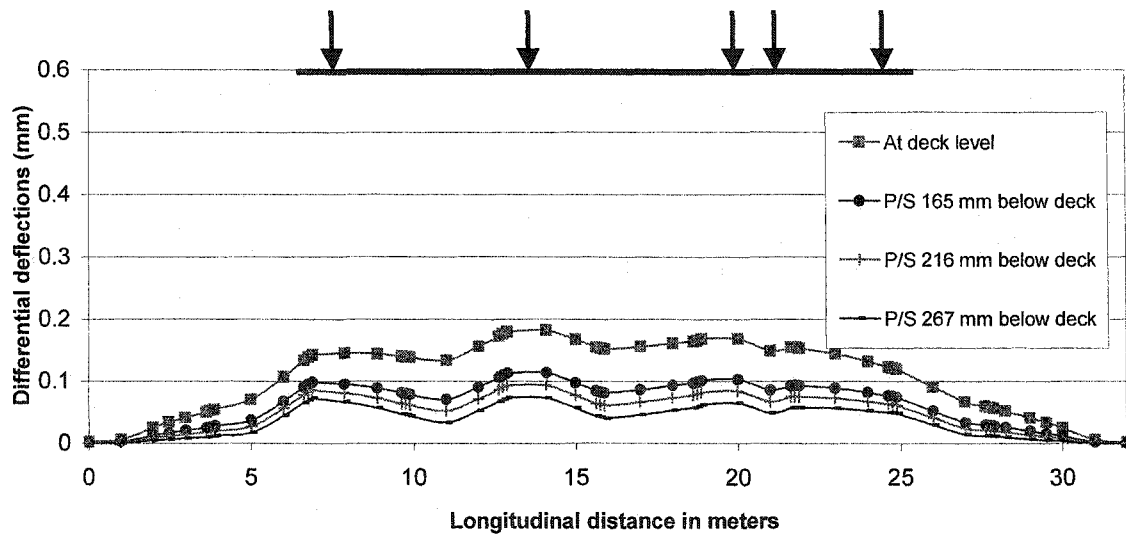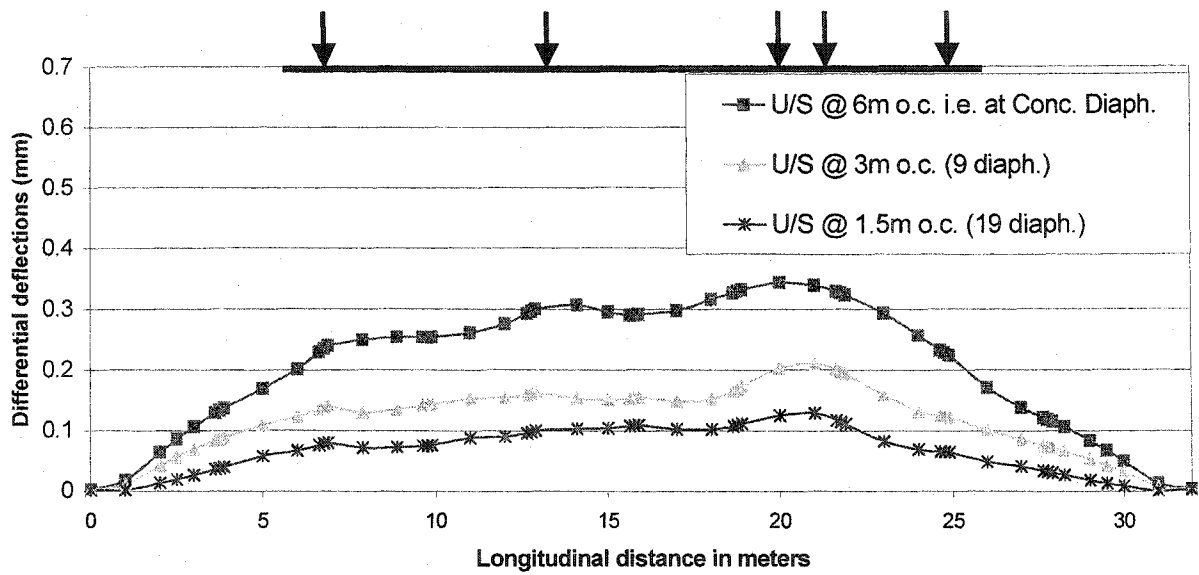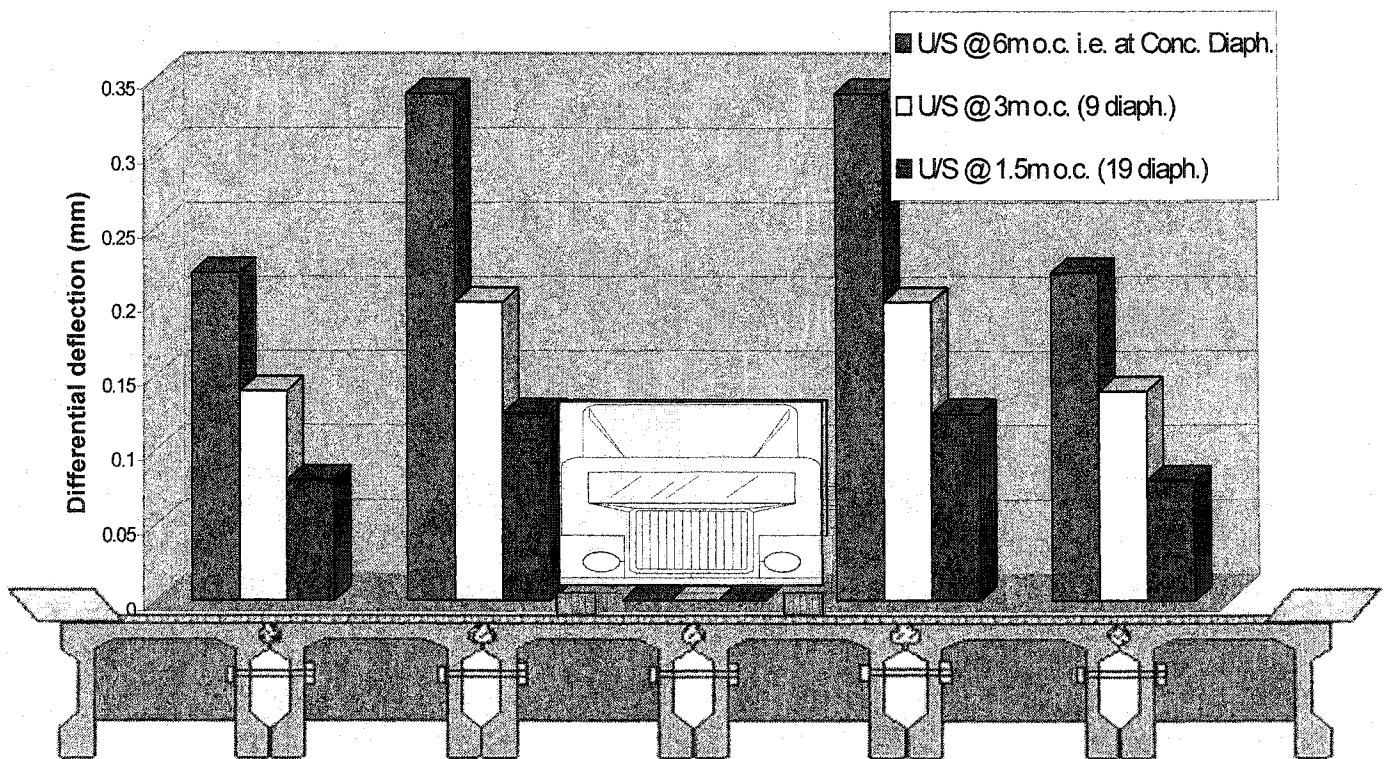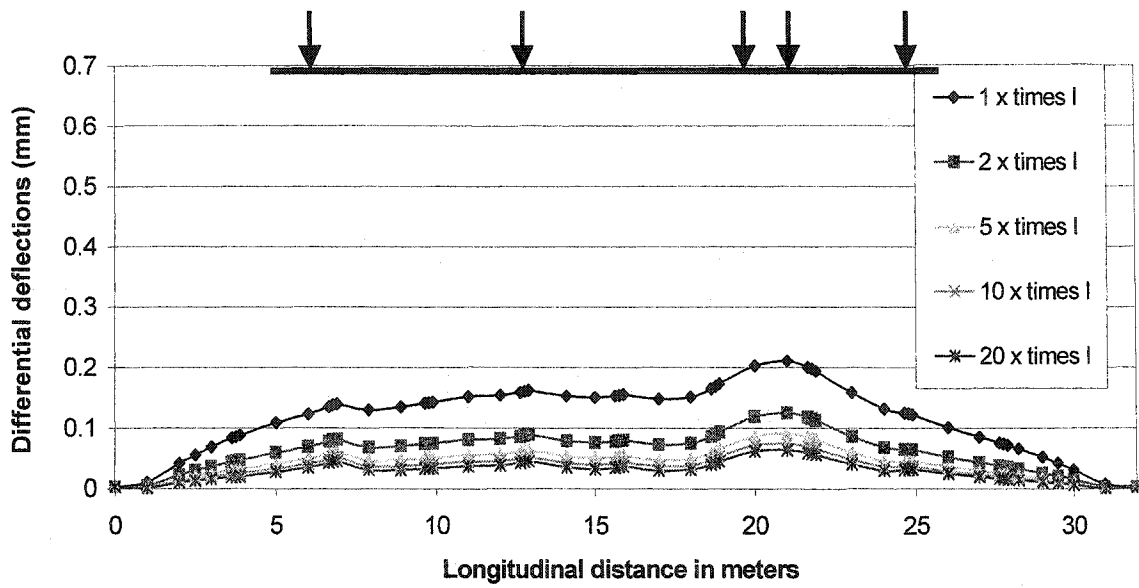

Figure 8.24: Differential deflections at one shear key at a longitudinal section
Rehabilitation Scheme = Prestressing (keeping force at 2x350 kN,
spaced at diaphragm locations and changing vertical location)
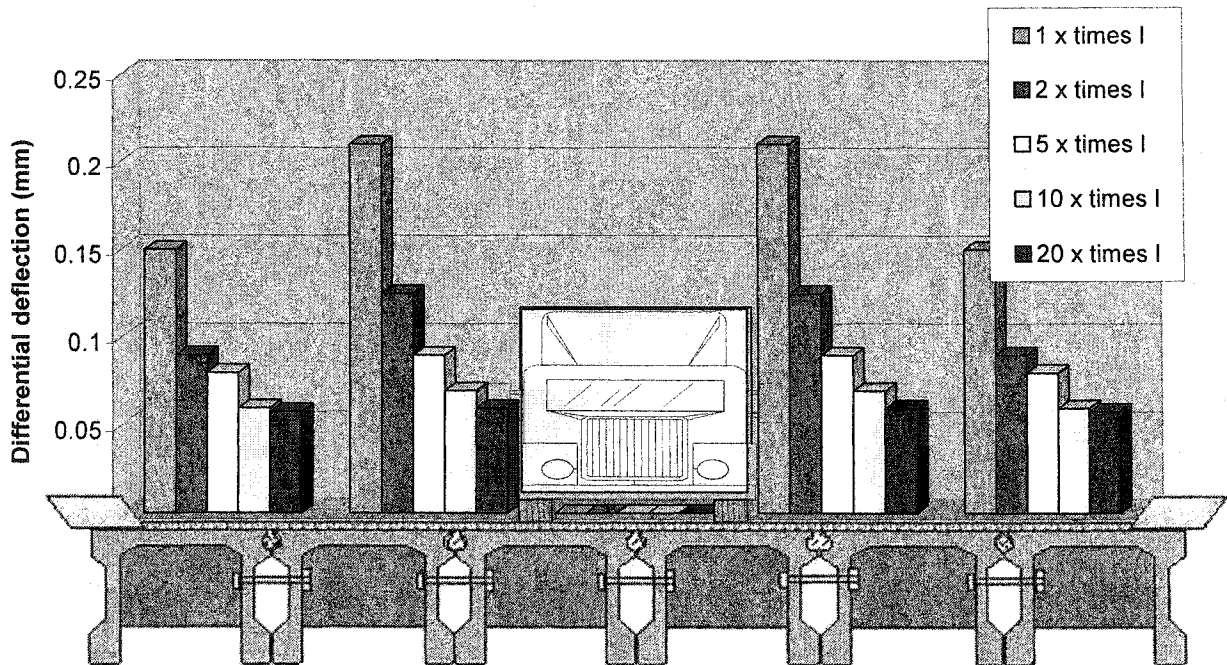
262
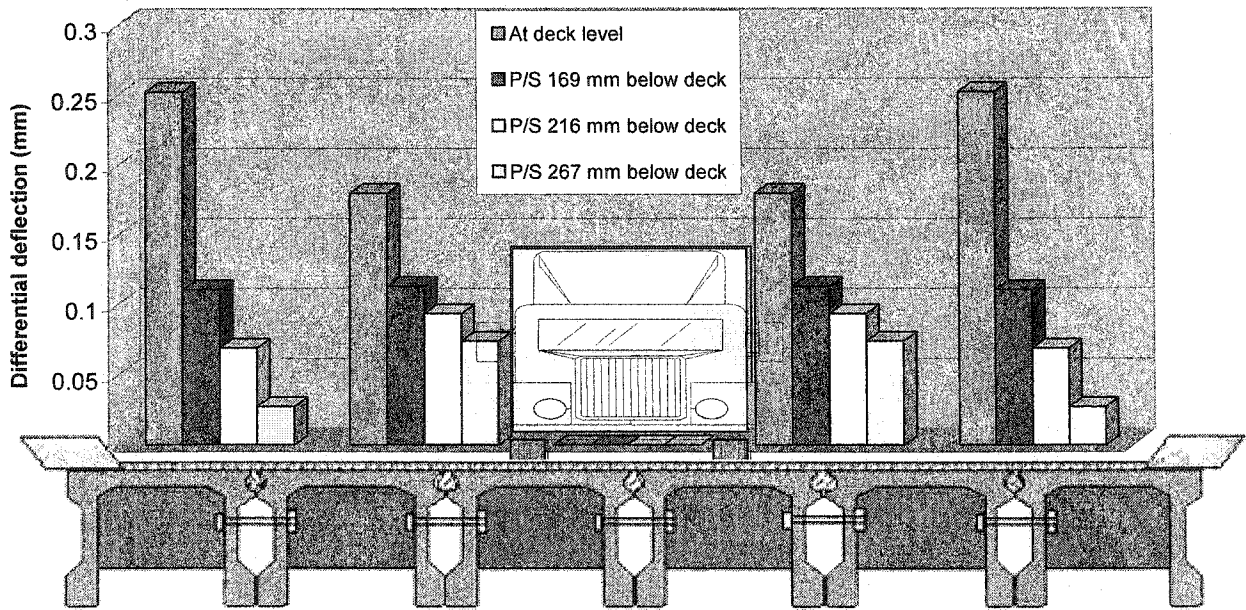
Figure 8.25: Maximum differential deflections at shear keys in mm.,
shown at a transverse cross section of the bridge at 13 m.
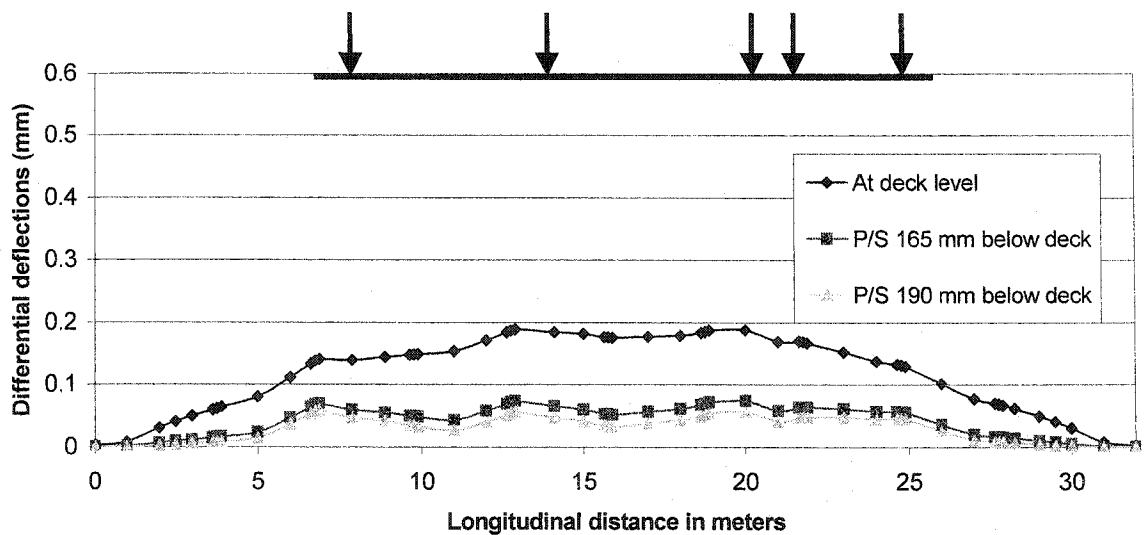
Figure 8.26: Differential deflections at one shear key at a longitudinal section
Rehabilitation Scheme = Prestressing (keeping force at 2x350 kN,
spaced at 3 metres on centers and changing vertical location)

263
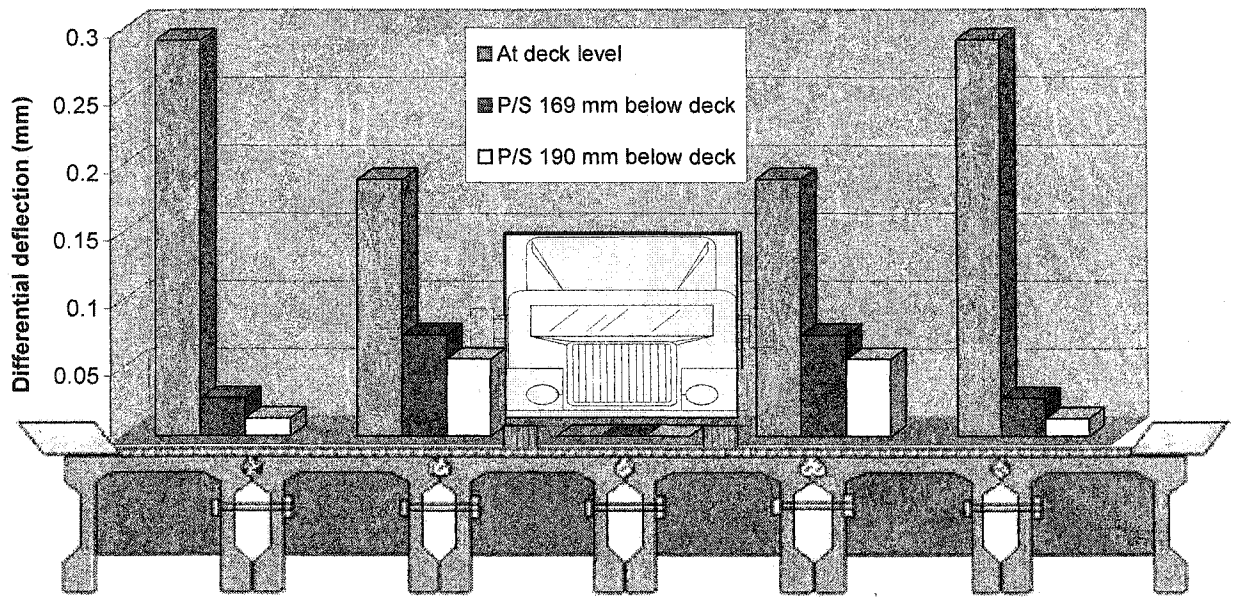
Figure 8.27: Maximum differential deflections at shear keys in mm.,
shown at a transverse cross section of the bridge at 13 m.
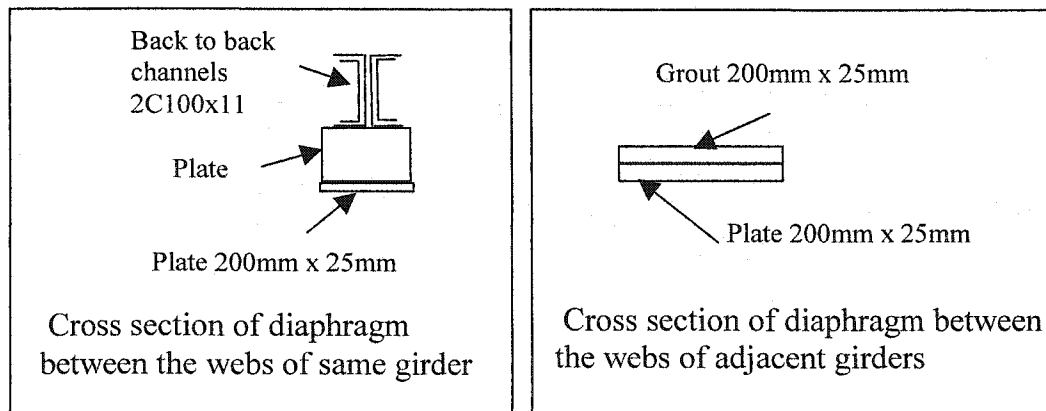
Figure 8.28: Cross sectional views of the Underslung diaphragm

264
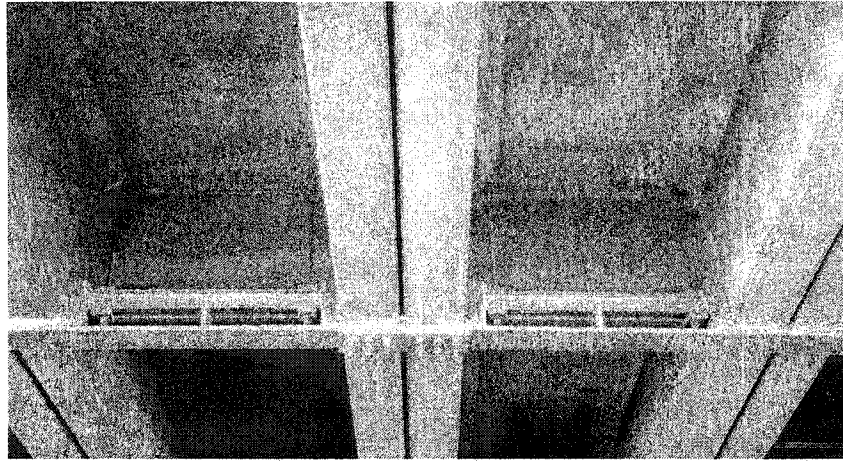
Figure 8.29: Rehabilitation by underslung diaphragms

Differential deflections (mm) of one shear key at a cross section at midspan
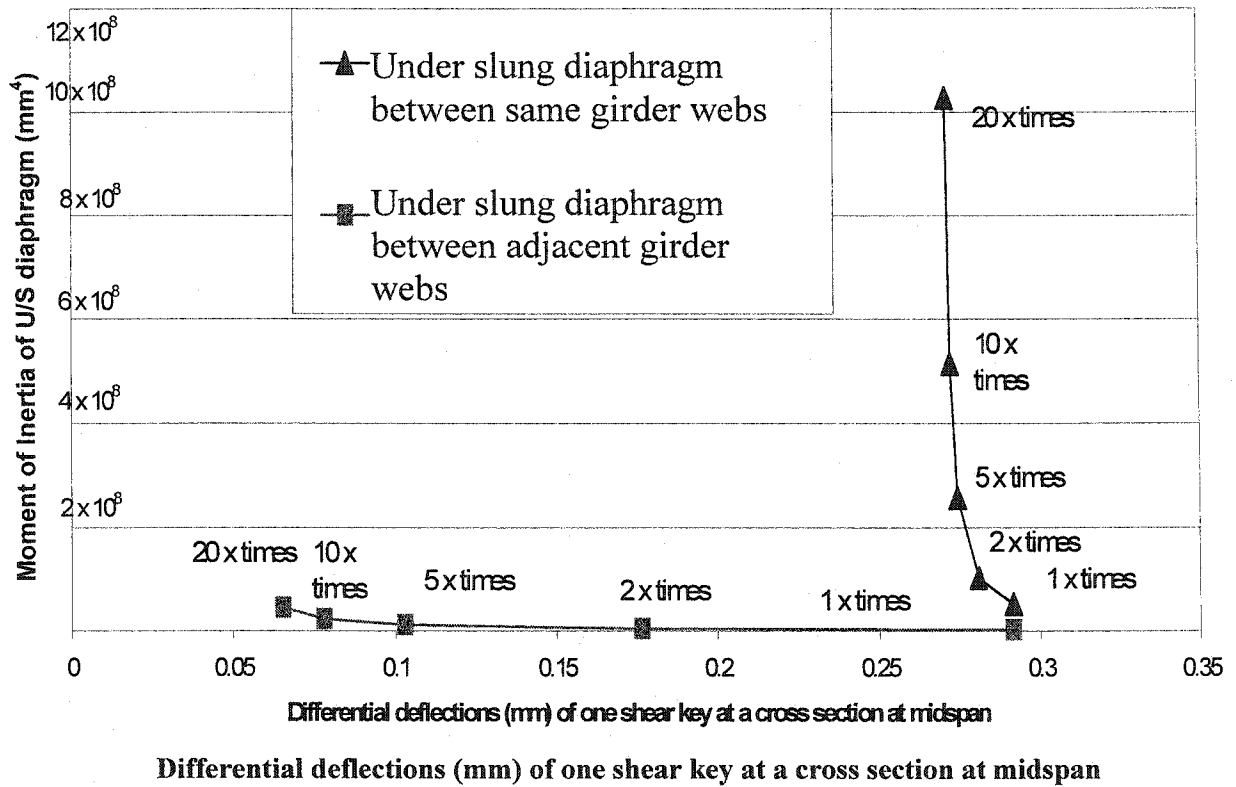
Figure 8.30: Rate of change of differential deflections with change in the
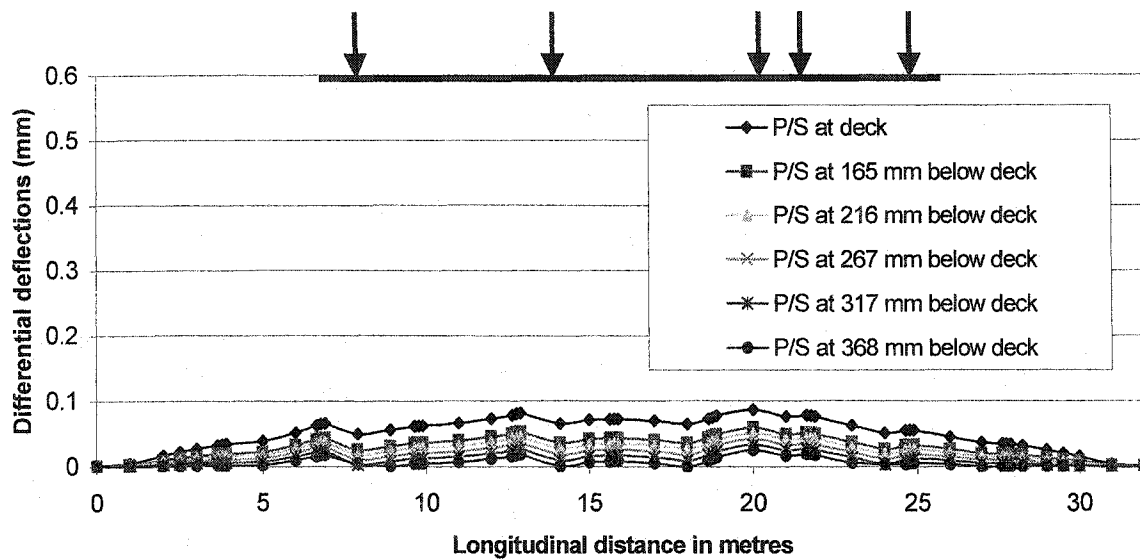moment of inertia of the Underslung diaphragm components

265

Figure 8.31: Differential deflections at one shear key at a longitudinal section
Rehabilitation Scheme = Underslung diaphragms (keeping sectional
properties constant, changing spacing)

Figure 8.32: Differential deflections at shear keys in mm., shown at a
transverse cross section at 21 m.

266

Figure 8.33: Differential deflections at one shear key at a longitudinal section
Rehabilitation Scheme: Underslung diaphragms (keeping spacing
@ 3m on centres and changing sectional properties)

Figure 8.34: Differential deflections at shear keys in mm., shown at a
transverse cross section at 21 m.

267

Figure 8.35: Differential deflections at one shear key at a longitudinal section
Rehabilitation Scheme: Underslung diaphragms plus prestressing.
(2x350 kN P/S force and USD applied at 3 metres on centres
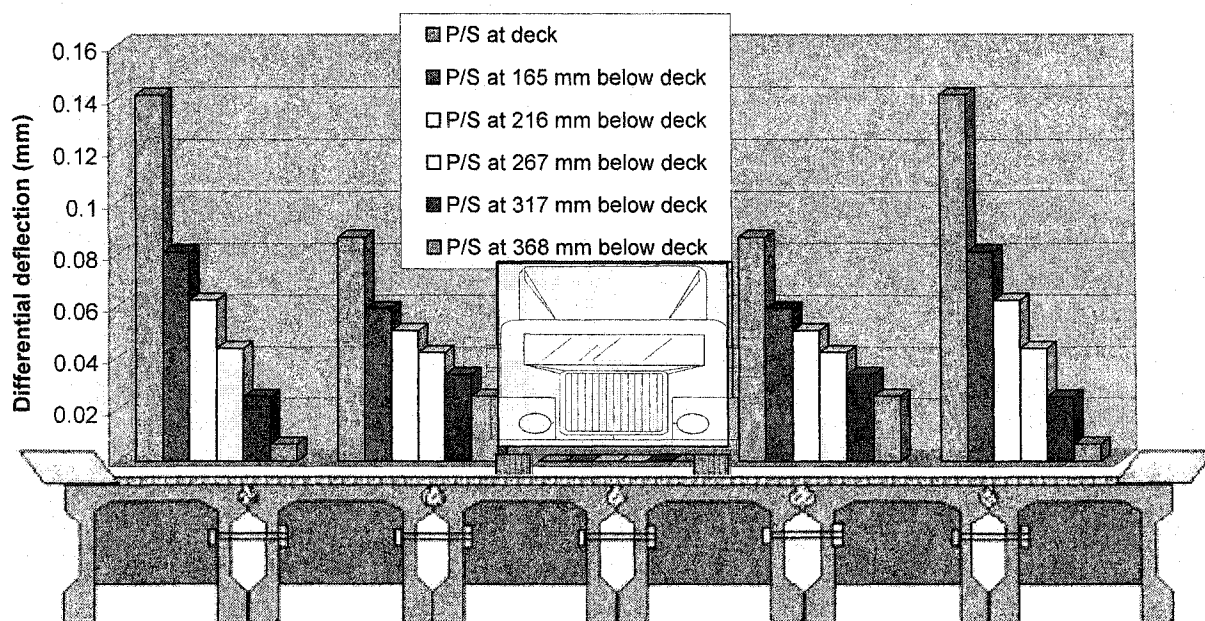
Figure 8.36: Differential deflections at shear keys in mm., shown at a
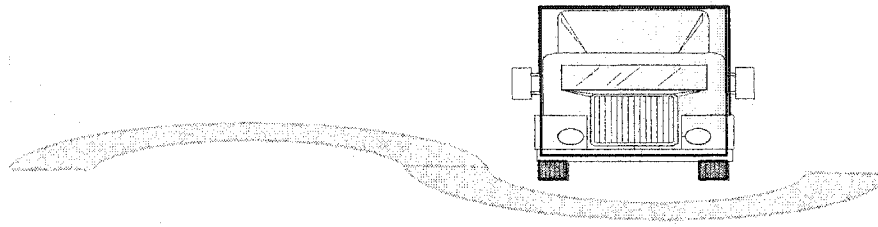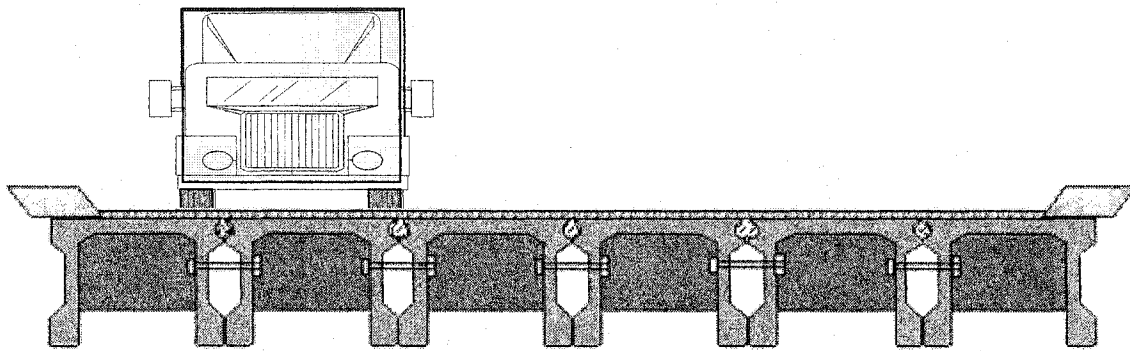transverse cross section at 20 metres.

268

Figure 8.37: Double curvature on bridge deck as a result of traffic on one lane

Shear key 1   Shear key 2   Shear key 3   Shear key 4   Shear key 5
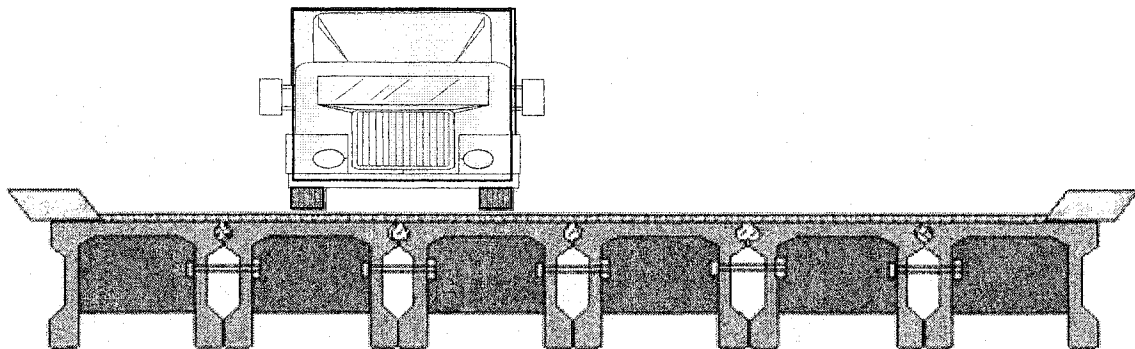
Figure 8.38: Transverse Load Position P1

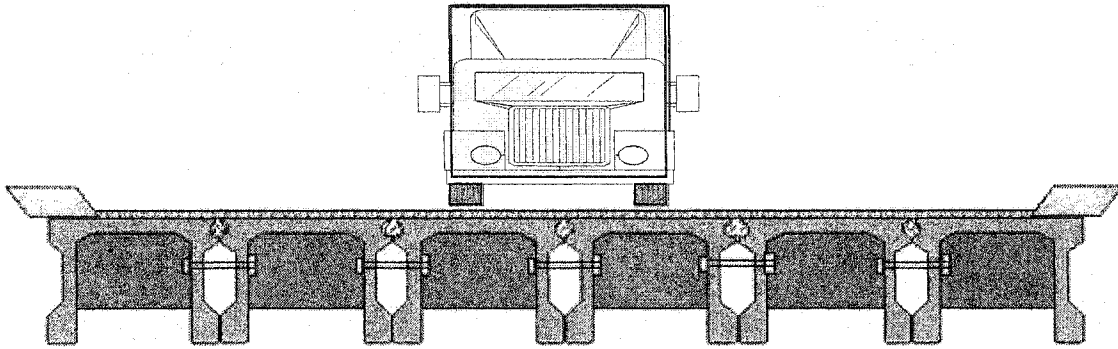Figure 8.39: Transverse Load Position P2
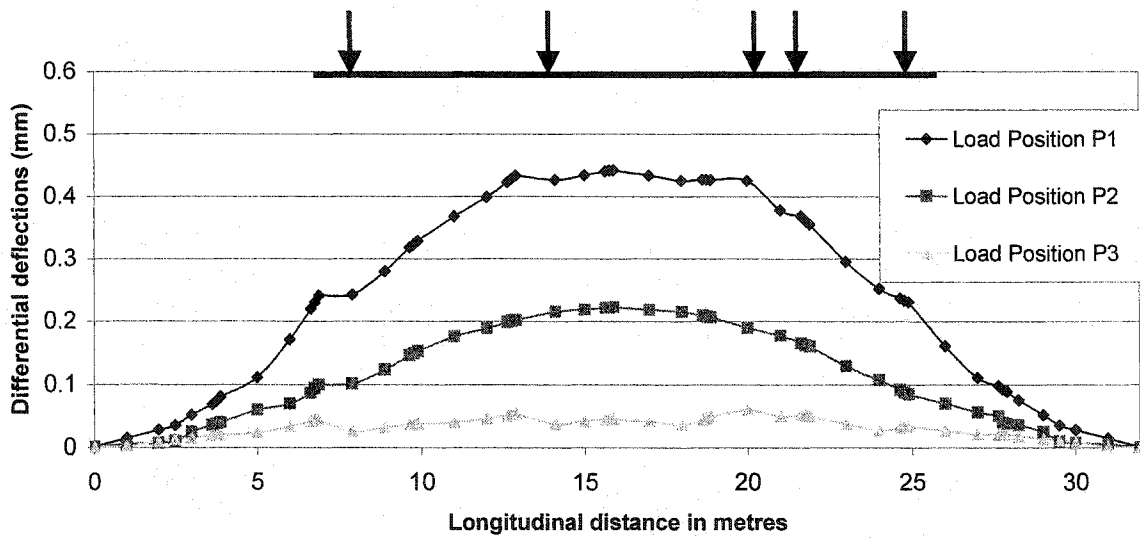
269

Figure 8.40: Transverse Load Position P3

Figure 8.41: Differential deflections at shear key 2, compared for different load positions
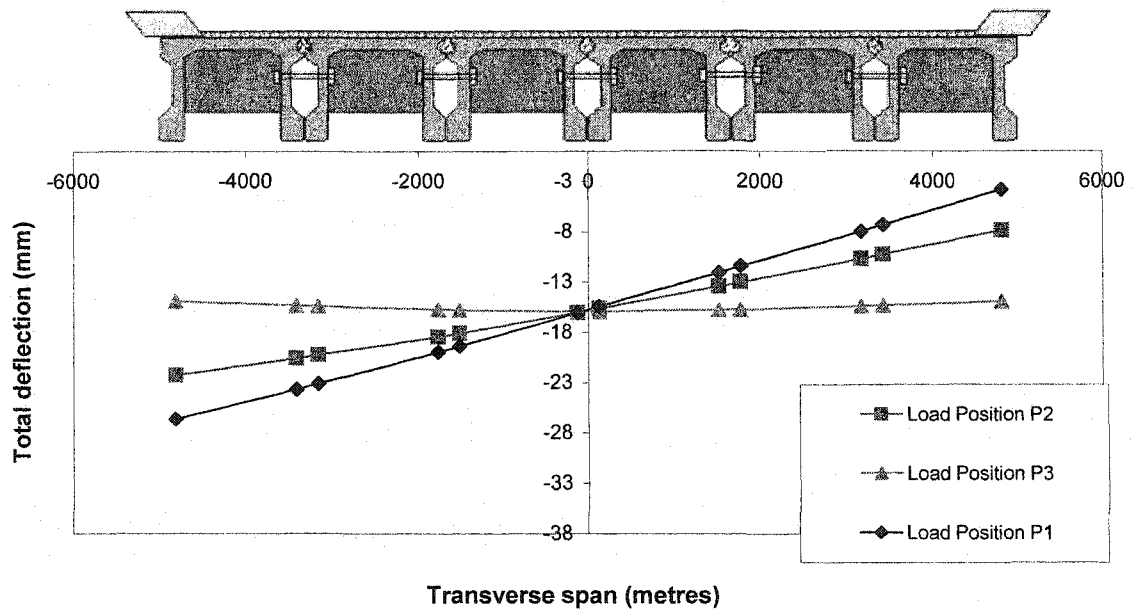
270

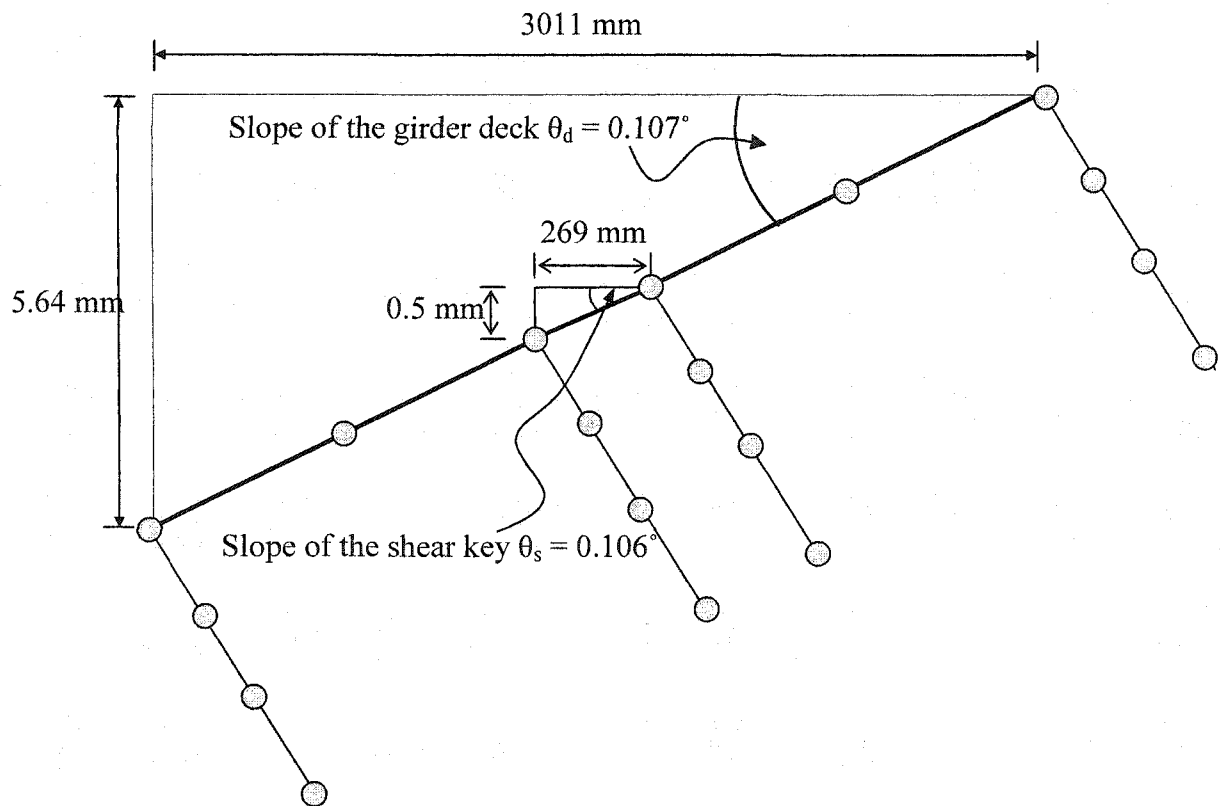Figure 8.42: Transverse deflection profile, compared for different load positions

Figure 8.43: Slope comparison of the shear key vs. adjacent girders

271
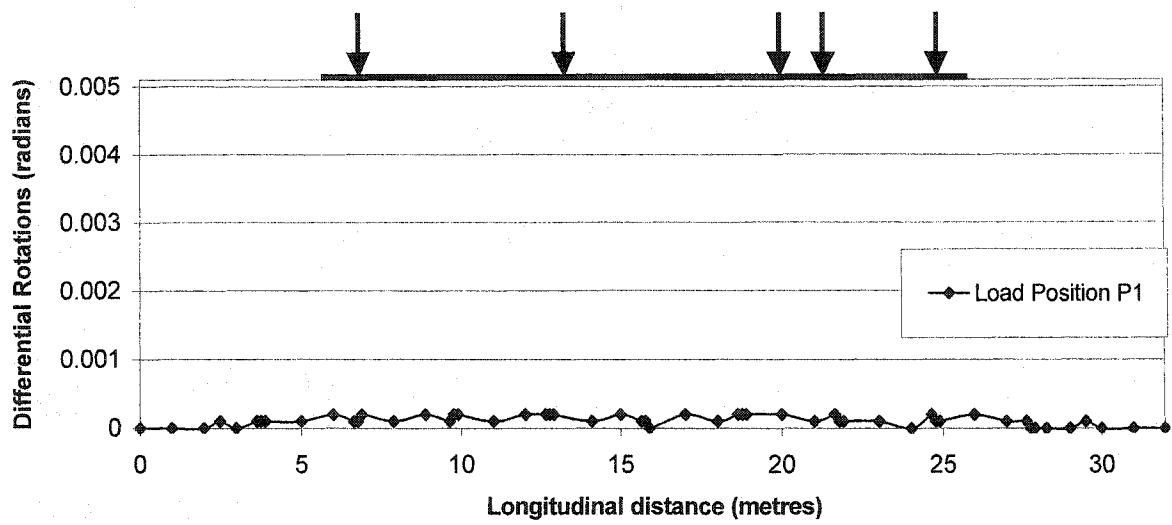
Figure 8.44: Differential rotations at shear keys with bridge under
combination scheme and under load position P1

Shear key 1   Shear key 2   Shear key 3   Shear key 4   Shear key 5
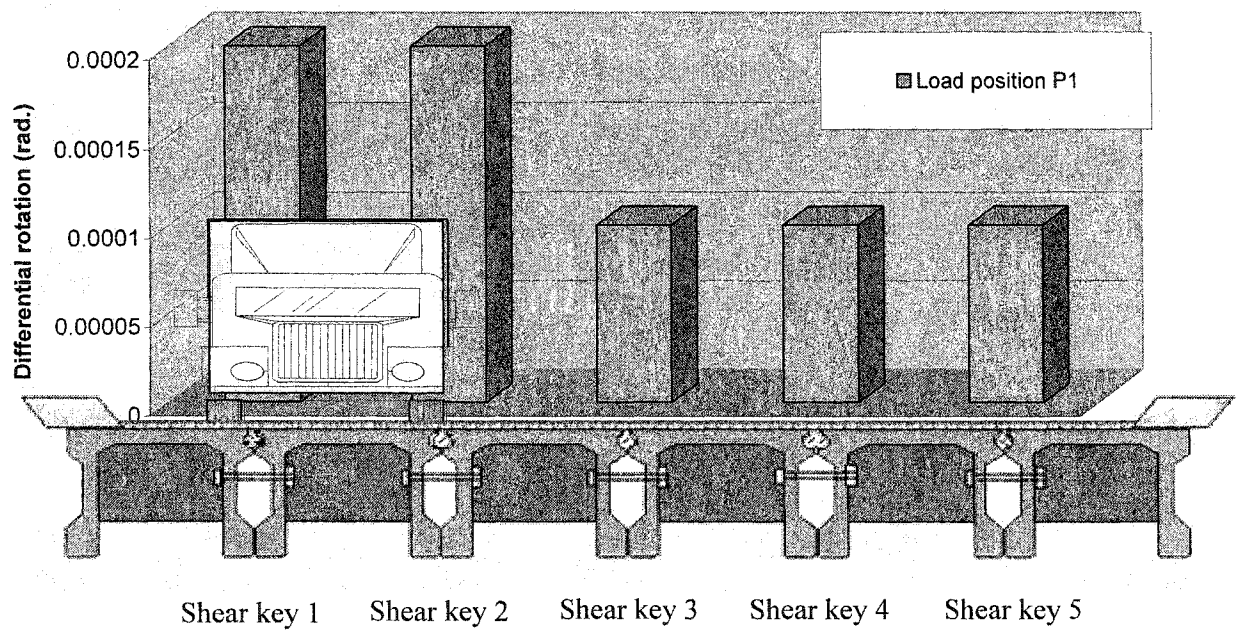
Figure 8.45: Differential rotations at a transverse cross section at 20 metres, with
bridge under combination scheme and load Position P1

272

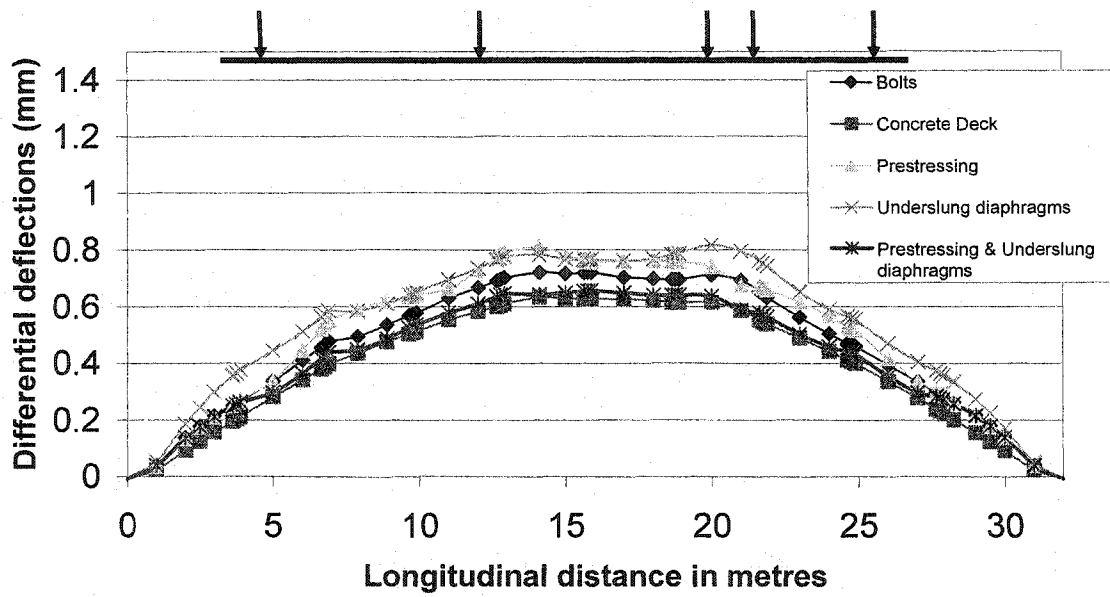Figure 8.46: Differential deflections at shear key 2 under different rehabilitation schemes and load position P1
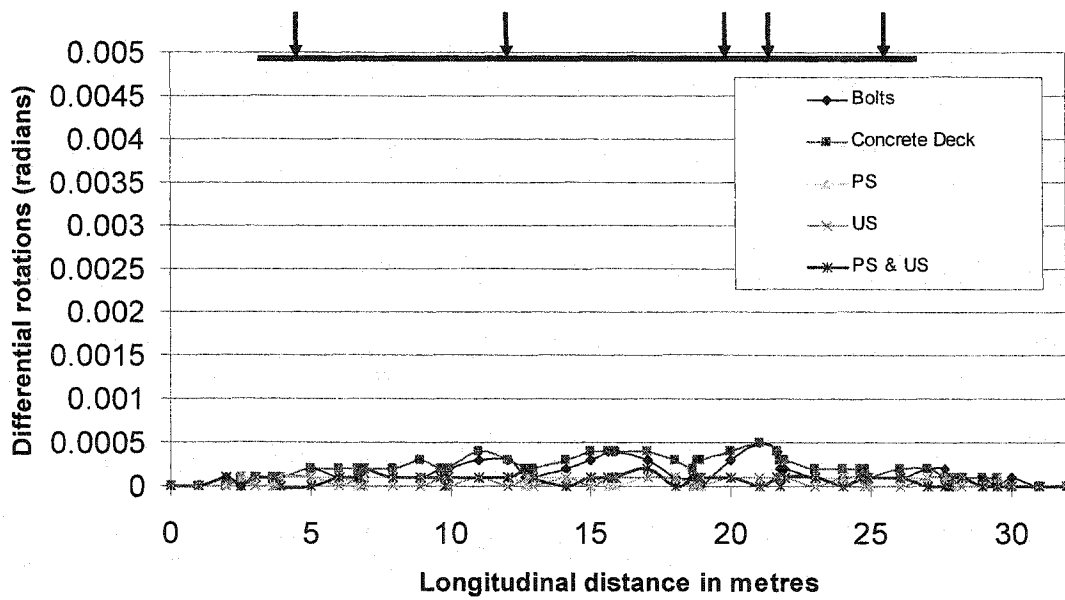
Figure 8.47: Differential rotations at shear key 2 under different rehabilitation schemes and load position P1

273
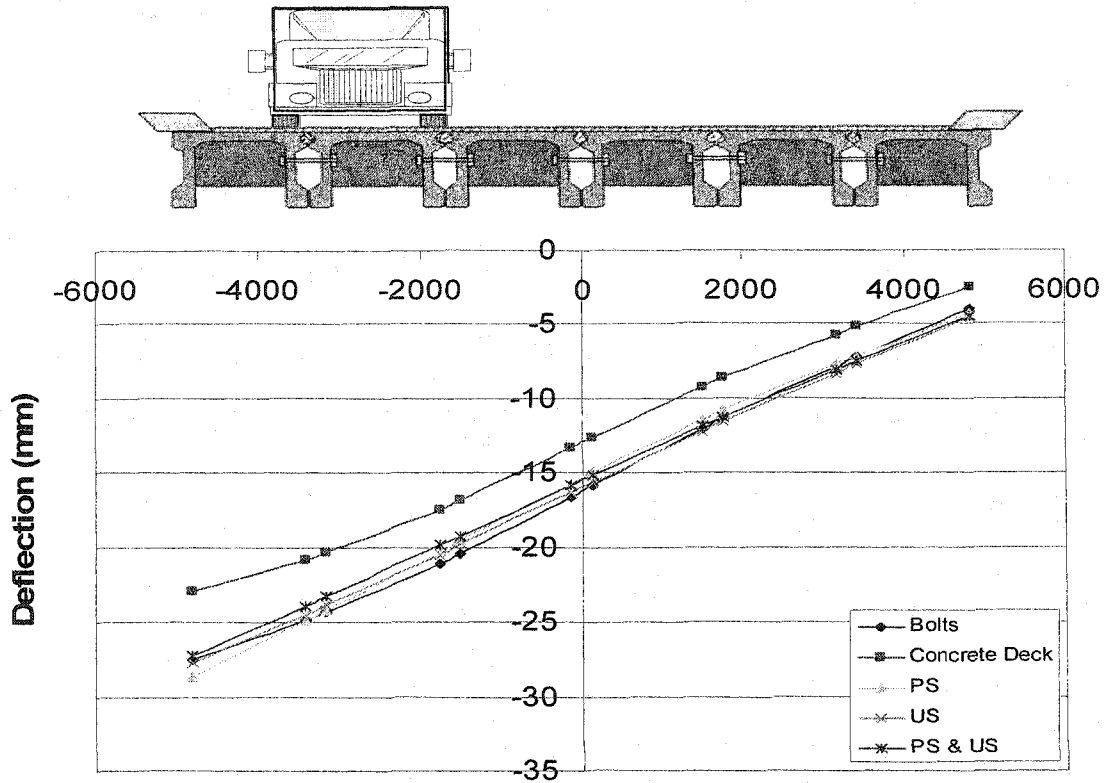
Figure 8.48: Transverse deflected profile at mid span

Figure 8.49: Slope of adjacent girders and shear keys at a cross section
at mid span, using bolts as rehabilitation scheme

274

Figure 8.50: Slope of adjacent girders and shear keys at a cross section
at mid span, using concrete deck as rehabilitation scheme

Figure 8.51: Slope of adjacent girders and shear keys at a cross section
at mid span, using prestressing as rehabilitation scheme

275

Underslung diaphragms

Figure 8.52: Slope of adjacent girders and shear keys at a cross section at mid span, using underslung diaphragms as rehabilitation scheme

Prestressing and Underslung diaphragms combined
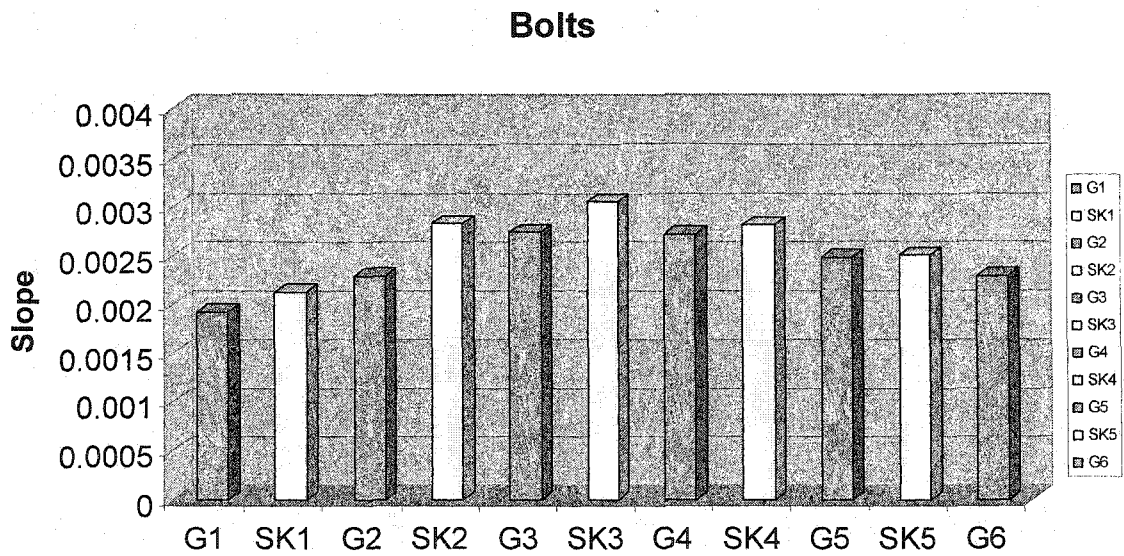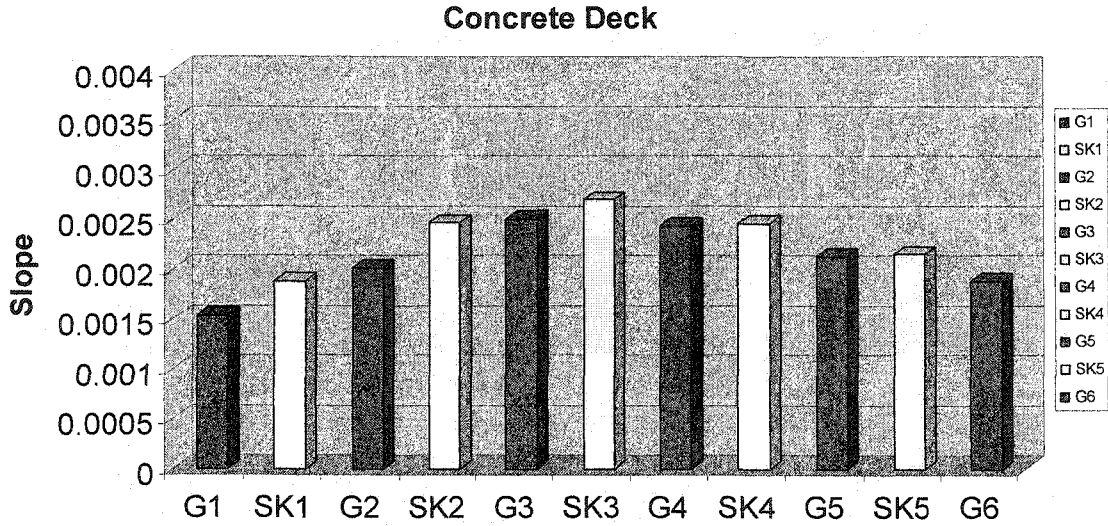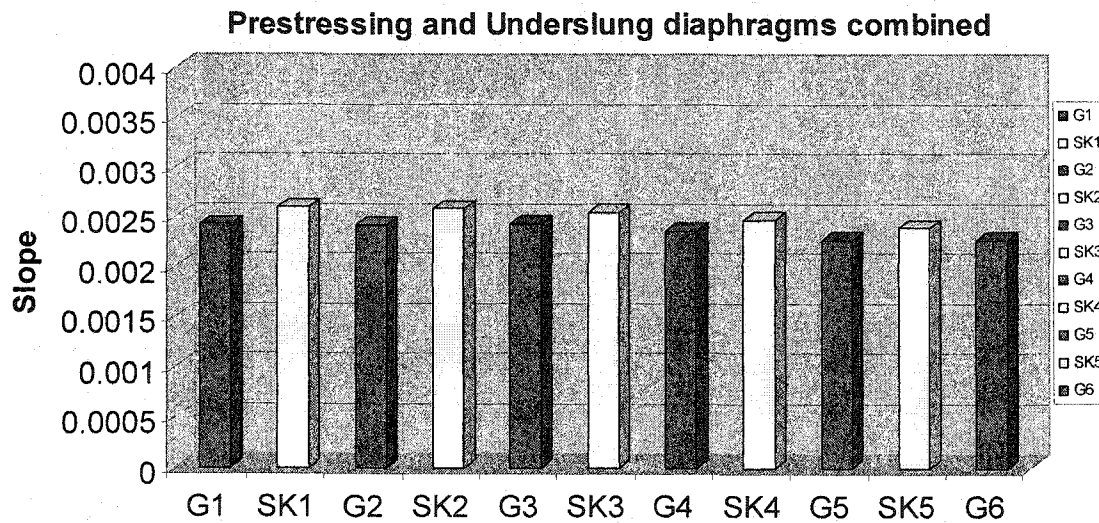

Figure 8.53: Slope of adjacent girders and shear keys at a cross section at mid span, using combination scheme as rehabilitation scheme
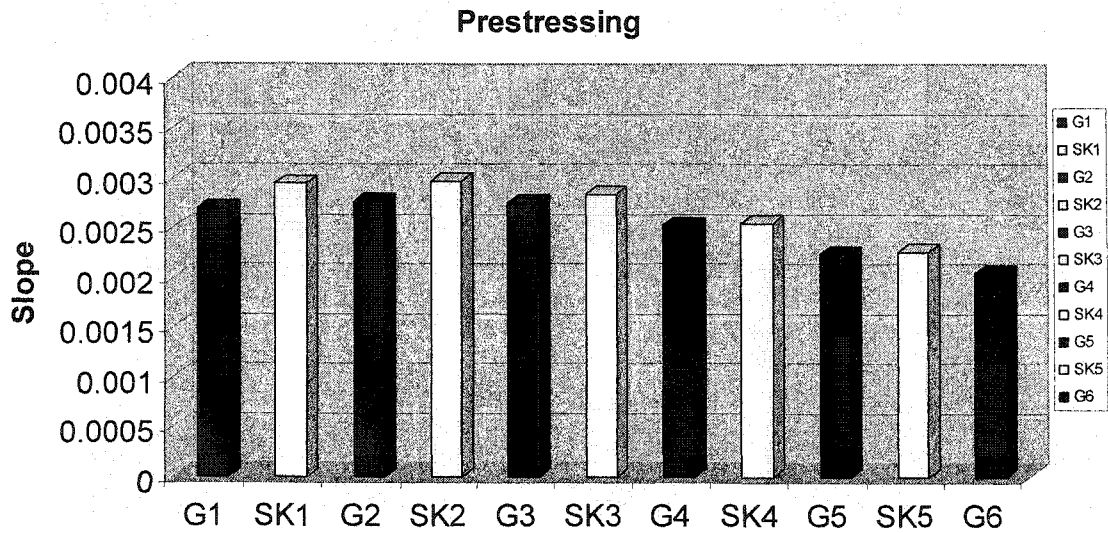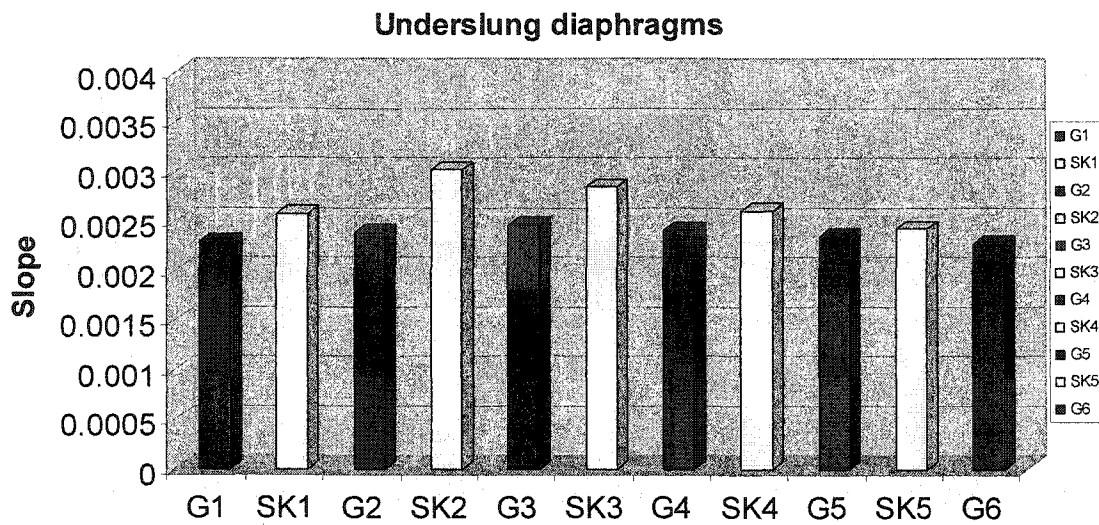
276
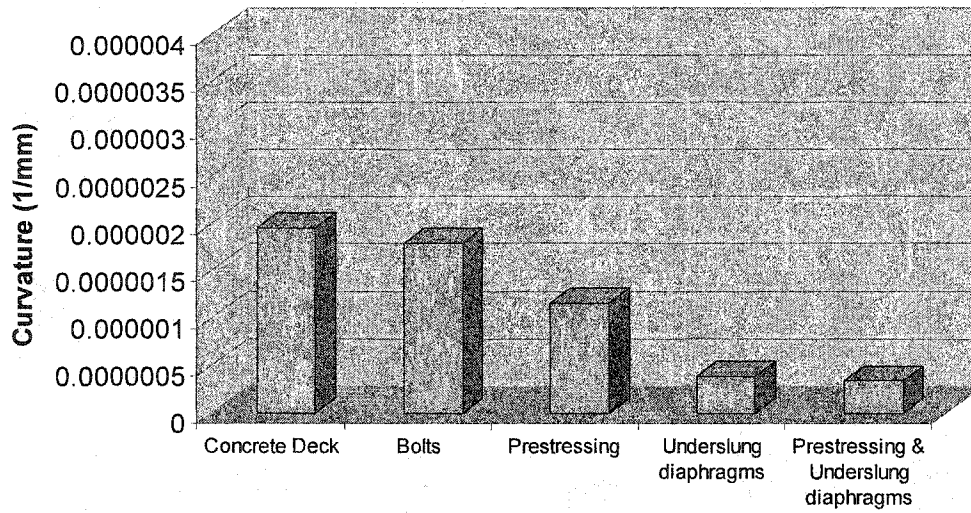
Figure 8.54: Largest shear key curvatures obtained by using different rehabilitation schemes

8.10 References

1. Alberta Transportation Bridge Records, "FC Girder Rehabilitation Data (1995 to 1999) & BIM (Bridge Inspection and Maintenance) system forms."

2. UMA Engineering Ltd., (1996), "Report on the finite element analysis of shear keys on FC Girder Bridges and the design of rehabilitation methods." Report prepared for Alberta Transportation & Utilities. January 1996.

3. CH2M Gore & Storrie Limited, (1998), " Report on the Lawrence River Bridge (BF 75694) Strengthening Analysis". Report prepared for Alberta Transportation.

4. Reid Crowther & Partners Ltd., (1996), "Highway 16A Overpass on Highway 16 (76339), finite element analysis report". Report prepared for Alberta Transportation and Utilities. April 1996.

5. CAN/CSA-S6-2000, (2000), " Canadian Highway Bridge Design Code – A National Standard of Canada". Canadian Standards Association.

6. Khattak, N.A. & Cheng, J.J.R., (2002), "Non destructive evaluation of single, medium span concrete bridges", Proceedings of the sixth international conference on short and medium span bridges, Vol.-II, Vancouver, BC Canada, July 31st – August 2. pp. 1295-1302.

9.0   SUMMARY, CONCLUSIONS & RECOMMENDATIONS

9.1 Summary

Most shear key based systems constructed around North America in the fifties, sixties and seventies have experienced cracking in the shear keys, regardless of the shape of the precast girder[1]. In the province of Alberta alone, almost fifty percent of the FC Girder Bridges, which were erected in the late sixties, seventies and even eighties, have undergone rehabilitation[2]. Most of these bridges have been rehabilitated by a random mix of various rehabilitation schemes and a thorough knowledge base does not exist about the suitability of these schemes towards the FC Girder Bridges[2].

The main objective of this research was to investigate the shear key field problem with FC Girder Bridges, to assess its severity in the field and to rationally evaluate the commonly used rehabilitation schemes on these bridges and discuss their individual merits and demerits, while commenting on the most suitable rehabilitation strategy for these bridges. Hence, this research aims at expanding the knowledge base available for rehabilitation needs of the FC Girder Bridges.

An extensive research program was designed to deal with the field problem at hand. The first part of this research plan consisted of a thorough literature review on similar work done on FC Girder Bridges in Alberta as well as any research done on shear key based bridge systems anywhere around the world. This was followed by a visual inspection survey of 20 percent of the FC Girder Bridges in the province of Alberta to assess the current condition of these bridges. To supplement the information from the visual inspections, a number of bridges were selected to conduct load and vibration testing in the field.

The bridge tests[3,4] yielded useful information on the current condition and dynamic characteristics of that particular bridge and provided data to formulate and calibrate a finite element model, which could then be used and extrapolated to other bridges. The finite element model was then used to conduct a study, which took into consideration the

279

use of various rehabilitation schemes. On the basis of deformation and stiffness criteria, a direct comparison of the performance of the optimum variation of the various rehabilitation schemes was conducted.

9.2 Conclusions

With the help of a thorough literature and field survey, it was established that longitudinal cracking in these bridge decks initiate and progress at the longitudinal shear key locations[1,2]. It was observed by some researchers that the shear keys actually crack because of thermal effects, which start to act almost immediately, after the bridge has been erected[1]. Once the shear keys have cracked, successive loading cycles will cause these cracks to grow and reach the surface. This same effect was verified by the natural frequency of the transverse bending mode shape, during a number of field tests. These natural frequencies essentially remained the same whether the bridge exhibited cracked shear keys or was in undamaged state[4]. This observation proves the point that even if the shear keys did not show cracking on the deck surface, they were still cracked from inside.

During the visual inspection field survey, it was observed that traffic loads and the age of the bridge had a direct impact on shear key cracking[2]. Hence we can conclude that the shear key cracks will grow faster and reach the surface if the bridge is subjected to a larger number of loading cycles whereas bridges, which are under light vehicular traffic, will probably take a longer to build cracking in the shear keys, which reaches the surface. Once a crack has formed in the longitudinal shear keys, the impact of the vehicle wheel load induces differential movement in the form of vertical deflection and transverse rotation at the cracked planes. This relative motion between the two cracked planes, with more and more loading cycles, cause the cracks to grown in width over time.

As the shear keys crack, they start to behave as hinges, hence transferring transverse shear but no moment. To model this mechanism beam elements with a hinge in the middle was used as shear key elements in the finite element model[5]. The finite element was compared with test results and it was observed that cracking reduces the stiffness of the shear keys, an effect which was then incorporated within the finite element model to

obtain excellent agreement between the test and the model with respect to three independent test measurements of deflections, strains and natural frequencies and mode shapes of vibration[5, 6].

The calibrated finite element model was then used with a number of different rehabilitation strategies and their performance evaluated on the basis of two characterizing parameters[5], i.e. differential deflections at shear key lines and natural frequency of the flexural bending in the transverse direction or the width span. Both these parameters are quite easily measurable in the field with the help of deflections transducers and accelerometers and were hence considered as useful indicators in gauging the performance of the rehabilitation schemes. Moreover, a change in the magnitude of both these parameters was directly and physically linked to the performance of the shear keys. In other words, an intact shear key would not permit differential movement between the adjacent webs of the girders and a low value of the transverse bending natural frequency would show inadequate flexural stiffness of the cross section in the transverse direction. The finite element model with a centrally placed truck load and using a healthy shear key showed differential deflections of 0.1 mm and natural frequency of 7.1 Hz. for the transverse bending mode shape. The same model after having been calibrated with the field tests and subjected to the light test load, showed differential deflections of around 2 mm and a natural frequency of 5.4 Hz. for the transverse bending mode shape. Needless to mention that the shear keys in the actual bridge were cracked and that these two parameters were reasonably good indicators to conduct the finite element study on the rehabilitation schemes.

Load sharing concerns are also directly related to the differential movement at adjacent girder webs and were shown with the help of lateral live load distribution factors (LLDF)[3]. Though partial load sharing was still taking place in the bridges that were tested, rehabilitation procedures did indeed improve the load sharing which could be easily spotted by the decrease in differential deflections, increase in the transverse bending natural frequency and a better distribution of the lateral load distribution factors.

281

Finally, a performance comparison of the rehabilitation schemes indicates that most of the rehabilitation schemes used to date are effective in improving the load sharing between the girders. However, the use of a combination of transverse prestressing and continuous steel underslung diaphragms would yield the best results[5], give torsional rigidity to the bridge cross section, arrest all differential movement between adjacent girders and hence improve load sharing between the girders. This combination scheme is the best alternative to prevent shear key cracks from occurring. However, in most cases, the underslung diaphragms are not extended all the way to the last web of the extreme girders for aesthetic purposes. This causes the extreme girders to flex a little and hence produce reverse curvature in the transverse bending profile which sometimes generates tension in the two end shear keys. To avoid this problem, it is recommended that the transverse steel diaphragms be extended all the way from one extreme web to the other.

9.3 Recommendations for Further Research

A laboratory test of full scale FC girders is highly recommended to study the cracking mechanism of the shear keys under cyclic loading representing the vehicular traffic. The laboratory test to failure will assess the role of the rehabilitation schemes in preventing recracking of the shear keys after the bridge has been rehabilitated and the shear keys regrouted.

Additional field tests on the different rehabilitated bridges will also be very beneficial in expanding the data base on the performance of different rehabilitation schemes in the field.

Finally, a life cycle cost analysis on the use of each rehabilitation scheme would give useful insight on the cost to benefit ratio of using these rehabilitation strategies.

282

9.4 References to Chapters

1.   Chapter 2

2.   Chapter 3

3.   Chapter 5

4.   Chapter 7

5.   Chapter 8

6.   Chapter 6